“Application of optical spectroscopy for the identification of agro-foods (olive oil and tsikoudia), quality control and adulteration of extra virgin olive oil”

Master Thesis

M.Sc. Micro-Optoelectronics, Physics Department, University of Crete

Antigoni Papadaki

BSc in Physics

Physics Department, UOC

Supervisors: Prof. Peter Rakintzis *(UOC)*

Dr. Michalis Velegrakis *(IESL-FORTH)*

February 23, 2017

Table of Contents

Acknowledgements:

First of all, I would like to thank my supervisor Dr. Michalis Velegrakis (Researcher Director, IESL-FORTH) for giving me the opportunity to cooperate with him during this Thesis and introduced me to his Cluster Physics and Chemistry Laboratory at Institute of Electronic Structure and Laser at Foundation of Research and Technology-Hellas (IESL-FORTH). He guided me to the facilities and applications of his laboratory, inspired me to work like a professional in a scientific environment and specially, in a "new" field for his group, Food Industry. His advice, kindness and full support during these years are invaluable!

Special thanks to Prof. Peter Rakintzis (Professor, Physics Department, University of Crete) and Prof. Stelios Tzortzakis (Associate Professor, Department of Materials Science and Technology, University of Crete) that accepted to be members of my evaluation committee for my Master Thesis. I appreciate their collaboration with me and my supervisor.

During these years, I collaborated with a lot of scientists and students at FORTH, University of Crete and other companies. I am thankful to Dr. Aggelos Philippidis, an excellent cooperator and man. Through our long-term conversations, he advised me for several reasons, helped me understand a lot of new things, which were unknown to me, making experiments together and communicated his knowledge to me. I am grateful that I met him and had such a perfect collaboration in the lab and the office.

Moreover, I would like to thank my lab colleagues Manos Poulakis, Dr. Claudia Mihesan and Pavle Glodić for their kindness and help in and out of the lab. Many thanks to the undergraduate students Aris Velegrakis, Maria Peloni and Giannis Daskalakis for helping me during experiments.

This Thesis would not have been performed without the collaboration of companies, which provided the samples and their knowledge. These are: Μποτζάκης Α.Ε. (specially to Λευτέρης Αρχάβλης), Μιχαήλ Ε. Παπαδάκης Ο.Ε., ΕΡΓΑΣΤΗΡΙΟ ΤΕΧΝΟΛΟΓΙΑΣ ΤΡΟΦΙΜΩΝ (Δρ. Αντωνίου Χρυσούλα – Χημικός και Ελένη Μπαρμποπούλου) for the oil samples and olive oil characteristics, Prof. Dimitris Lydakis (TEI of Crete) for discussion and tsikoudia samples supply and κ. Γερμανάκη Ελευθερία from ΕΑΣΡ (Εργαστήριο του Αγροτικού Συνεταιρισμού Ρεθύμνης) for samples and tasting results. Special thanks to Dr. George Kennanakis, for providing me the portable spectrophotometer (K-MAC spectrometer) and his trust of working on it every time I wanted to use it.

Last but not least, I would like to thank Dr. Petros Samartzis (ITSSUED/ERC-03 grant funded from Greece and EU under NSRF2007-2013) and Prof. Spiros Anastasiadis (SIMENES-IESL-NANOTECHNOLY, ΔΕΘ00200-30) for the financial support during these years.

Special Thanks to my family and friends that supported me through the years and at special situations.

Abstract:

In recent years, the need for identification, quality and authentication control of agro-products is intense, because of their high nutritional and commercial values. For this purpose, precise and well-established analytical techniques are employed, but they require time, specialized scientists, chemical reagents and high-cost equipment, in order to identify the agro-products.

For this purpose, there is a quest for alternative and innovative methods, so that the agro-products can be analyzed in a fast way and with low-cost equipment. The application of Optical Spectroscopic techniques seems to be an innovative approach, to record the “fingerprint” of the agro-products in a rapid and non-invasive way.

In this Thesis, the Absorption and Fluorescence Spectroscopic techniques are applied, to record and study samples of extra virgin olive oil, seed oil, and their mixtures, and samples of tsikoudia, which is a local Cretan alcoholic drink.

The objective of this work is to study the applicability of Optical Spectroscopy (Absorbance and Fluorescence), for discriminating the extra virgin olive oils based on their geographical origin, olive variety and harvest’s year, and also the detection of adulteration of the extra virgin olive oil with seed oils. Furthermore, a preliminary study of monovarietal tsikoudia is presented in this work, to discriminate the samples by their grape’s variety.

In conclusion, the results from this Thesis demonstrate the possibility for identifying extra virgin olive oil and monovarietal tsikoudia, controlling the quality and detecting the adulteration of extra virgin olive oil in low detection limits, by applying the Optical Spectroscopic techniques.

Περίληψη:

Τα τελευταία χρόνια υπάρχει έντονη η ανάγκη για ταυτοποίηση, έλεγχο ποιότητας και γνησιότητας των γεωργικών προϊόντων διατροφής, λόγω της υψηλής διατροφικής και εμπορικής τους αξίας. Για τον σκοπό αυτό χρησιμοποιούνται ακριβείς και καθιερωμένες αναλυτικές τεχνικές που όμως απαιτούν χρόνο, εξειδικευμένο προσωπικό, χημικά αντιδραστήρια και ακριβό εξοπλισμό για την ταυτοποίηση των διατροφικών προϊόντων.

Στα πλαίσια αυτά γίνεται προσφάτως αναζήτηση εναλλακτικών και καινοτόμων μεθόδων για γρήγορη και χαμηλού κόστους ανάλυση προϊόντων διατροφής.

Η εφαρμογή Οπτικών Φασματοσκοπικών τεχνικών ολοένα και πιο πολύ δείχνει να είναι μια τέτοια καινοτόμα προσέγγιση για την γρήγορη και μη επεμβατική καταγραφή του «δαχτυλικού αποτυπώματος» των προϊόντων αυτών.

Στην παρούσα εργασία έγινε εφαρμογή της φασματοσκοπίας απορρόφησης φωτός και φασματοσκοπίας εκπεμπόμενου φθορισμού για τη καταγραφή και μελέτη δειγμάτων εξαιρετικά παρθένου ελαιολάδου, σπορέλαιων και μιγμάτων αυτών, καθώς και τσικουδιάς, που είναι τοπικό Κρητικό ποτό.

Σκοπός της μελέτης ήταν να εξεταστεί η δυνατότητα εφαρμογής της Οπτικής Φασματοσκοπίας (Απορρόφησης και Φθορισμού) στο διαχωρισμό των ελαιολάδων βάσει γεωγραφικής προελεύσεως, ποικιλίας ελιάς κι έτους συγκομιδής, καθώς και ανίχνευση της νοθείας του εξαιρετικά παρθένου ελαιολάδου με σπορέλαια. Επίσης, θα παρουσιαστεί προκαταρκτική μελέτη για τον διαχωρισμό μονοποικιλιακών δειγμάτων τσικουδιάς.

Συμπερασματικά, τα αποτελέσματα αυτής της διατριβής δείχνουν την δυνατότητα για τη ταυτοποίηση του εξαιρετικά παρθένου ελαιολάδου και μονοποικιλιακής τσικουδιάς, τον ποιοτικό έλεγχο και την ανίχνευση της νοθείας στο παρθένο ελαιόλαδο σε χαμηλά όρια ανίχνευσης με την εφαρμογή των προαναφερθεισών οπτικών φασματοσκοπικών τεχνικών.

Chapter 1:

Motivation of the Thesis:

1.1 Agro-products

Agro-products are known to be valuable and suitable for the human nutrition. As Cretan, I have focused on two products: *Virgin Olive Oil* and *Tsikoudia* (grape distillation, also known as *Raki*). They are natural products that are produced on Crete and constitute main parts of the Cretan diet.

The virgin olive oil is considered to be the most valuable oil for the human nutrition. The Cretan olive oil is known to be one of the best olive oils that are produced worldwide *(Bendini, et al., 2007) (Guimet, Ferré, & Boqué, 2005)*. Its quality is related with the ideal climatic conditions of Crete, the production process that is applied and the olive tree varieties that are grown.

Tsikoudia is a crystal clear drink. It is the typical spirit that is consumed on Crete and it is offered to visitors in any Cretan house upon arrival. This comes from the distillation of the fermented grape residues after the wine production. Its quality is mainly related to the grape varieties that are used.

1.2 Optical Spectroscopy and Benefits

Several research groups have reported specialized analytical techniques, such as HPLC (High Performance Liquid Chromatography) or NMR (Nuclear Magnetic Resonance) techniques, in order to control the quality and the identification of the products. These techniques are of high cost, demand specialized researchers and the samples must be pre-treated, so the need for alternative and fast techniques is required. In this direction, we performed experiments by using Optical Spectroscopy, by means of Optical Absorption and Fluorescence techniques. These spectroscopic techniques are fast and non-invasive, while sample pretreatment is low or none.

Moreover, we implement Optical Spectroscopy to identify and control the quality of products in a rapid way, by using Spectrophotometers and computers. Absorption and Fluorescence techniques are easy to deal with, fast and non-destructive for our samples. As a result, identification and quality control of the products, combined with Statistical Analysis, can report a database of these products and can be used for the information of consumers and companies.

1.3 Adulteration of olive oil

Taking into account that Cretan Virgin Olive oil is one of the most nutritious juice with excellent quality in contrast to seed oils, it is more expensive than other

vegetable oils. This can lead to adulteration of virgin olive oil with lower quality oils, a common phenomenon in the production line. Consequently, it is important to authenticate and control the adulteration of virgin olive oil for consumers' health and safety by using fast and reliable techniques. Optical spectroscopy is promising in this field and will be presented in this Thesis.

1.4 State-of-the-Art

Through these years, various analytical techniques have been implemented to provide qualitative and quantitative information for the quality control of agro-products. Classification and authentication of oils were successfully achieved by chromatographic analytical techniques that discriminated edible oils, control of quality and detection of adulteration of oils successfully. These analytical methods have disadvantages in comparison with Optical Spectroscopy; they are sophisticated, time-consuming, need experts to work with and the samples must be pretreated.

The detection of adulteration can be achieved in low limits by using sophisticated, expertized and time consuming analytical techniques, such as HPLC (High Performance Liquid Chromatography) and GC-MS (Gas Chromatography-Mass Spectroscopy) and NMR (Nuclear Magnetic Resonance). Vibrational spectroscopic techniques, such as infrared and Raman, have been employed to determine olive oil adulteration. By using infrared spectroscopy, Obeidat *et.al*. classified virgin olive oil (Obeidat, S.M., Khanfar, M.S., & Obeidat, W.M., 2009), while Yang *et.al*. determined the adulteration of extra virgin olive oil with pomace oil *(Yang, 2001)*. Several scientific groups reported the employment of Raman spectroscopy in olive oil authentication and adulteration, combined with Chemometrics (L-Diez, 2003) (Zhang, Quantitative detection of adulterated olive oil by Raman spectroscopy and chemometrics, 2011) (Zou, 2009) (Zhang, 2011).

Recently, Philippidis et. al. conducted a scientific work, wherein Raman and Visible spectroscopy were employed with Multivariate Statistical Analysis, in order to characterize the spectral properties of extra virgin olive oil (evoo), sunflower oil, and binary mixtures and investigate the adulteration of Greek (Cretan) evoo with sunflower oil *(Phillipidis, Poulakis, Papadaki, & Velegrakis, 2016)*. Our experimental results in the laboratory were published, where a mobile Raman spectrometer with a laser source at the IR region (786nm) and a spectrophotometer at the visible region (400-800nm) were used for the detection of adulteration of extra virgin olive oil.

Combination of techniques was also performed to examine the authentication and adulteration of olive oil. Mass spectroscopy combined with n-IR and UV-Vis spectroscopy and n-IR, mid-IR and UV-Vis spectroscopy results were presented by Casale *et.al*. (Casale, 2010). More recently, the capability of spectroscopic techniques, especially absorption and fluorescence measurements, in combination with

statistical analysis was examined by Wójcicki, in order to detect the adulteration of extra virgin olive oil with deodorized and refined olive oil (Wójcicki, 2015).

Chapter 2:

Agro-products and Optical Spectroscopy

2.1 Olive oil

Olive oil is acquired solely from the olive, the fruit of Olea europaea, which is the traditional crop of Mediterranean basin, since the early Minoan times (about 3500BC). It is produced from the olive fruit by using only physical treatments that not affect /deteriorate the oil quality.

Talking about the production of olive oil in the European Union, more specifically in the Mediterranean basin, Greece produced about the 11% of world production of olive oil in 2013 (about 0.31 millions of tons) *(Olive oil virgin, crops processed, production data for 2013, 2013).* The virgin olive oil is considered to be the most valuable oil for the human nutrition, due to the low levels of unsaturated fatty acids and the high presence of vitamin E, an anti-oxidant that is important for human's health. The Mediterranean diet includes the virgin olive oil, as it appears to have several health benefits, such as decrease of risk for heart diseases, amendment of immune response and anticipation of some cancer types *(Bendini, et al., 2007), (Guimet, Ferré, & Boqué, 2005)* . The olive oil contains a variety of compounds, that may be responsible for its pleasant flavor, nutritious values and therapeutic characteristics *(Stark, 2002)*.

The olive oil can be classified into several categories, based on their purity and quality parameters, such as free acidity and other organoleptic characteristics. According to the Regulation (ECC) 2568/91 olive oil is distinguished in different categories as follow *(IOOC, 1991)*:

- **Extra virgin olive oil (EVOO)** is the virgin olive oil having a free acidity percentage of less than 0.8 g/kg, with the positive organoleptic attributes and without any defects. This is the highest quality rating for an olive oil (See Fig. 2.1.1). Consequently, its commercial price is higher than the other oils.
- **Virgin olive oil (VOO)** with a free acidity lower than 2 g/kg and organoleptic defects rating less than 2.5. It is of lower quality than extra virgin olive oil.
- **Lampante virgin olive oil** with a free acidity greater than 2 g/kg or defects rated more than 2.5. These oils come from bad olive fruit or from improper processing. It is not fit for human nutrition.
- **Refined olive oil** has a free acidity of less than 0.3. The refining process consists of different chemical and physical treatments (i.g. treatment with sodium hydroxide, in order to neutralize the free acidity, deodorization etc.).
- **Olive oil** that is a mixture of refined and virgin oil.
- **Olive Pomace oil (crude)** is obtained by treating olive pomace with solvents. It does not include any mixture with seed oils and is not fit for human consumption.
- **Olive Pomace oil (refined).**

Figure 2.1.1: Extra virgin olive oil

2.1.1 History of olive oil

Olives were transformed into olive oil by 6000BC *(Schuster, December 2014).* Since 1500BC, eastern coastal areas of the Mediterranean were most heavily cultivated. It is also suggested that olives were being growing in Crete as long ago as 2500BC. Olive oil trees were certainly cultivated by the Late Minoan period (1500BC) in Crete, and perhaps as early as the Early Minoan *(Riley, 2002)*. In Crete, the cultivation of olive trees became more intense in the post-palatial period and played an important role in the island's economy.

Besides food, olive oil has been used for religious rituals, medicines, as a fuel in oil lamps, soap-making, and skin care application. The Minoans used olive oil in religious ceremonies. The oil became a principal product of the Minoan civilization, where it is thought to have represented wealth.

Olive oil was common in ancient Greek and Roman cuisine. According to Herodotus, Apollodorus, Plutarch, Pausanias, Ovid and other sources, the city of Athens obtained its name because Athenians considered olive oil essential, preferring the offering of the goddess Athena (an olive tree) over the offering of Poseidon (a spring of salt water gushing out of a cliff). The Spartans and other Greeks used oil to rub themselves while exercising in the gymnasia. From its beginnings early in the 7th century BC, the cosmetic use of olive oil quickly spread to all of the Hellenic city states *(Kennell, 2001)*. Olive trees were planted throughout the entire Mediterranean basin during evolution of the Roman republic and empire. According to the historian Pliny the Elder, Italy had "excellent olive oil at reasonable prices" by the 1st century AD, "the best in the Mediterranean", he claimed.

2.1.2 Production of olive oil

Olive oil is produced by grinding olives and extracting the oil by mechanical means. Green olives usually produce more bitter oil. In order to have a good extra virgin olive oil, the olives must be perfectly ripened. In general (see Fig. 2.1.2), the process is described below:

1. The olives are ground into paste by using steel drums (In the past, large millstones were used instead of drums).

2. After grinding, the paste is stirred slowly for another 20 to 30 minutes in a particular container (malaxation basin), where the microscopic oil drops unite into bigger drops, which facilitates the mechanical extraction.
3. After grinding, in the traditional olive mills, the olive paste was spread on fiber disks, which were stack on top of each other in a column and then pressed.
4. Centrifugation is the process that is used in modern facilities instead of pressing. In the centrifuges (Decanters) the malaxed olive paste is separated into oil, vegetal liquid and olive paste residues.
5. Sometimes the produced oil will be filtered to eliminate remaining solid particles that may reduce the shelf life of the product.
6. The remaining paste (pomace) still contains a small quantity (about 5–10%) of oil. This part of oil is normally extracted using solvents in special industries and it is known as "pomace oil".

Figure 2.1.2: Olive oil factory

2.1.3 Chemical Composition of extra virgin olive oil

Extra virgin olive oil is a fat obtained by the olive. It is mainly composed of mixed triglyceride esters ($C_{55}H_{98}O_6$) of oleic and palmitic acid, traces of squalene ($C_{30}H_{50}$) – up to 0.7% - a variety of free fatty acids and phosphatides *(Kiritsakis)*.

- Triglycerides constitute the **saponified** compounds in olive oil (~98%).

Table 2.1 shows the most characteristic fatty acids ($CH_3(CH_2)nCOOH$) (where n is an even number between 12 and 22) contained in evoo.

Fatty acids	Chemical formula	Percentages
Oleic acid	$CH_3(CH_2)_7CH=CH(CH_2)_7COOH$	55-83%
Linoleic acid	(C18:2) $C_{18}H_{32}O_2$	3.5-21%
Palmitic acid	$CH_3(CH_2)_{14}COOH$	7.5-20%
Stearic acid	$CH_3(CH_2)_{16}COOH$	0.5-5%
a-Linolenic acid	(C18:3) $C_{18}H_{30}O_2$	0-1.5%

Table 2.1: Fatty acids, their chemical formula and percentages of them in evoo

Oleic, linoleic and a-linolenic acids (two cis double bonds; with the first double bond located at the sixth carbon from the methyl end) are unsaturated fatty acids, and palmitic and stearic acids are saturated fatty acids. The chemical structures of oleic and linoleic acids are shown at Fig. 2.1.3 and 2.1.4, respectively.

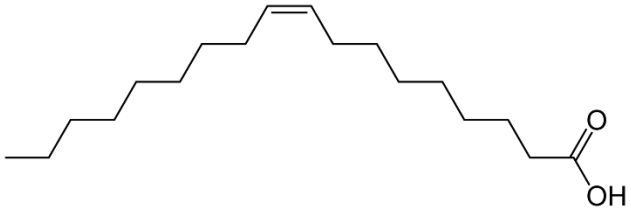

Figure 2.1.3: Oleic acid

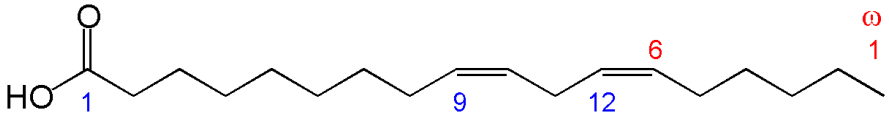

Figure 2.1.4: Linoleic acid

- The **unsaponifiable** compounds in olive oil (~1-2%) are hydrocarbons,

tocopherols, phenols, phospholipids, volatile compounds, sterols (0.2% phytosterol and tocosterols), carotenoids (take the form of a polyene hydrocarbon chain which is sometimes terminated by rings. Polyenes are poly-unsaturated organic compounds that contain at least three alternating double and single carbon–carbon bonds) and pigments. Phenolics, such as esters of tyrosol, hydroxytyrosol, oleocanthal and oleuropein are included. These compounds give the aroma, bitter and pungent taste to extra virgin olive oil.

- Phenols (a class of chemical compounds consisting of a hydroxyl group (—OH) bonded directly to an aromatic hydrocarbon group), as shown in Fig. 2.1.5, are compounds that contain at least one benzene ring and one or more hydroxyls at the ring. They can be simple phenols, phenolic acids, flavonoids or phenolic alcohols. Tyrosol and hydroxytyrosol (2-(3,4-Di-hydroxyphenyl)-ethanol or DHPE) are the most remarkable antioxidants of olive oil.. A great variety of phenolic compounds, including elenolic acid, is a marker for maturation of olives.

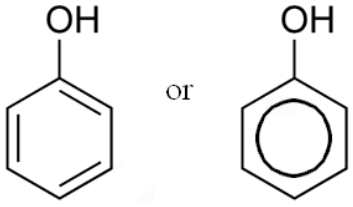

Figure 2.1.5: Simplest phenol

- Tocopherols are heterocyclic compounds of high molecular weight and their chemical structure is shown at Fig. 2.1.6. In olive oil, the percentage of α-

tocopherol is 88.5%, β, γ-tocopherol are 9.9% and δ-tocopherol is 1.6%. They are physical antioxidants of olive oil and due to them, there is stability of olive oil in oxidation.

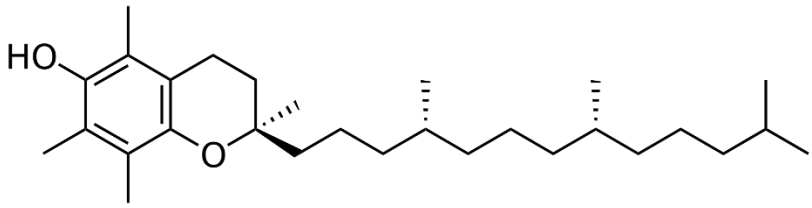

Figure 2.1.6: Tocopherol-a

- Pigments, such as chlorophyll, are responsible for the color of olive oil. Chlorophyll is the main reason for the oxidation of oil, if it comes close to light. This kind of oxidation of olive oil is called photo-oxidation. One type of the chlorophylls' group, chlorophyll- a, is shown in Fig. 2.1.7:

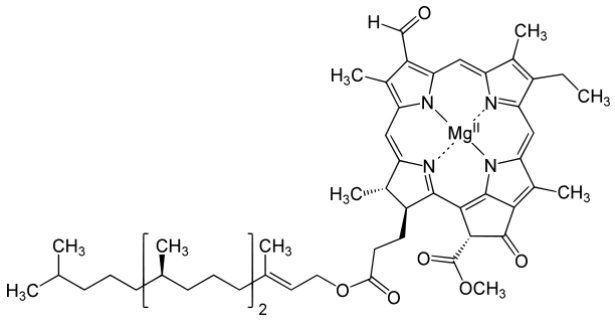

Figure 2.1.7: Chlorophyll-a

- Olive oil is poor in phospholipids and most of their components come from the olive core. Usually, lecithin and cephalin are found.
- The main characteristic of hydrocarbons in olive oil is squalene, which also contributes to the antioxidant effect of olive oil.

2.1.4 Adulteration of extra virgin olive oil

Extra virgin olive oil (Evoo) can be adulterated with low-grade oils or seed oils, in terms of economical profit, so the need for detecting the adulteration of the evoo is important. Seed oils, such as sunflower and corn oil, are vegetable oils, that contain mainly a mixture of monounsaturated/polyunsaturated fatty acids and this is the reason that they can be oxidized very easily. Antioxidants are absent in seed oils.

There has been a lot of journals and scientific articles which are focused on this direction, by using different methods, such as analytical techniques, spectroscopic techniques, combined with statistical analysis.[*(Sikorska, et al., 2004)*, *(Sikorska, Góreckib, Khmelin, Sikorskid, & Kozioła, 2005)*, *(Guimet, Boqué, & Ferré, 2004)*, *(Guimet,*

Ferré, & Boqué, 2005), *(Downey, McIntyre, & Davies, 2002)*, *(ÖZDEMIR & ÖZTÜRK, 2007)*, *(Boskou, Blekas, & Tsimidou, 1996)*]

Spectroscopic techniques have been used to analyze the olive oils. Mignani *et.al.* presented the adulteration of extra virgin olive oils with lower-grade olive oil by using diffuse-light absorption spectroscopy in the visible and near-infrared region of electromagnetic spectrum *(Mignani, 2011)*. Torrecilla *et.al.* quantified the adulteration of oil with lower quality oil by means of ultraviolet-visible spectroscopy *(Torrecilla, 2010)*. Combining near-IR spectroscopy with multivariate calibration models, identification of adulteration of olive oil was also achieved by Özdemir and Özturk (2007) *(ÖZDEMIR & ÖZTÜRK, 2007)*. Fluorescence Spectroscopy was also employed to this direction. Guimet *et.al.* reported the clustering of commercial Spanish olive oil using excitation-emission fluorescence spectroscopy *(Guimet, Boqué, & Ferré, 2004)*. Another scientific group carried out the adulteration of virgin olive oil and discriminated two different grades of olive oils *(Poulli K. I., 2005) (Poulli K. I., 2007)*.

Authentication and control of adulteration of extra virgin olive oil are important and complicated issues for the olive oil industry, so a lot of processes have been demonstrated for this purpose. Seed oils, especially sunflower and corn oils, as the low-grade oils are the most appropriate candidates to become the adulterants of evoo. This is because they are chemically similar to evoo, but of lower cost *(Poulli K. M., 2006)*. By mixing virgin olive oil with low quality oils and low price oils, consumers' health and safety can be put in danger *(Guimet, Ferré, & Boqué, 2005)*.

Optical Absorption and Fluorescence techniques provide qualitative information of detecting the adulteration of extra virgin olive oil. When combined with Chemometrics, by means of Partial Least Squares (PLS) Regression, quantitative information such as the detection limits can be extracted in a simple and user-friendly way.

2.2 Tsikoudia

Tsikoudia is produced from grapes. Usually, a combination of grape varieties is used for the production of tsikoudia. Since tsikoudia is legally produced only from the wine grape varieties grown on Crete and some Aegean Islands, a simple method of analysis that can relate the final product with the grape varieties is required. It has been the "trademark" of Cretan hospitality.

Lately, there is an increasing interest for the production of mono-varietal tsikoudia. The special aromatic characteristics and health related substances (e.g. methanol) of different mono – varietal tsikoudia products are investigated in aim to produce tsikoudia of excellent quality and safe for the consumers.

2.2.1 How Tsikoudia is made

Tsikoudia is made by the distillation of the fermented grape residues (straffyla) in a special apparatus known as “kazani”. Kazani is a copper made apparatus consisted of four parts: the pot, the lid, the connecting tube and the cooler. The pot is placed on a heat source. The distillation starts when the temperature in the pot arise to approximately 80 ^{o}C The produced vapors are driven through the lid and the connecting tube to the cooler where they are condensed.

The distillate is divided normally in three parts. The first part (1-2 liters) contains a high percentage of methanol, ethyl esters and other undesired substances. This part must not be used for human consumption. The second part is the best regarding quality and safety. The distillation process continues till the average ethanol content of the distillate is between 35-40 vol. This is the part of distillate that is used for consumption. The third part of the distillate contains low ethanol, acetic and other organic acids. Normally, the first and the third part of the distillate are used in the next distillation.

Figure 2.2.1: “Kazani” and tube

2.2.2 Analytical techniques for the Grape distillates

Various scientific reports have been published employing near-infrared spectroscopic methods to study food’s authentication, identification and geographical origin *(Xie, Ye, Liu, & Ying, 2009) (Cozzolino, et al., 2008)*. Near-infrared region spectrum combined with chemometrics could determine chemical and physical characteristics of the distillates under study *(Rogovaya, Sinitsyn, & Khodasevich, 2014)*. Spectrophotometric analysis in the UV region showed that wine distillates are characterized by a maximum absorption peak at 280nm and a minimum at 250nm, defined by the aromatic aldehydes. Rogovaya *et.al.* reported the transmission spectra of a 7-year-old distillate sample at the spectral range of 190-2600nm, divided into three categories, UV, Visible to n-IR and IR regions *(Rogovaya, Sinitsyn, & Khodasevich, 2014)*. Tothova *et.al.* reported the differences between brandies and wine distillates, by employing total luminescence spectroscopy combined with PCA (Principal Component Analysis) and HCA (Hierarchical Component Analysis) *(Tothova, Sadecka, & Majek, 2009)*. They diluted the brandies and wine distillates and measured at the right-angle geometry, in order to

observe the fluorescence intensities of samples, because of their high absorption at the UV region.

NMR spectroscopy was also employed to investigate the differences between Cypriot alcoholic beverage *Zivania* and other spirits, similar to zivania from other countries, combined with Statistical Analysis *(Petrakis, et al., 2005)*, *(Kokkinofta & Theocharis, 2005)*. ^{1}H NMR approach was applied to Greek grape spirits tsipouro and tsikoudia to monitor the metabolic signature, combined with PCA and PLS regression techniques *(Fotakis, et al., 2013)*. Atomic absorption spectrometry and total reflection X-ray fluorescence techniques were also applied to Cretan wines and wine products *(Galani-Nikolakaki, Kallithrakas-Kontos, & Katsanos, 2002)*. Rodriguez *et.al.* studied orujo distillate alcoholic samples from Galicia by applying electrothermal atomic absorption spectrometry and inductively coupled plasma optical emission spectrometry and compared the data with different chemometric techniques *(Rodriguez, et al., 2010)*.

Chapter 3:

Physics Background

3.1 Absorption Theory

Absorption of electromagnetic radiation is the process whereby the intensity of the light beam is attenuated in passing through a material medium by conversion of the energy of the radiation to an equivalent amount of energy which appears within the medium. The radiant energy is converted into heat or some other form of molecular energy. A perfectly transparent medium permits the passage of a beam of radiation without any change in intensity other than that caused by the spread or convergence of the beam, and the total radiant energy emergent from such a medium equals that which entered it, whereas the emergent energy from an absorbing medium is less than that which enters, and, in the case of highly opaque media, is reduced practically to zero *(West, 2014)*.

There is not any known medium that is opaque to all wavelengths of the electromagnetic spectrum, which extends from radio waves, whose wavelengths are measured in km, through the infrared, visible and ultraviolet spectral regions, to x-rays and gamma rays, of wavelengths down to 10^{-13} m. Similarly, no material medium is transparent to the whole electromagnetic spectrum. A medium which absorbs a relatively wide range of wavelengths is said to exhibit general absorption, while a medium which absorbs only restricted wavelength regions of no great range exhibits selective absorption for those particular spectral regions. Ordinary window glass is transparent to visible light, but shows general absorption for ultraviolet radiation of wavelengths below about 310nm, while colored glasses show selective absorption for specific regions of the visible spectrum. The color of objects which are not self-luminous and which are seen by light reflected or transmitted by the object is usually the result of selective absorption of portions of the visible spectrum *(West, 2014)*.

3.1.1 Laws of absorption

The capacity of a medium to absorb radiation depends on a number of factors, mainly the electronic and nuclear constitution of the atoms and molecules of the medium, the wavelength of the radiation, the thickness of the absorbing layer and the variables which determine the state of the medium, of which the most important are the temperature and the concentration of the absorbing agent. In special cases, absorption may be influenced by electric or magnetic fields *(West, 2014)*.

Usually, the absorption of waves does not depend on their intensity (linear absorption), although in certain conditions, the medium changes its transparency dependently on the intensity of waves going through, and saturating absorption (or nonlinear absorption) occurs. The **absorbance** of an object quantifies how much of the incident light is absorbed by it (instead of being reflected or refracted). This may

be related to other properties of the object through the **Beer–Lambert law**. Precise measurements of the absorbance at many wavelengths allow the identification of a substance via absorption spectroscopy, where a sample is illuminated from one side, and the intensity of the light that exits from the sample in every direction is measured. A few examples of absorption are ultraviolet–visible spectroscopy, infrared spectroscopy, and X-ray absorption spectroscopy.

3.1.2 Beer-Lambert's Law

This law refers to the effect of the concentration of the absorption medium - that is the mass of absorbing material per unit of volume – on the absorption. This relation is of prime importance in describing the absorption of solutions of an absorbing solute, since the concentration of the solute may be varied over wide limits. According to Beer's law, each individual molecule of the absorbing material absorbs the same fraction of the radiation incident upon it, no matter whether the molecules are closely packed in a concentrated solution or highly dispersed in a dilute solution. The effects of thickness *d* and concentration *c* on absorption of monochromatic radiation can therefore be combined in a single mathematical expression (Eq. 3.1), given in:

$$\mathrm{I} = \mathrm{I}_0 \cdot \mathrm{e}^{-\mathrm{k}'\mathrm{cd}} \qquad \text{Equation 3.1}$$

in which k' is a constant for a given absorbing substance (at constant wavelength and temperature), independent of the actual concentration of solute in the solution. In logarithms, the relation (Eq. 3.2) becomes as:

$$\log_{10}\left({}^{\mathrm{I}_0}\!/_{\mathrm{I}}\right) = \left({}^{\mathrm{k}'}\!/_{2.303}\right) \cdot \mathrm{c} \cdot \mathrm{d} = \varepsilon \cdot \mathrm{c} \cdot \mathrm{d} \qquad \text{Equation 3.2}$$

The values of the constants $k'$and ε in Eq. (3.1, 3.2) depend on the units of concentration. The quantity $\mathbf{\log_{10}\left({}^{I_0}\!/_{I}\right)}$ is often called the **optical density**, or the **absorbance (A)** of the medium. The ratio $\left({}^{\mathbf{I}}\!/_{\mathbf{I_0}}\right)$ is called **Transmittance (T)**. Absorbance and Transmittance are related as:

$$\mathbf{\log T = -A} \qquad \text{Equation 3.3}$$

If the concentration of the solute is expressed in moles per liter, the constant ε is called the molar extinction coefficient. It is also employed by the symbol α_m , which is called the molar absorbance index, instead of ε. If Beer's law is adhered to, the molar extinction coefficient does not depend on the concentration of the absorbing solute, but usually changes with the radiation's wavelength, the temperature of the solution and with the solvent.

The dimensions of the molar extinction coefficient are reciprocal concentration multiplied by reciprocal length, the usual units being $[litre\ /\ ((mole)\cdot(cm)\ )]$. If Beer's law is true for a particular solution, the plot of $\log\left({}^{\mathrm{I}_0}\!/_{\mathrm{I}}\right)$ against the concentrations for solutions of different concentrations, measured in cells of

constant thickness, will yield a straight line, the slope of which is equal to the molar extinction coefficient *(West, 2014)*.

3.1.3 Absorption measurements

The measurement of the absorption of homogeneous media is usually accomplished by absolute or comparative measurements of the intensities of the incident and transmitted beams, with corrections for any loss of radiant energy by processes other than absorption. The most important of these losses is by reflection at the various surfaces of vessels which may contain the medium, if the medium is liquid or gaseous. Such losses are usually automatically compensated for by the method of measurement employed.

For the most organic molecules, the electrons are classified in 3 categories: σ-electrons, π-electrons and n-electrons or non- bonding electrons, which don't take place in bonds and are held weakly, so they can be transited. The σ-electrons are more stable, adherent to the nuclei and need higher energy in order to transit to other energy levels, while for the π- and n-electrons that need lower energy. Usually, the n-electrons need lower energy than the π-electrons.

In organic molecules, UV and Visible radiation absorption is restricted to certain functional groups (chromophores) that contain valence electrons of low excitation energy. The spectrum of molecules containing these chromophores is complex, because of the superposition of rotational and vibrational transitions on the electronic transitions that gives a combination of overlapping lines. This appears as a continuous absorption band. Possible electronic transitions of π, σ and n electrons are shown below (Fig. 3.1.1):

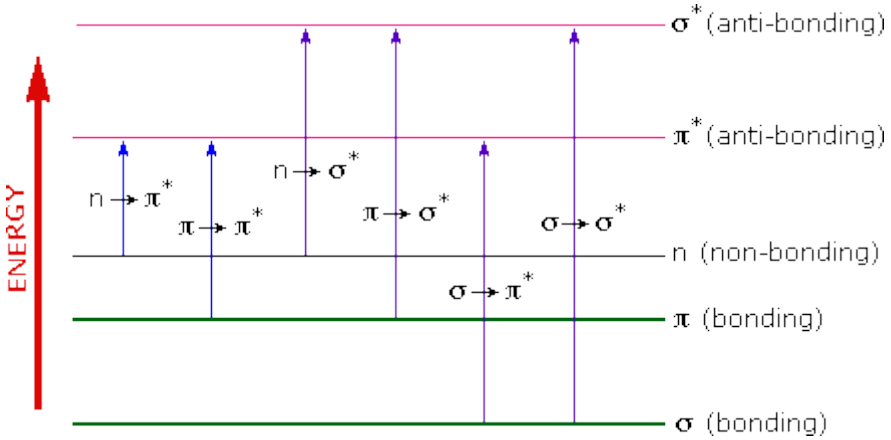

Figure 3.1.1: Electronic transitions of π, σ and n electrons *(Reusch, n.d.)*

- $\sigma \rightarrow \sigma^*$ Transitions

An electron in a bonding σ orbital is excited to the corresponding antibonding orbital. The energy required is large. For example, methane (which has only C-H bonds, and can only undergo $\sigma \rightarrow \sigma^*$ transitions) shows an absorbance maximum at 125 nm. Absorption maxima due to $\sigma \rightarrow \sigma^*$ transitions are not seen in typical UV-Vis spectra (200- 700 nm).

- $n \rightarrow \sigma^*$ Transitions

Saturated compounds containing atoms with lone pairs (non-bonding electrons) are capable of $n \rightarrow \sigma^*$ transitions. These transitions usually need less energy than $\sigma \rightarrow \sigma^*$ transitions. They can be initiated by light whose wavelength is in the range 150 - 250 nm. The number of organic functional groups with $n \rightarrow \sigma^*$ peaks in the UV region is small.

- $n \rightarrow \pi^*$ and $\pi \rightarrow \pi^*$ Transitions

Most absorption spectroscopy of organic compounds is based on transitions of n or π electrons to the π^* excited state. This is because the absorption peaks for these transitions fall in an experimentally convenient region of the spectrum (200 - 700 nm). These transitions need an unsaturated group in the molecule to provide the π electrons. Molar absorbtivities from $n \rightarrow \pi^*$ transitions are relatively low and range from 10 to $100 \mathrm{L} \cdot \mathrm{mol}^{-1} \mathrm{cm}^{-1}$. Transitions $\pi \rightarrow \pi^*$ normally give molar absorbtivities between 1000 to $10000 \mathrm{L} \cdot \mathrm{mol}^{-1} \mathrm{cm}^{-1}$.

The solvent in which the absorbing species is dissolved also has an effect on the spectrum of the species. Peaks resulting from $n \rightarrow \pi^*$ transitions are shifted to shorter wavelengths *(blue shift)* with increasing solvent polarity. This arises from increased solvation of the lone pair, which lowers the energy of the n orbital. For $\pi \rightarrow \pi^*$ transitions, peaks are often shifted to longer wavelengths *(red shift)* and this is caused by attractive polarization forces between the solvent and the absorber, which lower the energy levels of both the excited and unexcited states. This effect is greater for the excited state, so the energy difference between the excited and unexcited states is slightly reduced - resulting in a small red shift. This effect also influences $n \rightarrow \pi^*$ transitions but is overshadowed by the blue shift resulting from solvation of lone pairs.

Simple chromophore groups with double and triple bonds follow the $\pi \rightarrow \pi^*$ transitions, which absorb at low wavelengths at the UV region. Other groups, such as –OH, have non-bonding electrons and they can make transitions from 190nm and longer wavelengths *(Βαλαβανίδης, 2008)*.

There are some important changes at the UV-Vis spectra that are caused by the presence of two or more double bonds in organic molecules. If the bonds are conjugated, the transitions $\pi \rightarrow \pi^*$ and $n \rightarrow \pi^*$ are amplified and they absorb at longer wavelengths.

Absorption of radiation by matter always involves the loss of energy by the radiation and a corresponding gain in energy by the atoms or molecules of the medium. The energy absorbed from radiation appears as increased internal energy, or in increased vibrational and rotational energy of the atoms and molecules of the absorbing medium. As a general rule, translational energy is not directly increased by radiation's absorption, although it may be indirectly increased by degradation of

electronic energy or by conversion of rotational or vibrational energy to that of translation by intermolecular collisions.

Absorption measurements are obtained by exciting the samples into a range of wavelengths from an excitation source. Light passes through the sample, is analyzed by a monochromator and the transmitted light is detected, as shown in Figure 3.1.2:

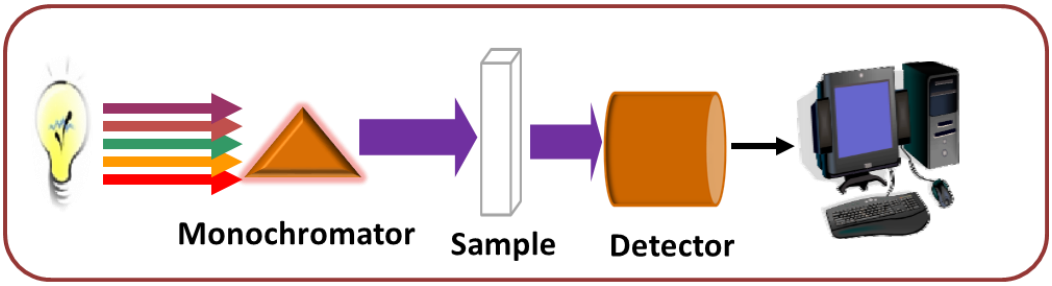

Fig. 3.1.2: Absorption Setup

As mentioned before (Equation 3.3), absorbance and transmittance are the "two sides of the same coin". Consequently, when transmittance is measured, absorbance is just a transformation of the transmittance spectrum, taking into account the relation between them.

3.1.4 Quantum theory

In order to construct an adequate theoretical description of the energy relations between matter and radiation, it has been necessary to amplify the wave theory of radiation by the quantum theory, according to which the energy in radiation occurs in natural units, called quanta *(Τραχανάς, 2005)*. The value of the energy in these units, expressed in ergs or calories, for example, is the same for all radiation of the same wavelength, but differs for radiation of different wavelengths. The energy *E* in a quantum of radiation of frequency *ν* is directly proportional to the frequency, or inversely proportional to the wavelength *λ*, according to the Eq. 1:

$$E = h\nu \qquad \textit{Equation 1}$$

$$\text{Frequency } \nu = {}^{c}/_{\lambda} \qquad \textit{Equation 2}$$

where *c* is the velocity of the radiation in a given medium, *λ* the wavelength in the same medium and *h* is a universal constant known as Planck's constant. The value of *h* is $6.63 \cdot 10^{-34}$ Joule · sec. If ν is expressed in sec^{-1}, E is given in Joules/quantum.

In order to excite the more loosely bound valence electrons, less energy is required, which can be accomplished by the absorption of quanta of visible radiation (wavelength 700nm (red light) to 400nm (blue light)) or of Ultraviolet radiation, of wavelength down to about 100nm. Absorption of UV radiation of shorter wavelengths, down to those on the border of the x-ray region, excites electrons bound to the nucleus with intermediate strength. The absorption of relatively low-energy quanta of wavelength from about 1 to 10 μm suffices to excite vibrating atoms in molecules to higher vibrational states, while changes in rotational energy, which are of still smaller magnitude, may be excited by absorption of radiation of still longer wavelength, from the short wavelength radio region of about 1cm to long-wavelength infrared radiation.

3.1.5 Liquids Absorption

Liquids usually absorb radiation in the same general spectral region as the corresponding vapors. Liquid water, for example, like water vapor, absorbs strongly the infrared radiation (vibrational transitions), is largely transparent to visible and near-UV radiation and begins to absorb strongly in the far-UV. A universal difference between liquids and gases is the disturbance in the energy states of the molecules in a liquid caused by the great number of intermolecular collisions. This has the effect of broadening the very fine lines observed in the absorption spectra of vapors, so that sharp-line structure disappears in the absorption bands of liquids.

3.2 Fluorescence Theory

3.2.1 What Fluorescence is

Fluorescence is the emission of light by a substance that has absorbed light or other electromagnetic radiation and occurs from electronically excited states. In most cases, the emitted light has a longer wavelength, and therefore lower energy, than the absorbed radiation. The most striking example of fluorescence occurs when the absorbed radiation is in the ultraviolet region of the spectrum, and thus invisible to human eye, while the emitted light is in the visible region, which gives the fluorescent substance a distinct color that can only be seen when exposed to UV light. However, unlike phosphorescence, where the substance would continue to glow and emit light for some time after the radiation source has been turned off, fluorescent materials would stop glowing immediately upon removal of the excitation source.

3.2.2 Physical Principles

Fluorescence occurs when an orbital electron of a molecule, relaxes to its ground state by emitting a photon from an excited singlet state, after the absorption of visible and UV radiation:

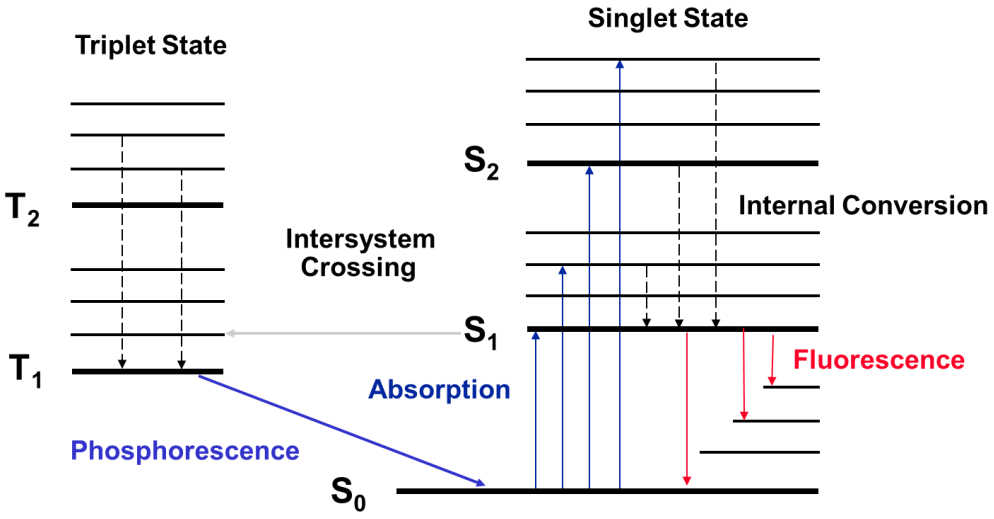

Fig. 3.2.1: Simple Jablonski diagram *(Perkin Elmer Fluorescence Spectroscopy)*

When a photon, of energy equal to the difference of the two energy states of the molecule, is absorbed by the electrons of the ground state, the electrons are excited to some higher vibrational levels of the first excited singlet state (see Fig. 3.2.1). At each of the electronic energy levels, the fluorophores can exist in a number of vibrational energy levels. S_0 is called the singlet ground state of the fluorescent molecule, with g_1 degeneracy, and S_1 is its first, electronically, excited singlet state. A molecule in S_1 can relax by various competing pathways. It can undergo *non-radiative* relaxation, also known as internal conversion and occurs in 10^{-12} s or less, in which the excitation energy can be dissipated as heat (vibrations) to the solvent. Fluorescence lifetimes are typically 10^{-8} s, so the internal conversion is generally complete before emission. The fluorescence emission results generally from the lowest- energy vibrational state of S_1.

Relaxation from S_1 can also occur through interaction with a second molecule through fluorescence quenching. Molecules in the first electronic singlet state S_1 can undergo a spin conversion to the first triplet state, T_1. This emission from state T_1 is called phosphorescence and is generally shifted to longer wavelengths – lower energy – than fluorescence. The conversion of S_1 to T_1 is called intersystem crossing. Transitions from T_1 to the singlet electronic ground state is forbidden because the parity does not change (in order to have a transition from excited state to the ground state, the parity should change), rate constants for triplet states are several orders of magnitude smaller than those of fluorescence.

Degeneracy: As mentioned, degeneracy, often represented by symbol g, is referred to different arrangements of a physical system which have the same energy and is calculated as $g = 2S + 1$, where S is the total electron spin angular momentum. When S=0 and g=1, the diradicals are singlet. This means that there are two electrons with spins ½ and -½ in one orbital. Triplet diradicals have 2 electrons with the same spin ½ in two orbitals, so S=1 and g=3 *(Τραχανάς, 2005)*.

Fluorescence typically occurs from aromatic molecules, due to low energy $\pi \rightarrow \pi^*$ transitions. Compounds consisting of carbonyl group or structures with many conjugated double bonds could also present fluorescence.

In most cases, the emitted light has a longer wavelength, and therefore lower energy, than the absorbed radiation. This phenomenon is known as the Stokes shift.

Fluorescence quantum efficiency denotes the ration of the total energy emitted by any molecule per quantum of energy absorbed:

$$\Phi_f = \frac{\text{number of quanta emitted}}{\text{number of quanta absorbed}} = \text{quantum yield or efficiency} \qquad \text{Equation 3.4}$$

The higher the value of Φ, the greater the observed fluorescence of the compound *(Guilbault, 1990)*. Fluorescence is connected to the absorption of radiation. As mentioned in section 3.1.2, absorption can be described by the Beer-Lampert's law. So, the fluorescence intensity can be described by:

$$I_f = I_0 \cdot \Phi_f \cdot (1 - 10^{-A}) \qquad \text{Equation 3.5}$$

where I_f is the fluorescence intensity, I_0 is the incident light intensity, Φ_f is the fluorescence quantum yield and A is the absorbance (see Eq. 3.2), which is transformed to (McLaren expansion):

$$I_f = 2.3 \cdot I_0 \cdot \Phi_f \cdot A + \text{constant}$$ Equation 3.6

This means that the fluorescence emission is proportional to lamp intensity I_0, quantum yield Φ_f, absorbance A and concentration c. If the absorbance A is less than 0.005, then the constant causes 0% error to the predicted fluorescence intensity. If the absorbance is equal to 0.01, the constant causes 1% error to the predicted intensity.

3.2.3 Fluorescence Spectroscopy

Fluorescence Spectroscopy is a type of electromagnetic spectroscopy in which the fluorophore groups included in the samples are excited using a light beam. Conventional fluorescence spectroscopy provides an emission spectrum for a fixed excitation wavelength, or an excitation spectrum for a fixed emission wavelength. The emission spectra are obtained by recording the signal of an emission monochromator at different wavelengths (λ_{em}) for a constant excitation wavelength (λ_{exc}), usually at a wavelength of high absorption. On the other hand, the excitation spectra are obtained by recording the signal from the excitation monochromator at different wavelengths (λ_{exc}), maintaining a constant emission wavelength (λ_{em}). The spectra provide both qualitative and quantitative information about fluorophore groups present in the sample *(Garcia-Gonzalez & et.al.)*.

Although molecular fluorescence spectroscopy is a highly sensitive technique, a severe overlap of excitation and emission makes the spectra difficult to interpret. The fluorescence spectra can also be affected by the attenuation of the absorption intensity due to the absorption of the excitation wavelength (primary inner effect) and the emission wavelength (secondary inner effect). These phenomena are more evident when working with Right Angle (RA) instruments. In this geometry (Right Angle), the collection of the fluorescence beam is collected at a right angle to the incident beam. In other words, emission is measured at 90^{o} in relation with the excitation (Fig. 3.2.2). Front Face (FF) geometry minimizes the inner filter effects compared to the RA geometry *(Sadecka & Tothova, 2007)*.

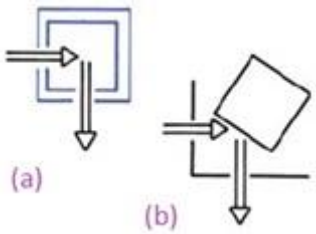

Fig. 3.2.2: Fluorescence Geometries (a) Right Angle and (b) Front Face

In vibrational spectroscopy, the probability of excitation for a particular vibration is determined by the selection rules, which can be derived from the application of group theory to atomic vibrations in the molecules belonging to different classes of symmetry *(Atkin)*. Considering fluorescence spectroscopy, to study the band position and intensity, it is necessary to consider the following issues:

i. The excitation wavelength used to obtain the emission spectra should be strongly absorbed by the fluorescent compounds. It is recommended to obtain the full absorption spectrum of the sample and then select the most appropriate wavelength based on the maximum absorption intensities. It is important to use an excitation wavelength that is strongly absorbed because the emission fluorescence intensity is proportional to the absorption intensity (Foot).
ii. Not all of the emission spectrum obtained with the selected excitation wavelength corresponds to the fluorescent compounds present in the sample. According to Stoke's law of fluorescent states, the wavelength of fluorescence radiation is greater than the exciting radiation. Consequently, the emission wavelength should be at least five or ten units larger than the excitation wavelength.
iii. The overtone area is located at twice the wavelength of excitation in the emission spectrum. In the interpretation of the spectra, it is also convenient to omit the region of the spectrum that is located too far from the excitation wavelength.
iv. Primary and secondary inner filter effects are other considerations that should be taken into account in the traditional Right Angle techniques. The inner filter effects imply the attenuation of the emission intensity due to the absorption of the incident excitation light and emitted light. These effects are avoided by working with diluted samples, but this solution also prevents saturation in the spectrum *(Garcia-Gonzalez & et.al.)*.

Fluorescence can be affected by several factors:

1. A rise in temperature or in the viscosity of the solvent can lead to decrease in fluorescence because of the more collisions occurring between the molecules.
2. Solvents containing heavy atoms, such as carbon tetrabromide, could also reduce fluorescence.
3. Fluorescence may be affected by the pH of solutions, if the fluorophore is consisted of acid or basic substituents.
4. For highly concentrated solutions, there are many collisions between the molecules, which produce self-absorption phenomena, as primary and secondary inner filter effects.
5. Quenching involves a reduction in fluorescence by a competing deactivating process, resulting from the interaction between a fluorophore and another substance present in the system.

Scattering artifacts in Luminescence Spectroscopy can also affect the fluorescence of a sample. The incident light that hits the sample could be scattered. There are two types of scatter, elastic, where the energy is not changed and there is no wavelength shift, and inelastic, where the energy is changed and there is a red wavelength shift.

At this section, the Rayleigh (elastic) and Raman (inelastic) scattering will be discussed in brief.

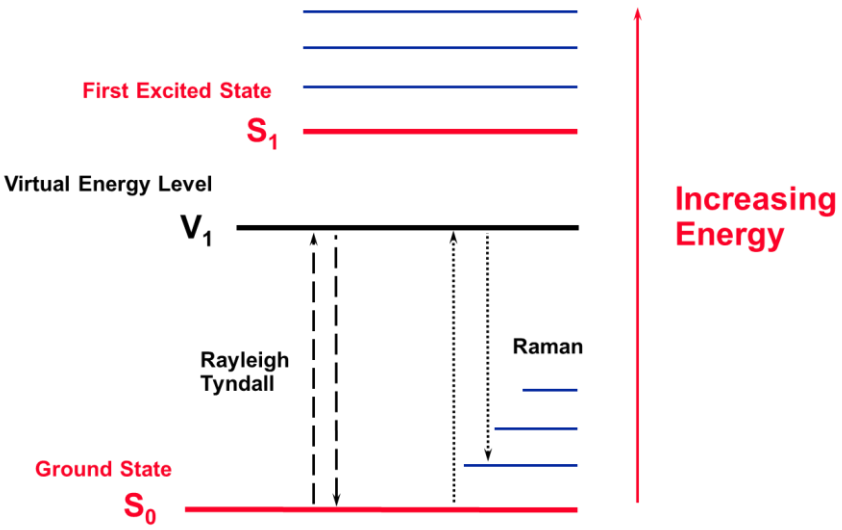

Figure 3.2.3: Types of scatter taking place, when a molecule is excited.

In Raman scattering, an absorbed photon is re-emitted with lower energy; the difference in energy between the incident and scattered photons corresponds to the energy required to excite a molecule to a higher vibrational mode. Typically, in Raman spectroscopy high intensity laser radiation with wavelengths in either the visible or near-infrared regions of the spectrum is passed through a sample. Photons from the laser beam produce an oscillating polarization in the molecules, exciting them to a virtual energy state. The oscillating polarization of the molecule can couple with other possible polarizations of the molecule, including vibrational and electronic excitations. If the polarization in the molecule does not couple to these other possible polarizations, then it will not change the vibrational state that the molecule started in and the scattered photon will have the same energy as the original photon. This type of scattering is known as Rayleigh scattering *(Bertolucci, 1989)*.

3.2.4 Fluorescence Measurements

In order to obtain a fluorescence spectrum, it is necessary to excite the sample with an energy – specific excitation wavelength (λ_{exc}), which comes from an excitation source, passes through a monochromator or a filter and strikes the sample. Then a fluorescent light is emitted in all directions. Some of this fluorescent light passes through a second monochromator or filter, dividing the light into different emission wavelengths (λ_{em}), which reach a detector.

Various light sources may be used as excitation sources, including lasers, photodiodes, and lamps as xenon arcs and mercury-vapor lamps. Only xenon arc lamp has a continuous emission spectrum, with nearly constant intensity in the range of 300-800nm and a sufficient irradiance for measurements down to just

above 220nm. The detectors can be classified as single-channel or multichannel. The difference between them is based on the number of wavelengths that they can detect at a time. So, single-channel detector can only detect the intensity of one wavelength at a time, in contrast to multichannel type that detects the intensity at all wavelengths simultaneously.

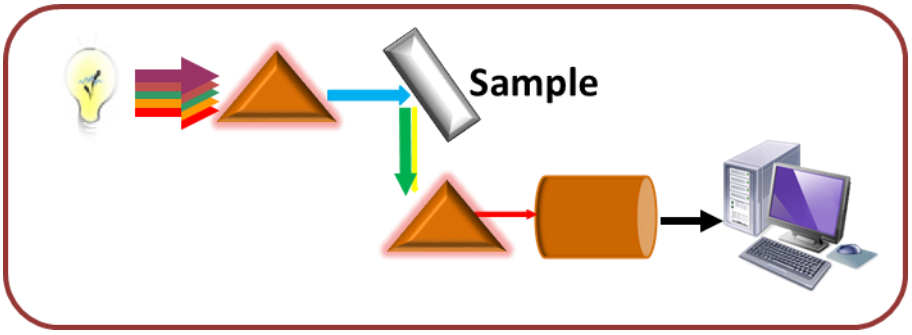

Fig. 3.2.4: Fluorescence Setup with FF Geometry

As seen in Figure 3.2.4, the light source emits light of all wavelengths, passes through the excitation monochromator, in order to choose the desired wavelength, which excites the sample. The fluorophore groups emit light in all directions, the fluorescence light is collected from the emission monochromator and finally passes to the detector. The emission spectrum can be seen to the computer screen. The Front Face geometry is used to collect the fluorescence from the surface of the solution and, consequently avoid diluting the sample and the inner-filter effects.

Mostly, when the sample is liquid, quartz cuvettes with different paths, internal widths and volumes are used to analyze the fluorescence spectrum. In addition to the conventional collection of emission spectra with a single excitation wavelength, some fluorometers can be adapted to conduct analyses under two particular modes that provide some advantages over the conventional mode. These particular ways are known as excitation-emission fluorescence spectroscopy (EEFS) and synchronous fluorescence spectroscopy (SFS) *(Garcia-Gonzalez & et.al.)*.

3.2.5 Potential of Fluorescence Spectroscopy in Olive oils

Fluorescence spectroscopy is a rapid analytical technique with high sensitivity to determine the overall presence of series of compounds. Frehse first proposed the use of fluorescence to analyze olive oils, studying the possibility of detecting the presence of refined oil in voo, by examining the oils under a quartz lamp with a Wood filter *(Frehse, 1925)*. Fluorescence spectroscopy has considerable potential to characterize virgin olive oils because of the large variety of fluorescent compounds (chlorophylls, tocopherols, pheophytins, vitamin E and oxidized compounds) present in them. The use of this technique for authentication purposes is encouraging, because of the remarkable differences between virgin olive oil and other seed oils *(Garcia-Gonzalez & et.al.)*.

3.3 Laser Induced Fluorescence

Laser Induced Fluorescence (LIF) spectroscopy is well known as a sensitive and powerful technique for detecting molecules and atoms, measuring species concentration, etc. It is easy to implement, highly characteristic and mostly non-invasive, which is important for the detection and possible separation of molecules *(Enderlein, Ambrose, Goodwin, & Keller)*. In a LIF experiment, atoms (or molecules) are excited from the ground state to an excited state, by absorbing laser radiation. Once they are excited, molecules can decay to their ground electronic level by spontaneous emission of a photon (or fluorescence). The relaxation of the molecules at an excited electronic state has a duration of a few nanoseconds. Every group of compounds has a different decay time, so there can be a discrimination between the different fluorophores by the decay time. This is called Time-Resolved Spectroscopy and has been employed as a preliminary study of this Thesis, focused on one sample of extra virgin olive oil.

A pulsed laser beam is of high power. This means that the energy transferred to the sample is high enough to destroy or damage the sample, causing photochemical deterioration to the sample. Using an attenuator before the sample, the power of the laser beam is decreased and the photodamage of the sample is eliminated. When the attenuator is placed at 45°, the initial power is decreased at its half power. If the attenuator is placed in a smaller attenuator, a bigger portion of power will pass through the sample. As seen in Figure 3.3.1, when the average power is 20mW, PMT will detect a higher voltage signal.

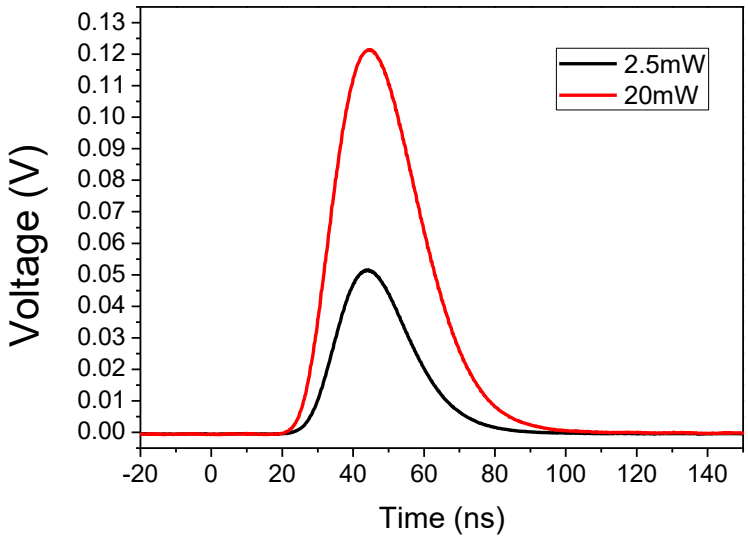

Figure 3.3.1: Olive oil fluorescence signal when excited in different powers.

The repetition of the laser was 10Hz. This can be changed manually, so we adjusted the repetition rate of the laser, in order to have one pulse per second, or 1Hz, and

we compared the fluorescence signal of the oil, fluctuating the power of the laser beam before the sample (Fig. 3.3.2).

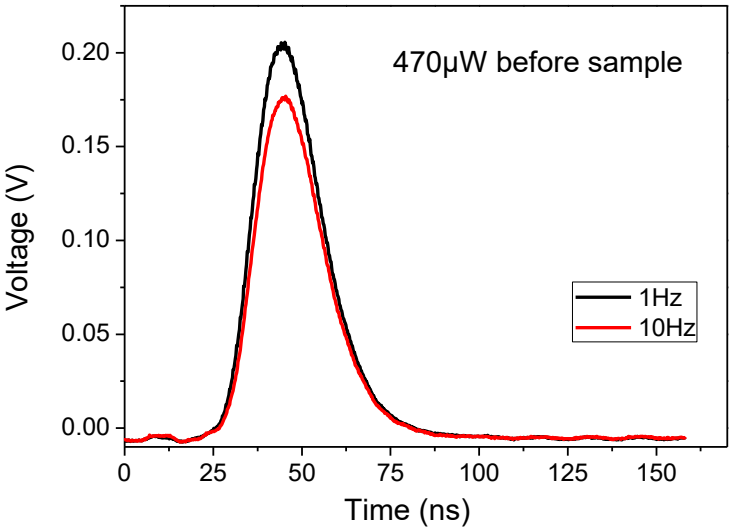

(a)

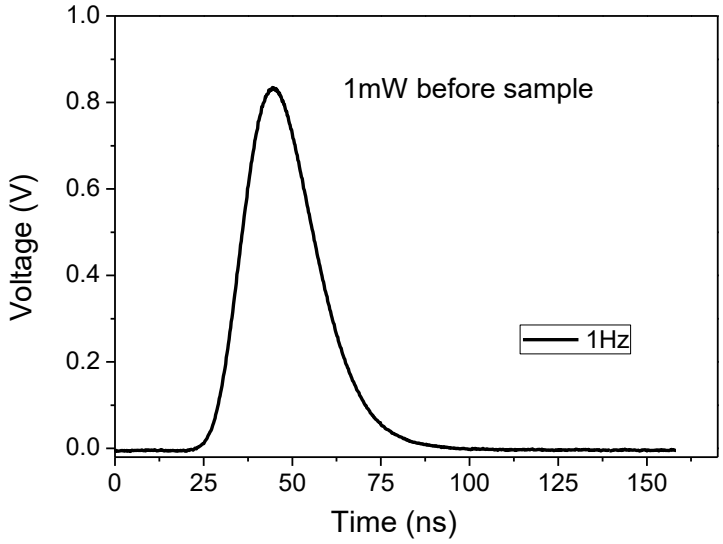

(b)

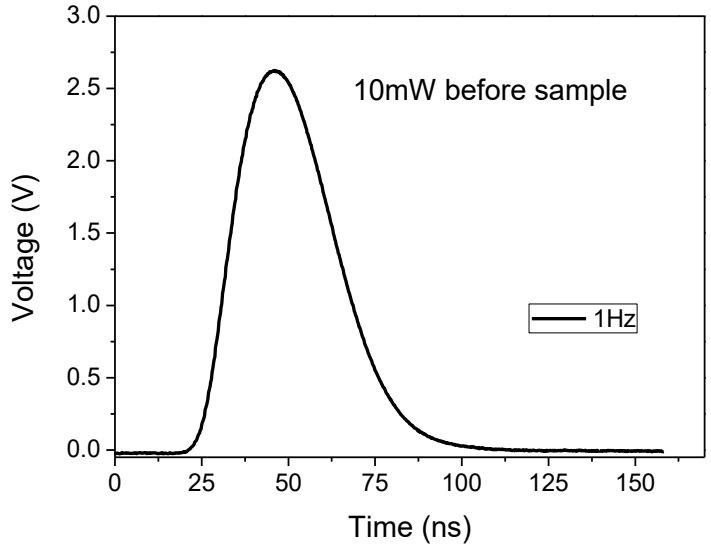

(c)

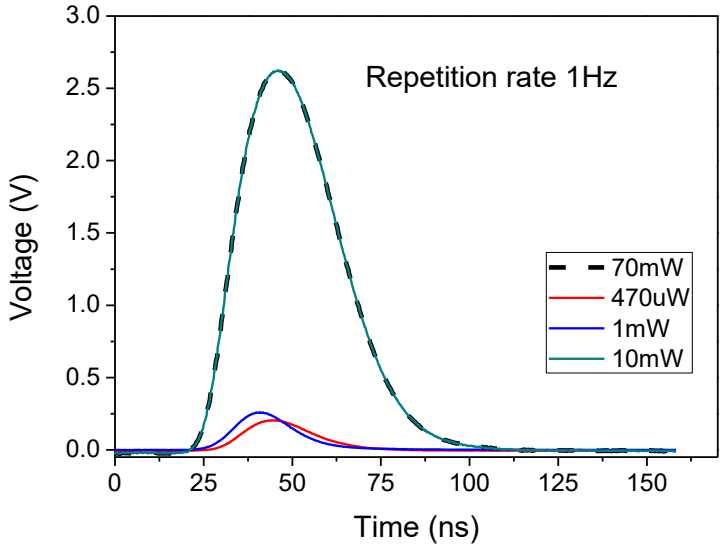

(d)

Figures 3.3.2 (a-d): Fluorescence signal of oil sample at 355nm. (a) power of 470 µW, 1 and 10Hz (b) power of 1mW, 1Hz (c) power of 10mW, 1Hz (d) repetition rate 1Hz and different powers

The energy per pulse transferred to the sample is calculated as *(http://www.coherent.com/downloads/AboutMeasuringLaserPowerndEnergyOutputFinal, n.d.)*:

$$\mathrm{E(J)} = \frac{\text{average Power (W)}}{\text{Repetition rate (Hz)}} \qquad \text{Equation 3}$$

When the power is low ($\sim 470\mu W$), the voltage signal reaches 200mV at repetition rates of 1 and 10Hz. The energies per pulse are 470µJ and 47µJ, respectively. Keeping the repetition rate in 1Hz, the average power increases to 1mW, the energy per pulse is 1mJ and the signal voltage is 900mV. Increasing the average power to 10mW, the energy per pulse is 10mJ, signal voltage increases to 2.6V and the sample

is photodamaged. Concerning the photodamage, there are phenomena that cause photochemical processes to the sample and the fluorescence signal becomes lower. In Fig. 3.3.2 (d), all the signals have been put together, so we can see the differences in the voltage signal that PMT detects.

When the average power is 20mW and the repetition rate is 10Hz, the energy is 2mJ/pulse, the oil sample is not photodamaged. When the repetition rate decreases to 1Hz, but the average power is 10mW, the energy transferred to the sample is 10mJ/pulse. This is a high energy and the oil sample suffers from photodamage.

We found that the threshold of average power at the olive oil fluorescence, with less damage in photochemistry of the sample, is 20mW or 2mJ/pulse when the repetition rate is 10Hz and the attenuator at 45^{o} to the incident laser beam, where the signal voltage is about 70mV.

Chapter 4:

Experimental Setup and Samples:

4.1 Samples

The oils used for the performance of this Thesis were obtained from local companies, in order to authenticate the quality, origin of olive oils, discriminate the changes between olive and seed oils and their mixtures and the correlation between the spectroscopic results and tasting tests from a panel of oil experts. The oils obtained come from all Crete, Greece, Turkey, Africa and South Europe. They are discriminated by the year of cultivation, olive variety and quality, based on storage.

Tsikoudia samples were of different varieties of grapes and every sample contained one variety of grapes. This is a preliminary study of tsikoudia, due to the few samples that were available.

4.2 Sample Preparation

Olive and seed oil were kept at room temperature in the dark, before measured, without any pretreatment. Tsikoudia was kept in fridge, at $4^{o}C$ without any pretreatment, before measurement. The quartz cuvettes were cleared with n-hexane.

4.2.1 Tsikoudia

Samples were kept out of fridge, in order to come to a room temperature, for about half an hour, before measured. For absorption measurements (230-450nm), no dilution was made and the path length of the quartz cuvette was 10mm. As a background measurement, a solution of water: ethanol (70:30) was used, because samples contained about 30% alcohol. For Fluorescence measurements, no dilution was made, the cuvette path length was 10mm and the geometry used was Front Face (FF) (Fig. 3.2.2). We performed an Excitation-Emission Fluorescence spectrum (EEF) for each sample and obtained the 2D contour map (see paragraph 3.2.4).

4.2.2 Oils

Fluorescence measurements were performed in a 10mm path length cuvette in the Front Face Geometry for all samples.

Absorption measurements were divided in three regions:

- UV region (220-280nm), dilution 1% (v/v) in n-hexane, cuvette path length 2mm
- UV region (260-400nm), dilution 1% (v/v) in n-hexane, cuvette path length 10mm

- Visible and n-IR region (>400nm), undiluted, cuvette path length 2mm

Dilution:

The solution that we made for the UV region contained 1% (v/v) oil in the solvent n-hexane (*>99.9% pure, GC, Sigma Aldrich*). This solvent was capable of diluting the oil and is used widely for HPLC measurements and for authentication of virgin olive oils, according to IOOC *(IOOC, 1991)*. Other scientific groups have used other solvents, isooctane and cyclohexane, which are also mentioned at the European instructions *(IOOC, 1991)*. For all solvents, n-hexane, cyclohexane and isooctane, the % Transmittance was measured by applying the same parameters – quartz cuvette of 10mm path length, background of distilled water, at the spectral range of 215-280nm. As mentioned in the international instructions for the olive oil, the solvents should have the following characteristics *(http://eur-lex.europa.eu/legal-content/en/ALL/?uri=CELEX:31991R2568, n.d.)*:

- Spectrophotometrically pure iso-octane (2,2,4-trimethylpentane). With reference to distilled water this should have a transmittance of not less than 60 % at 220 nm and not less than 95 % at 250 nm, or
- Spectrophotometrically pure cyclohexane: with reference to distilled water this should have a transmittance of not less than 40 % at 220 nm and not less than 95 % at 250 nm, or
- Another suitable solvent capable of completely dissolving the fat (e.g. n-hexane, widely used at HPLC measurements).

At the following figure (Figure 4.2.1), the transmittance spectra of the solvents are presented. It is clear that the solvent cyclohexane measured is not pure enough. The other two solvents n-hexane and isooctane fulfill the requirements for being used as oil solvents.

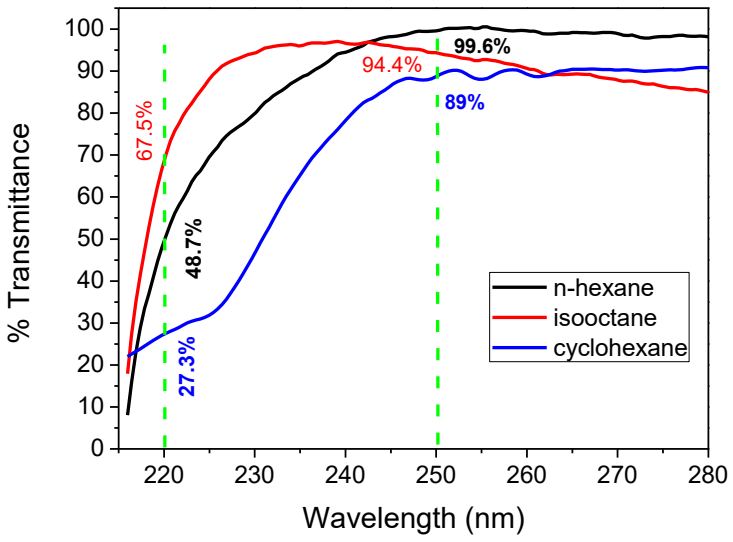

Figure 4.2.1: Transmittance spectra of the three basic solvents used in olive oil characterization.

Furthermore, the absorption spectra of the solvents were recorded in the UV region, at the wavelength range of 220-280nm. The path length of the quartz cuvette was 10mm, the background recorded was pure air and the spectra were printed in the following graph (Fig. 4.2.2):

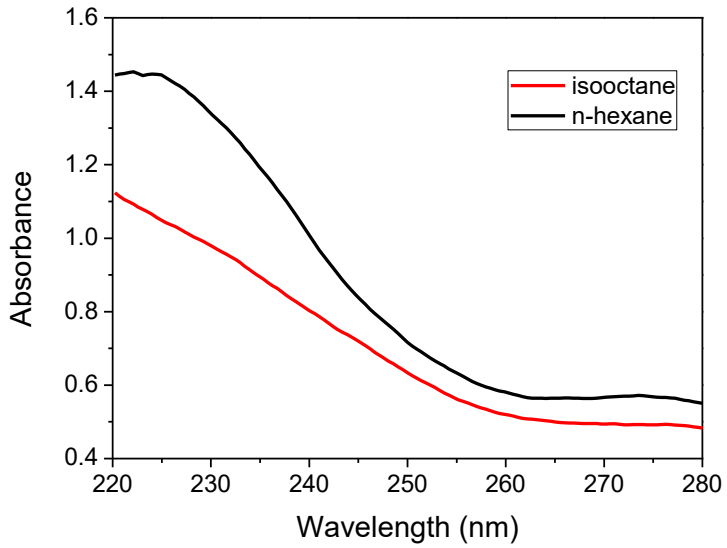

Figure 4.2.2: Absorption spectra of solvents at the UV wavelength range of 220-280nm.

It can be observed that n-hexane presents higher absorbance than isooctane (Fig. 4.2.2). These solvents are used in order to calculate the indexes K and ΔK of the oils and classify them to different quality categories (see section 2.1). As seen at Fig. 4.2.2, the multiplying factor that connects the widely used solvent isooctane and n-hexane is 1.35 for the wavelength 232nm and 1.16 for the wavelength 270nm, for the calculation of K indexes.

When olive oils were diluted in these different solvents, the absorbance intensity of the dilutions at 232nm was higher, when n-hexane was used. This was the reason we chose to use a lower path length cuvette, specifically 2mm, when n-hexane was the solvent at the UV range of 220-280nm, so as the absorbance intensity to be in the boundaries of 0.1 to 0.8, as must be for liquids absorption.

In order to control the quality and authentication of oils, we took into account the rules from IOOC *(IOOC, 1991)* about the quality parameters. The special issues include the absorption of oils at the UV region of the electromagnetic spectrum. More specifically, absorbance at 232nm is due to the formation of hydroperoxides and conjugated dienes. Absorbance at 270nm is due to the formation of secondary oxidation products (carbonylic compounds, conjugated trienes). Measuring the absorbance at these specific wavelengths, indexes K can be calculated (Eq. 4.1) as:

$$K_\lambda = \frac{E_\lambda}{c \cdot s}$$ Equation 4.1

where K_λ is the index, E_λ is the absorbance measured at wavelength λ, *c* is the concentration of solution in g/100ml and *s* is the path length of cuvette in cm.

The absorbance measured should have values 0.1<A<0.8 and the background (I_0) was the respective cuvette full of the solvent (n-hexane).

The index K_{270} is an indicator of how fresh the olive oil is. There is one more index, ΔK_λ, measured (Eq. 4.2) as:

$$\Delta K = K_\lambda - \frac{K_{\lambda-4} + K_{\lambda+4}}{2}$$ Equation 4.2

where K_λ is the index K as referred above and λ is the wavelength 270nm (ΠΑΡΑΡΤΗΜΑ ΙΧ, 1991). ΔK is a criterion of discriminating the quality and purity of virgin olive oils. Especially, for extra virgin olive oils, the criteria for authentication, using any solvent, are below, as shown in Eq. 4.3:

a. $1.5<K_{232}<2.5$
b. $0.15<K_{270}<0.22$ Equation 4.3
c. $\Delta K<0$ and $\Delta K \leq 0.01$

Thereafter, the dilution was made as mentioned in the European instructions (1% v/v or 1gr oil/100ml solution). The usage of two different path length cuvettes was important, in order to achieve the desirable and acceptable values of absorbance. More specifically, at the UV range of 220-280nm, n-hexane was the solvent, cuvette had a path length of 2mm and the index K_{232} was calculated as:

$$K_{232} = \frac{E_{232}}{(1\%\ v/v) \cdot (0.2/1)} = 5 \cdot E_{232}$$ Equation 4.4

As provided by the European instructions, the concentration of the oil is 1% v/v in n-hexane, in order to measure the UV absorbance of the oils, and the path length of the cuvette is 10mm (or 1cm). As observed from the Eq. 4.4, the index K_{232} is calculated as 5 times the absorbance, because the cuvette used is of 2mm path length and the dilution is 1% v/v oil in the solvent n-hexane, as mentioned *(IOOC, 1991)*.

Filtration:

Olive oils consist of several organic components. In order to assume that larger molecules do or do not affect the absorbance or fluorescence intensities, a filtration of samples took place before the measurements, by using a *Whatman* 0.2μm TF. Then, the absorbance at the Visible wavelength region was measured (Fig. 4.2.3):

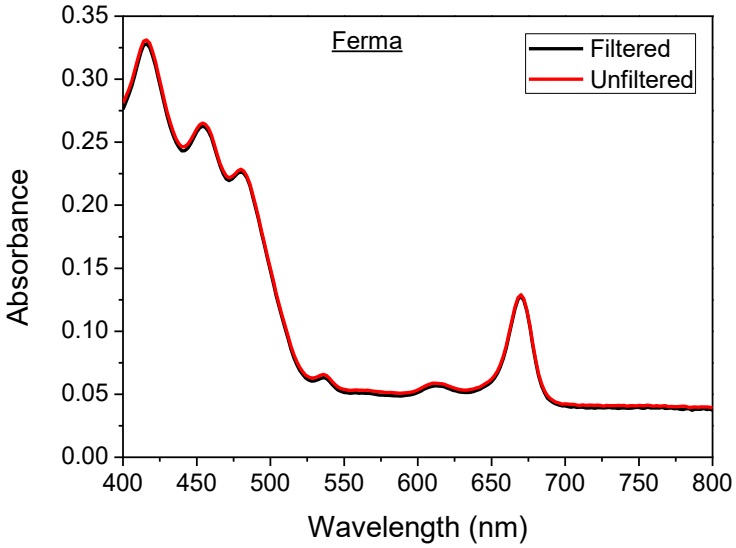
Ferma
Filtered
Unfiltered
Absorbance
Wavelength (nm)
0.35
0.30
0.25
0.20
0.15
0.10
0.05
0.00
400
450
500
550
600
650
700
750
800

(a)

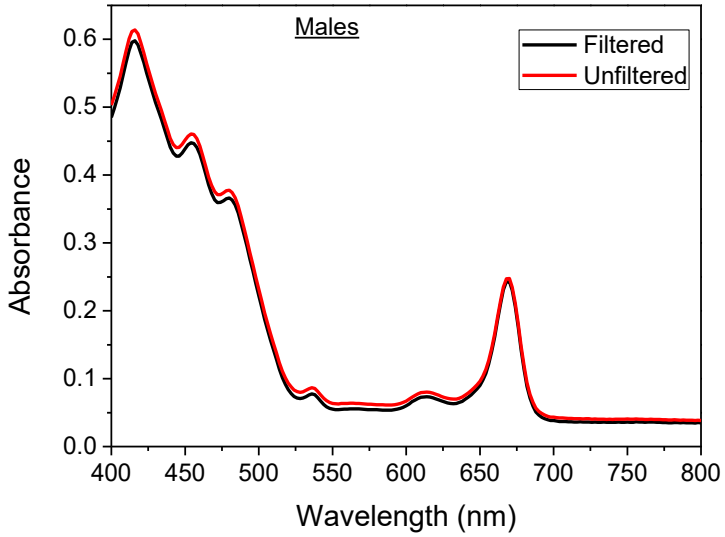
Males
Filtered
Unfiltered
Absorbance
Wavelength (nm)
0.6
0.5
0.4
0.3
0.2
0.1
0.0
400
450
500
550
600
650
700
750
800

(b)

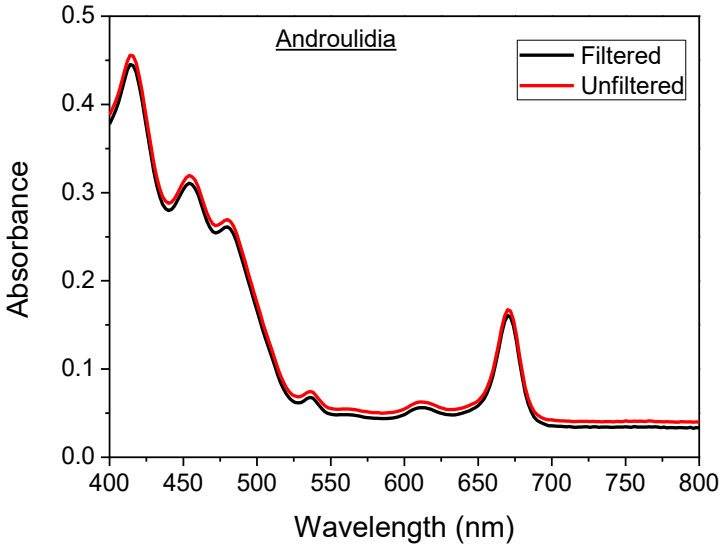

(c)

Figure 4.2.3 (a- c): Absorption spectra of filtered and unfiltered virgin olive oil at the Visible region 400-800nm

It can be observed that the absorption spectra of filtered and unfiltered virgin olive oils measured, coming from different geographical origin but of the same olive variety, do not present any significant differences. As a conclusion, the oils tested and measured in this Thesis are all unfiltered, because the filtration does not affect the absorption spectrum of the olive oil, neither in shape nor in the absorbance units.

4.3 Absorbance Measurements

Absorption measurements were obtained, by using two different commercial devices. The first one is a laboratory device, connected with an integrating sphere, so Reflectance measurements can also be obtained. This is the Perkin-Elmer Lambda 950 spectrophotometer, operating in a range of 190-2500nm, where the UV-Vis resolution is 0.05nm, while the near-IR resolution reaches up to 0.2nm (Fig. 4.3.1). The excitation light sources are a Deuterium lamp, emitting from 190-318nm, and a Wolframium (or Tungsten), emitting from 318-2500nm. The detector is a gridless Photo Multiplier Tube (PMT) with Peltier-controlled PbS to achieve high-performance testing across the spectral range up to 2500nm. It also contains dual sample compartments, so the user can put both solvent and sample in the compartments and measure I and I_0 simultaneously *(Elmer, n.d.)*.

Fig. 4.3.1: Perkin-Elmer spectrophotometer

The second device is a portable spectrophotometer, K-MAC UV-Vis spectrometer, operating in the range of 220-850nm, with an optical resolution of about 2nm. The light sources are Deuterium/Tungsten lamps for the UV-Vis region and a Tungsten lamp for the visible region (Fig. 4.3.2) *(K-MAC spectrometer)*. The detectors are CCD arrays, with 600lines/nm gratings.

Fig. 4.3.2: K-MAC spectrometer

Both spectrophotometers are connected with a computer and run their own hardware.

Finally, taking into account the advantages of both spectrometers and the experimental setup, as it is described in section 3.1.3 and Figure 3.1.1, performance of the experiments shall begin.

4.4 Fluorescence measurements

Fluorescence measurements were obtained by using the Horiba FluoroMax-3 device, as seen in the following figure (Fig. 4.4.1) *(Fluoromax-3, 2001)*.

(a)

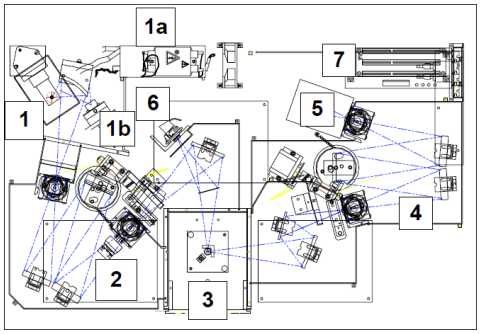

(b)

Fig. 4.4.1(a, b): Fluorometer from outside (Fig. a) and inside (Fig. b)

One can see the different positions in this “black box”:

1. Light source (150W ozone-free xenon-arc lamp)
2. Excitation monochromator
3. Sample compartment
4. Emission monochromator
5. PMT
6. Photodiode and current-acquisition module
7. Instrument control

The gratings contain 1200grooves/mm. The spectrum accuracy that can be achieved is better than 0.5nm. The detectors of Fluorometer are:

- A reference detector, that monitors the xenon lamp and it is a UV-enhanced silicon photodiode, set just before the sample compartment, and
- A signal detector for the fluorescence detection, which is a photomultiplier tube.

The user can manage to change the integration time of the measurement and the slits of excitation and emission spectrometers. Integration time is the length of time that data are collected for each data point. By changing the Slits, width of all slits in the optical path can be set. Slit width affects the amount of light reaching the detectors. Slits of excitation spectrometer determine the amount of light that passes through the excitation spectrometer and reaches the sample. Slits of emission spectrometer control the amount of fluorescence that the signal detector sees. The wider the slits are, the more light falls on the sample and detector, but the resolution decreases. When a large portion of fluorescence reaches the signal

detector, the signal gets saturated and then the slits of emission spectrometer should be decreased.

All samples are not chemically pre-treated and are placed in the Front Face (FF) geometry, and more specifically at 35^{o} to the incident beam, in order to avoid all inner filter effects, that were discussed before (section 3.2.3), and the fluorescence signal comes from the surface of the sample. An example of a fluorescence spectrum of sunflower oil when excited at 355nm is shown in Figure 4.4.1:

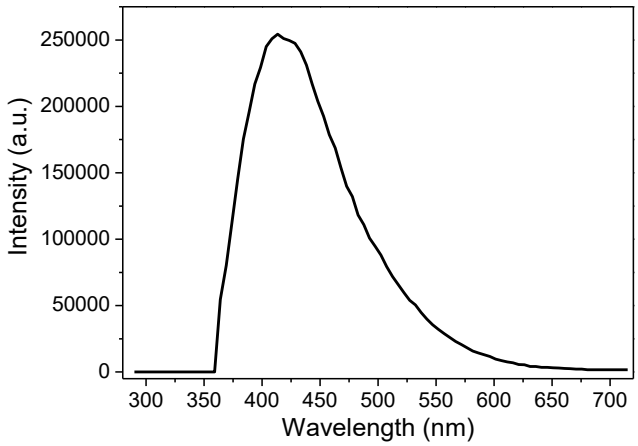

Fig. 4.4.1: Fluorescence spectrum of sunflower oil, when excited at 355nm.

As mentioned in section 3.2.4, we employed Excitation-Emission Fluorescence spectroscopy for the sample recording. The result of this spectroscopic technique is a contour map, as seen in Figure 4.4.2. We excite the sample in different excitation wavelengths and record the emission spectrum, avoiding the Rayleigh scattering (first or second order), and then we combine all these emission spectra. The contour map has 3 directions: x-axis represents the excitation wavelength, y-axis represents the emission wavelength and the intensity of the colors represents the fluorescence intensity.

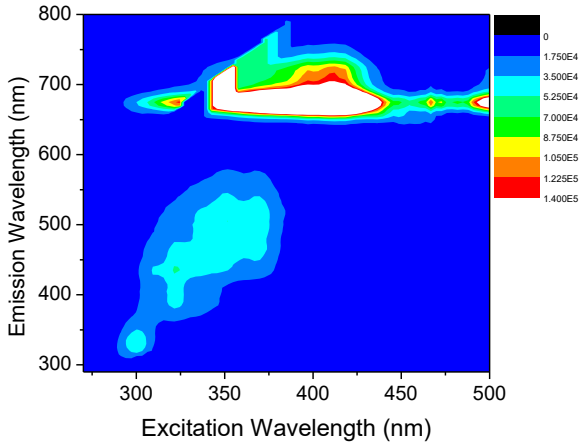

Figure 4.4.2: Contour map of extra virgin olive oil

4.5 LIF measurements and parameters

Laser Induced Fluorescence Setup contains a pulsed Nd:YAG laser, operated at 1064nm, power of about 40mW (400mJ/pulse), with a repetition rate of 10Hz and pulse duration of 8ns. Extra virgin olive oils were measured by employing the third harmonic generation frequency at 355nm (UV).

Fig. 4.5.1: Laser spot on a black paper, before the sample

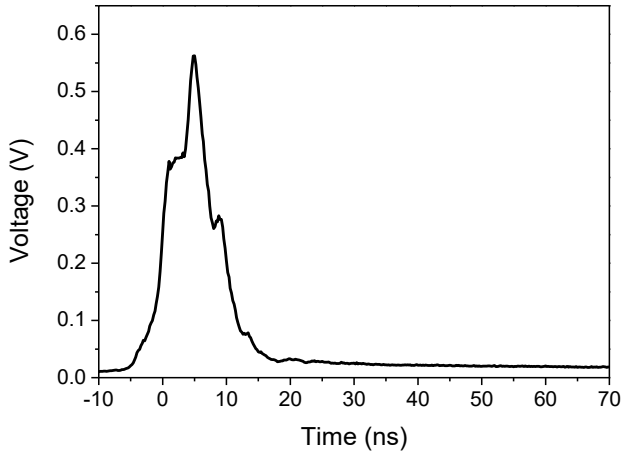

Figure 4.5.2: Laser pulse signal recorded on the oscilloscope.

The laser beam, of 6mm diameter, (Figure 4.5.1) was guided to the sample, which is perpendicular to the direction of the incident beam, as shown in Figure 4.5.3. The laser pulse, as seen in Figure 4.5.2, is recorded to the oscilloscope. The sample was put in a 10mm path length quartz cuvette, undiluted. Specifically, the incident laser beam stroke the cuvette perpendicularly at the opening and the fluorescence was collected at 90^{o} from the incident beam, but on the surface of the liquid. Taking into account that the quartz cuvette does not absorb at the UV region, the fluorescence signal was poor of inner filter effects. The fluorescence signal is guided through an optical fiber, that is placed at the surface of the oil sample, to a slit of 1mm in a monochromator, so as to choose manually the selected emission wavelength, then

to a Photomultiplier Tube (PMT), in order to avoid scattering or back-reflection light and multiply the signal, and the resulting signal is recorded to an oscilloscope. The PMT indicator is fixed, so all measurements can be compared at the same rate.

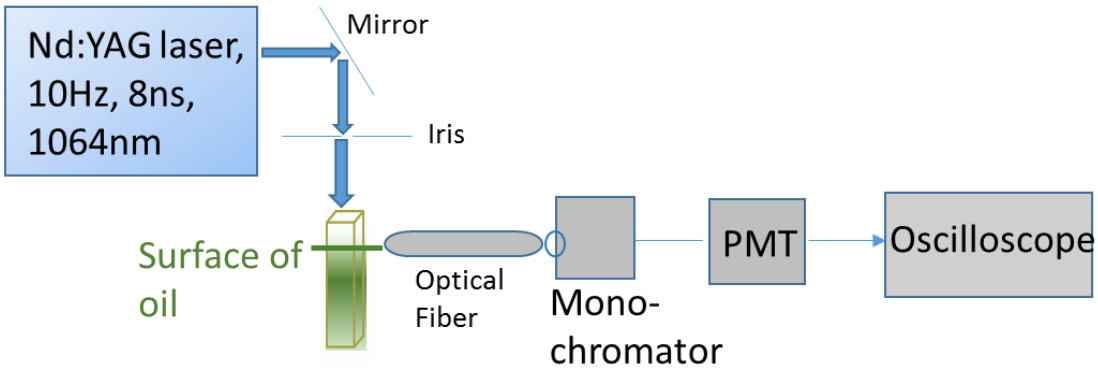

Figure 4.5.3: LIF setup

Employing this experimental setup to an olive oil, the laser beam of 1064nm passes through appropriate crystals, in order to generate the third harmonic generation (THG) frequency (wavelength of 355nm). This laser frequency (355nm) passes through the experimental components and irradiates the sample and the fluorescence of chlorophyll can be recorded. The fluorescence signal is printed to the oscilloscope screen as a function of time (ns) at the selected emission wavelengths. Then, the recorded fluorescence intensity is plotted versus the emission wavelength (in nm scale) and the resulting emission spectrum is shown below (Fig. 4.5.4):

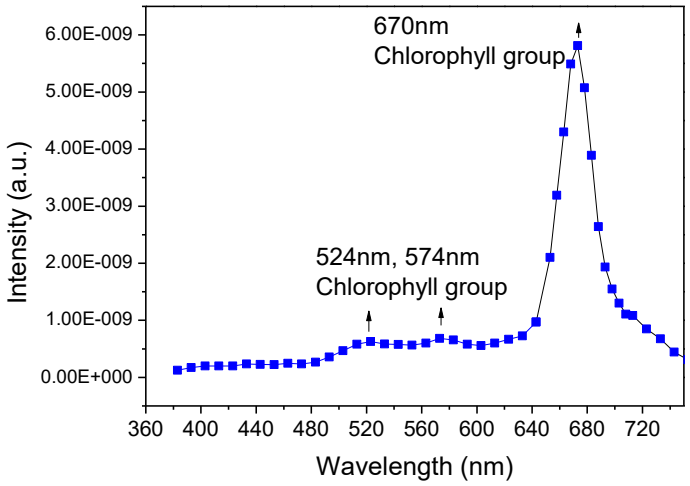

Figure 4.5.4: Fluorescence spectrum of olive oil excited at 355nm by LIF

Chapter 5:

Statistical Analysis - Chemometrics

5.1 Principal Component Analysis (PCA)

Principal component analysis (PCA) is a statistical procedure that uses an orthogonal transformation to convert a set of observations of possibly correlated variables into a set of values of linearly uncorrelated variables called **principal components**. The number of principal components is less than or equal to the number of original variables. This transformation is defined in such a way that the first principal component has the largest possible variance (that is, accounts for as much of the variability in the data as possible), and each succeeding component in turn has the highest variance possible under the constraint that it is orthogonal to the preceding components. The resulting vectors are an uncorrelated orthogonal basis set. PCA is sensitive to the relative scaling of the original variables.

PCA is mostly used as a tool in exploratory data analysis and for making predictive models. PCA can be done by eigenvalue decomposition of a data covariance (or correlation) matrix or singular value decomposition of a data matrix, usually after mean centering (and normalizing or using Z-scores) the data matrix for each attribute *(Abdi. H., 2010)*. The results of a PCA are usually discussed in terms of component scores, sometimes called factor scores (the transformed variable values corresponding to a particular data point), and loadings (the weight by which each standardized original variable should be multiplied to get the component score) *(P.J.A., 2003)*.

5.2 Partial Least Squares Regression (PLS)

Partial least squares regression (PLS regression) is a statistical method that bears some relation to principal components regression; instead of finding hyperplanes of maximum variance between the response and independent variables, it finds a linear regression model by projecting the predicted variables and the observable variables to a new space. Because both the *X* and *Y* data are projected to new spaces, the PLS family of methods are known as bilinear factor models.

PLS is used to find the fundamental relations between two matrices (*X* and *Y*), i.e. a latent variable approach to modeling the covariance structures in these two spaces. A PLS model will try to find the multidimensional direction in the *X* space that explains the maximum multidimensional variance direction in the *Y* space. PLS regression is particularly suited when the matrix of predictors has more variables than observations, and when there is multicollinearity among *X* values *(Tenenhaus, Esposito Vinzi, Chatelinc, & Lauro, 2005) (Vinzi, Chin, Henseler, & et al., 2010)*. Matrix X represents the independent variables and matrix Y the dependent variables *(Wold, 2001)*.

Data inserted to the PLS model can be pre-treated in many ways, such as mean centering, SNV (standard deviation), Savitzky-Golay methods (n-order derivatives), etc. The most used cross validation are the leave-one-out (one variable is left out and the model is calculated, for several times) and venetian blinds (a group of variables is left out and the model is calculated, for several times) cross validation processes *(Wold, 2001)*.

Both Statistical methods are employed as a useful tool for presenting the correlation between the Optical Spectroscopy and the origin of oils and tsikoudia samples, tasting results and the adulteration of olive oils.

Chapter 6:

Experimental Results of Olive oil study and Discussion

6.1 Absorption and Fluorescence of olive oils based on their geographical origin

Extra virgin olive oils from different geographical regions were obtained by two local companies.

6.1.1 Absorption measurements

First of all, we should take a look at the typical absorption spectra of an extra virgin olive oil in the Ultraviolet (UV), Visible (Vis) and near Infrared (near-IR) regions, divided as:

a. UV wavelengths region of 220-280nm, where the sample was diluted in n-hexane (1% v/v) and placed in a 2mm path length quartz cuvette,

b. UV wavelengths region of 260-410nm, where the sample was diluted in n-hexane (1% v/v) and placed in a 10mm path length quartz cuvette *(Dankowska)*,

c. Visible wavelengths region of 400-800nm, where the sample was undiluted and placed in a 2mm path length quartz cuvette,

d. Near-IR wavelengths region of 800-1600nm, where the sample was undiluted and placed in a 10mm path length quartz cuvette, and

e. Near-IR wavelengths region of 1800-2200nm, where the sample was undiluted and placed in a 10mm path length quartz cuvette.

The near-IR wavelengths region of 1600-1800nm was excluded, because of the absorbance intensity saturation of oils. The absorption spectra are printed below (Fig. 6.1 (a-e)) for the different wavelength regions, respectively, including the components that absorb at these regions.

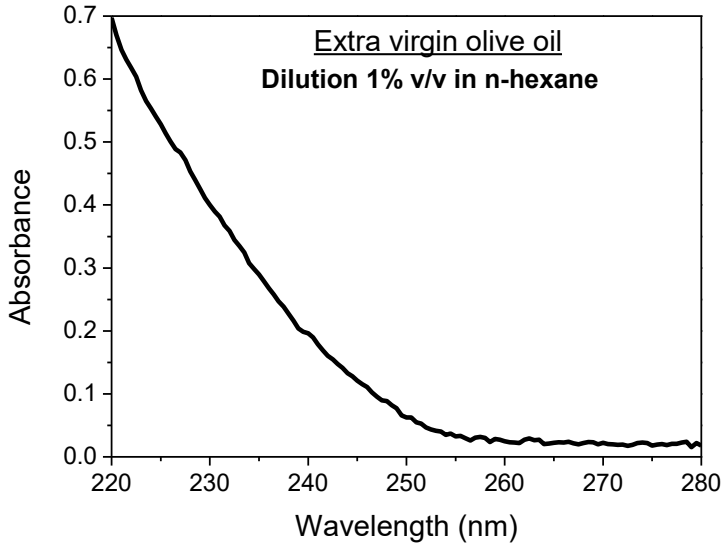
Extra virgin olive oil
Dilution 1% v/v in n-hexane
Absorbance
0.0
0.1
0.2
0.3
0.4
0.5
0.6
0.7
220
230
240
250
260
270
280
Wavelength (nm)

(a)

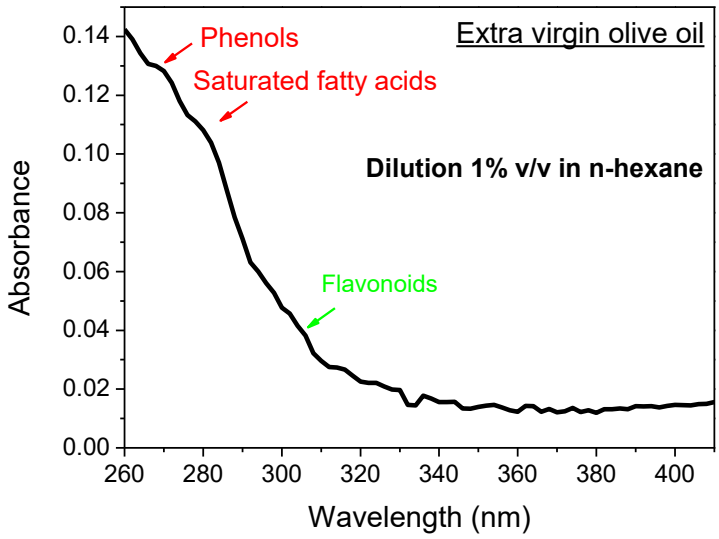
Extra virgin olive oil
Phenols
Saturated fatty acids
Dilution 1% v/v in n-hexane
Flavonoids
Absorbance
Wavelength (nm)
0.00
0.02
0.04
0.06
0.08
0.10
0.12
0.14
260
280
300
320
340
360
380
400

(b)

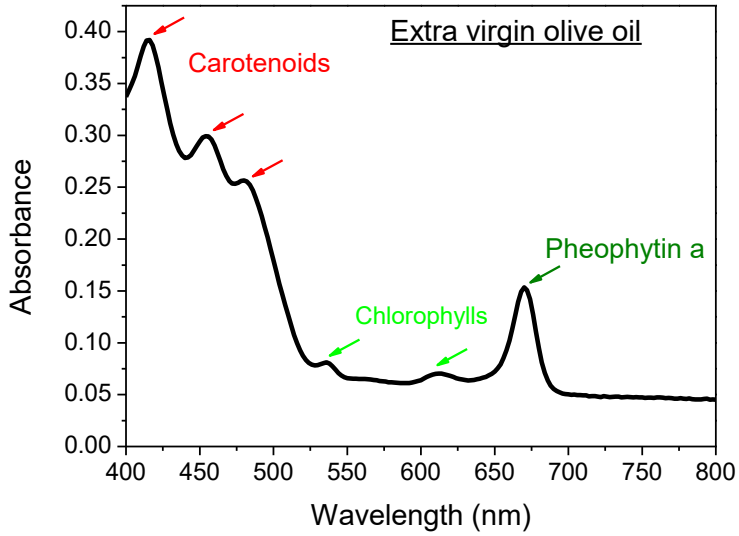
Extra virgin olive oil
Carotenoids
Pheophytin a
Chlorophylls
Absorbance
Wavelength (nm)
0.00
0.05
0.10
0.15
0.20
0.25
0.30
0.35
0.40
400
450
500
550
600
650
700
750
800

(c)

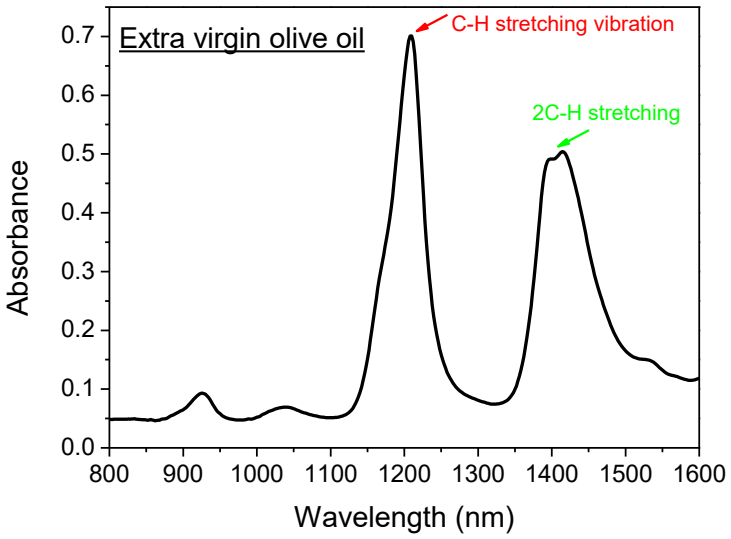

(d)

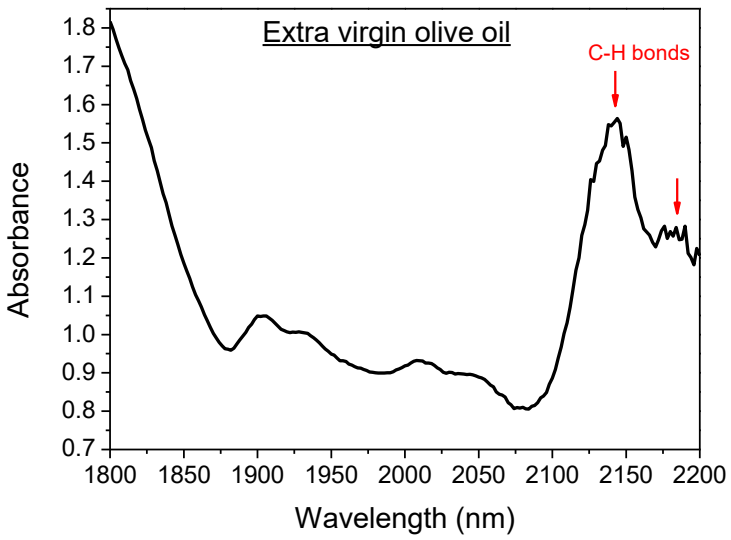

(e)

Fig. 6.1 (a- e): Absorption spectra of evoo. (a) UV region 220-280nm, (b) UV region 260-410nm, (c) Visible region 400-800nm, (d) IR region 800-1600nm, (e) IR region 1800-2200nm.

At the UV region two main absorbance peaks at 275 and 280nm are noted, corresponding to phenols and saturated fatty acids *(Angerosa, Campestre, & Giansante, 2006)*, and a shoulder at 305nm, corresponding to flavonoids *(Passaloglou-Emmanouilidou, 1990)*, *(Fuentes, Báez , Bravo, Cid, & Labra, 2012)*. At the wavelength region of 220-260nm there is no significant absorbance peaks, as shown in Fig. 6.1 (b), but, when the olive oil has been kept in non-appropriate conditions, such as in an iron barrel or has been illuminated, an absorbance peak at 225nm would arise, corresponding to conjugated dienes *(White, 1995)*. Several scientific groups reported the correlation between the absorbance at 225nm and the phenolic compounds content with the bitterness of virgin olive oil *(RAQUEL MATEOS, CONCEPCIOÄ N*

GARCIÄA-ORTIÄZ CIVANTOS, & JUAN CASTRO, 2005), *(GUTIÉRREZ, Albi, Palma, Rios, & Olias, 1989), (Rosales, Perdiguero, Gutiérrez, & Olias, 1992), (Beltrán, Ruano, Jiménez, Uceda, & Aguilera, 2007)*. Extra virgin olive oil presents 6 main peaks at the visible region at 414, 458 and 483nm, corresponding to carotenoids, at 530 and 610nm, corresponding to chlorophyll and at 675nm, corresponding to chlorophylls' group *(Downey, Mcintyre , & Davies, 2003)* and more specifically to pheophytin a *(Domenici, et al., 2014)*. 800-1600nm, by a 2mm step, the absorption spectra of olive oils, as seen in Fig. 6.1 (d), present main peaks, at 1208nm and a broad peak 1391-1420nm, which correspond to C-H stretching of CH_3 and CH_2 and 2C-H stretching, respectively *(Holman & Edmondson, 1956)*. These peaks are the same for all oils, even for seed oils, as we will discuss later. At this absorbance spectrum, there are two main absorbance peaks at 2141 and 2190nm corresponding to C-H bonds and these peaks are the same in all oils *(Fuentes, Báez , Bravo, Cid, & Labra, 2012)*.

6.1.1.1 UV region

Extra virgin olive oils were tested, using the Perkin-Elmer spectrometer, in the UV region 250-400nm by a 2nm step, in a cuvette of 10mm path length and 1% v/v diluted in n-hexane. As a background measurement, a 10mm path length cuvette full of n-hexane was used. The samples used are from different geographical origins, but coming from the same olive variety, Korwneiki. The first results are recorded in Fig. 6.1.1:

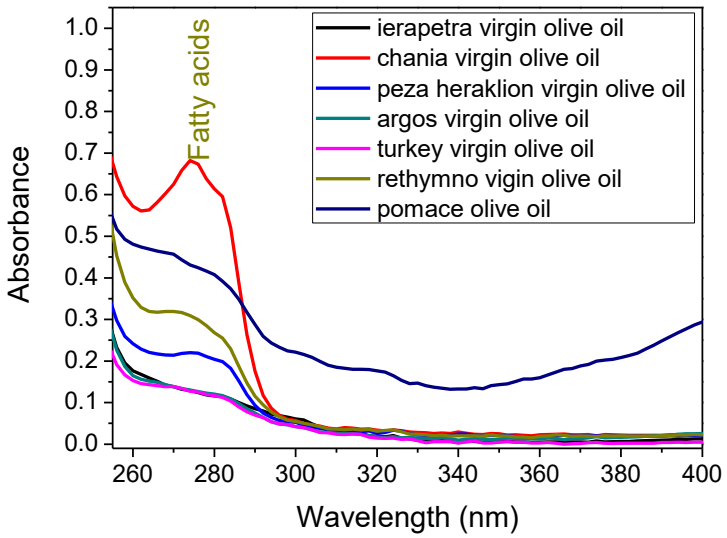

Figure 6.1.1: Absorption spectra of extra virgin olive in the UV region (250-400nm), 1% diluted in n-hexane

The absorbance peaks at 275-280nm correspond to saturated fatty acids *(Angerosa, Campestre, & Giansante, 2006)*, as seen in Fig. 6.1.1. No other absorption peak is present at this region. According to the European instructions for the quality of extra virgin oils (see section 4.2.2), a table for indexes K_{270} and ΔK was made (Table 6.1):

Olive Oil	**K_{270}**	**ΔK_{270}**
Argos	0.14	0
Chania	0.64	0.01
Harakas	0.16	0.005
Ierapetra	0.14	0.005
Italy	0.15	0.005
Panagia Heraklion	0.31	0.006
Peza Heraklion	0.22	0.002
Rethimno	0.32	0.007
Turkey	0.14	0.004
Tynisia	0.14	0.0005
Pyrinelaio	0.46	0.016

Table 6.1: K_{270} and ΔK indexes for some olive oils

Olive pomace oil (named as pyrinelaio - πυρηνέλαιο - in the table 6.1) seems to have values of indexes K_{270} and ΔK significantly greater than the values of extra virgin olive oil (evoo).

Let's move on and observe the absorption spectra of some olive oils from different geographical origins at the UV region (230-280nm), using a 2mm path length, and the samples are diluted 1% v/v in n-hexane (Fig. 6.1.2). The following measurements have been taken by Mrs. Maria Peloni and Mr. Aris Velegrakis, within the context of their Practical exercise in the laboratory.

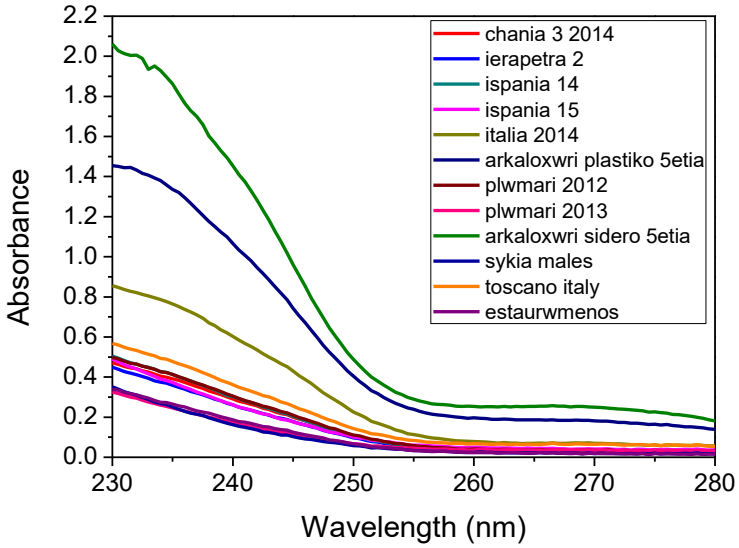
Absorbance
Wavelength (nm)
chania 3 2014
ierapetra 2
ispania 14
ispania 15
italia 2014
arkaloxwri plastiko 5etia
plwmari 2012
plwmari 2013
arkaloxwri sidero 5etia
sykia males
toscano italy
estaurwmenos

(a)

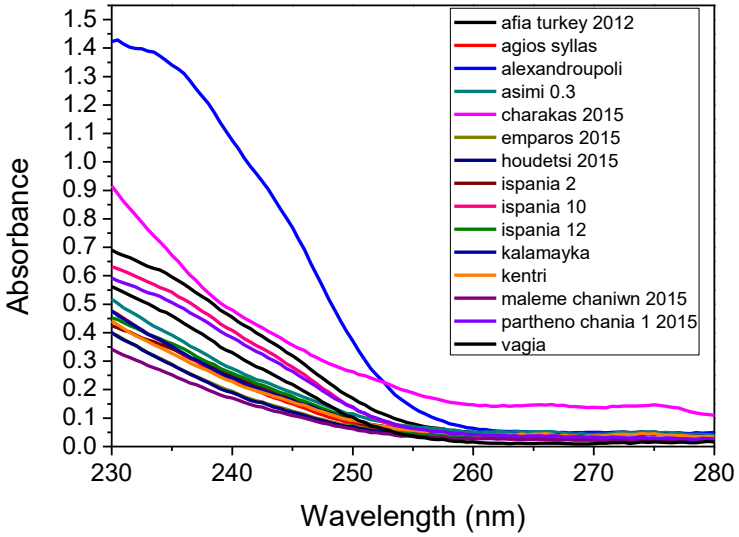
Absorbance
Wavelength (nm)
afia turkey 2012
agios syllas
alexandroupoli
asimi 0.3
charakas 2015
emparos 2015
houdetsi 2015
ispania 2
ispania 10
ispania 12
kalamayka
kentri
maleme chaniwn 2015
partheno chania 1 2015
vagia

(b)

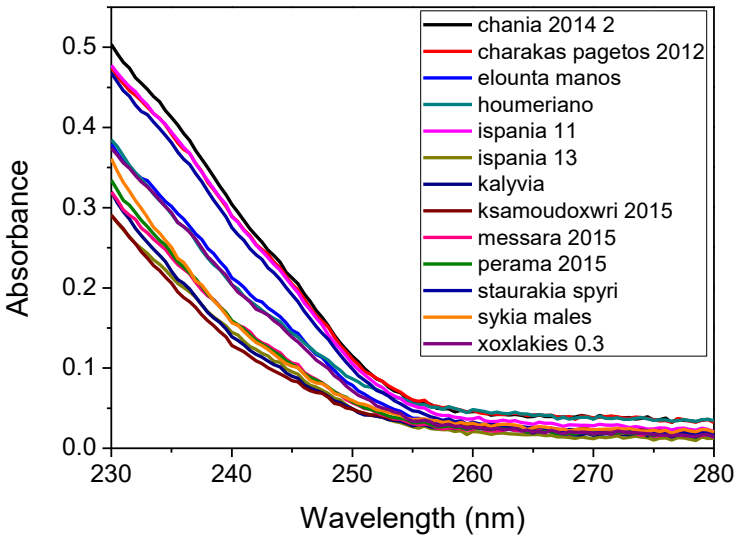
chania 2014 2
charakas pagetos 2012
elounta manos
houmeriano
ispania 11
ispania 13
kalyvia
ksamoudoxwri 2015
messara 2015
perama 2015
staurakia spyri
sykia males
xoxlakies 0.3
Absorbance
Wavelength (nm)
0.0
0.1
0.2
0.3
0.4
0.5
230
240
250
260
270
280

(c)

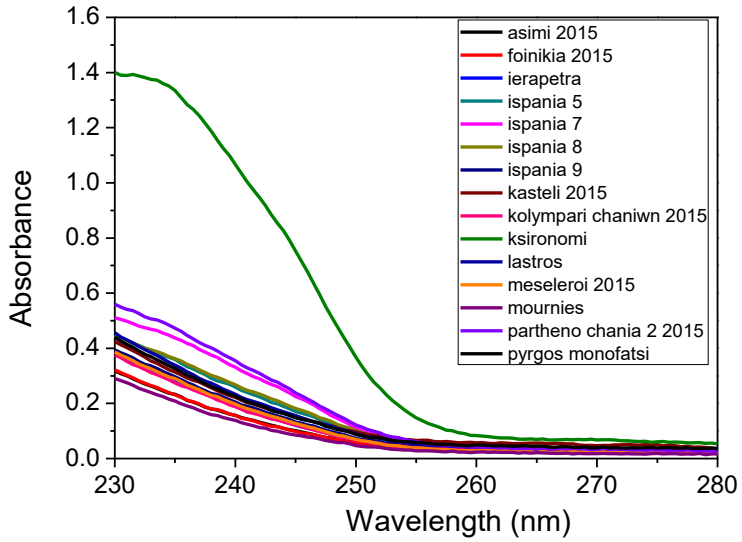
asimi 2015
foinikia 2015
ierapetra
ispania 5
ispania 7
ispania 8
ispania 9
kasteli 2015
kolympari chaniwn 2015
ksironomi
lastros
meseleroi 2015
mournies
partheno chania 2 2015
pyrgos monofatsi
Absorbance
Wavelength (nm)
0.0
0.2
0.4
0.6
0.8
1.0
1.2
1.4
1.6
230
240
250
260
270
280

(d)

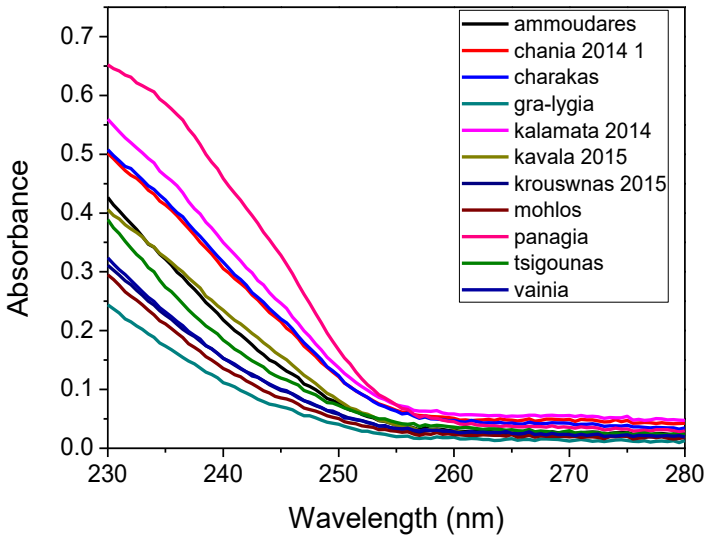
Absorbance
Wavelength (nm)
ammoudares
chania 2014 1
charakas
gra-lygia
kalamata 2014
kavala 2015
krouswnas 2015
mohlos
panagia
tsigounas
vainia

(e)

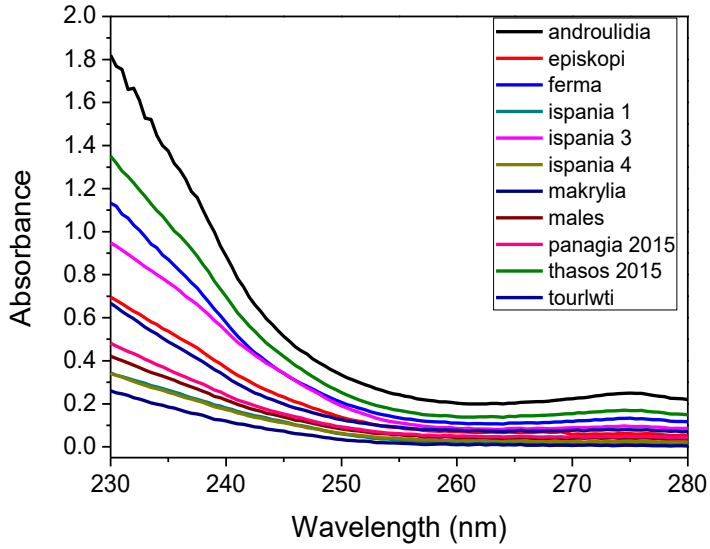
Absorbance
Wavelength (nm)
androulidia
episkopi
ferma
ispania 1
ispania 3
ispania 4
makrylia
males
panagia 2015
thasos 2015
tourlwti

(f)

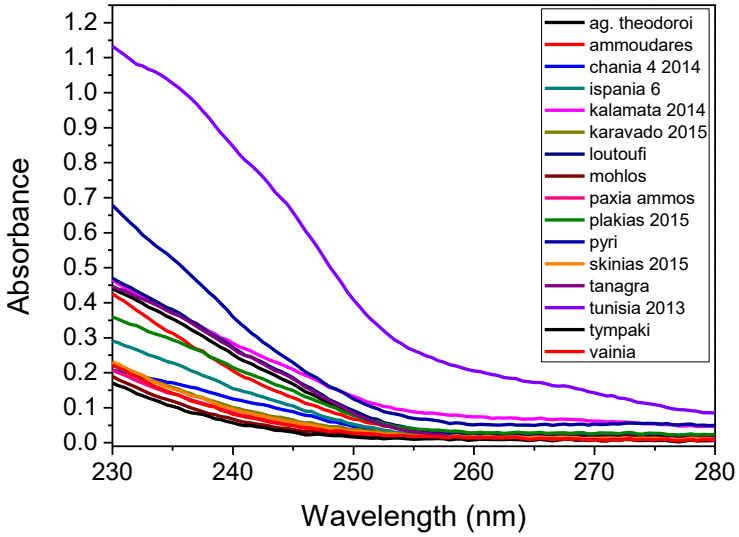

(g)

Figure 6.1.2 (a-g): Absorption spectra in the UV region (230-280nm) of olive oils coming from different geographical origin

Olive oils could present an absorption peak at 235nm in the UV region 230-280nm. This peak may correspond to conjugated dienes. Taking into account the values of absorbance at 232nm, indexes K_{232} can be extracted by the Eq. 4.1 and the following figures show these values (Fig. 6.1.3):

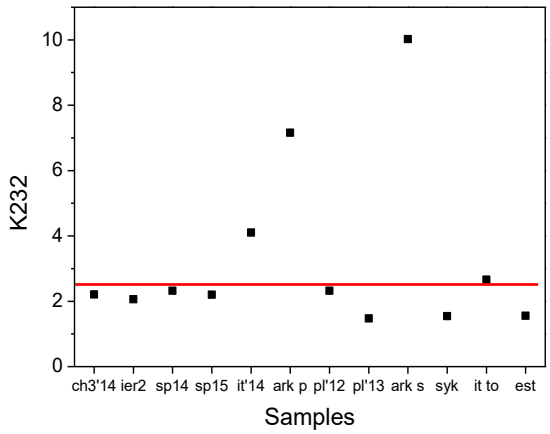

(a)

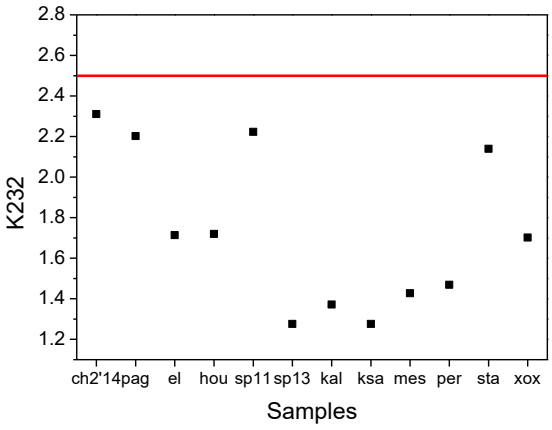
K232
2.8
2.6
2.4
2.2
2.0
1.8
1.6
1.4
1.2
ch2'14pag el hou sp11 sp13 kal ksa mes per sta xox
Samples

(b)

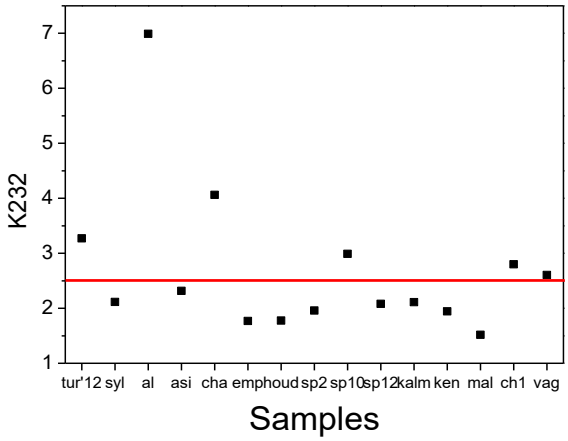
K232
7
6
5
4
3
2
1
tur'12 syl al asi cha emphoud sp2 sp10 sp12 kalm ken mal ch1 vag
Samples

(c)

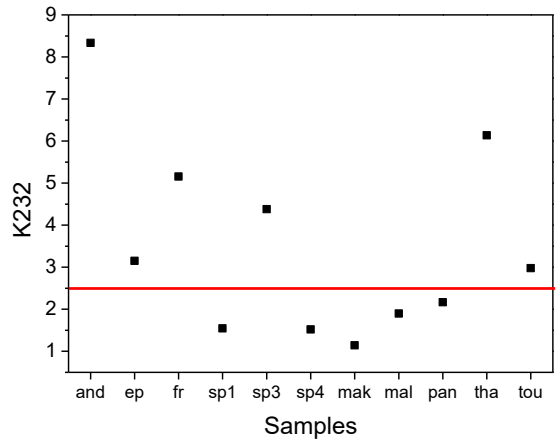
K232
9
8
7
6
5
4
3
2
1
and ep fr sp1 sp3 sp4 mak mal pan tha tou
Samples

(d)

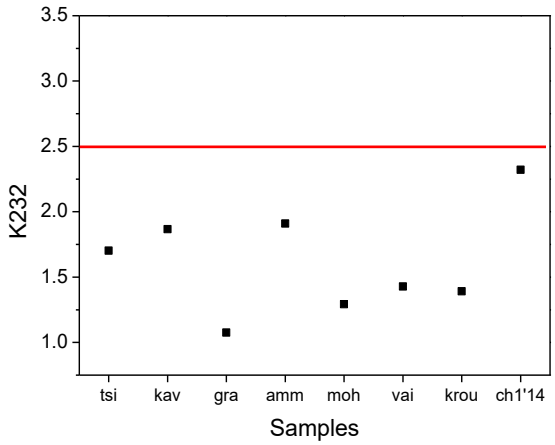
K232
3.5
3.0
2.5
2.0
1.5
1.0
tsi kav gra amm moh vai krou ch1'14
Samples

(e)

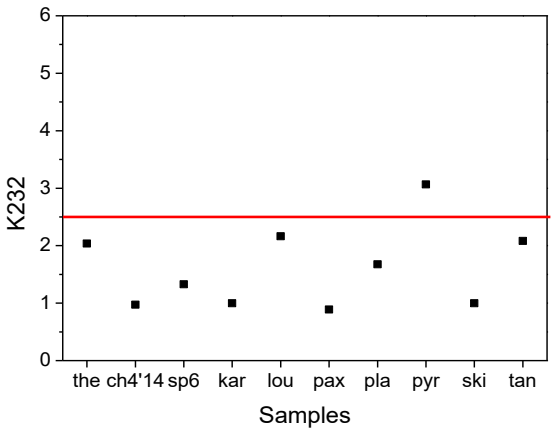
K232
6
5
4
3
2
1
0
the ch4'14 sp6 kar lou pax pla pyr ski tan
Samples

(f)

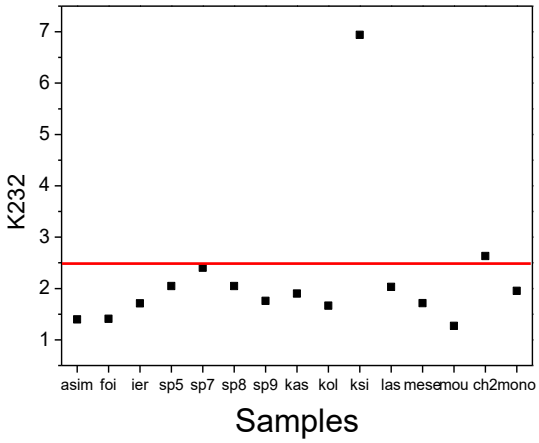

(g)

Figures 6.1.3 (a-g): Indexes K_{232} vs Samples of olive oils. Red line indicate the value limit of K_{232} for extra virgin olive oil.

According to the European instructions *(IOOC, 1991)*, values of index K_{232} should be lower than 2.5 for extra virgin olive oils. It is observed that some oils have a value of K_{232} higher than 2.5. As observed, these oils are olive oil samples that were cultivated the previous years. In conclusion, the olive oils that were cultivated a few years ago and were stored in non-appropriate conditions, present a higher value of index K_{232}.

Moving on to the absorption spectra of olive oils in the UV region (260-410nm), olive oils were diluted 1% v/v in n-hexane and put in a 10mm path length cuvette, using the solvent n-hexane as a background. In figures 6.1.4, the absorption spectra are presented.

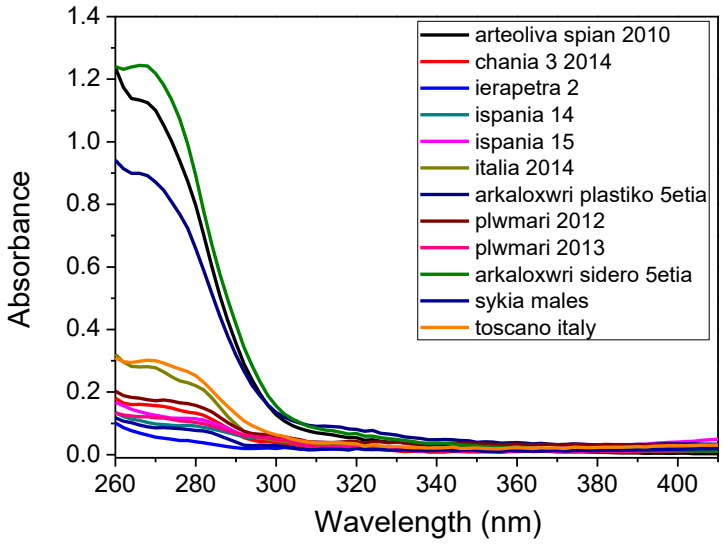

(a)

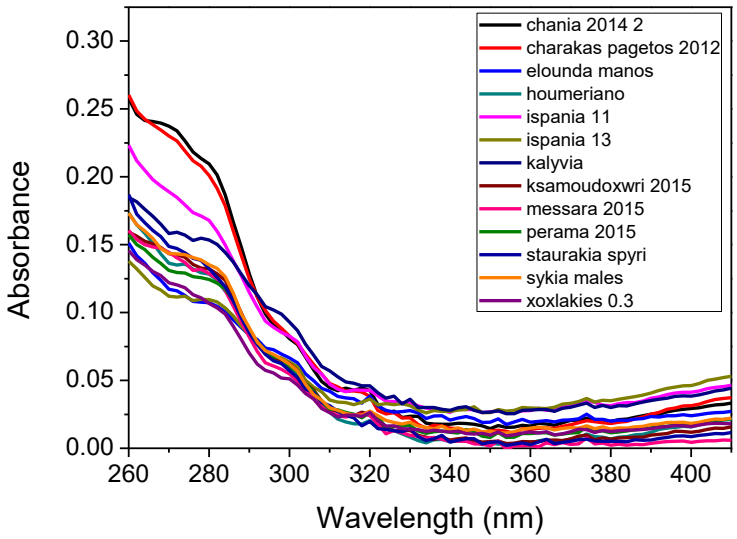
chania 2014 2
charakas pagetos 2012
elounda manos
houmeriano
ispania 11
ispania 13
kalyvia
ksamoudoxwri 2015
messara 2015
perama 2015
staurakia spyri
sykia males
xoxlakies 0.3
Absorbance
0.00
0.05
0.10
0.15
0.20
0.25
0.30
260
280
300
320
340
360
380
400
Wavelength (nm)

(b)

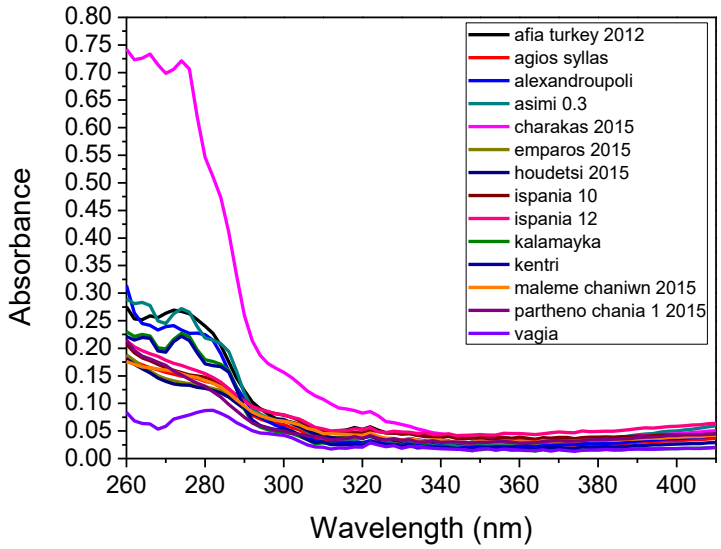
afia turkey 2012
agios syllas
alexandroupoli
asimi 0.3
charakas 2015
emparos 2015
houdetsi 2015
ispania 10
ispania 12
kalamayka
kentri
maleme chaniwn 2015
partheno chania 1 2015
vagia
Absorbance
0.00
0.05
0.10
0.15
0.20
0.25
0.30
0.35
0.40
0.45
0.50
0.55
0.60
0.65
0.70
0.75
0.80
260
280
300
320
340
360
380
400
Wavelength (nm)

(c)

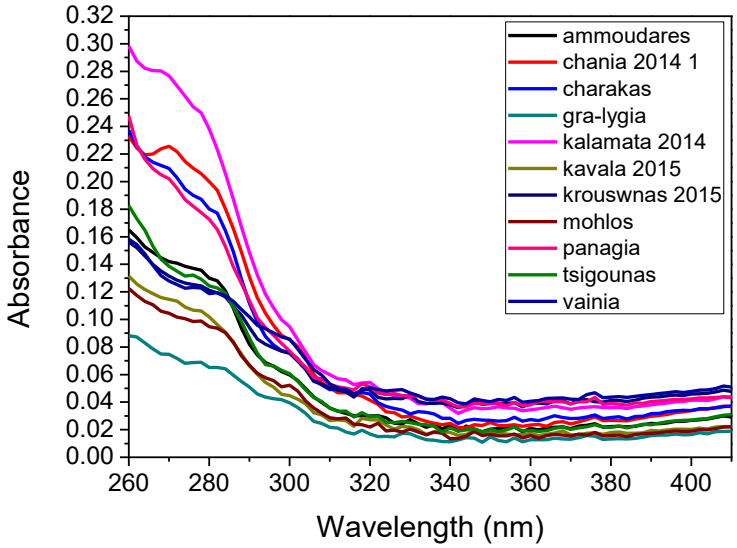
Absorbance
Wavelength (nm)
ammoudares
chania 2014 1
charakas
gra-lygia
kalamata 2014
kavala 2015
krouswnas 2015
mohlos
panagia
tsigounas
vainia

(d)

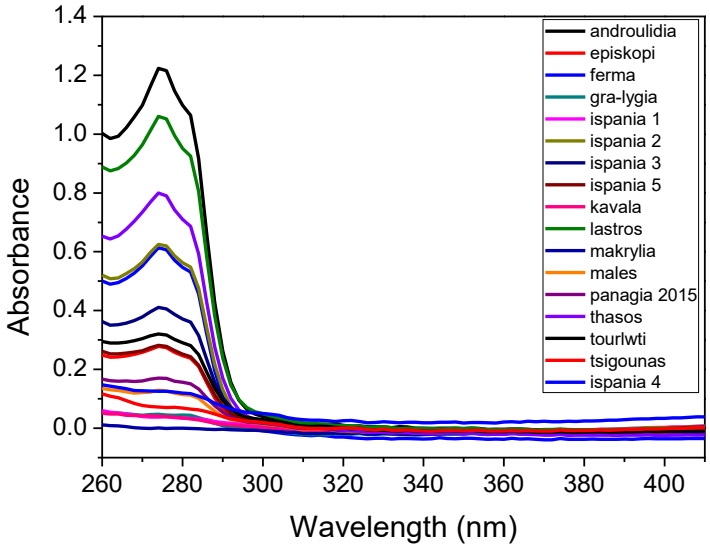
Absorbance
Wavelength (nm)
androulidia
episkopi
ferma
gra-lygia
ispania 1
ispania 2
ispania 3
ispania 5
kavala
lastros
makrylia
males
panagia 2015
thasos
tourlwti
tsigounas
ispania 4

(e)

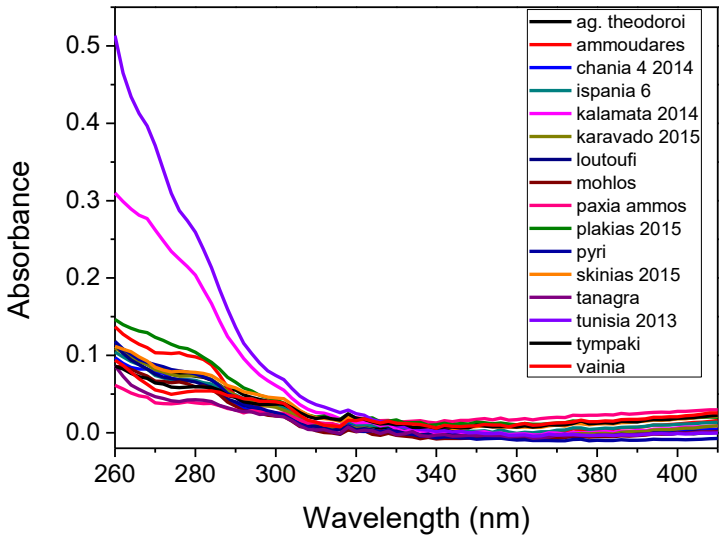

(f)

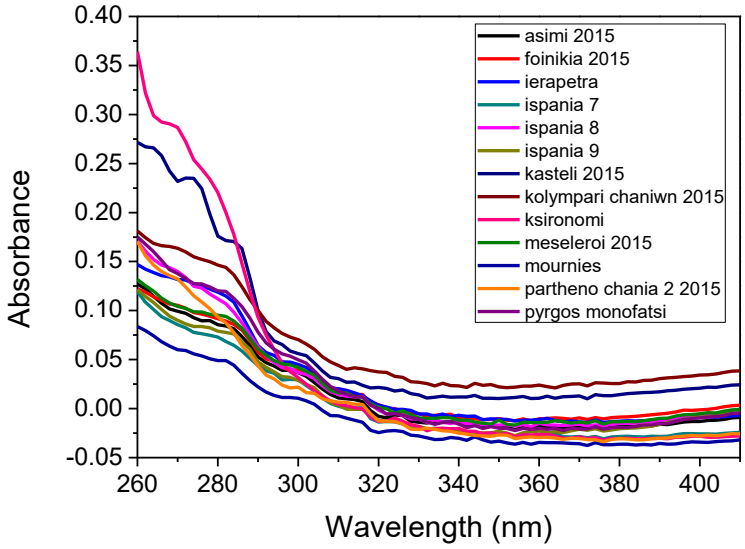

(g)

Figures 6.1.4 (a-g): Absorption spectra at the UV region 260-410nm, 10mm path length cuvette, 1% dilution in n-hexane, background the solvent.

As observed, olive oils have an absorption peak at 275-280nm, which correspond to saturated fatty acids *(Angerosa, Campestre, & Giansante, 2006)*. When the olive oil is fresh, there is no absorption peak at this wavelength. Consequently, we can conclude from the absorption spectra at this UV region that fresh olive oils do not present any absorbance peaks at 275nm. Considering the values of absorbance at 270, 266 and 274nm, we calculated the indexes K_{270} and ΔK according to Eq. 4.1 and 4.2. The following graphs (index K vs samples) show the values of K_{270} and ΔK of the samples (Fig. 6.1.5):

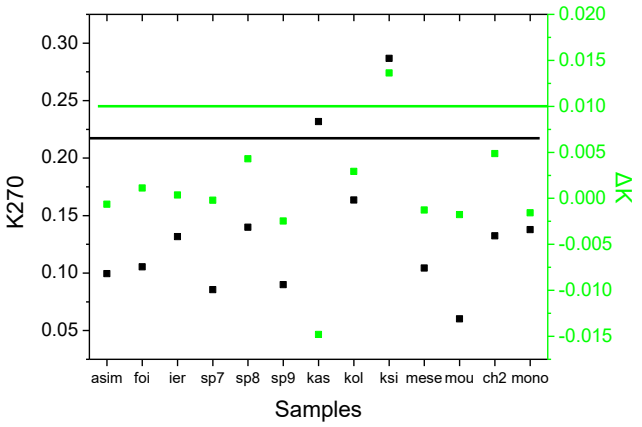
K270
ΔK
0.30
0.25
0.20
0.15
0.10
0.05
0.020
0.015
0.010
0.005
0.000
-0.005
-0.010
-0.015
asim foi ier sp7 sp8 sp9 kas kol ksi mese mou ch2 mono
Samples

(a)

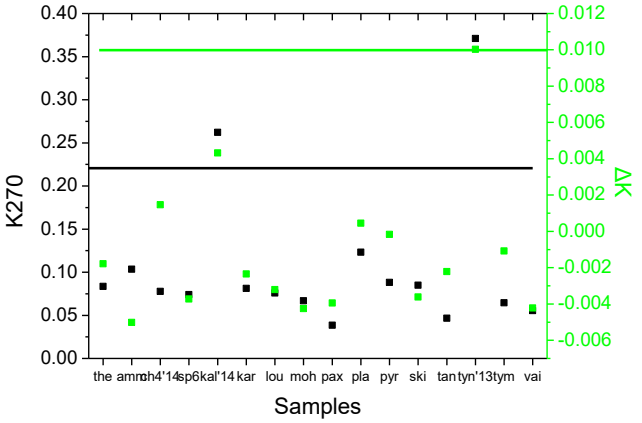
K270
ΔK
0.40
0.35
0.30
0.25
0.20
0.15
0.10
0.05
0.00
0.012
0.010
0.008
0.006
0.004
0.002
0.000
-0.002
-0.004
-0.006
the amm ch4'14 sp6 kal'14 kar lou moh pax pla pyr ski tan tyn'13 tym vai
Samples

(b)

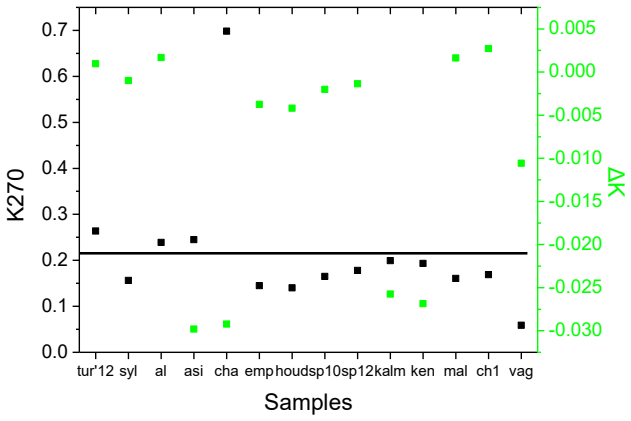
K270
ΔK
0.7
0.6
0.5
0.4
0.3
0.2
0.1
0.0
0.005
0.000
-0.005
-0.010
-0.015
-0.020
-0.025
-0.030
tur'12 syl al asi cha emp houd sp10 sp12 kalm ken mal ch1 vag
Samples

(c)

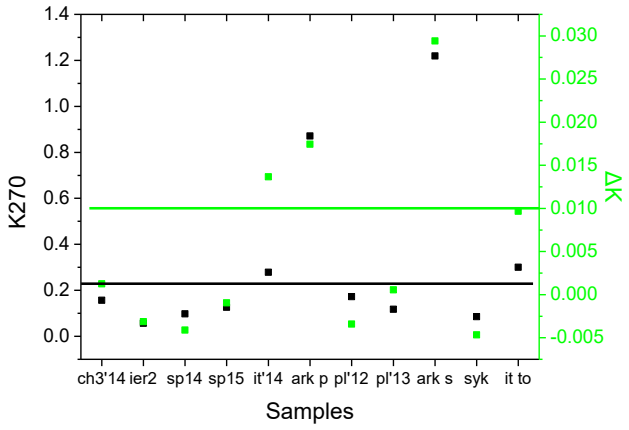
K270
ΔK
Samples
ch3'14 ier2 sp14 sp15 it'14 ark p pl'12 pl'13 ark s syk it to

(d)

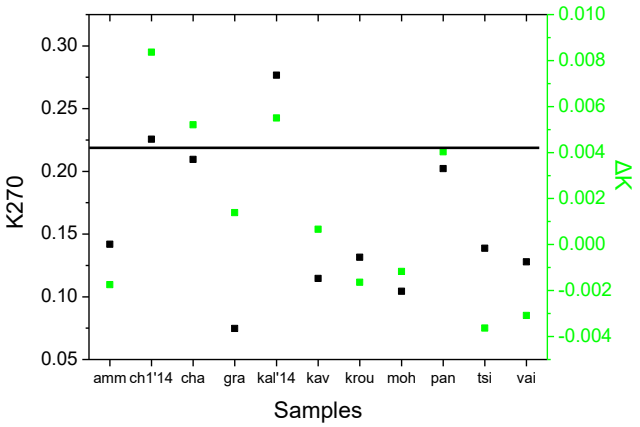
K270
ΔK
Samples
amm ch1'14 cha gra kal'14 kav krou moh pan tsi vai

(e)

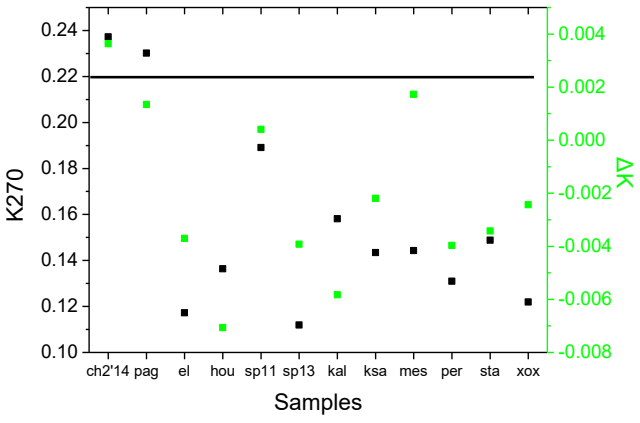
K270
ΔK
Samples
ch2'14 pag el hou sp11 sp13 kal ksa mes per sta xox

(f)

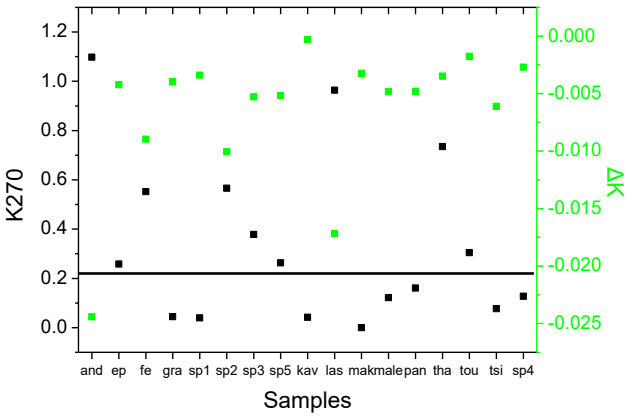

(g)

Figures 6.1.5 (a-g): Index K_{270} and ΔK vs Samples. Black line indicates the value limit of K_{270} for extra virgin olive oil. Blue line indicates the value limit of ΔK for virgin olive oil.

As remarked from the K indexes, there are some olive oils that present higher values of K_{270} and ΔK, showing that they cannot be characterized as extra virgin olive oils, according to European instructions *(IOOC, 1991)*. Note that $0.15<K_{270}<0.22$, $\Delta K<0$ and $\Delta K \leq 0.01$ (Eq. 4.3) so an olive oil to be characterized as extra virgin olive oil. In particular, ΔK index constitutes a criterion of the purity of the oil. The samples that have higher values of these indexes are oils that were cultivated previous years or have not been stored properly.

Collecting all these absorption data at this UV region (260-410nm), PCA was employed (Matlab (R2015b) and PLS-Toolbox used) and the score plot is printed (Fig. 6.1.6). The different colors represent the different geographical origins of olive oils. More specifically:

- Red dots: olive oils coming from Crete, harvested in 2015
- Green dots: olive oils coming from Greece, excluding oils from Crete
- Light Blue dots: olive oils coming from Spain, Italy and other countries out of Greece
- Blue dots: olive oils coming from Greece, excluding oils from Crete, harvested the previous years (before 2015)
- Pink dots: olive oils harvested in 2010

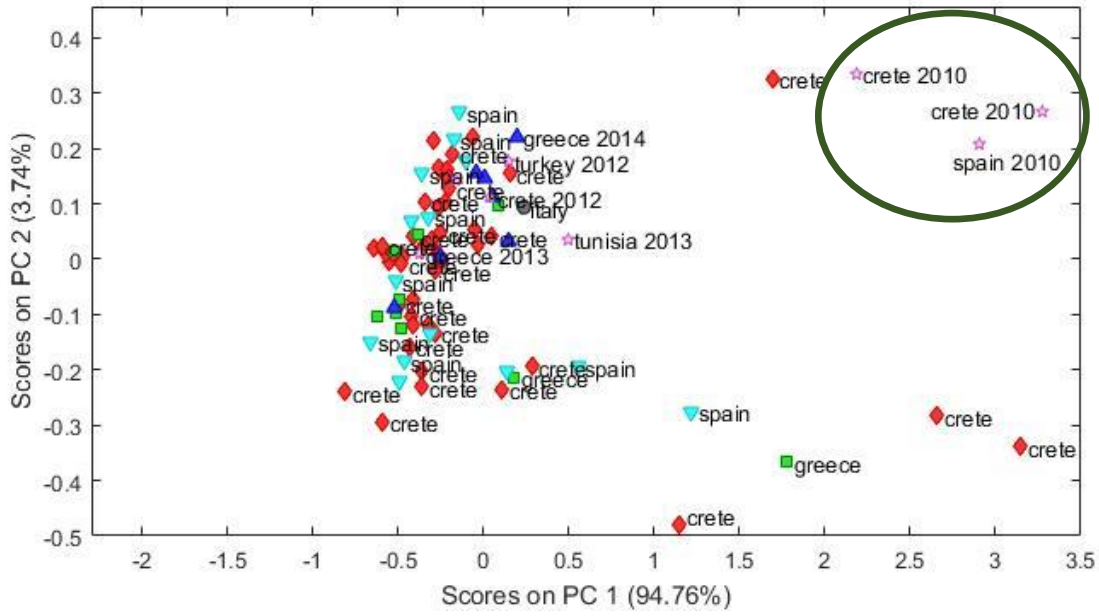

(a)

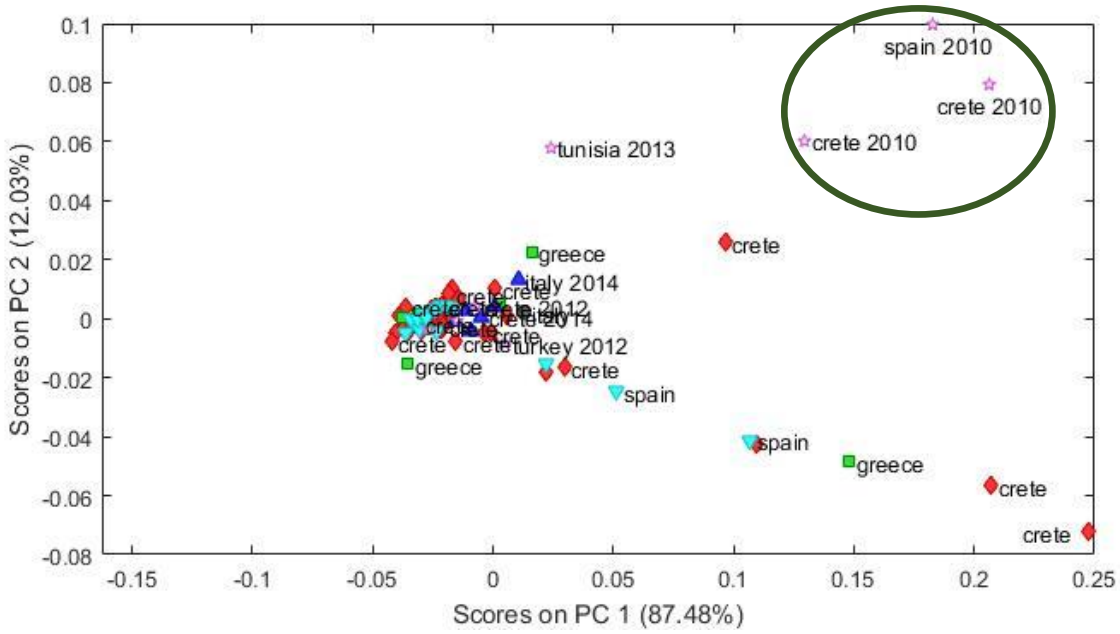

(b)

Figure 6.1.6: Score plot of absorption data at the UV region (260-410nm). (a) Mean-centering pre-treatment of data and leave-one-out cross validation (b) Mean-centering + Savgol 1st derivative pre-treatment of data and leave-one-out cross validation.

As seen in Fig. 6.1.6 (a), Principal Component 1 (PC1) explains the 94.76% of correlation matrices and Principal Component 2 (PC2) the 3.74%. As the absorption data are more pre-treated (Fig. 6.1.6 (b)), PC1 explains the 87.48% and PC2 the 12.03% of the correlation matrices.

Both PCA score plots show a discrimination of older olive oils (harvested in 2010), but there is no other discrimination of oils, based on their absorption spectra at the UV region.

6.1.1.2 Visible region

Measuring the absorbance of olive oils in the visible region 400-800nm with a 2nm step, using a 10mm path length quartz cuvette, different compounds of oils seem to absorb, as seen in Fig. 6.1.7:

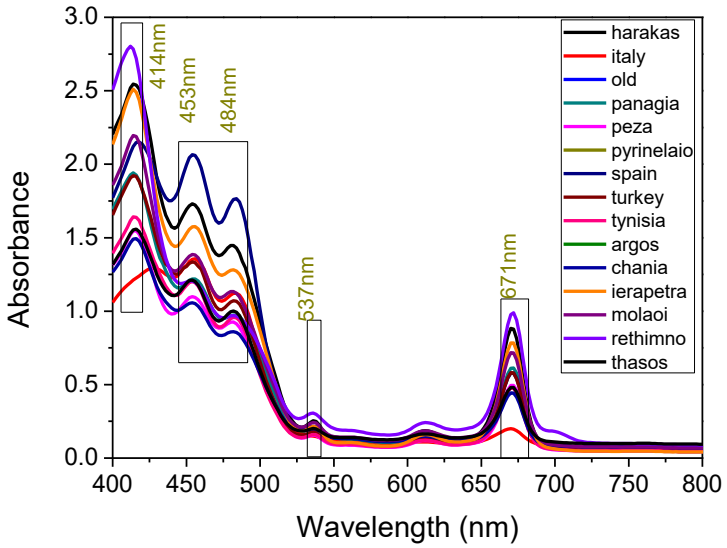

Figure 6.1.7: Absorption spectra of extra virgin olive oils in the visible region (400-800nm) in a 10mm path length quartz cuvette

Absorption peaks at ~ 414, 453 and 484nm correspond to carotenoids, peak at ~537nm to chlorophyll a and the absorbance peak at 671nm is related to the chlorophyll group. Moving on at the near infrared region at wavelengths 800-1600nm, by a 2mm step, the absorption spectra of olive oils, as seen in Fig. 6.1.8 below, present main peaks, at 1208nm and a broad peak 1391-1420nm, which correspond to C-H stretching of CH_3 and CH_2 and 2C-H stretching, respectively. These peaks are the same for all oils, even for seed oils, as we will discuss later.

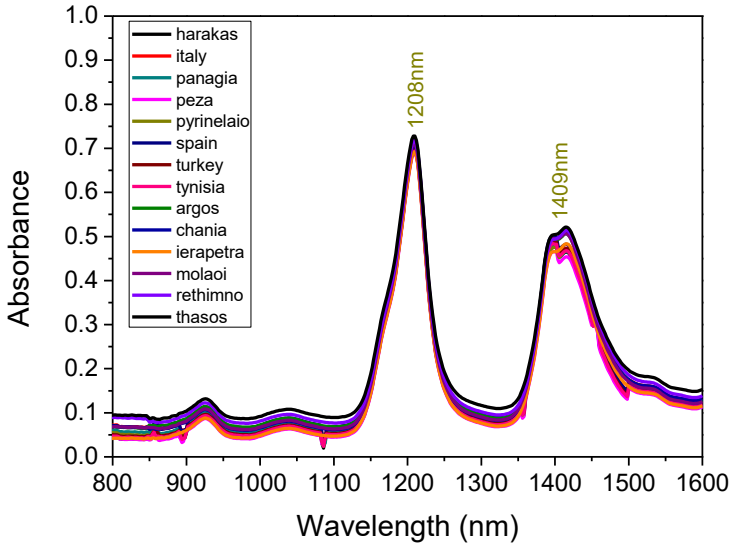

Figure 6.1.8: Absorption spectra of extra virgin olive oils in the near-IR region (800-1600nm) in a 10mm path length quartz cuvette

Moving on to the infrared region 1800-2200nm, with a step of 2nm, employing a quartz cuvette of 10mm path length without any dilution, an absorption spectrum of olive oils is made, as seen in Figure 6.1.9:

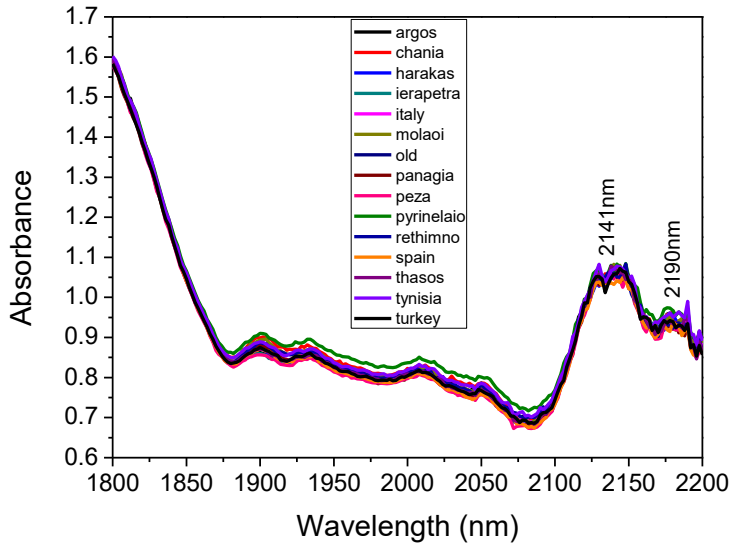

Figure 6.1.9: Absorption spectra of oils at the near IR region (1800-2200nm), step 2nm, cuvette 10mm, undiluted

At this absorbance spectrum, there are two main absorbance peaks at 2141 and 2190nm corresponding to C-H bonds and these peaks are the same in all oils.

Adding more extra virgin olive oil samples from Crete, north Greece and Spain, Italy, Tunisia, Turkey and measure their absorbance at the Visible region 400-800nm, by

2nm step, using a 2mm path length cuvette, without any dilution and air was the background measurement, the absorption spectra is recorded and printed in Figure 6.1.10 below:

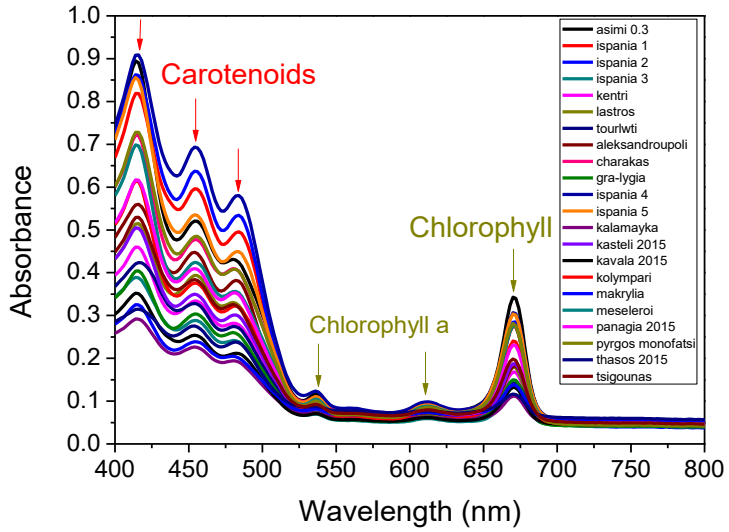

(a)

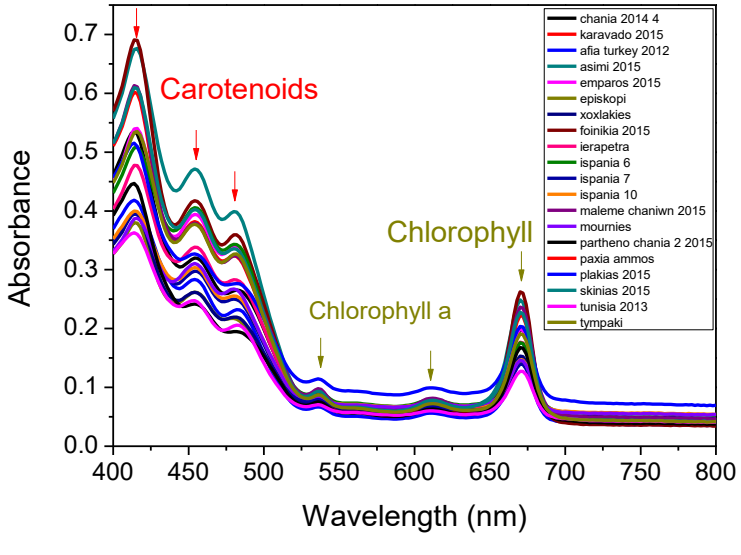

(b)

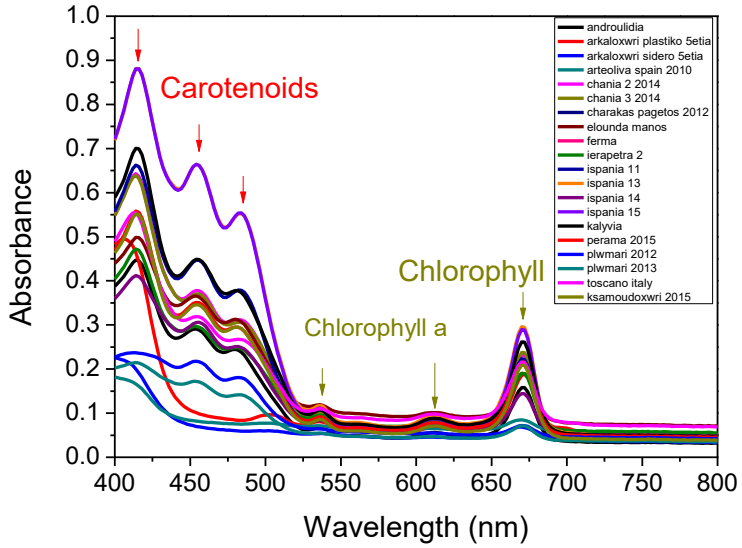
Absorbance
Wavelength (nm)
Carotenoids
Chlorophyll
Chlorophyll a
androulidia
arkaloxwri plastiko 5etia
arkaloxwri sidero 5etia
arteoliva spain 2010
chania 2 2014
chania 3 2014
charakas pagetos 2012
elounda manos
ferma
ierapetra 2
ispania 11
ispania 13
ispania 14
ispania 15
kalyvia
perama 2015
plwmari 2012
plwmari 2013
toscano italy
ksamoudoxwri 2015

(c)

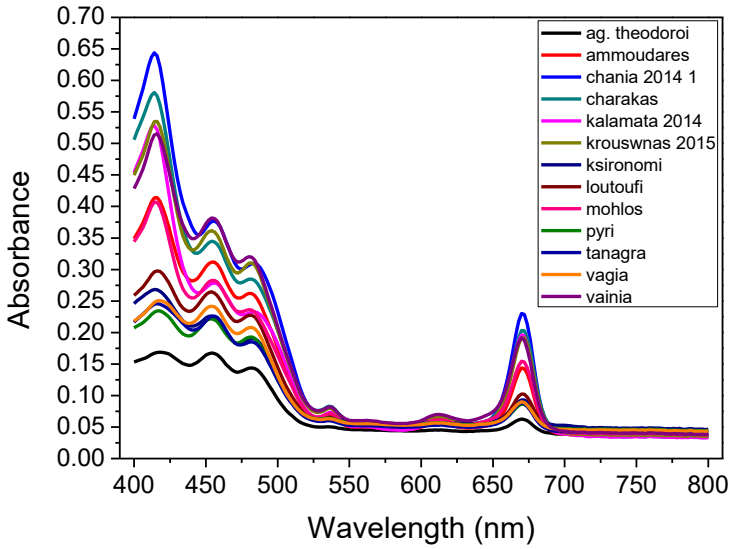
Absorbance
Wavelength (nm)
ag. theodoroi
ammoudares
chania 2014 1
charakas
kalamata 2014
krouswnas 2015
ksironomi
loutoufi
mohlos
pyri
tanagra
vagia
vainia

(d)

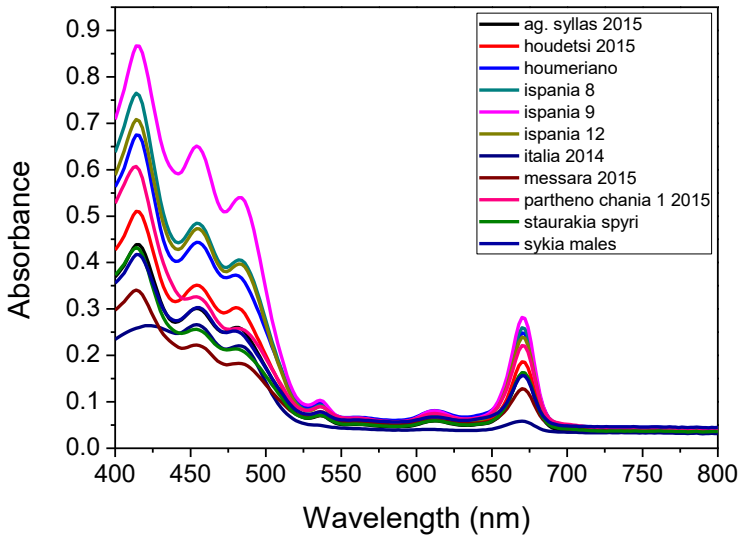

(e)

Figure 6.1.10 (a- e): Absorption spectra of more oils in the visible region 400-800nm, step 2nm, cuvette 2mm path length, undiluted, background is air.

Absorption peaks at 414, 453 and 484nm correspond to carotenoids, peak at 537nm and 625nm to chlorophyll a and the absorbance peak at 671nm is related to the chlorophyll group. Note that most of the olive oils measured were cultivated this year. There are some olive oil samples that were cultivated the previous years and were tagged with their cultivation year. Having all the absorption spectra of the visible region 400-800nm, we categorized the olive oils from their derivation; Crete (oils coming from the island of Crete), Greece (oils coming from Greece, except from Crete), Spain (oils coming from Spain), Italy (oils coming from Italy), Turkey (oils coming from Turkey), Tunisia (oils coming from Tunisia). If oils were cultivated in previous years, the year of cultivation follows the origin. A PCA plot was implemented – using the Matlab2015b and PLS-Toolbox, in order to classify the olive oils by their geographical origin.

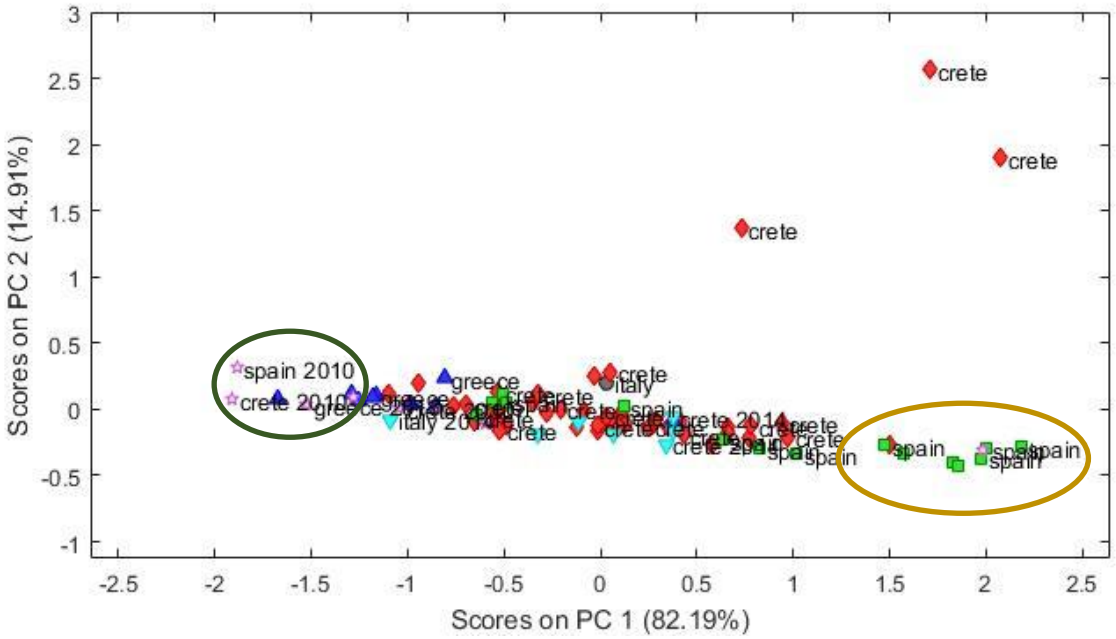

Figure 6.1.11: Score plot of absorbance of olive oils in the visible region, with mean-centering pre-treatment of the data.

As seen at the score plot (Fig. 6.1.11), where PCs correspond to Principal Components of the PCA, there is a good discrimination between the oils of Cretan and Spanish oils. The absorption data were pre-treated with mean centering pre-treatment. Principal Component 1 explains the 82.19% of the correlation matrix and the Principal Component 2 explains the 14.91% of the correlation matrix. It seems that there is a discrimination between the Spanish olive oils and the Cretan olive oils. Additionally, there is a cluster of olive oils that were cultivated the previous years.

Moreover, an extra pre-treatment to the absorption data was used, the SNV (standard normalized variation) pre-treatment and the score plot that is arising is the following (Fig. 6.1.12):

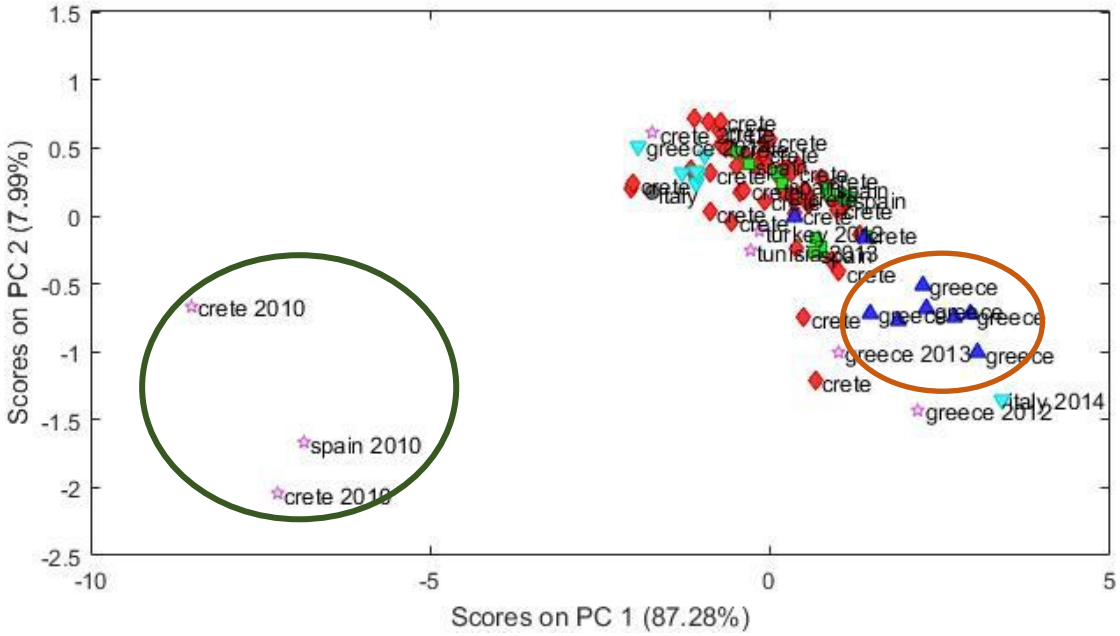

Figure 6.1.12: Score plot of absorbance of olive oils in the visible region, pre-treatment of the data with mean-centering and SNV

Here, the PC1 and PC2 explain the 87.28% and 7.99% of the correlation matrices respectively, showing a group between the oils coming from Greece and a group of oils that are cultivated in previous years, especially in 2010. When mean-centering and second derivative pre-treatments of the absorption data are employed, the result that comes out is shown in the score plot below (Fig. 6.1.13):

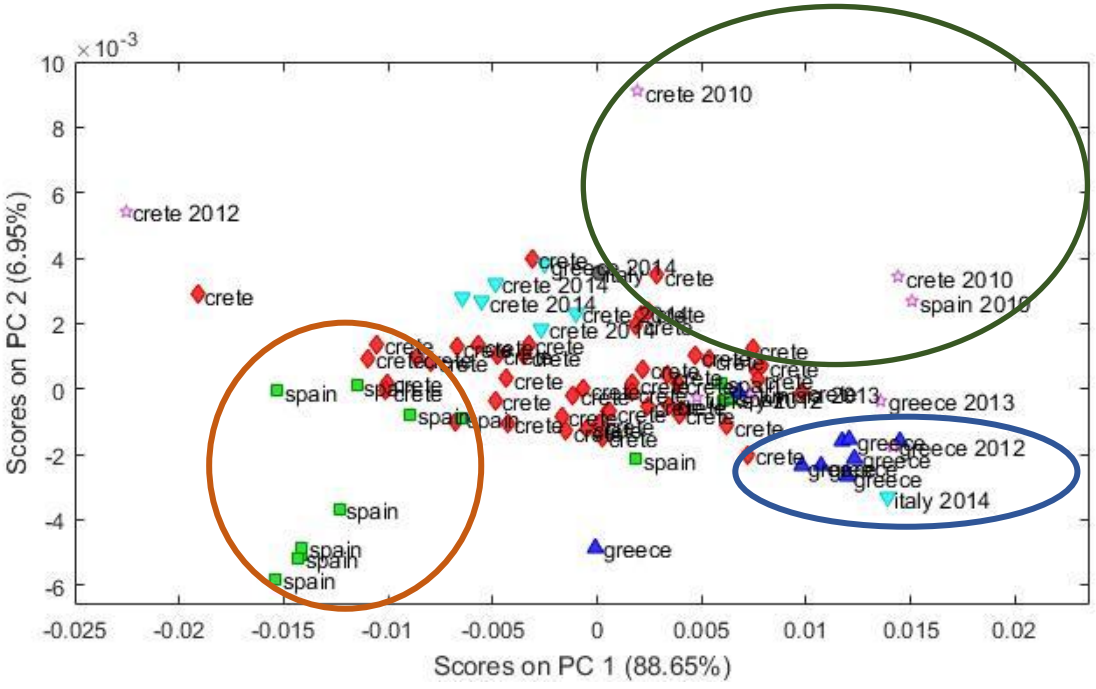

Figure 6.1.13: Score plot of absorbance of olive oils in the visible region, pre-treatment of the data with mean-centering and 2nd derivative.

At this score plot, PC1 and PC2 explain the 88.65% and 6.95% of the correlation matrices, respectively. Again, the olive oils coming from Spain create a cluster and olive oils from Greece create another cluster.

Focusing on a smallest absorption region (400-500nm), where carotenoids absorb – there are three absorption peaks at this region, as shown in Figures 6.1.11 – a new score plot comes out (Fig. 6.1.14), with mean-centering pre-treatment:

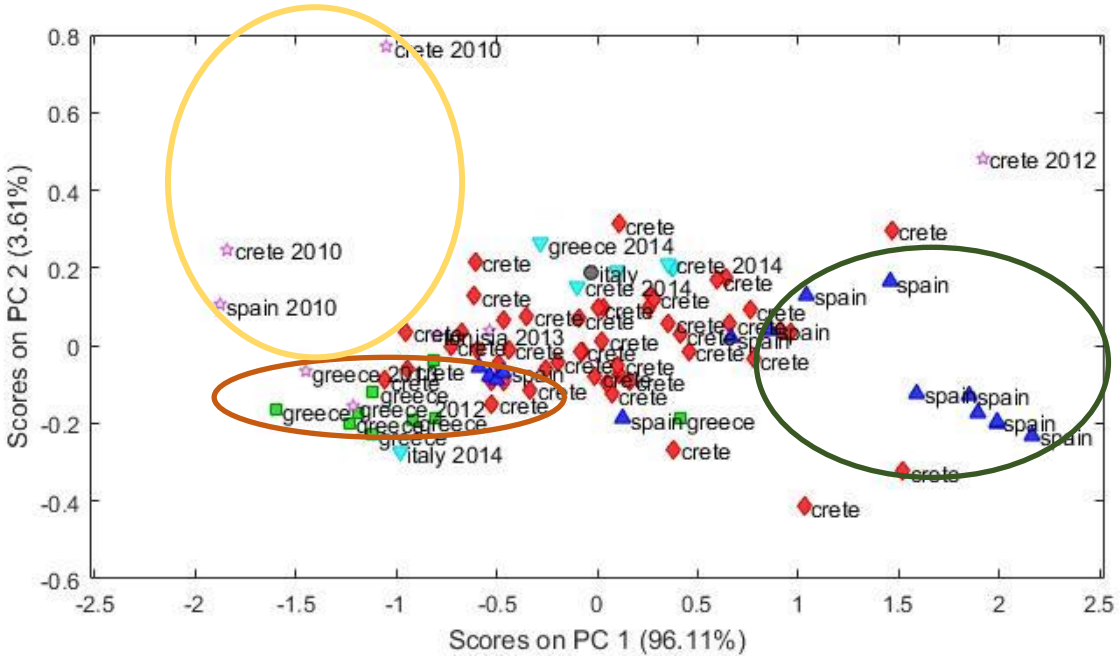

Figure 6.1.14: Score plot of absorbance of olive oils in the visible region (400-500nm), pre-treatment of the data with mean-centering.

At this score plot, PC1 and PC2 explain the 96.11% and 3.61% of the correlation matrices, respectively. A better discrimination of olive oils, based on their geographical origin, is shown. Olive oils from Spain create a cluster, olive oils from Greece create another group and olive oils that were cultivated in 2010 also create a cluster.

SNV pre-treatment of the data is also used to this region (400-500nm) and the score plot is presented in Figure 6.1.15:

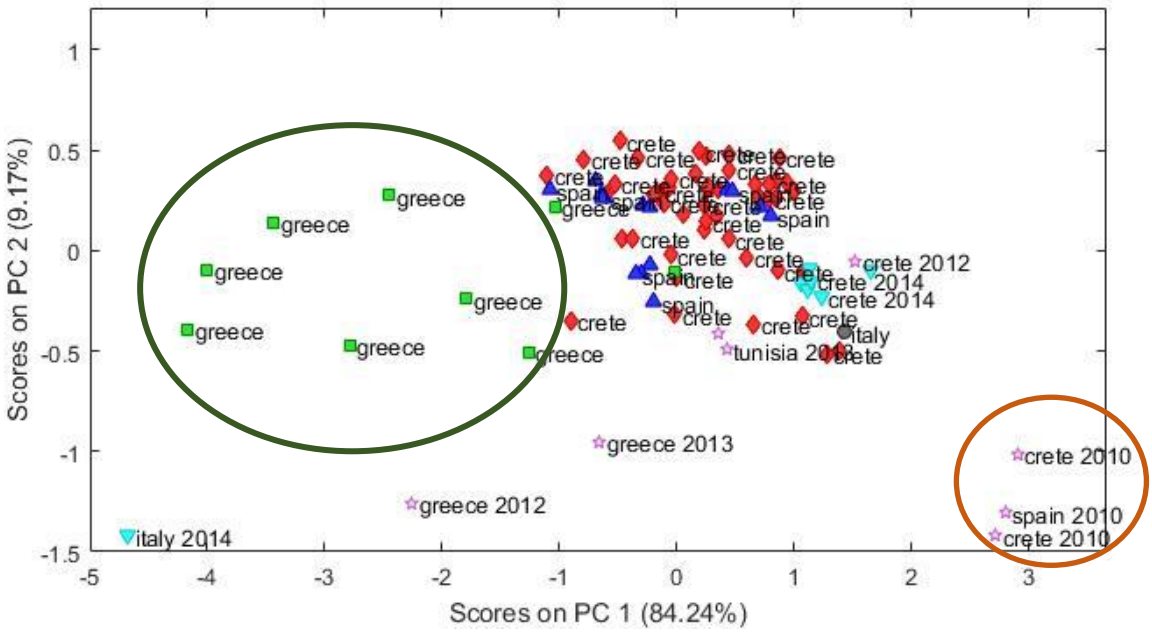

Figure 6.1.15: Score plot of absorbance of olive oils in the visible region (400-500nm), pre-treatment of the data with mean-centering and SNV.

At this score plot, PC1 and PC2 explain the 84.24% and 9.17% of the correlation matrices. As seen in the Figure 6.1.16, the discrimination of the olive oils is getting better. It is clear that there are groups of olive oils, regarding their geographical origin. The olive oils coming from Greece are a special group and are differentiated from the Cretan and Spanish olive oils. Furthermore, olive oils that were cultivated the previous years also make a group.

Consequently, there is a good discrimination between the olive oils coming from different geographical origins, when the absorption in the visible region (400-800nm) is measured. Keep in mind that the olive oils were not diluted with any solvent in order to be measured at this region.

6.1.2 Fluorescence measurements

Olive oil samples that were obtained by the local companies were measured by employing EEFS (Excitation-Emission Fluorescence Spectroscopy). As mentioned in section 4.4, a creation of contour map was achieved as emission spectra were combined when samples were excited in different excitation wavelengths. Front Face geometry was used in all experiments, where the sample was placed at 35^{o} to the incident beam. As already mentioned (see section 4.4), samples were not chemically pre-treated and were placed in a 10mm path length quartz cuvette.

The excitation and emission wavelengths were kept the same in all measurements and these are:

Excitation wavelength region: 270-500nm by a 3nm step

Emission wavelength region: 290-800nm by a 5nm step

Slit of excitation spectrometer: 1nm

Slits of emission spectrometer: 2nm

Integration time: 0.2sec

As observed at the following figure (Fig. 6.1.16), when olive oils are excited at the region 290-300nm, the emission spectrum shows a fluorescence peak at the region 320-340nm, where polyphenols, or more specifically tocopherols emit *(Sikorska, et al., 2004)*. This assignment is based on its similarity to the total luminescence spectrum of α-tocopherol dissolved in n-hexane, Fig. 6.1.18 *(Sikorska, et al., 2004)*. At the excitation region of 320-340nm, the emission spectrum shows the fluorescence of phenolic compounds at 420-460nm. Chlorophylls and pheophytins emit at the region 650-690nm, when excited at 350-430nm *(Eitenmiller, Ye, & Landen, 2008) (Ward, Scarth, Daun, & Thorsteinson, 1994) (Undenfriend, 1962) (Díaz, Merás, Correa, Roldan, & Cáceres, 2003)*.

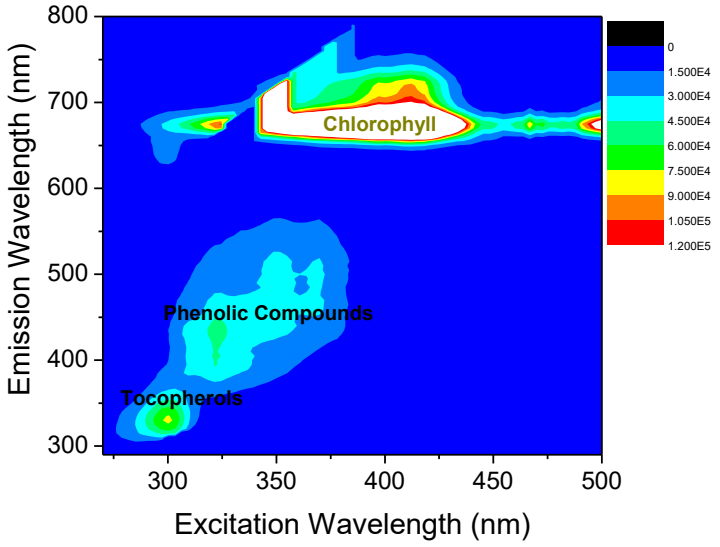

Figure 6.1.16: Contour map of extra virgin olive oil

At the following figure, we can see some characteristic contour maps of virgin olive oils, coming from different geographical origin (Fig. 6.1.17):

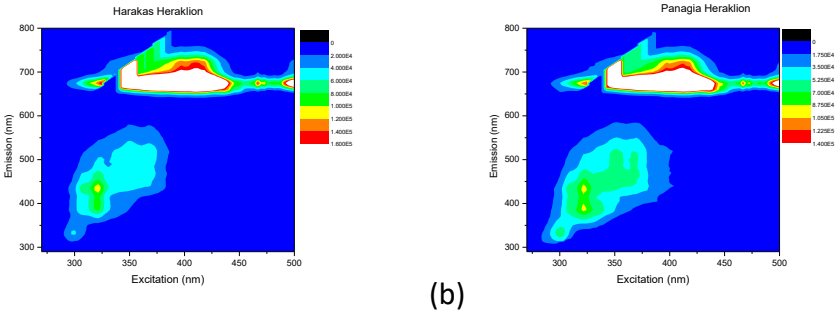

(a) (b)

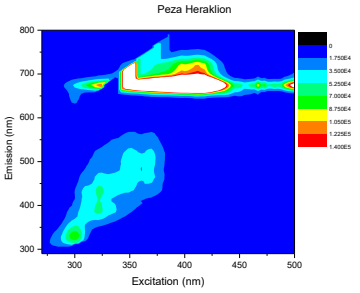
Peza Heraklion
Emission (nm)
Excitation (nm)

(c)

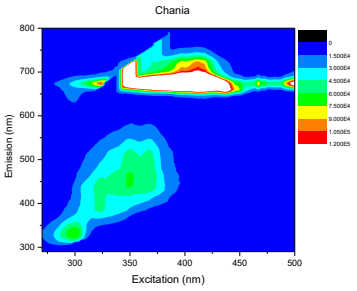
Chania
Emission (nm)
Excitation (nm)

(d)

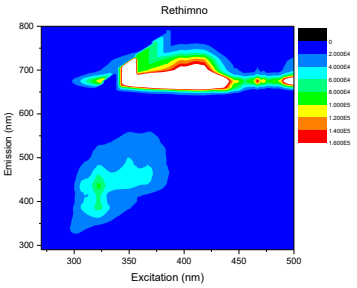
Rethimno
Emission (nm)
Excitation (nm)

(e)

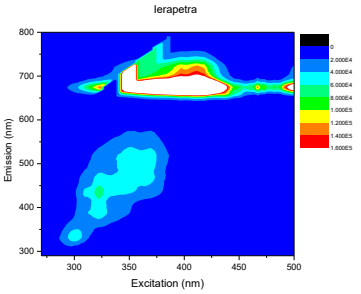
Ierapetra
Emission (nm)
Excitation (nm)

(f)

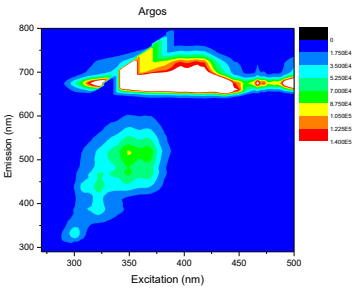
Argos
Emission (nm)
Excitation (nm)

(g)

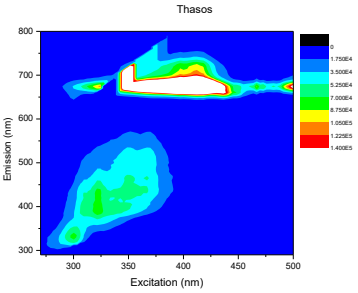
Thasos
Emission (nm)
Excitation (nm)

(h)

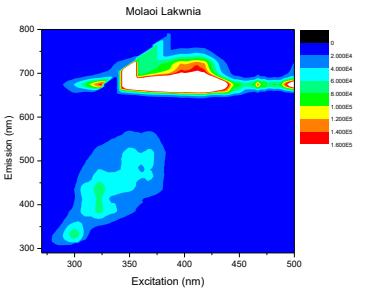
Molaoi Lakwnia
Emission (nm)
Excitation (nm)

(i)

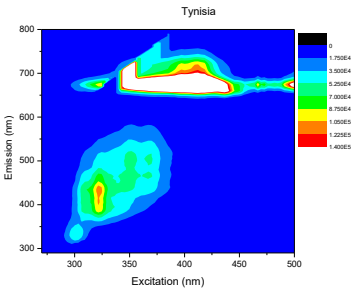
Tynisia
Emission (nm)
Excitation (nm)

(j)

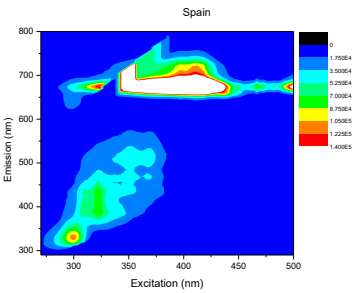
Spain
Emission (nm)
Excitation (nm)

(k)

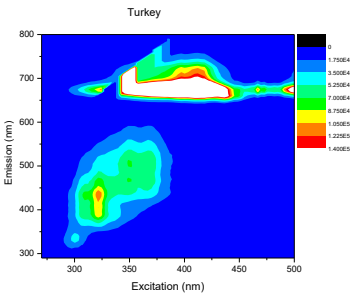
Turkey
Emission (nm)
Excitation (nm)

(l)

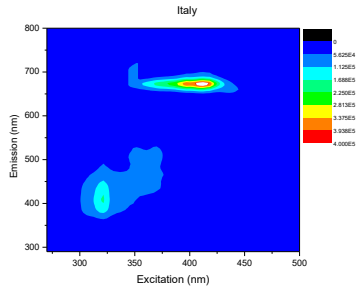

(m)

Figures 6.1.17 (a-m): Contour maps of olive oils from different geographical origin.

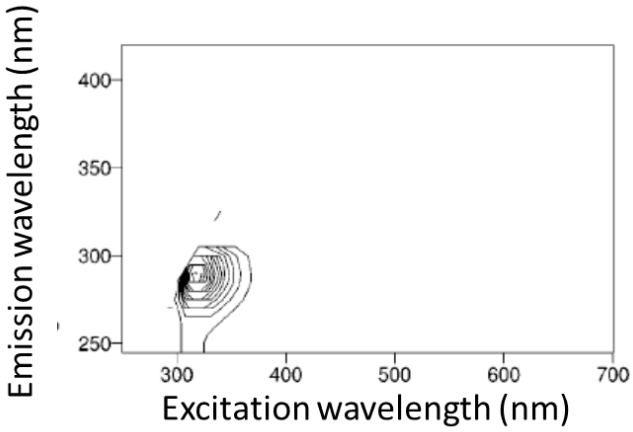

Figure 6.1.18: Contour map (in gray scale) of α-tocopherol in n-hexane

From the contour maps, some small differences between the olive oils are observed. The chlorophylls' fluorescence is very intense compared to the tocopherols' *(Sikorska, et al., 2004)* (Fig. 6.1.18) and the other phenolic compounds' fluorescence. When a discrimination of olive oils is needed and these data are inserted to a statistical model, emission range over 600nm is excluded, because of the intense emission of chlorophylls.

6.2 Absorption and Fluorescence of olive oils based on the olive's variety

Olive oils come from the crop of olive tree. There are some varieties of olives through Crete. As a result, the olive oils consumed contain either one variety of olive or a mixture of the varieties, depending on the region of cultivation, the olive press and the ground. In this section, three different varieties of olives cultivated generally in Crete will be studied from their products, olive oils. The three varieties of olives studied are: Korwneiki (κορωνέικη ή ψιλολιά in Greek), Tsounati (τσουνάτη in Greek) and Xontrolia (χοντρολιά in Greek). These olives are cultivated in Crete, in various regions of the island. Samples of Tsounati and Xontrolia come from the south coast of Heraklion (Γερμανάκη Ελευθερία, ΕΑΣΡ) and the samples of Korwneiki come from Rethymno, Chania and Ierapetra (Παπαδάκης Ε. Μιχαήλ Ο.Ε.).

6.2.1 Absorption measurements

6.2.1.1 UV region (220-410nm)

The absorbance measurements of the olive oils, being made from one variety of olives, have been prepared by using the Perkin Elmer spectrophotometer. All samples were diluted 1% v/v in n-hexane and were put in 2mm and 10mm path length quartz cuvettes, depending on the region of wavelengths measured. In all measurements, the background measured was the solvent n-hexane placed in the respective cuvette for the desirable wavelength region used.

At the UV region and more specifically at the wavelength region of 220-280nm (0.5nm interval), the olive oil absorbance measured is recorded, by using a 2mm path length cuvette and is shown in Fig. 6.2.1 below:

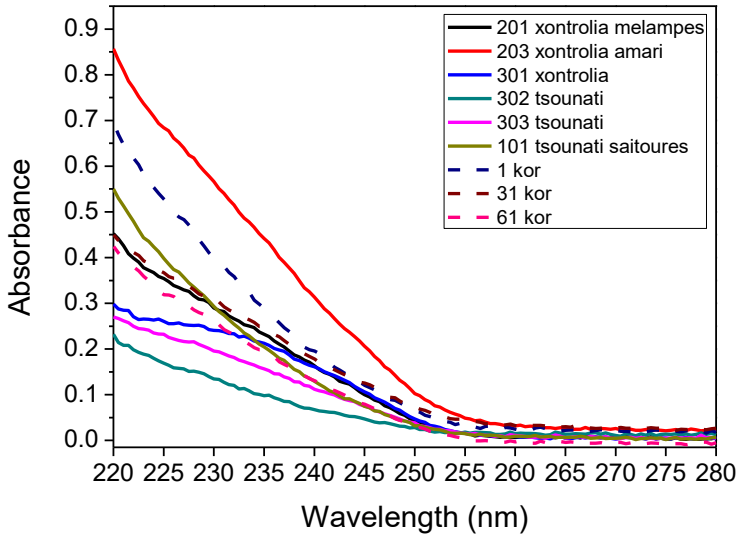

Figure 6.2.1: Absorbance measurements of different varieties of olive oils at 220-280nm wavelength region.

From the absorption spectrum above (Fig. 6.2.1), a discrimination of the varieties cannot be extracted. It can be observed that olive oils coming from Tsounati variety show lower absorbance values than Korwneiki variety. Taking into account the values of absorbance at 232nm, we calculated the index K_{232} for these oils and the graph presenting these results is cited below (Fig. 6.2.2):

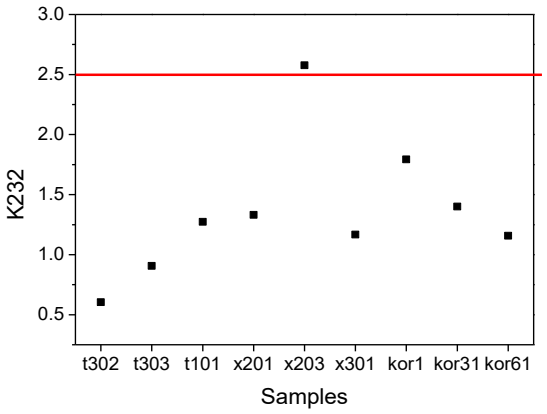

Figure 6.2.2: Index K_{232} vs Samples. Symbols: t corresponds to variety Tsounati, x to variety Xontrolia and k to variety Korwneiki

Samples are coded as: t corresponds to Tsounati olive variety, x corresponds to Xontrolia olive variety and k to Korwneiki olive variety. Numbers show the number of sample, as the company coded them. One can observe that sample "203 x", corresponding to Xontrolia olive variety has a little higher value of index K_{232}. This may be a mistake while measured.

Moving on to the UV region of 260-410nm wavelengths (step was 2nm), olive oils were diluted 1% v/v in n-hexane and were put in a 10mm path length quartz cuvette. The following figure (Fig. 6.2.3) shows the absorbance measured for the different olive oil varieties:

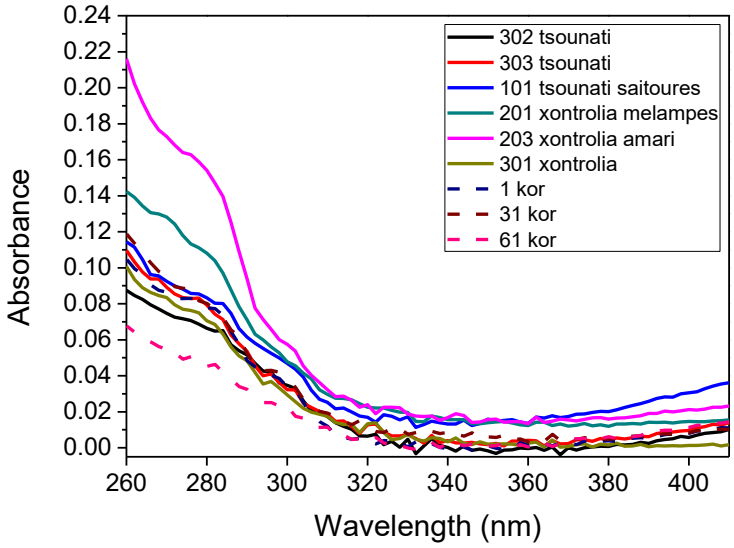

Figure 6.2.3: Absorbance measurements of olive oils at the wavelength region of 260-410nm

The variety of olive Xontrolia presents higher values of absorbance compared to the other varieties, showing a peak absorption at 280nm, which correspond to phenols.

As mentioned before, all codes used are the same. Considering the absorbance values at 266, 270 and 274nm and equations 4.1 and 4.2, the graph presenting the indexes K_{270} and ΔK versus the samples is shown below (Fig. 6.2.4):

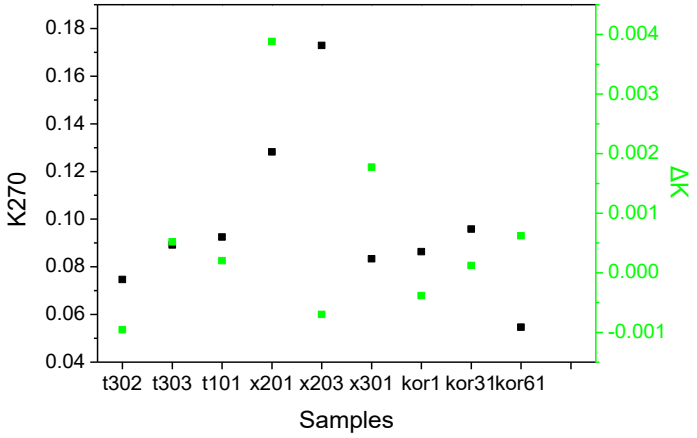

Figure 6.2.4: Indexes K_{270} and ΔK vs Samples. Symbols: t corresponds to variety Tsounati, x to variety Xontrolia and k to variety Korwneiki

Both K indexes values are lower than the limits for extra virgin olive oil. That means that all olive oil samples can be characterized as extra virgin olive oil, taking into account these calculations. The variety Xontrolia seem to have higher values of K_{270} and ΔK indexes than the other two varieties, but it is not significant.

6.2.1.2 Visible region (400-800nm)

Measuring the absorbance at the visible region of the electromagnetic spectrum, at wavelengths 400-800nm, by a 2nm interval, the oils were undiluted and a 2mm path length quartz cuvette was employed. The absorption spectra are printed (Fig. 6.2.5):

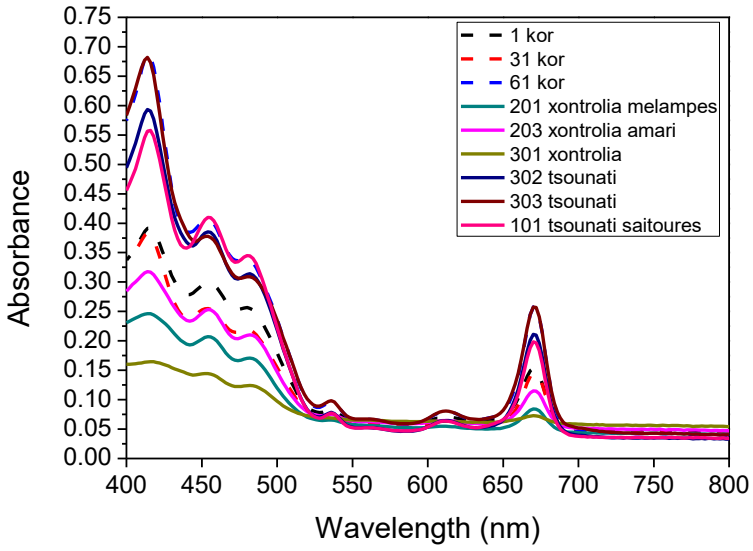

Figure 6.2.5: Absorption spectra of olive oils coming from different varieties of olives in the visible region 400-800nm.

A discrimination of the oils coming from different olive varieties is observed. Tsounati variety presents higher values of absorbance, Korwneiki variety follows and Xontrolia variety presents the lower absorbance values. The main absorbance peaks at this wavelength region are:

- Peaks at wavelengths 414, 453 and 484nm correspond to carotenoids,
- Peaks at 537nm and 620nm to chlorophyll a and pheophytins, and
- Peak at 671nm is related to the chlorophyll group.

Consequently, discrimination of the olive variety can be achieved by the absorption spectra in the visible region (400-800nm).

6.2.1.3 Correlation of absorbance spectra with PCA

In the visible region (400-800nm) we entered the absorbance spectra in the PCA model (via Statistica), in order to see if the different olive varieties can be discriminated. The results are shown in the following graph (Fig. 6.2.6):

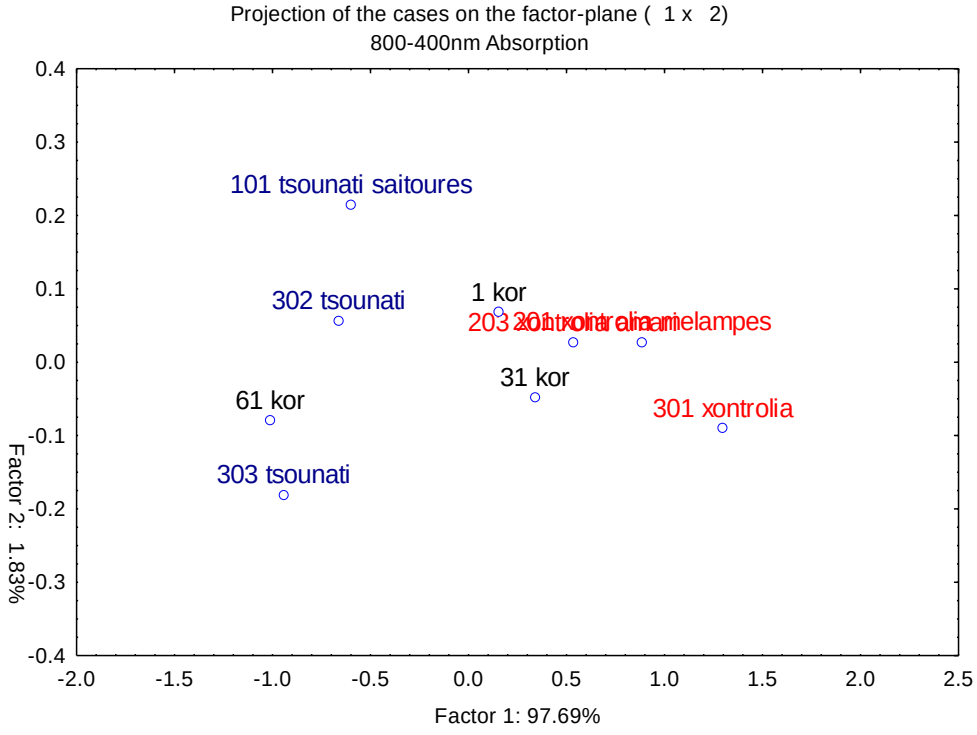

Figure 6.2.6: Score plot of the different olive varieties in the visible region.

Factors 1 and 2 are the principal components 1 and 2 respectively, explaining the 97.69% and 1.83% of the data. It is observed that the Xontrolia variety oils are grouped.

Moving on to the absorption spectra in the UV region (260-410nm), the score plot printed below does not present any olive discrimination (Fig. 6.2.7):

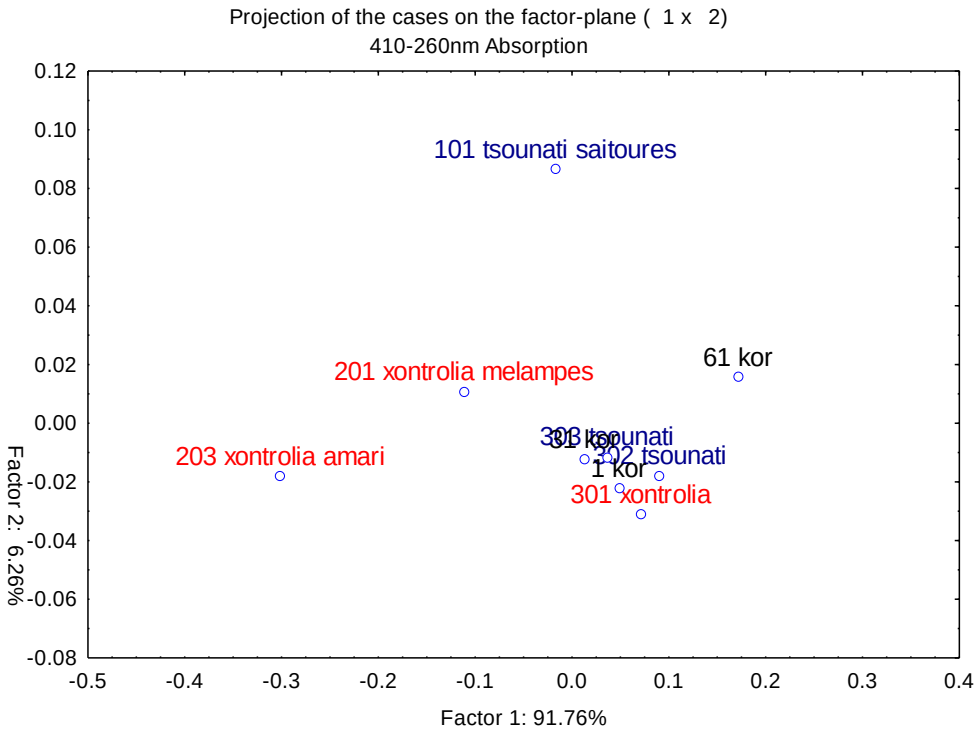

Figure 6.2.7: Score plot of the different olive varieties in the UV region (260-410nm) (PC1: 91.76%, PC2: 6.26%)

The last absorbance region studied is 220-280nm. The score plot is presented below (Fig. 6.2.8):

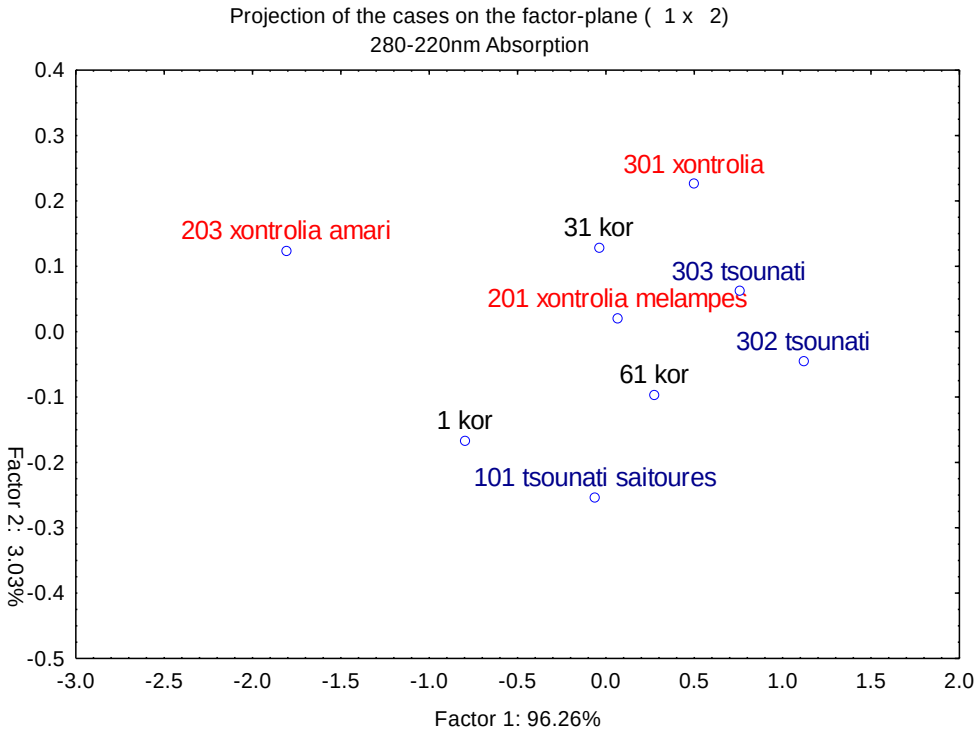

Figure 6.2.8: Score plot of the different olive varieties in the UV region (220-280nm) (PC1: 96.26%, PC2: 3.03%)

The discrimination of olive varieties by employing absorption measurements and PCA cannot be achieved, due to the fact that the samples are few.

6.2.2 Fluorescence measurements

By employing EEFS (see section 4.4), a creation of contour map was achieved as emission spectra were combined when samples were excited in different excitation wavelengths. Front Face geometry was used in all experiments, where the sample was placed at 35° to the incident beam. As already mentioned (see section 4.4), samples were not chemically pre-treated and were placed in a 10mm path length quartz cuvette.

The excitation and emission wavelengths were kept the same in all measurements and these are:

Excitation wavelength region: 270-500nm by a 3nm step

Emission wavelength region: 290-800nm by a 5nm step

Slit of excitation spectrometer: 1nm

Slits of emission spectrometer: 2nm

Integration time: 0.2sec

The contour maps following show the fluorescence of the oils made from different olive varieties (Fig. 6.2.9):

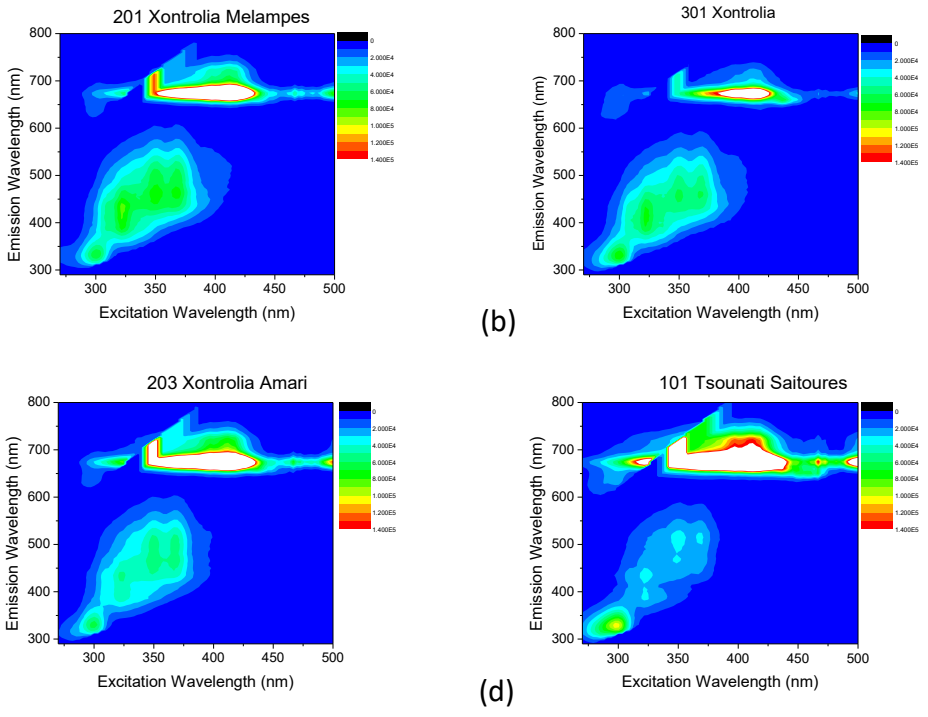

(a) (b)

(c) (d)

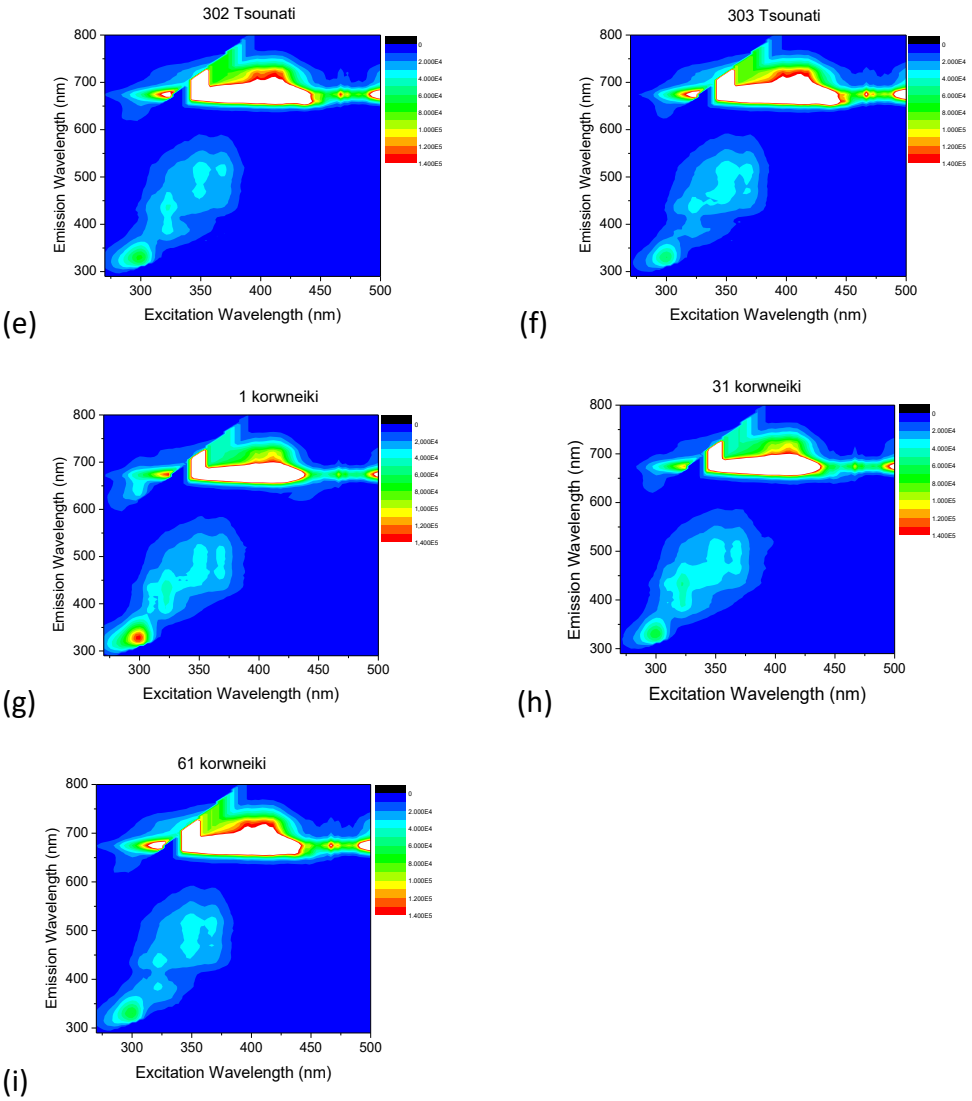

Figures 6.2.9 (a-i): Contour maps of oils from different olive varieties

When olive oils are excited at the region 290-300nm, the emission spectrum shows a fluorescence peak at the region 320-340nm, where polyphenols, or more specifically, tocopherols emit (Sikorska, et al., 2004). At the excitation region of 320-340nm, the emission spectrum shows the fluorescence of phenolic compounds at 420-460nm. Chlorophylls and pheophytins emit at the region 650-690nm, when excited at 350-430nm *(Eitenmiller, Ye, & Landen, 2008) (Ward, Scarth, Daun, & Thorsteinson, 1994) (Undenfriend, 1962) (Díaz, Merás, Correa, Roldan, & Cáceres, 2003)*.

It can be observed that there are differences at the fluorescence maps of the different varieties of olives. Tsounati variety, such as Korwneiki variety, presents intense fluorescence at the wavelength region 320-340nm, when excited at 290-310nm, corresponding to tocopherols' fluorescence *(Sikorska, et al., 2004)*. In contrast to Xontrolia variety, that present an intense fluorescence at the wavelength region 420-460nm, when excited at 320-360nm, which correspond to phenolic compounds. Chlorophylls' fluorescence is about the same for all varieties of olives.

Because the chlorophyll's fluorescence is high enough and information from the excitation-emission map could be "lost" for the compounds that fluoresce at the wavelength region under 600nm, excitation-emission maps were collected, by measuring the fluorescence of oil's compounds, when excited at wavelength regions of 270-397nm and emitted at 290-595nm:

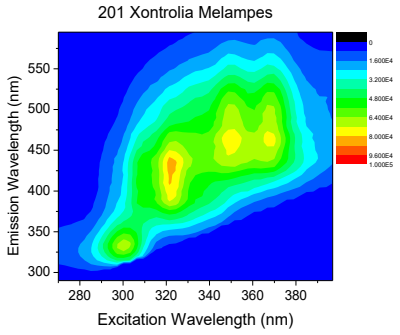

(a)

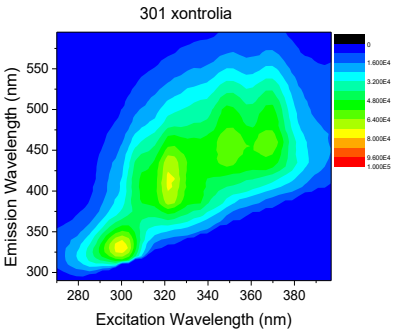

(b)

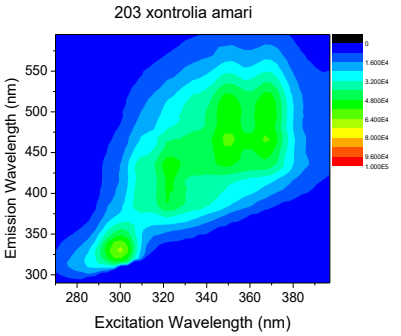

(c)

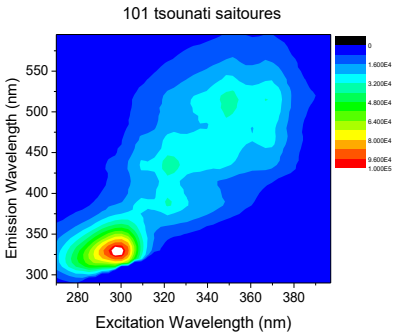

(d)

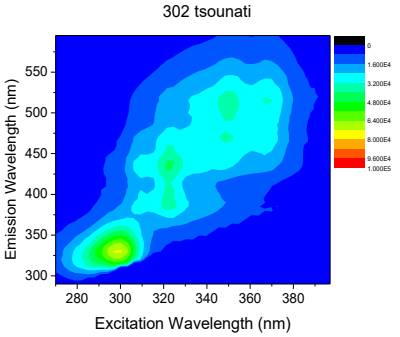

(e)

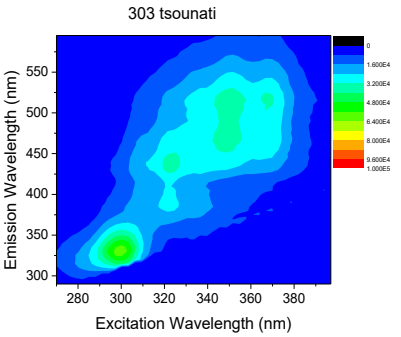

(f)

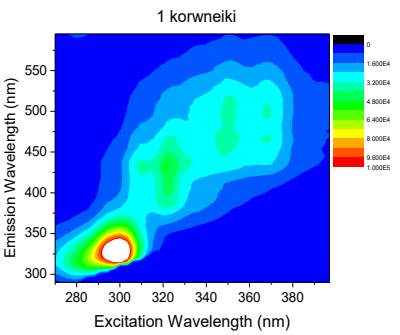

(g)

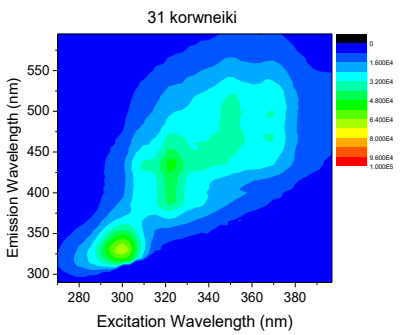

(h)

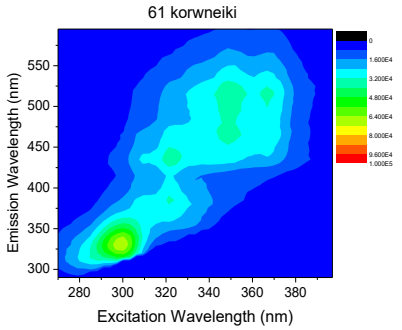

(i)

Figures 6.2.10 (a-i): Contour maps of oils from different olive varieties, excluding the chlorophylls's fluorescence

It can be observed clearly from Fig. 6.2.10 that the olive oil varieties present different fluorescence profiles. Xontrolia variety presents a higher fluorescence band at 425-430nm, when excited at 320-325nm and two other bands at 460nm, when excited at 350 and 368nm, which correspond at phenolic compounds. Tsounati variety shows an intense fluorescence at 330nm, when excited at 300nm, which correspond to tocopherols, and two other fluorescence bands at 435 and 510nm, when excited at 325 and 350nm, respectively. Korwneiki variety seems to fluoresce intensely at 330nm, when excited at 300nm, which correspond to tocopherols, and there are also three other bands of excitation/emission at 323/425, 350/467 and 370/494nm.

6.3 Absorption and Fluorescence of olive oils based on the olive's variety and cultivation year

Virgin olive oils were collected from ΕΡΓΑΣΤΗΡΙΟ ΤΕΧΝΟΛΟΓΙΑΣ ΤΡΟΦΙΜΩΝ in Chania in collaboration with Mrs. Barbopoulou and Dr. Antoniou. Different varieties of olives were collected to make the olive oils presented at this section in two serial years (2014 and 2015) and in two different maturation stages.

These olive varieties, the two different maturation stages and the years collected are shown in the following table (Table 6.3.1):

Olive varieties	2015 1st stage	2015 2nd stage	2014 1st stage	2014 2nd stage
Dafnelia	22/10/15	6/11/15		19/11/14
Korwneiki	22/10/15	6/11/15	31/10/14	19/11/14
Koutsourelia	30/10/15	12/11/15	13/11/14	25/11/14
Thiaki	30/10/15	12/11/15	13/11/14	25/11/14

Table 6.3.1: Four different olive varieties, cultivation year and maturation stages

The names in Greek are: Δαφνελιά for Dafnelia, Κορωνέικη for Korwneiki, Κουτσουρελιά for Koutsourelia and Θιακή for Thiaki.

We tested these samples employing Absorption and Fluorescence Spectroscopy and correlated with PLS regression the absorption spectra with characteristics of olive oils, provided by the collaborating lab in Chania.

6.3.1 Absorption measurements

The absorbance measurements were achieved using the portable spectrometer K-MAC.

6.3.1.1 Visible region (400-800nm)

Following the same process as in section 6.2.1.2, the absorption spectra are printed below (Fig. 6.3.1 and 6.3.2):

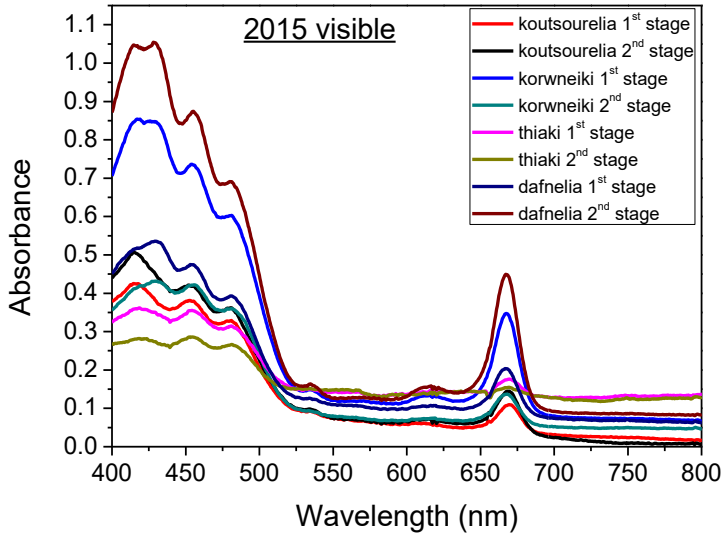

(a)

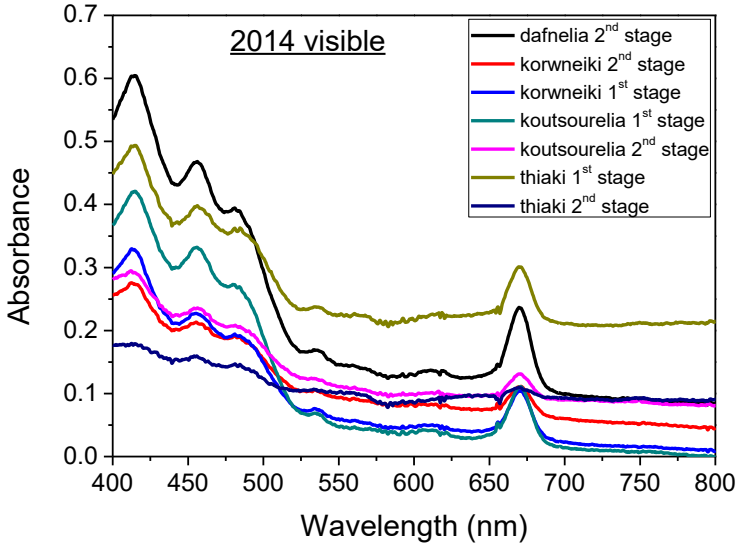

(b)

Figures 6.3.1 (a and b): Absorption spectra of the different olive varieties based on the cultivation year. (a) cultivation year 2015 and (b) cultivation year 2014

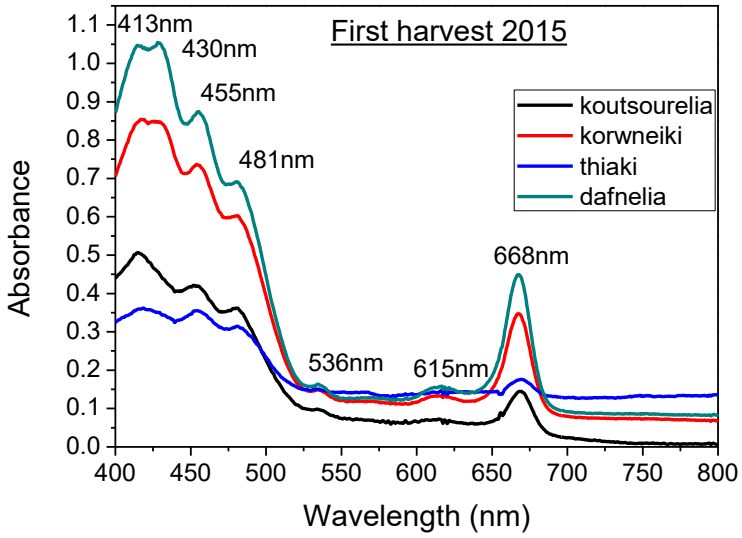

(a)

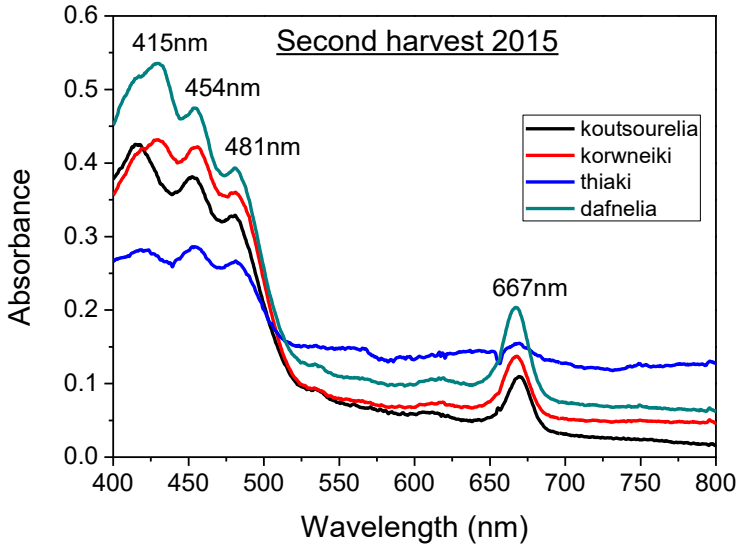

(b)

Figure 6.3.2 (a and b): Absorption spectra of the different olive varieties based on the stage of harvest in 2015. (a) First harvest 2015 and (b) Second harvest 2015

It can be observed that oils present four main absorption peaks and two shoulders of absorption:

- 413-430, 455, 480nm correspond to Carotenoids
- 536, 613nm correspond to Chlorophyll-a and pheophytins
- 667-670nm correspond to Chlorophyll

In both harvest periods of 2015, variety Dafnelia seems to have more intense absorbance peaks. Variety Korwneiki follows with lower intensity peaks, then variety Koutsourelia presents even lower intensity peaks and variety Thiaki seems to have

the lower intensity absorbance peaks. Note that, at the first harvest of 2015, the intensity of the absorbance peaks is higher than the second harvest's peaks. This means that the concentrations of chlorophylls and carotenoids were higher at the first harvest of 2015.

6.3.1.2 UV region (220-410nm)

All samples were diluted 1% v/v in n-hexane and were put in 2mm and 10mm path length quartz cuvettes, depending on the region of wavelengths measured. In all measurements, the background measured was the solvent n-hexane placed in the respective cuvette for the desirable wavelength region used.

At the UV region and more specifically at the wavelength region of 220-280nm, the olive oil absorbance measured is recorded, by using a 2mm path length cuvette. Characteristic absorption spectra are the following (Fig. 6.3.3):

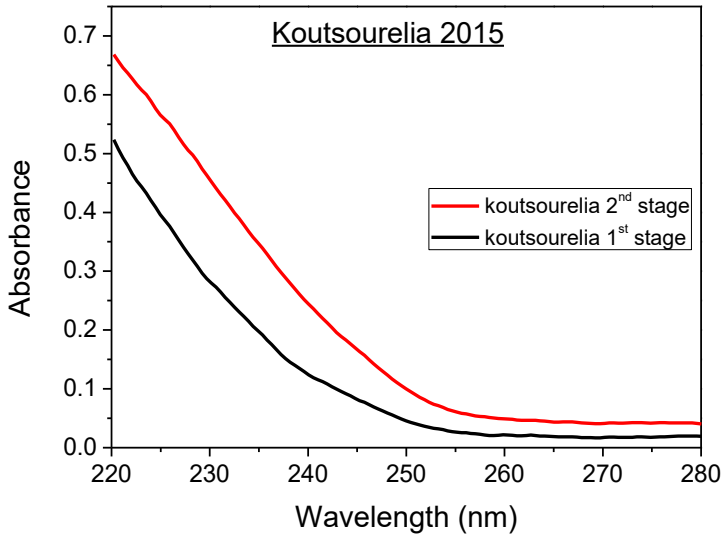

(a)

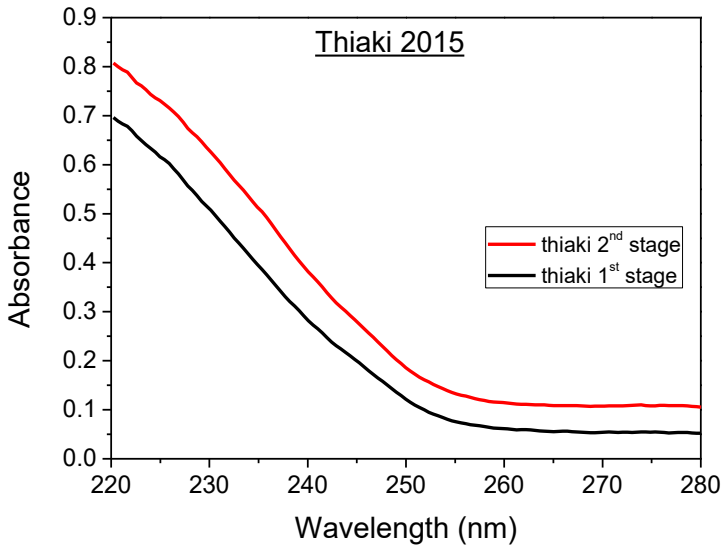

(b)

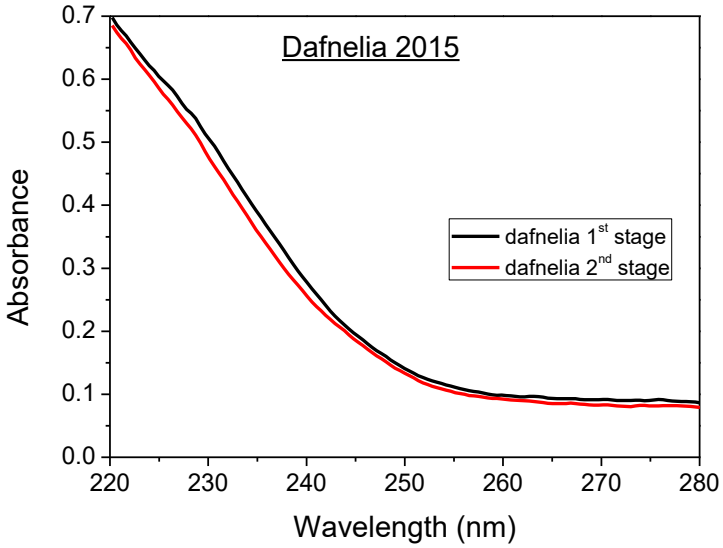
Dafnelia 2015
Absorbance
Wavelength (nm)
dafnelia 1st stage
dafnelia 2nd stage
0.0
0.1
0.2
0.3
0.4
0.5
0.6
0.7
220
230
240
250
260
270
280

(c)

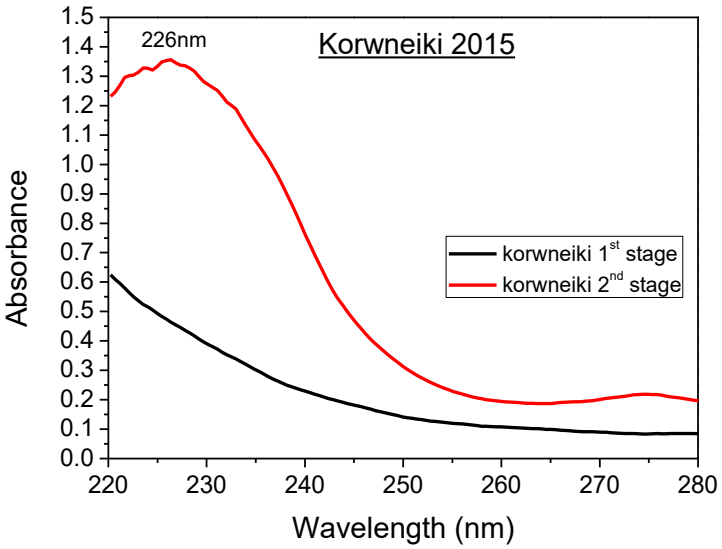
226nm
Korwneiki 2015
Absorbance
Wavelength (nm)
korwneiki 1st stage
korwneiki 2nd stage
0.0
0.1
0.2
0.3
0.4
0.5
0.6
0.7
0.8
0.9
1.0
1.1
1.2
1.3
1.4
1.5
220
230
240
250
260
270
280

(d)

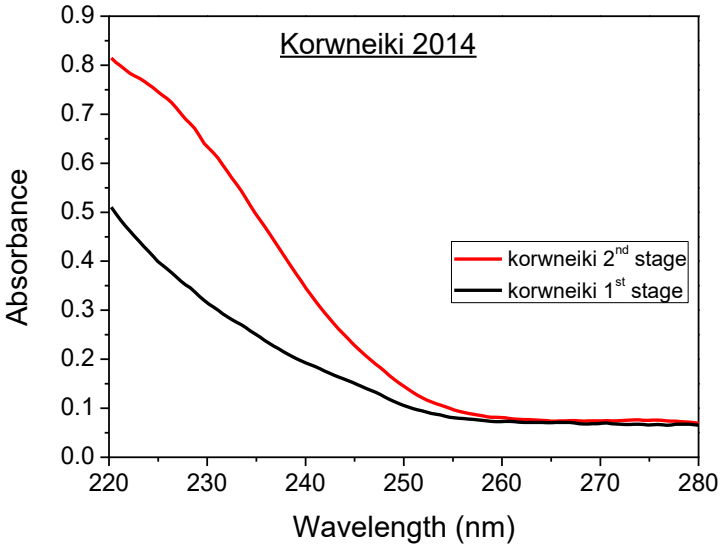
Korwneiki 2014
Absorbance
Wavelength (nm)
korwneiki 2nd stage
korwneiki 1st stage
0.0
0.1
0.2
0.3
0.4
0.5
0.6
0.7
0.8
0.9
220
230
240
250
260
270
280

(e)

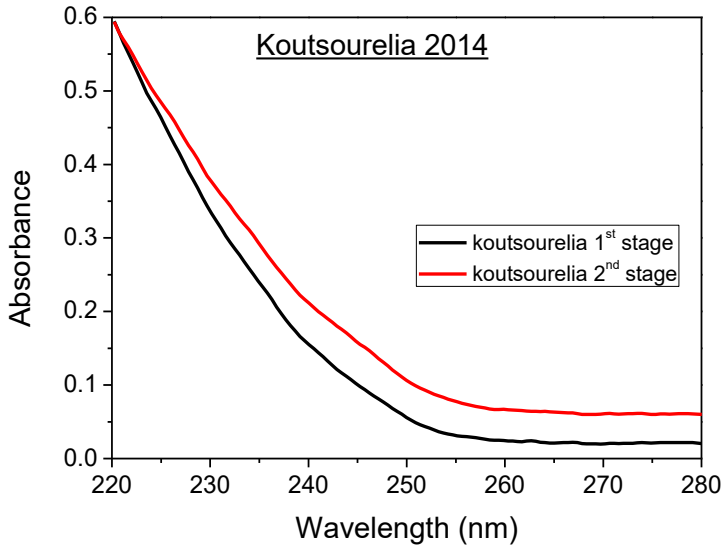
Koutsourelia 2014
Absorbance
Wavelength (nm)
koutsourelia 1st stage
koutsourelia 2nd stage
0.0
0.1
0.2
0.3
0.4
0.5
0.6
220
230
240
250
260
270
280

(f)

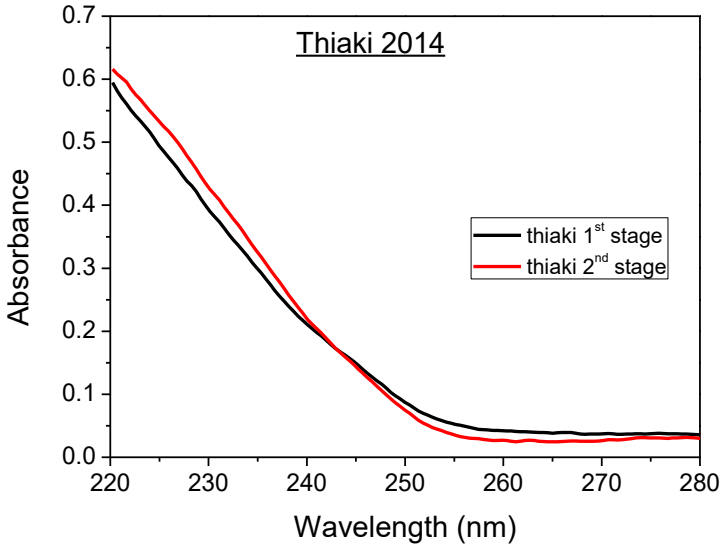

(g)

Figures 6.3.3 (a-g): Absorption spectra of olive oils from different olive varieties at the wavelength region (220-280nm). (a-d) Harvest of 2015, (e-g) Harvest of 2014

The different olive oil varieties seem to be differentiated by the UV absorption spectrum. The olive oils cultivated on the second stage presented higher absorption values at both harvest periods. Three oil samples, two from 2015's harvest period and one from 2014's harvest period, both at the second stage of cultivation (Thiaki 2015, Korwneiki 2015 and Korwneiki 2014), present an absorption peak at 226nm, corresponding to conjugated dienes. This could be probably due to the time the olives remained in trees more than the appropriated. Considering the absorbance values at 232nm and the equation 4.1, K_{232} indexes are calculated and presented below (Fig. 6.3.4):

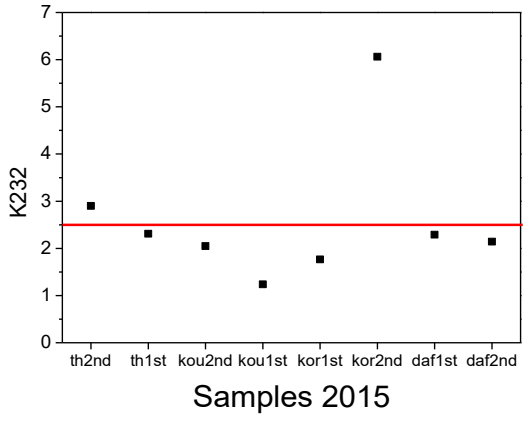

(a)

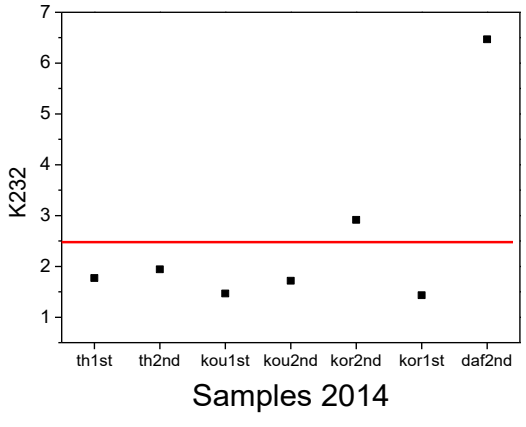

(b)

Figures 6.3.4 (a and b): Samples vs index K_{232}. (a) cultivation year 2015 and (b) cultivation year 2014.

As observed from the above graphs, two oil samples cultivated in 2015 have higher values of this index and two other oil samples cultivated in 2014 also have higher values of K_{232}, according to the limits of the index for being characterized as extra virgin olive oils. These values may be due to bad storage of the samples, the transfer conditions or the delay of measuring these oils, by means that these oils have been measured 4 months after harvesting, referring to cultivation of 2015.

Going on to the experimental process, oils were measured in the UV region at wavelengths 260-410nm, placed in a 10mm path length cuvette. Some indicative examples of the absorption spectra are shown in the following graphs (Fig. 6.3.5):

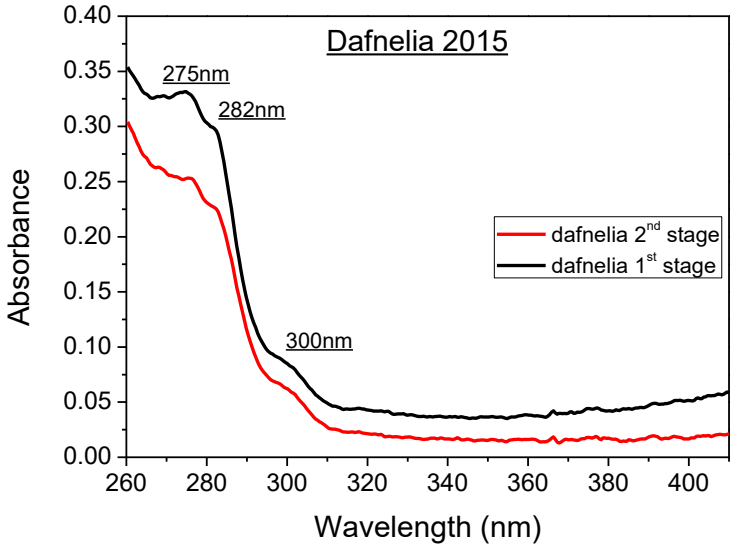
Dafnelia 2015
275nm
282nm
300nm
dafnelia 2nd stage
dafnelia 1st stage
Absorbance
Wavelength (nm)
0.40
0.35
0.30
0.25
0.20
0.15
0.10
0.05
0.00
260
280
300
320
340
360
380
400

(a)

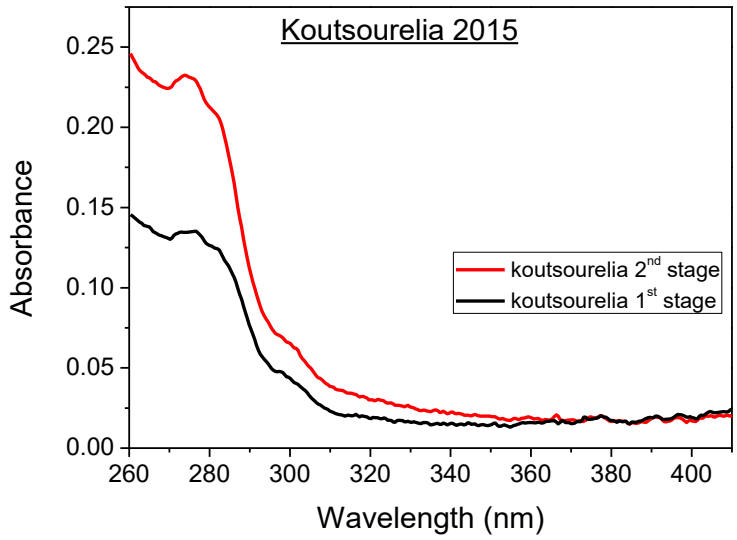
Koutsourelia 2015
koutsourelia 2nd stage
koutsourelia 1st stage
Absorbance
Wavelength (nm)
0.25
0.20
0.15
0.10
0.05
0.00
260
280
300
320
340
360
380
400

(b)

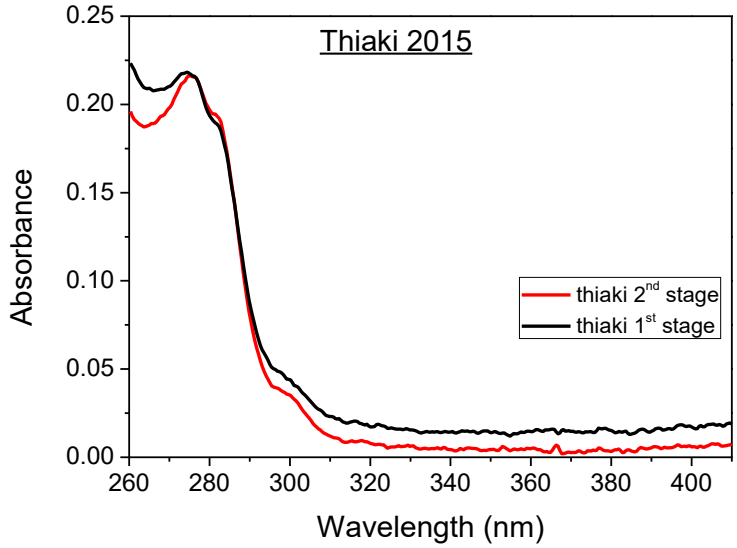

(c)

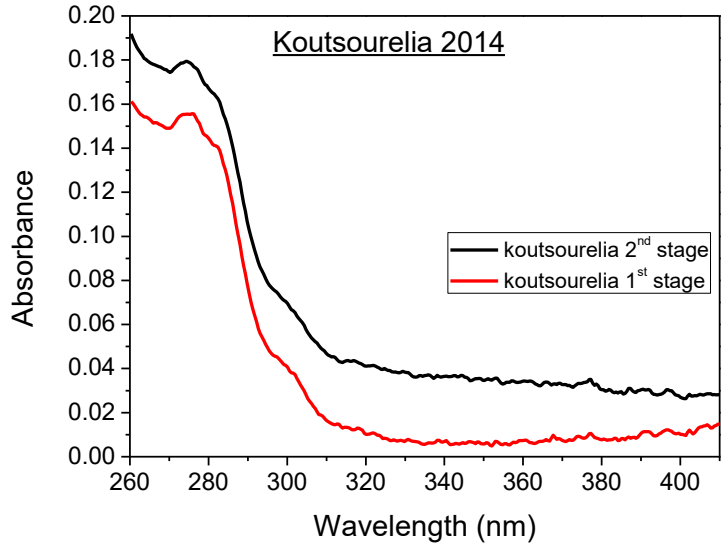

(d)

Figures 6.3.5 (a-d): Absorption spectra of olive oils from different olive varieties at the wavelength region (260-410nm)

It can be observed from Fig. 6.3.5, olive oils coming from different olive varieties behave in a different way. In this UV region (260-410nm), some oil samples show up some absorbance peaks at 275nm, related to unsaturated fatty acids, and at 282nm, related to phenols. There is also an absorption shoulder at 300nm, corresponding to phenolic compounds. In order to calculate the K_{270} and ΔK indexes, values of absorbance at 266, 270 and 274nm are inserted to equations 4.1 and 4.2 and the results are plotted vs Samples (Fig. 6.3.6):

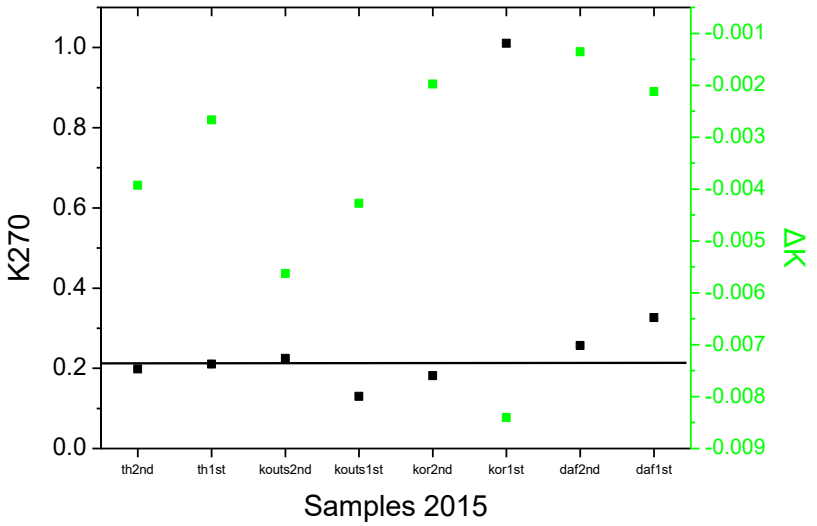

(a)

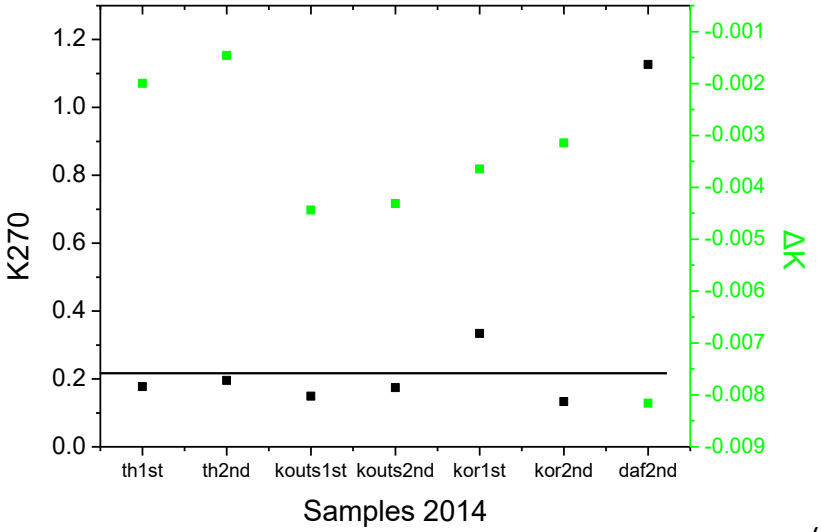

(b)

Figures 6.3.6 (a and b): Indexes K_{270} and ΔK vs Samples. (a) cultivated in 2015 and (b) cultivated in 2014

The index ΔK is lower than zero (0) for all samples and this means that the oils are pure olive oils. Concerning the index K_{270}, there are some oil samples whose K values are higher than 0.22 - criterion of characterization of extra virgin olive oil (IOOC, 1991) – but this is caused either in the absorption measurements or the storage and transfer conditions.

6.3.2 Correlation of Absorption Spectroscopy and Quality Characteristics

The quality characteristics of virgin olive oils include the acidity of the oils. At the following table, the acidity values of the oil samples is presented (Table 6.3.2):

(a) Cultivation of 2014

Variety of olive	Acidity
Dafnelia 2nd stage	0.19
Korwneiki 1st stage	0.42
Korwneiki 2nd stage	0.45
Thiaki 1st stage	0.23
Thiaki 2nd stage	0.22
Koutsourelia 1st stage	0.2
Koutsourelia 2nd stage	0.34

(b) Cultivation of 2015

Variety of olive	Acidity
Dafnelia 1st stage	0.14
Dafnelia 2nd stage	0.21
Korwneiki 1st stage	0.17
Korwneiki 2nd stage	0.16
Thiaki 1st stage	0.26
Thiaki 2nd stage	0.25
Koutsourelia 1st stage	0.29
Koutsourelia 2nd stage	0.36

Table 6.3.2 (a and b): Acidity values of olives

We employed PLS regression model in MATLAB (R2015b) and PLS Toolbox 8.1 in order to correlate the absorption spectra of these olive oils and their acidity. Plots of The PLS regression model are shown at figures below (Fig. 6.3.7, 6.3.8 and 6.3.9) and provide the values of RMSECV (Root Mean Squares Error of Cross Validation) and the line coefficient R^2 of cross validation (CV). The RMSECV shows the prediction error of the input data and the R^2 the fitting of the line.

Three different absorption region were correlated with the quality parameter:

- Visible region (400-800nm) – Acidity:

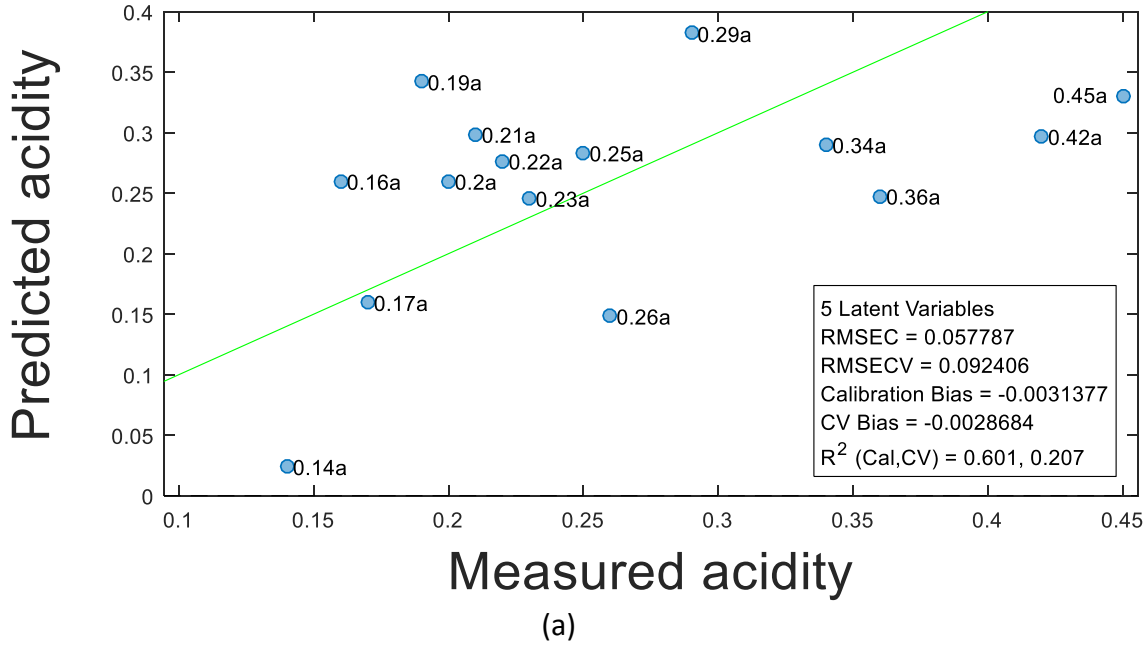

(a)

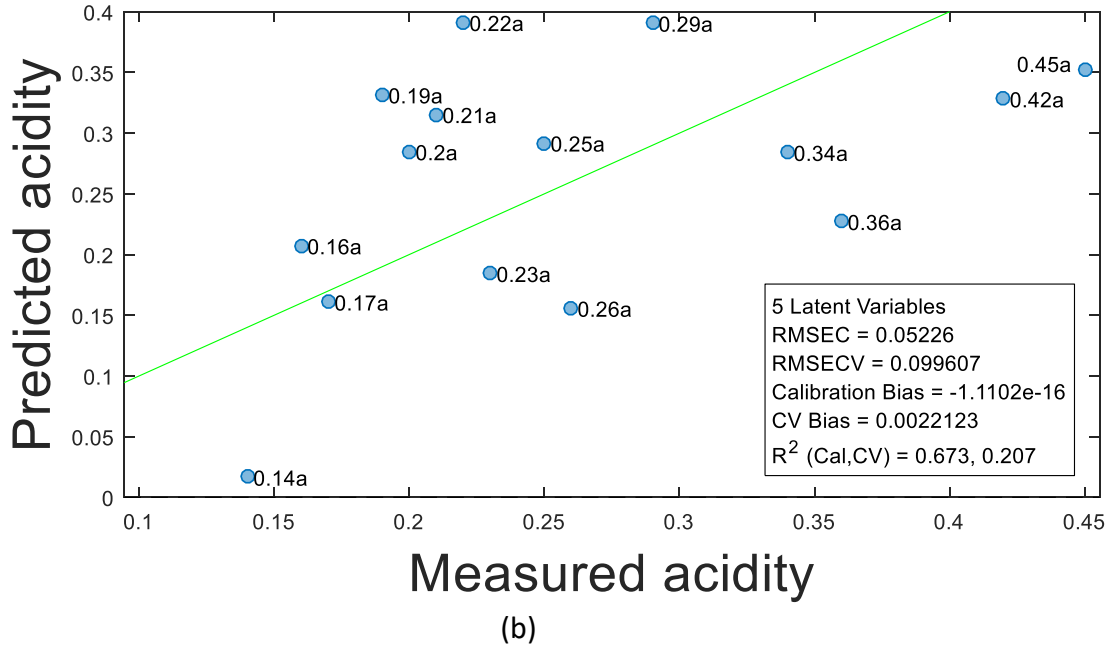

(b)

Figures 6.3.7 (a and b): PLS regression plots. (a) No pre-treatment of data, leave-one-out cross validation, RMSECV=9.2% (b) Mean-centering pre-treatment of data, leave-one-out cross validation, RMSECV=10%

- UV region (260-410nm) – Acidity:

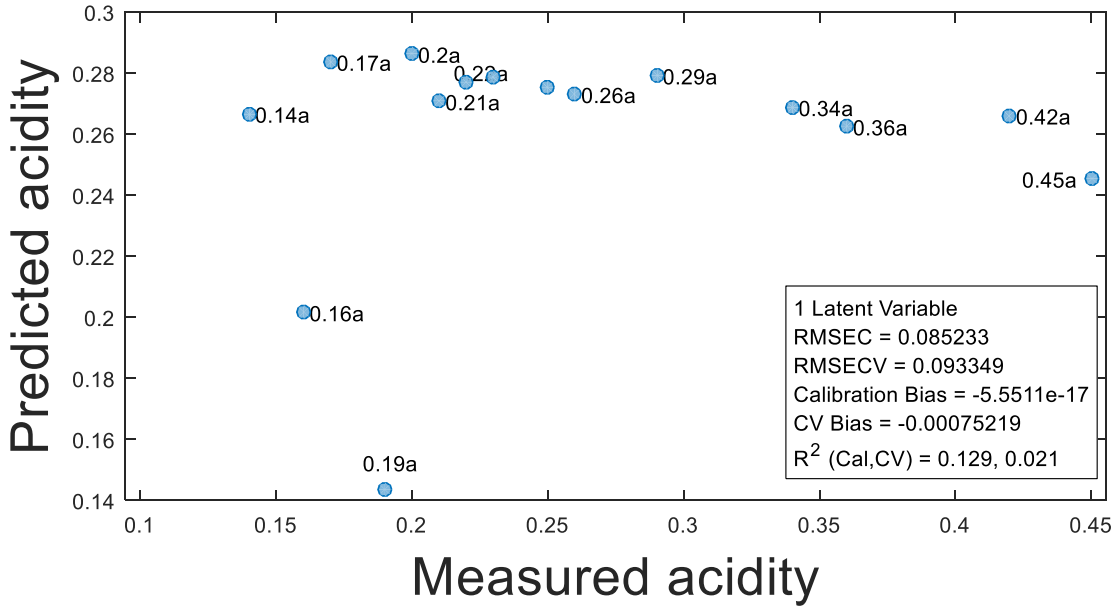
Predicted acidity
Measured acidity
0.17a
0.2a
0.22a
0.21a
0.14a
0.26a
0.29a
0.34a
0.36a
0.42a
0.45a
0.16a
0.19a
1 Latent Variable
RMSEC = 0.085233
RMSECV = 0.093349
Calibration Bias = -5.5511e-17
CV Bias = -0.00075219
R2 (Cal,CV) = 0.129, 0.021

(a)

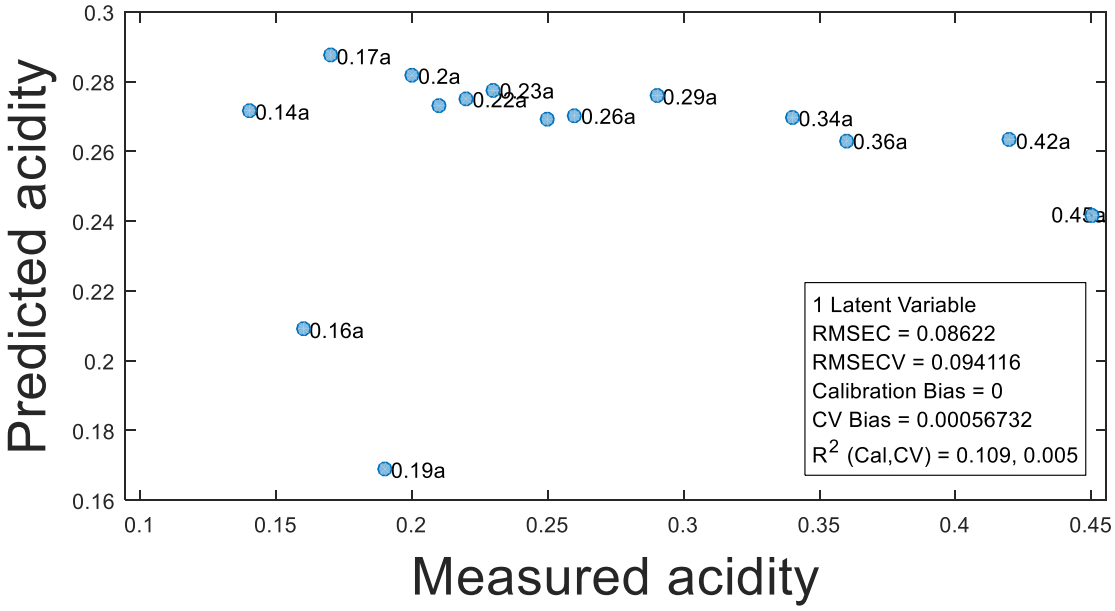
Predicted acidity
Measured acidity
0.17a
0.2a
0.23a
0.22a
0.14a
0.26a
0.29a
0.34a
0.36a
0.42a
0.16a
0.19a
1 Latent Variable
RMSEC = 0.08622
RMSECV = 0.094116
Calibration Bias = 0
CV Bias = 0.00056732
R2 (Cal,CV) = 0.109, 0.005

(b)

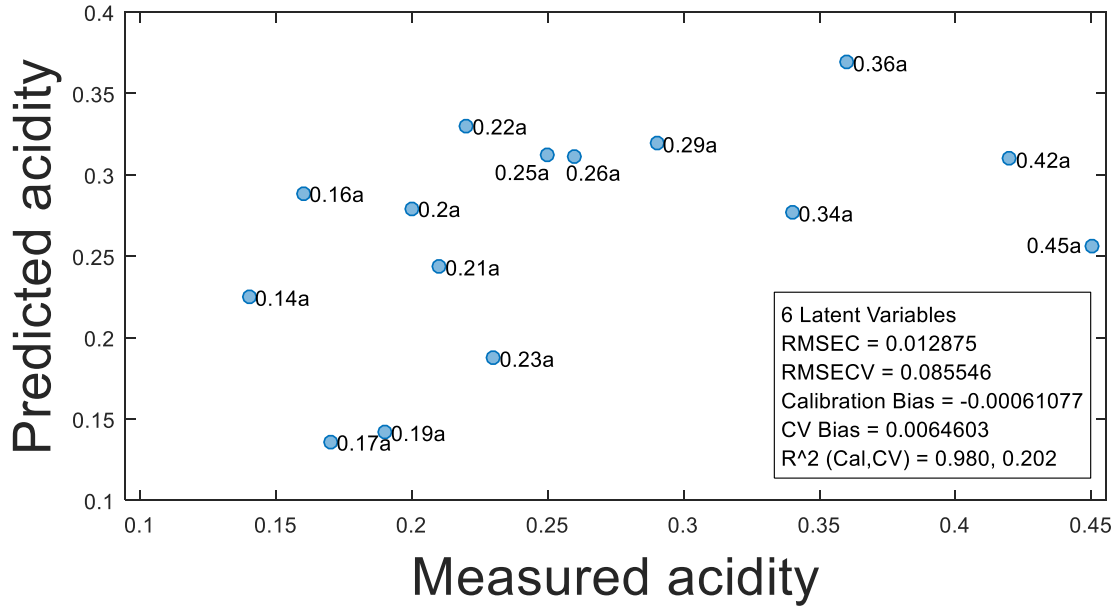

(c)

Figures 6.3.8 (a- c): PLS regression plots. (a) Mean-centering pre-treatment of data, leave-one-out cross validation, RMSECV=9.3% (b) Mean-centering + Savgol 1st derivative pre-treatment of data, leave-one-out cross validation, RMSECV=9.4% (c) Savgol 2nd derivative pre-treatment of data, leave-one-out cross validation, RMSECV=8.6%

- UV region (220-280nm) – Acidity:

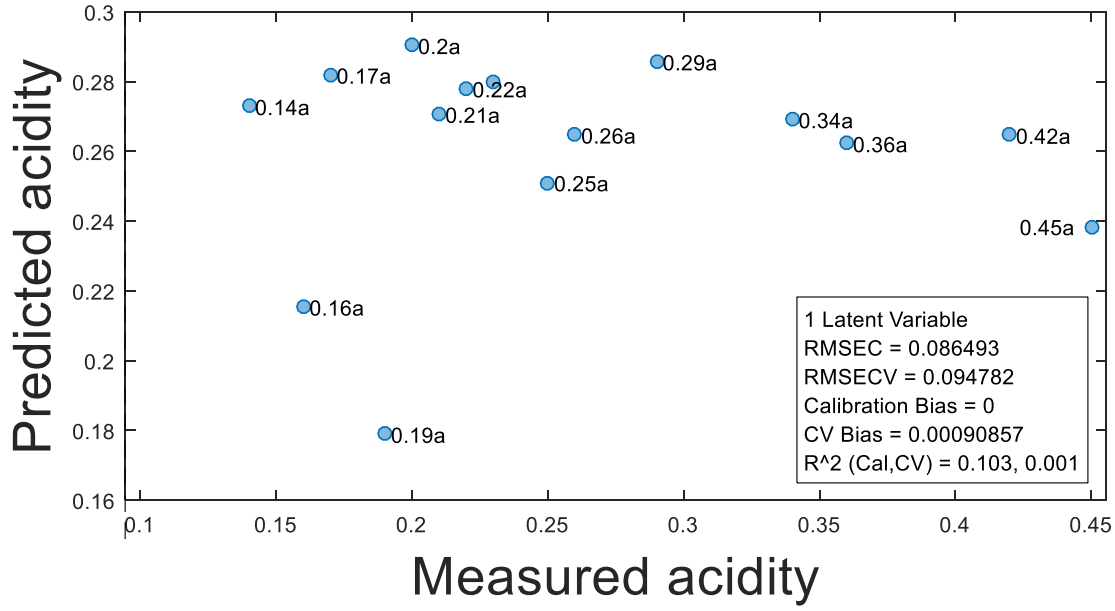

(a)

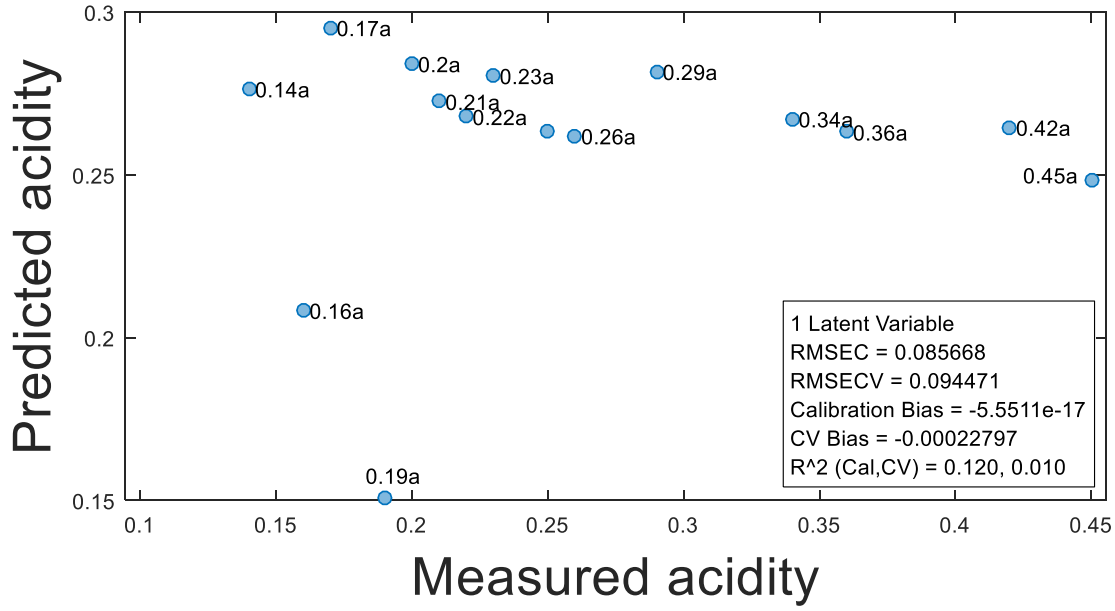

(b)

Figures 6.3.9 (a and b): PLS regression plots. (a) Mean centering pre-treatment of data, leave-one-out cross validation, RMSECV=9.5% (b) Mean center + Savgol 2nd derivative pre-treatment of data, leave-one-out cross validation, RMSECV=9.4%

As observed, RMSECVs are quite equal to all absorption regions. The quality parameter, acidity, is defined as a percentage as grams of free fatty acids (expressed as oleic acid, the main fatty acid present in olive oil) in 100 grams of oil. Due to the fact that free fatty acids absorb light of wavelengths about 275-280nm, the best prediction result comes from the PLS regression plot of absorption spectra at the UV region, 260-410nm. The prediction error of acidity (or RMSECV) is 0.086, when the data were pre-treated by means of 2nd derivative, as seen at Fig. 6.3.8 (c).

These results are good enough to correlate the absorption spectral data with the quality characteristics of olive oils, in this case, acidity, by employing a fast, non-destructive spectroscopic technique.

6.3.3 Fluorescence measurements

As previously, we employed EEFS (see section 4.4) in order to create the contour maps. Front Face geometry was used in all experiments, where the sample was placed at 35^{o} to the incident beam. The samples were not chemically pre-treated and were placed in a 10mm path length quartz cuvette.

The excitation and emission wavelengths were kept the same in all measurements and these are:

Excitation wavelength region: 270-500nm by a 3nm step

Emission wavelength region: 290-800nm by a 5nm step

Slit of excitation spectrometer: 1nm

Slits of emission spectrometer: 2nm

Integration time: 0.2sec

Thereinafter, characteristic contour maps of oil samples are presented (Fig. 6.3.10):

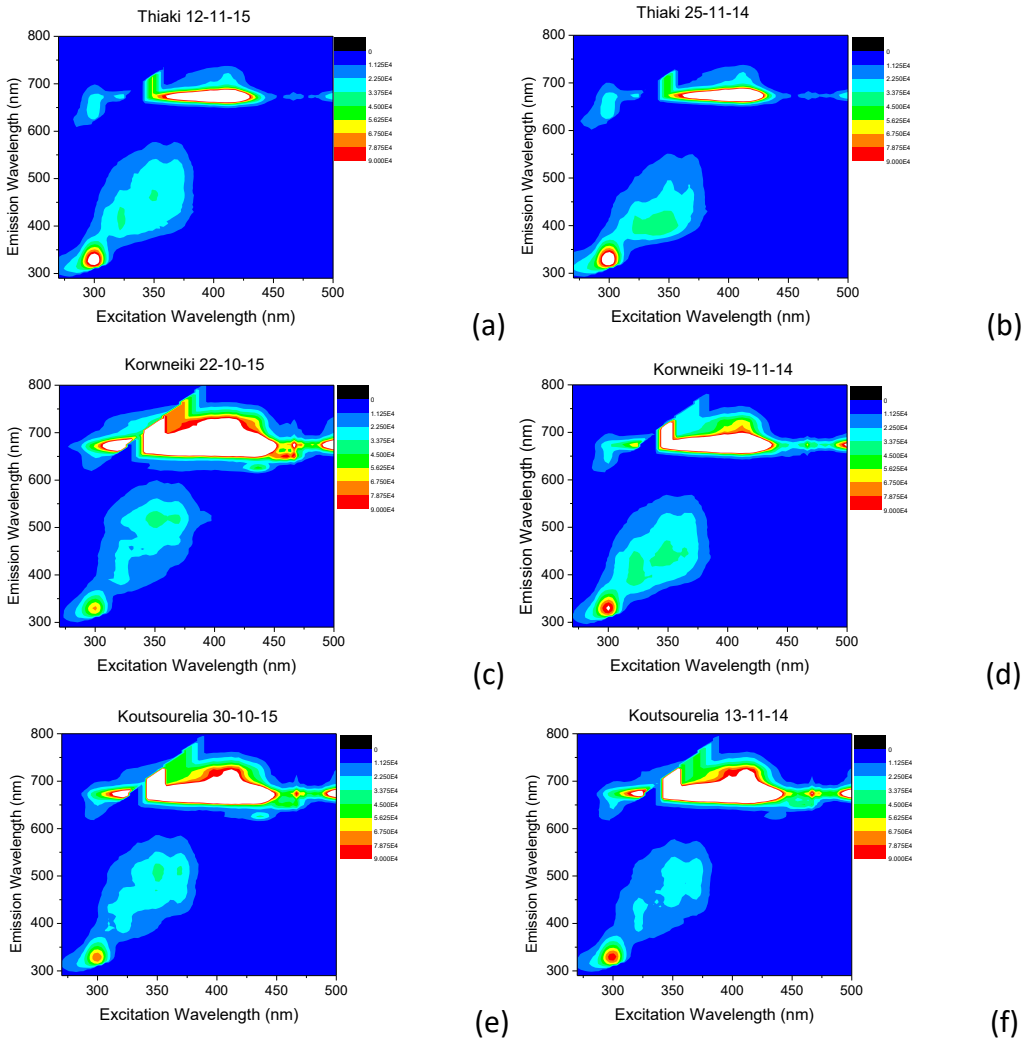

Figures 6.3.10 (a-f): Contour maps of oils from different olive varieties

The first harvest of both cultivation years show higher fluorescence intensities at λ_{em}=685nm, when excited at 325nm, than the second harvest. This emission is related to chlorophylls. Concerning the cultivation year of 2015, the second harvest shows more intense fluorescence at emission wavelengths region 320-340nm, when excited at about 300nm, corresponding to tocopherols, and at emission wavelengths region 390-420nm, when excited at 330-350nm, corresponding to phenolic compounds.

6.4 Tasting tests and Discrimination of olive oils

During the collaboration with ΕΑΣΡ and Mrs Eleftheria Germanaki, 30 samples of extra virgin olive oils have been received to the lab, which were tasted and marked by a tasting panel. These virgin olives were classified in three categories, based on the grades of the panel:

High quality olive oils: 1-10

Medium quality oils: 30-39

Low quality oils: 60-69

Note that the oil numbered 1 has the best grade and oil numbered 10 has the lowest grade among the high quality category. The same is applied to the other two categories.

Samples were placed in glass vials without any pre-treatment and coded with their grades.

6.4.1 Absorption measurements and correlation of UV-Vis Absorption Spectroscopy with PCA

We measured the samples in three wavelength regions: UV (220-280nm), UV (260-410nm) and Visible (400-800nm).

6.4.1.1 UV region (220-410nm)

Samples were diluted 1% v/v in the solvent n-hexane for being measured in the ultraviolet wavelength region, because the undiluted oil absorbance is saturated. Background was the solvent n-hexane placed in a cuvette of 2mm or 10mm path length, depending on the desired wavelength region.

The absorption spectra of oils in the UV region (220-280nm), by 0.5nm step, are presented below, separated in three different plots for the three categories (Fig. 6.4.1), as mentioned before. Samples were placed in a 2mm path length quartz cuvette, so was the solvent.

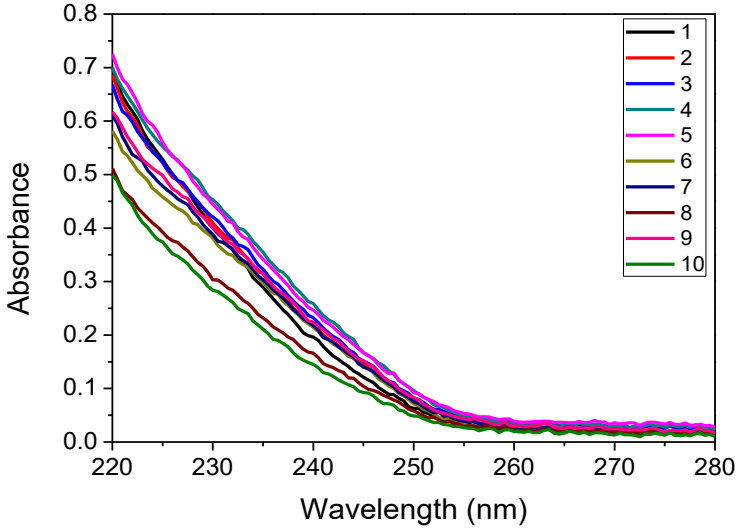
Absorbance
Wavelength (nm)
1
2
3
4
5
6
7
8
9
10

(a)

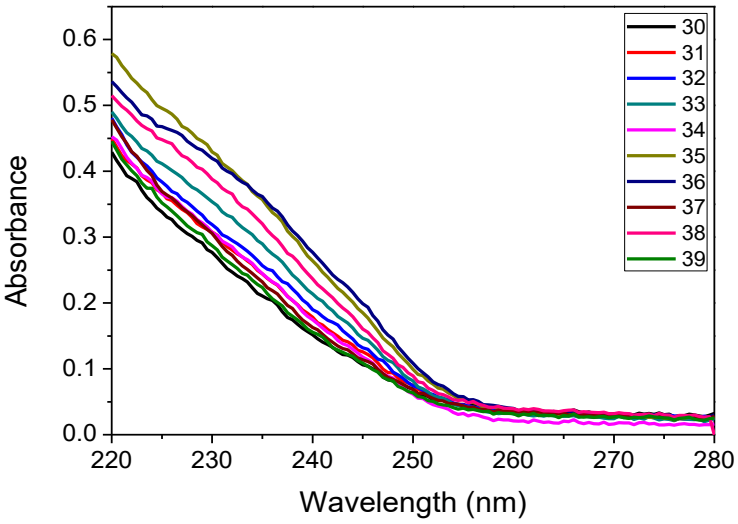
Absorbance
Wavelength (nm)
30
31
32
33
34
35
36
37
38
39

(b)

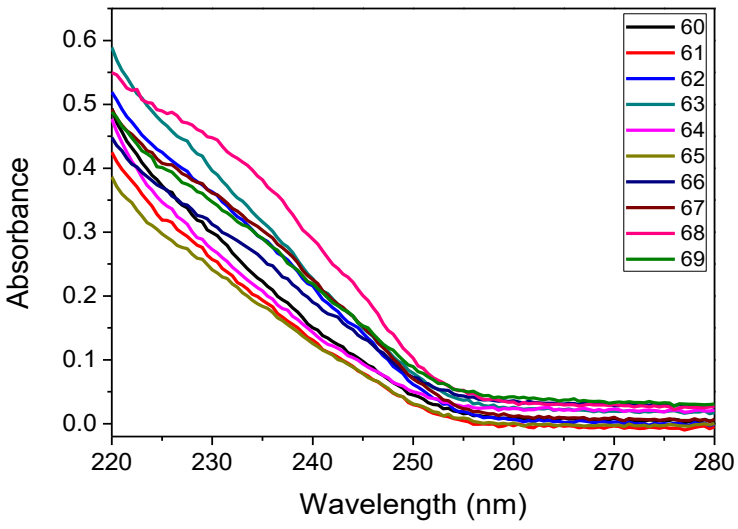
Absorbance
Wavelength (nm)
60
61
62
63
64
65
66
67
68
69

(c)

Figures 6.4.1 (a- c): Absorption spectra of olive oil samples. (a) oils graded 1-10, (b) oils graded 30-39 and (c) oils graded 60-69

Samples characterized as medium and low quality olive oils tend to present a shoulder at 235-240nm, which is related to conjugated dienes, in contrary to high graded olive oils, that do not present absorption peaks at this UV region.

As observed, we cannot discriminate the olive oils, based on their tasting grades, from the spectra. Taking into account the values of absorbance at 232nm, indexes K_{232} are calculated.

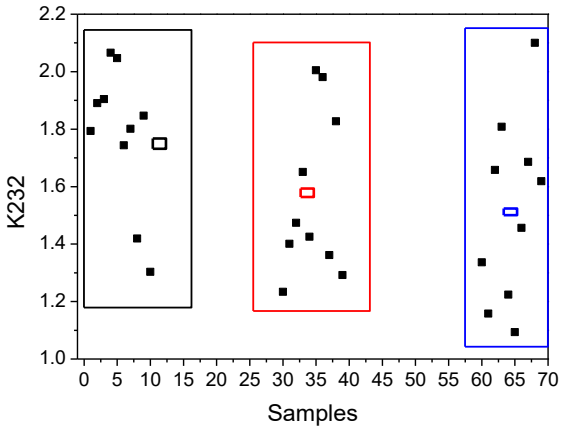

Figure 6.4.2: Plot of K_{232} for all samples at the UV region (220-280nm)

All samples present lower than 2.5 of index K_{232}. The distribution of these values is different for each category, confirming the group of grades taken. The 3 small boxes presented in Fig. 6.4.2 (black for 1-10, red for 30-39 and blue for 60-69) represent the mean values of K_{232}, showing that, as the quality of oils (according to the tasting grades) falls, the mean values of index K decreases.

PCA is employed (Fig. 6.4.3), in order to see if these categories are discriminated by the absorption spectra at this wavelength region (220-280nm).

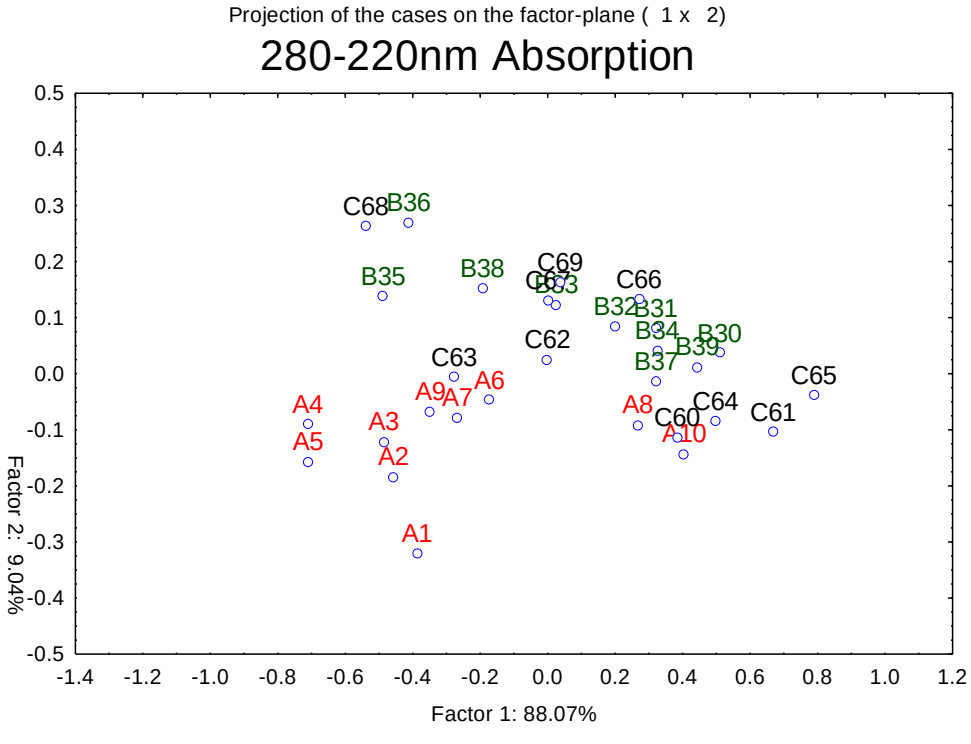

(a)

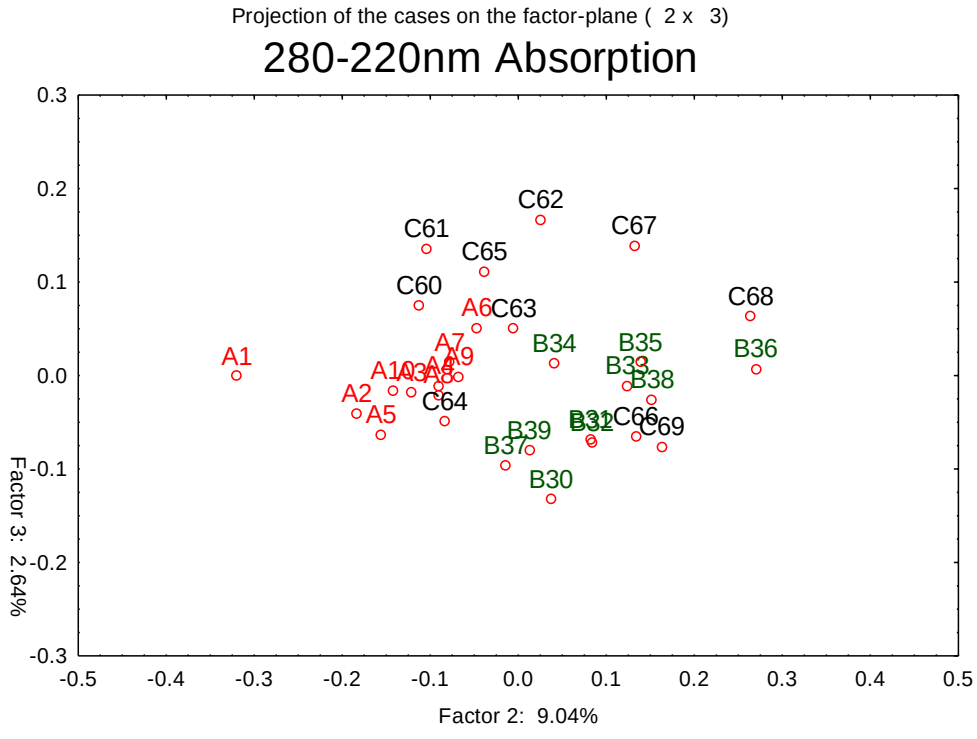

(b)

Figures 6.4.3 (a and b): Score plots of absorption spectra of olive oils in the wavelength region 220-280nm. (a) PC1: 88.07%, PC2: 9.04% (b) PC2: 9.04%, PC3: 2.64%

According to the score plots above, a discrimination of oils can be achieved, observing the group made for the high quality olive oils (symbol in plot is A). Especially, looking at the second score plot (Fig. 6.4.3 b), where PC2 and PC3 are

plotted, high quality olive oils (symbol A in the graph) create a cluster and the olive oil with the best grade, A1, is the olive oil that is differentiated from the others.

Moving on to the other UV region studied (260-410nm), by a 2nm interval, olive oil samples were placed in a 10mm path length cuvette, so was the solvent for the background measurement. Absorption spectra are shown below (Fig. 6.4.4):

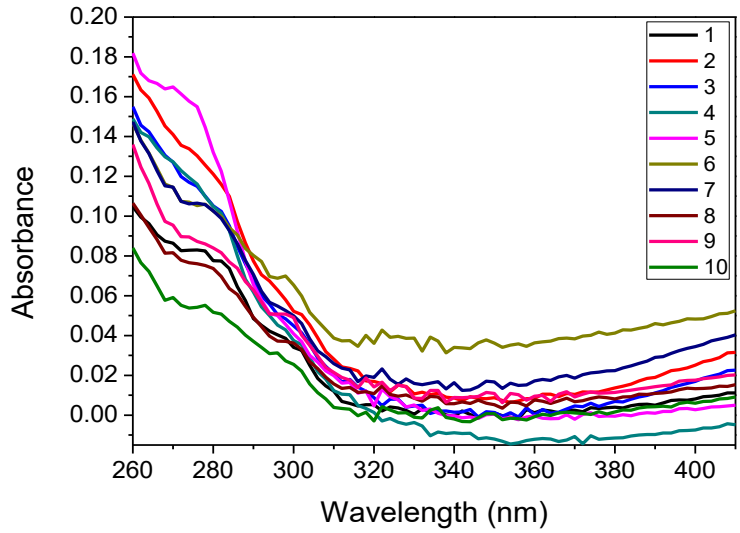
Absorbance
Wavelength (nm)
1
2
3
4
5
6
7
8
9
10

(a)

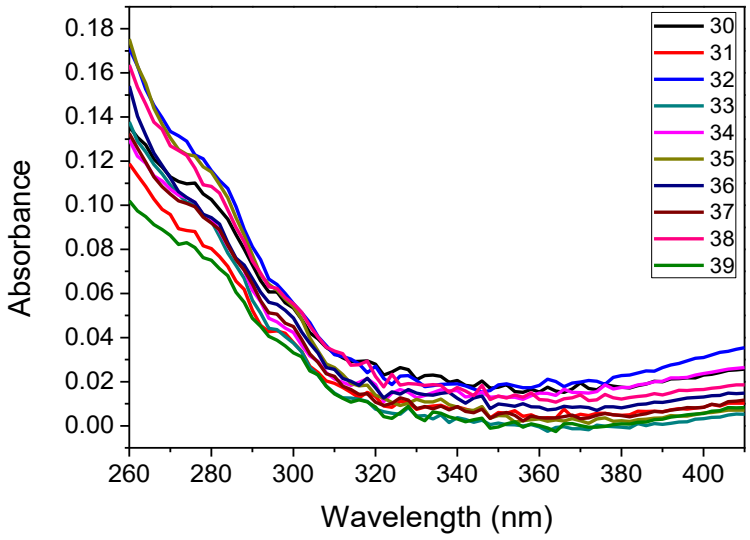
Absorbance
Wavelength (nm)
30
31
32
33
34
35
36
37
38
39

(b)

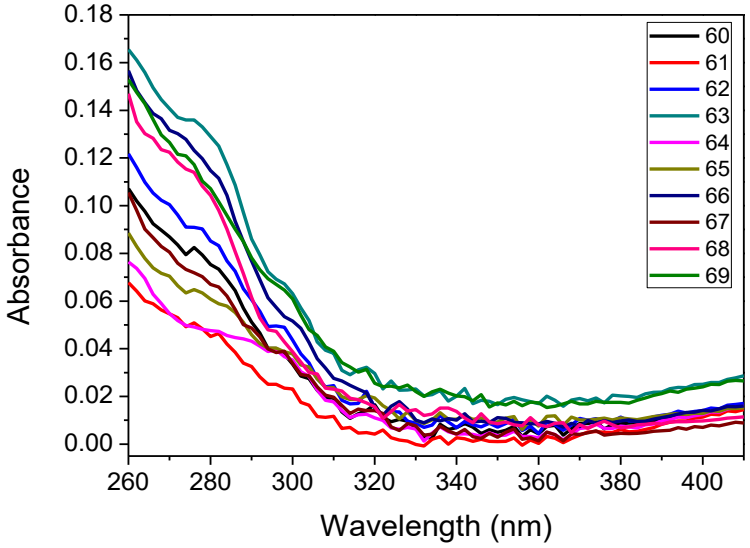
Absorbance
Wavelength (nm)
60
61
62
63
64
65
66
67
68
69

(c)

Figures 6.4.4 (a- c): Absorption spectra of olive oils at the wavelength region 260-410nm. (a) oils graded 1-10, (b) oils graded 30-39 and (c) oils graded 60-69.

In this UV region (260-410nm), all oil samples show up some absorbance peaks at 275nm, related to unsaturated fatty acids, and at 282nm, related to phenols. There is also an absorption shoulder at 300nm, corresponding to phenolic compounds. Considering the absorbance values at 266, 270 and 274nm, K_{270} and ΔK are calculated and plotted versus samples, as seen in Fig. 6.4.5:

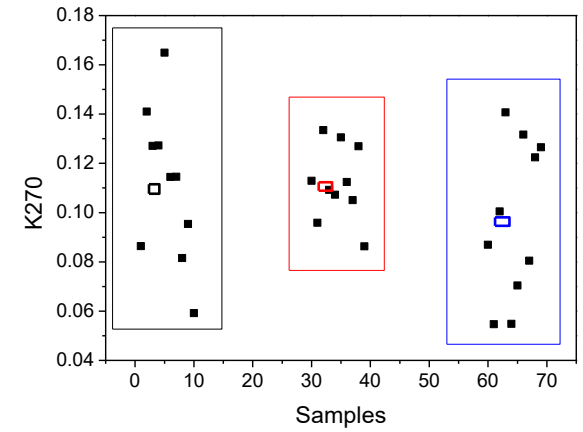

(a)

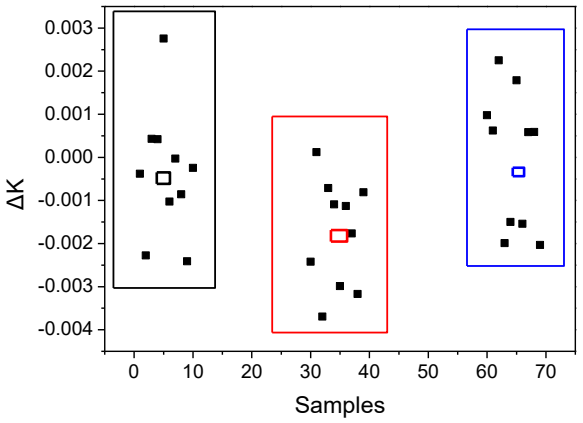

(b)

Figures 6.4.5 (a and b): Indexes K_{270} (a) and ΔK (b) of olive oils

K indexes values are less than the limits set by the European instructions *(IOOC, 1991)*, for characterization of an olive oil as extra virgin olive oil. In Fig. 6.4.5 (a), the mean values of K_{270} index values (presented as small boxes, colored as black for 1-10, red for 30-39 and blue for 60-69) decrease, as the quality of oils decrease. Concerning the values of ΔK indexes, all samples present low values.

Employing the PCA model, where no pre-treatment of the data was made, the score plots arising are printed below:

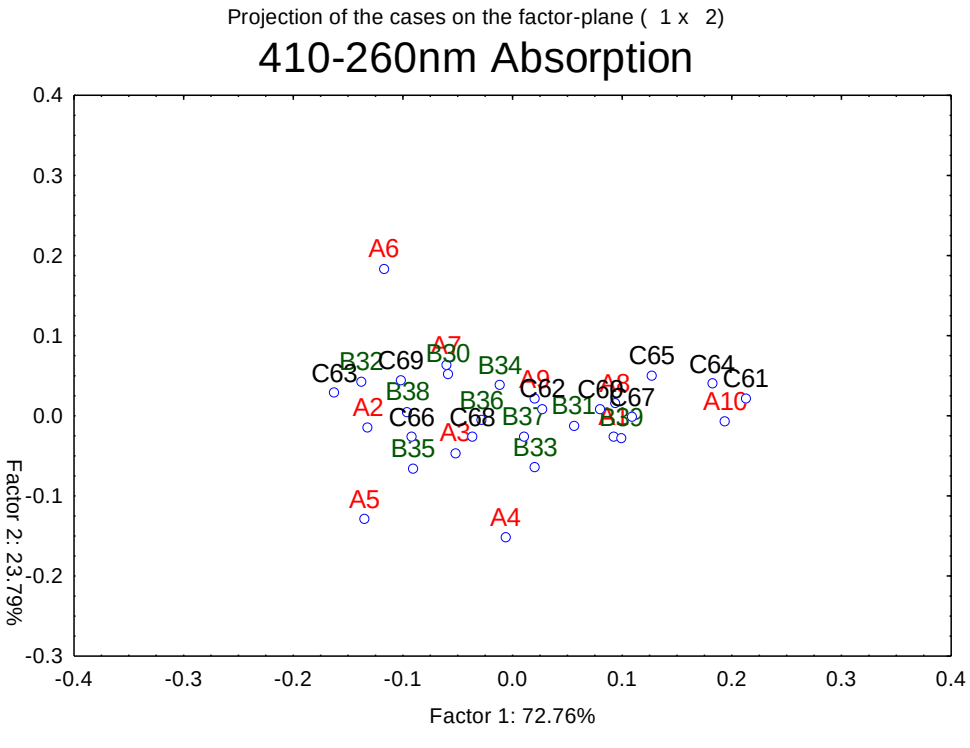

(a)

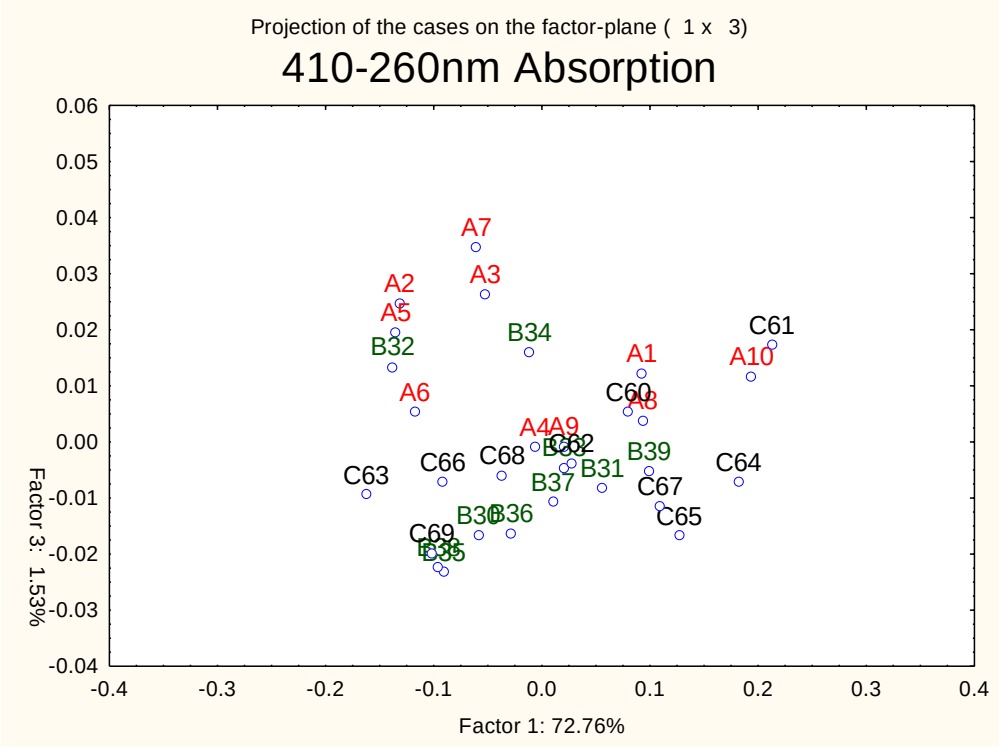

(b)

Figures 6.4.6 (a and b): Score plots of absorbance in the UV region (260-410nm). (a) PC1: 72.76%, PC2: 23.7% (b) PC1: 72.76%, PC2: 1.53%

According to these score plots, groups are not discriminated with these absorbance data.

6.4.1.2 Visible region (400-800nm)

Samples are not diluted in any solvent. In order to measure the absorbance of oils, samples were placed in a 2mm path length quartz cuvette and the air is measured as background.

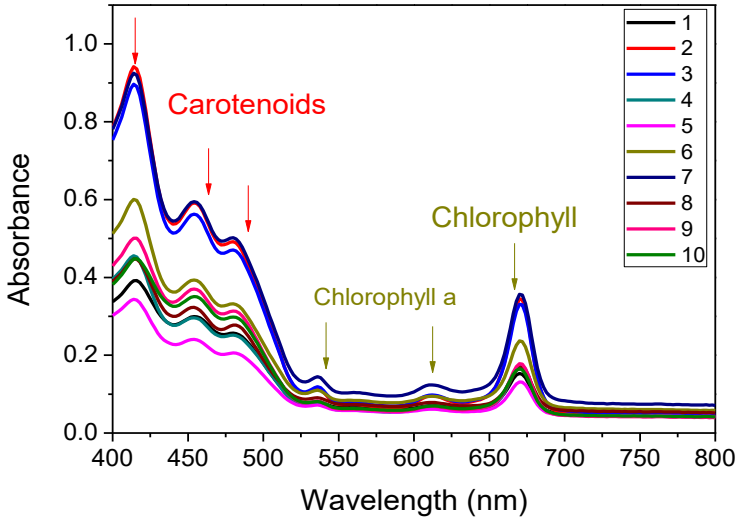
Carotenoids
Chlorophyll
Chlorophyll a
Absorbance
Wavelength (nm)
1
2
3
4
5
6
7
8
9
10

(a)

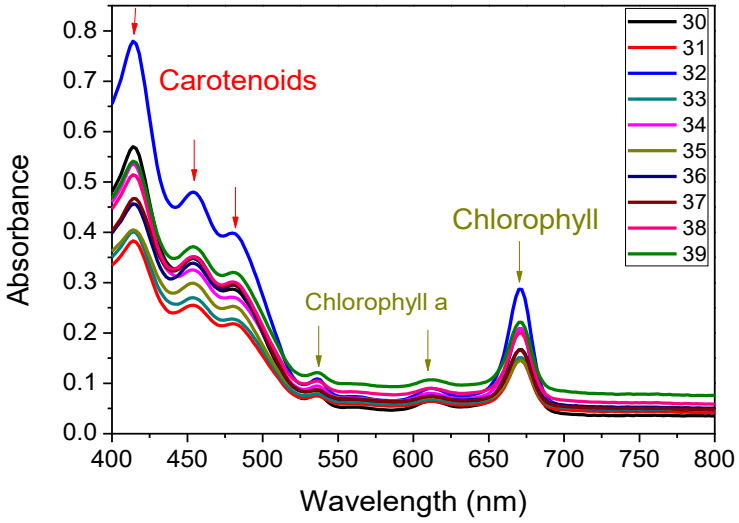
Carotenoids
Chlorophyll
Chlorophyll a
Absorbance
Wavelength (nm)
30
31
32
33
34
35
36
37
38
39

(b)

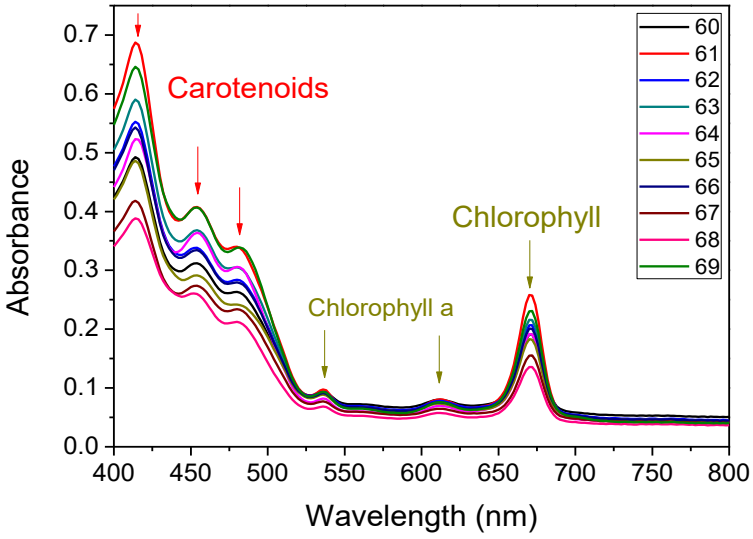
Carotenoids
Chlorophyll
Chlorophyll a
Absorbance
Wavelength (nm)
60
61
62
63
64
65
66
67
68
69

(c)

Figures 6.4.7 (a- c): Absorption spectra of olive oils at the visible region (400-800nm). (a) oils graded 1-10, (b) oils graded 30-39 and (c) oils graded 60-69

All olive oils present many absorbance peaks at the visible region. Carotenoids absorb at 414, 453 and 484nm, Chlorophyll a absorbs at 536 and 613nm, while the chlorophylls group absorbs at 667nm. As observed from the spectra (Fig. 6.4.7), the peak absorbance of carotenoids at 414nm decreases, as the quality of oil decrease. By means of the oil quality, we took into account the tasting results.

Employing the PCA model and the absorbance spectra at this region, we created the score plot below:

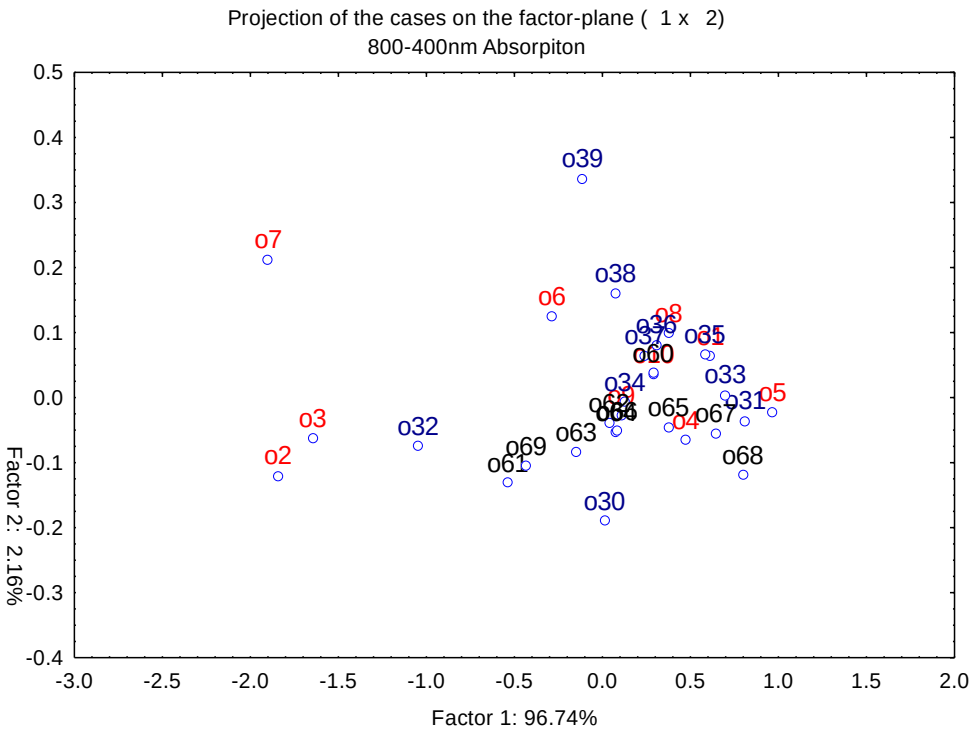

Figure 6.4.8: Score plot of Principal components 1, 2 for the absorption spectra of oils (PC1: 96.74%, PC2: 2.16%)

The statistical model (Fig. 6.4.8) provided no further information for the oil discrimination, based on the tasting results.

In conclusion, absorption spectra in the visible region 400-800nm show a good discrimination of the olive oils. In particular, the absorbance peak of carotenoids at 414nm decreases, as the grade of oil decreases.

6.4.2 Fluorescence measurements

Samples of oils were not diluted. We employed the Excitation-Emission Fluorescence Spectroscopy (EEFS) and Front Face (FF) geometry to measure the fluorescence of olive oils. The parameters were constant during all the experimental process:

Excitation wavelength region: 270-500nm by a 3nm step

Emission wavelength region: 290-800nm by a 5nm step

Slit of excitation spectrometer: 1nm

Slits of emission spectrometer: 2nm

Integration time: 0.2sec

The contour maps are presented indicatively below (Fig. 6.4.9):

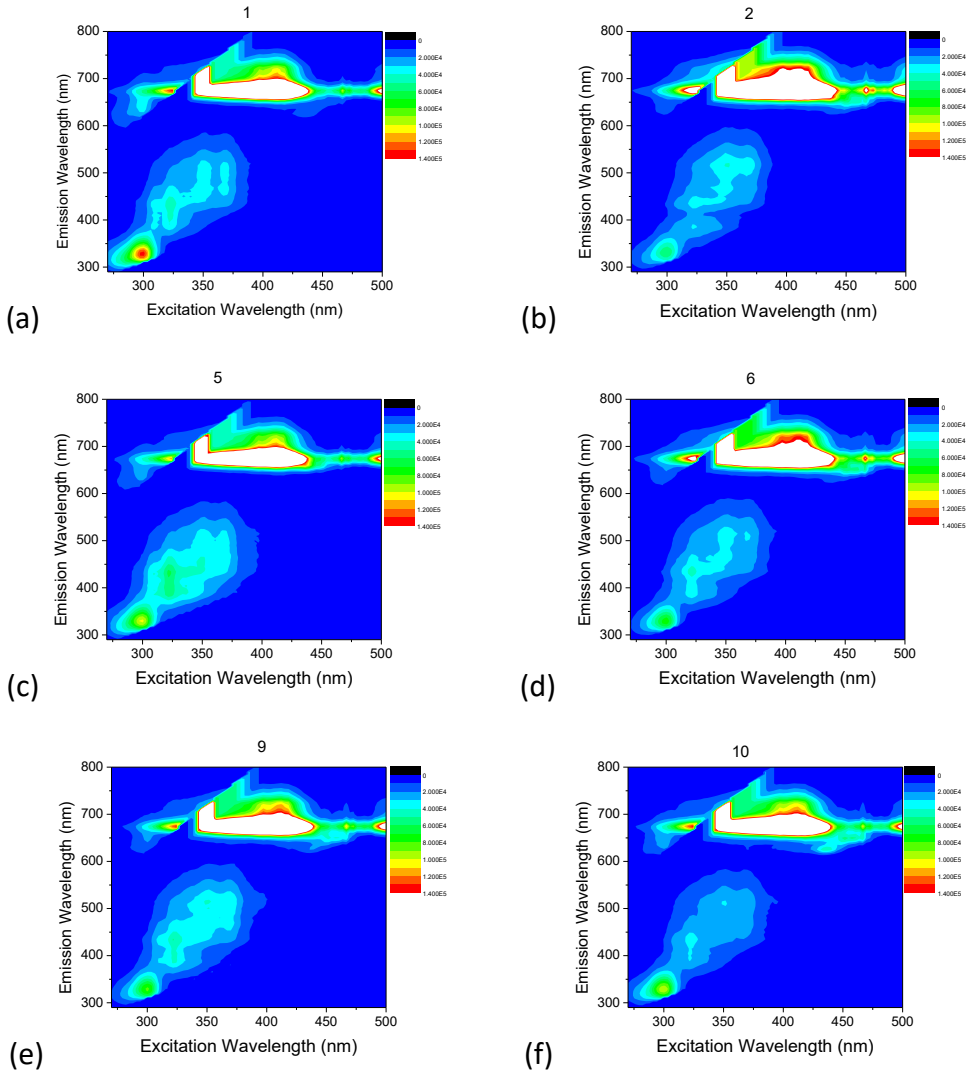

Figures 6.4.9 (a-f): Characteristic contour maps of the oils graded 1-10

The fluorescence at 660-690nm is related to chlorophylls and is very intense. Looking at the emission wavelengths 320-340nm, where the excitation wavelengths are 290-310nm, we observe the emission of tocopherols. At emission wavelengths 420-440nm, when excited at 320-340nm, the fluorescence is related to phenolic compounds. As the quality of oil decreases, the fluorescence of tocopherols decreases (Fig. 6.4.9). This is a sign that tocopherols included to the olive oil present lower fluorescence intensities, as the quality of oil decreases.

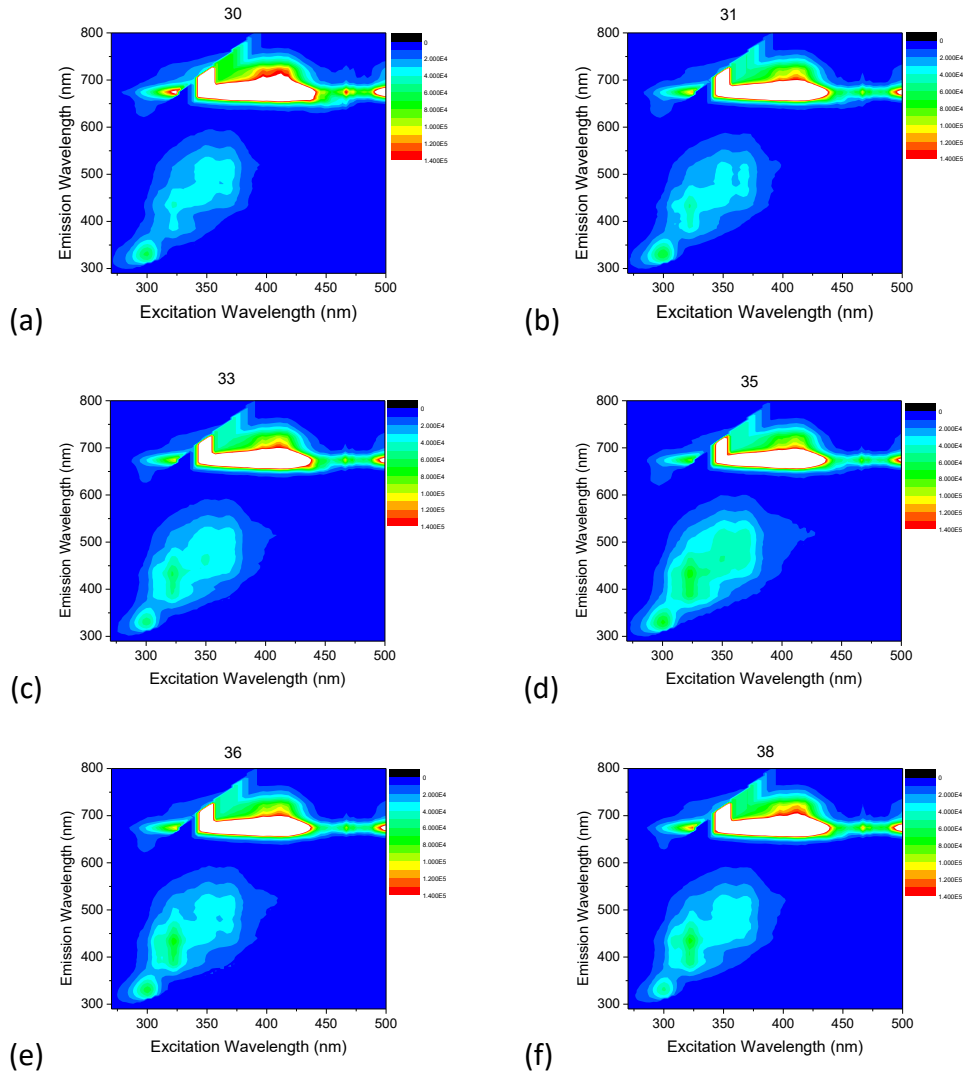

Figures 6.4.10 (a-f): Characteristic contour maps of the oils graded 30-39

The olive oils, characterized as olive oils of medium quality, present an intense fluorescence at emission wavelengths 660-690nm, which is related to chlorophyll pigments. Concerning the emission of tocopherols, the intensity decreases as the oil quality decreases, but the emission of phenolic compounds increases (Fig. 6.4.10). This behavior may be connected to the oxidation of phenolic compounds (Kyriakidis & Skarkalis, 2000).

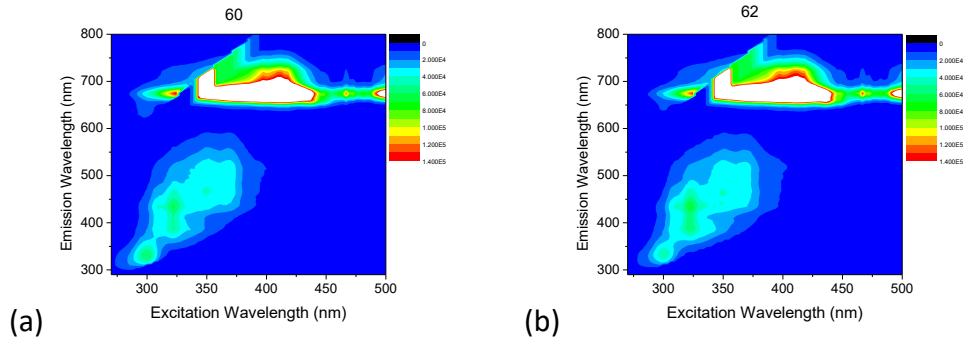

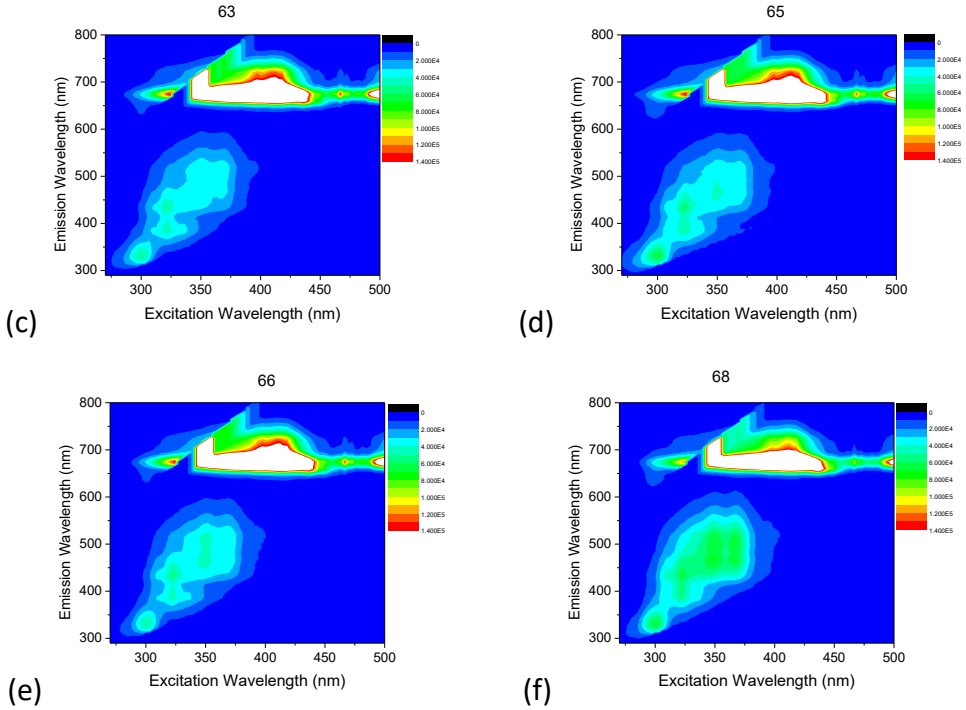

Figures 6.4.11 (a-f): Characteristic contour maps of the oils graded 60-69

As the oil quality decreases, the fluorescence intensity at emission wavelengths 450-500nm, excited at 350-380nm, is increased (Fig. 6.4.11). This effect is due to the oxidation of phenolic compounds, including vitamin E.

In conclusion, the excitation-emission fluorescence spectroscopy can discriminate the olive oils, based on the organoleptic characteristics and tasting tests. The fluorescence intensity of tocopherols is decreased, but the emission intensity of vitamin E (included in phenolic compounds) is increased, as the quality of oils decreases, because of the oxidation of phenolic compounds.

6.5 Adulteration of extra virgin olive oil

The adulteration of extra virgin olive oil with seed oils is a common practice in the oil industry. There have been a lot of journals focused on detecting the adulteration of extra virgin olive oils seed low-quality oils. Downey *et.al.* detected the adulteration of extra virgin olive oil with sunflower oil with detection limit of 0.8% via PLS regression, employing visible and near-IR transflectance spectra *(Downey, McIntyre, & Davies, 2002)*. Another scientific group reported the adulteration of extra virgin olive oil with refined olive pomace oil and sunflower oil, by employing the UV absorption spectra and more specifically the K indexes *(Skevin, et al., 2011)*.

Sunflower, corn and olive pomace oils are chemically similar to the virgin olive oil and the differences between them are their different composition in fatty acids. In order to control the quality of these seed oils, absorption and fluorescence spectroscopy were employed.

6.5.1 Absorption and Fluorescence measurements of seed and olive oils

6.5.1.1 Absorption measurements

At the UV region 250-400nm (2nm interval), the oil samples were diluted 1% v/v in n-hexane and placed in a 10mm path length cuvette.

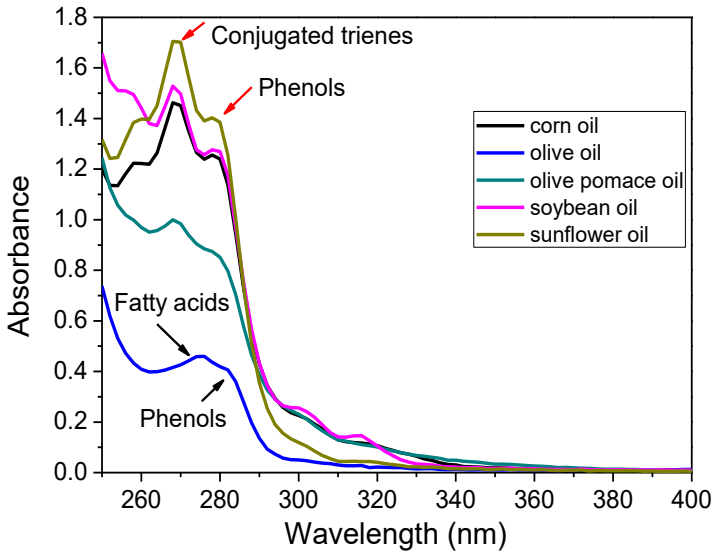

(a)

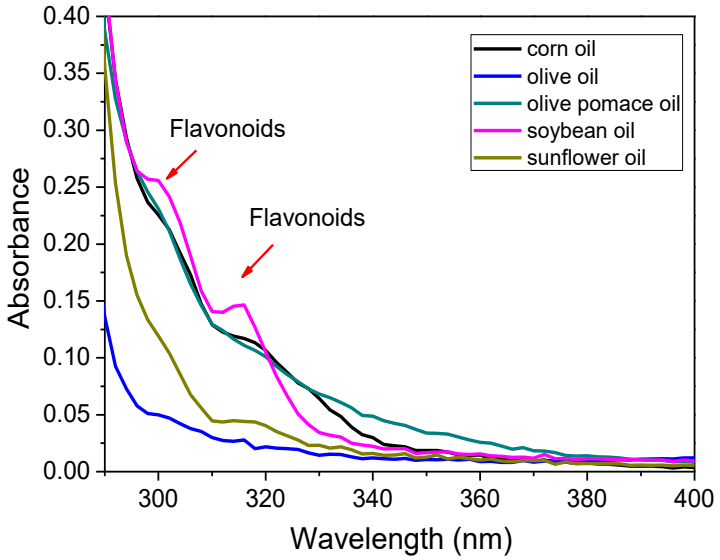

(b)

Figures 6.5.1: (a) Absorption spectra of oils at UV region (250-400nm),

(b) Zoom in of (a) in the region 300-330nm.

It is observed (Fig. 6.5.1) that olive oil absorbs at 270nm, which is attributed to fatty acids, and at 282nm, which is attributed to phenols. Seed oils absorb at 268nnm, which is attributed to conjugated trienes and at 279nm, as olive oil. Zooming in the spectra, soybean oil presents two other absorbance peaks, at 300 and 315nm, which are related to flavonoids (Fuentes, Báez , Bravo, Cid, & Labra, 2012).

Moving on to the visible and near-infrared region 400-1600nm (2nm interval), samples were undiluted and placed in a 10mm path length cuvette:

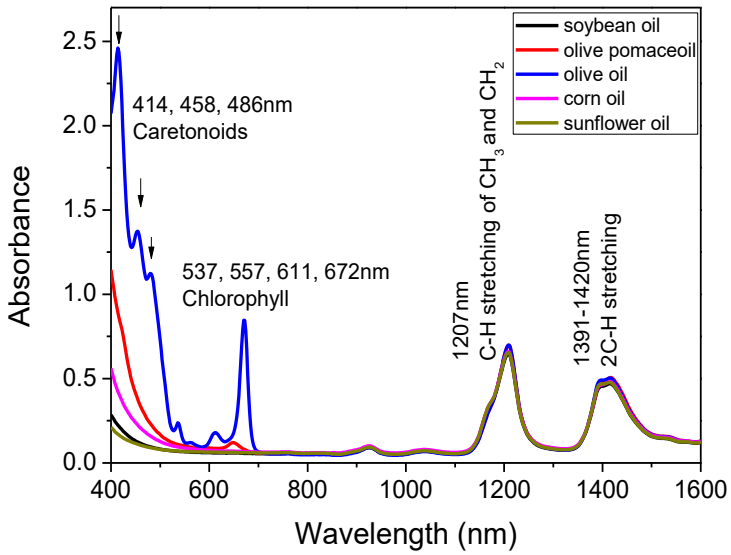

(a)

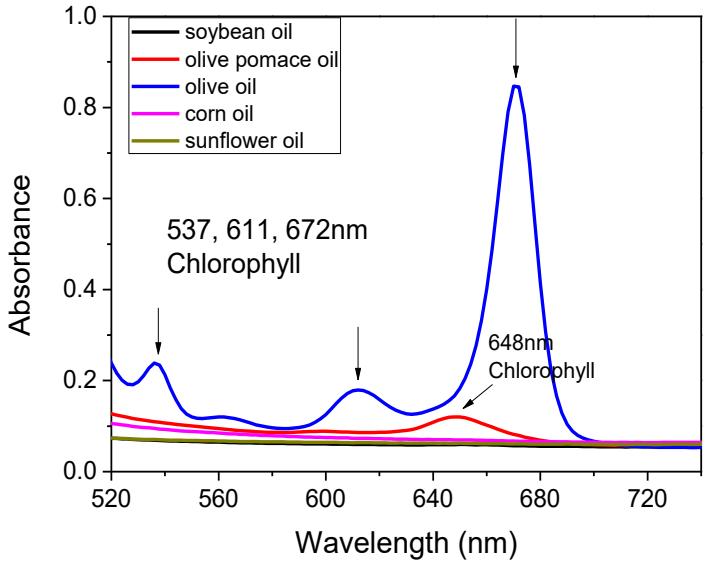

(b)

Figures 6.5.2: (a) Absorption spectra of oils at visible and near-IR region (400-1600nm),

(b) Zoom in of (a) in the region 520-740nm.

As seen in Fig. 6.5.2, at the visible region (400-700nm), olive oil presents three main peak absorbance peaks at 414, 458 and 486nm, related to carotenoids and three absorbance peaks at 537, 611 and 672nm, related to chlorophylls. Olive pomace oil presents a peak, but with lower absorbance, at 648nm, which is due to chlorophyll. This is essential, because the olive pomace oil comes from the olive core. The seed oils do not absorb at the visible region. There are two main absorbance peaks of all oils in the near-IR region, at 1207nm, coming from C-H stretching second overtone of CH_3 and CH_2 and a broad peak at 1391-1420nm, coming from 2C-H stretching. These two peaks are of the same intensity for all oil samples.

Near-IR region is interesting to study the vibrations of organic molecules. Measuring the absorbance of undiluted oils at the wavelengths 1800-2200nm, by an interval of 2nm, two main peaks are observed, as seen in Fig. 6.5.3:

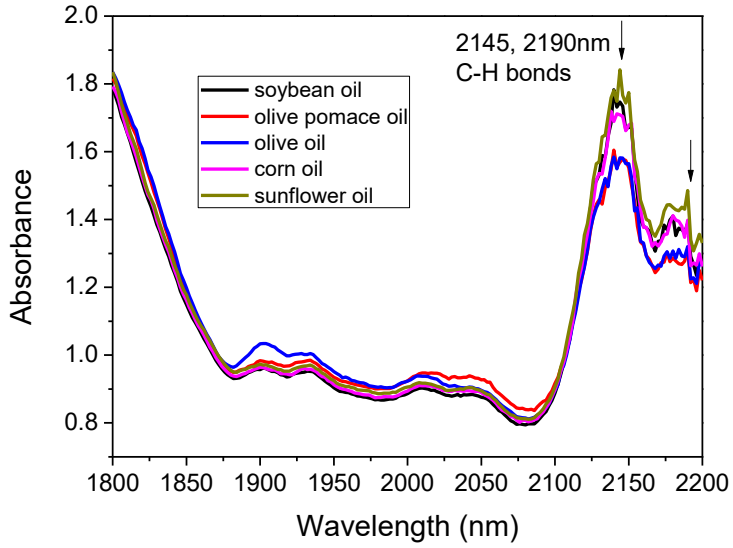

Figure 6.5.3: Absorption spectra of oils at near-IR region (1800-2200nm)

The absorbance peaks at 2145 and 2190nm show the vibration of C-H bonds. Olive and pomace olive oils present less absorbance than the seed oils. This information could be useful for FT-IR or Raman spectroscopy.

6.5.1.2 Fluorescence measurements

Excitation-emission fluorescence spectroscopy was employed in order to measure the fluorescence of oils. The experimental parameters were:

Excitation wavelengths region: 250-450nm, 3nm interval

Emission wavelengths region: 290-720nm, 5nm interval

Excitation/Emission Slits: 1/2nm

Integration time: 0.1sec

Undiluted oil samples were placed in a 10mm path length cuvette and measured at Front Face Geometry, 35° to the incident beam.

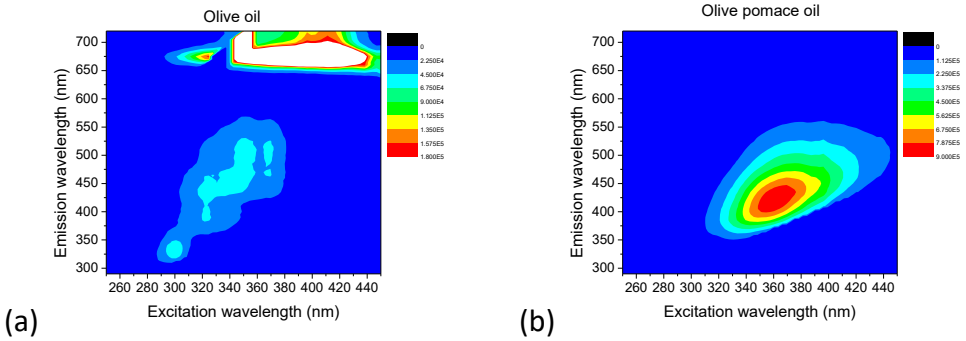

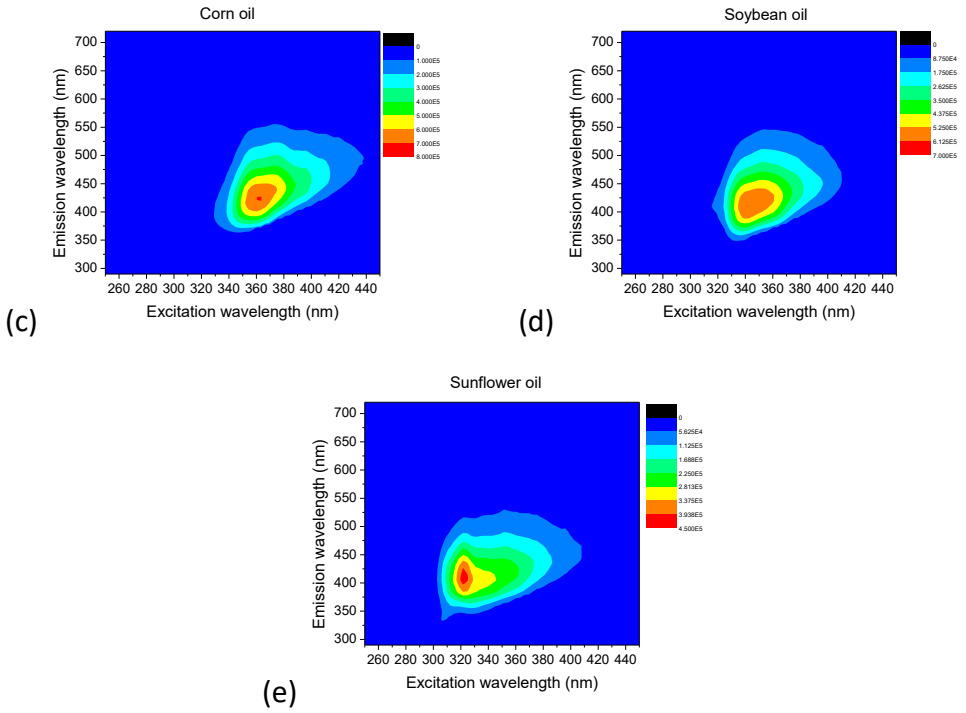

Figures 6.5.4 (a-e): Contour maps of oils. (a) olive oil, (b) olive pomace oil, (c) corn oil, (d) soybean oil, (e) sunflower oil

It is obvious from Fig. 6.5.4 that the olive oil is different, in comparison with seed oils. Concerning the contour map of olive oil, the fluorescence at 660-690nm is related to chlorophylls and is very intense. Looking at the emission wavelengths 320-340nm, where the excitation wavelengths are 290-310nm, we observe the emission of tocopherols. At emission wavelengths 420-440nm, when excited at 320-340nm, the fluorescence is related to phenolic compounds. Except from the chlorophyll fluorescence, sunflower oil presents fluorescence signal at 410nm, when excited at 315-345nm. Olive pomace oil, soybean and corn oils present vitamin E fluorescence at the region 410-430nm, when excited at 355-375nm.

The similarities of the seed oils with the virgin olive oil make them candidates for extra virgin olive oil adulteration.

Absorption and fluorescence measurements were performed for the adulteration of extra virgin olive oil with seed oils and especially with sunflower oil, corn oil and olive pomace oil. Mixtures of seed and extra virgin olive oils were performed in different volume percentages, as will be discussed at the next section.

6.5.2 Adulteration of extra virgin olive oil: Absorption measurements

6.5.2.1 Adulteration with olive pomace oil

The mixtures performed for the adulteration of extra virgin olive oil (evoo, as abbreviation) with olive pomace oil are: 10%, 20%, 30% and 50% v/v olive pomace oil in evoo. Oils samples were undiluted, placed in a 10mm path length cuvette and background was air.

Absorbance spectra at the near-IR and visible region are shown in Fig. 6.5.5 and 6.5.6:

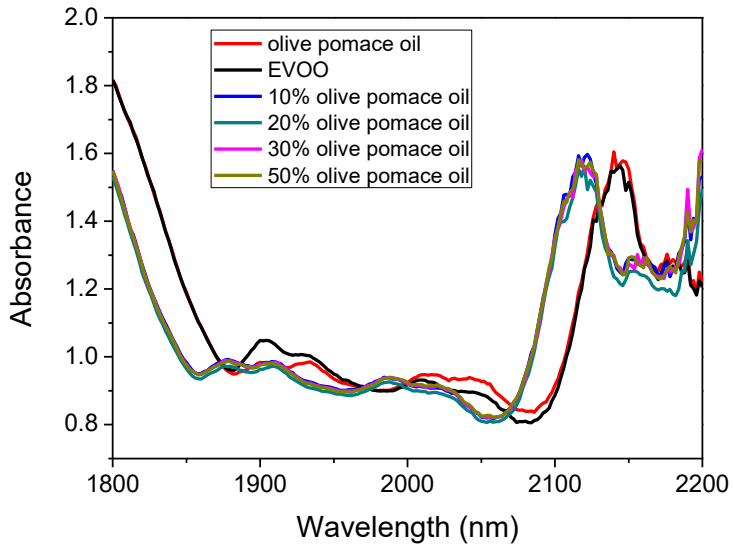

Figure 6.5.5: Absorption spectra of mixtures in near-IR region (1800-2200nm)

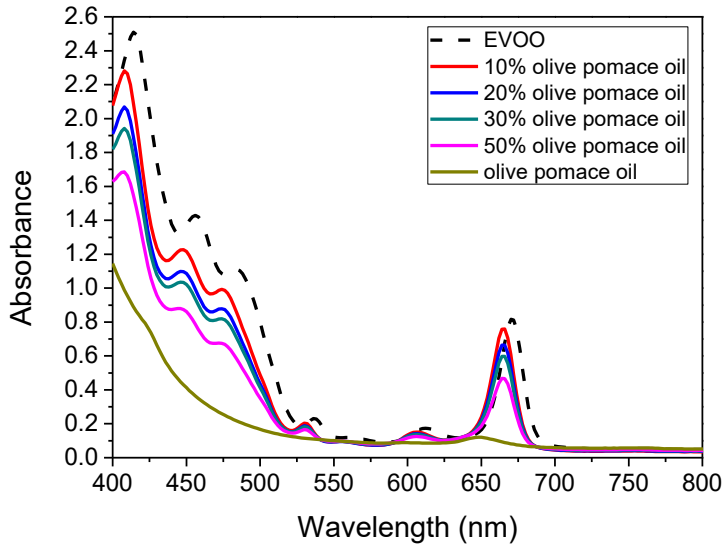

Figure 6.5.6: Absorption spectra of mixtures in visible region (400-800nm)

As seen in Fig. 6.5.5, at the near-IR region, a differentiation between the authentic oils and the mixtures is observed after 2100nm. The mixtures' spectra are blue shifted at 2120nm and the pure oils present their absorbance peak at 2140nm. This

is a mark for detecting the adulteration of evoo with olive pomace oil at the near-IR region.

Olive pomace oil has one absorbance peak at 648nm and the evoo presents 6 absorbance peaks, 3 peaks below 500nm, related to carotenoids and 3 others above 500nm. The mixtures are blue-shifted (about 10nm), because of a possible change in chemical composition in oil. Absorbance values of carotenoids are decreasing as pomace olive oil is added to evoo.

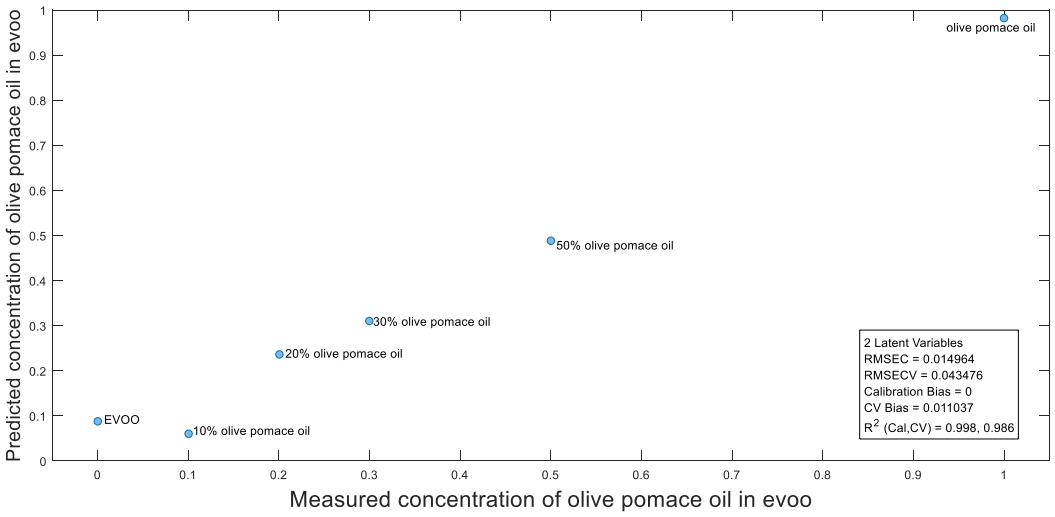

Figure 6.5.7: PLS plot at the visible region.

As seen in Fig. 6.5.7, PLS model was applied to the absorption spectra at the visible region (mean-centering pre-treatment of data and leave-one-out cross validation) and the RMSECV was 4.3%.

Fluorescence spectroscopy was employed, in order to try and discriminate the mixtures. Front Face geometry was used and the samples were placed in a 10mm path length cuvette. The experimental parameters were:

Excitation wavelengths region: 250-450nm, 3nm interval

Emission wavelengths region: 290-720nm, 5nm interval

Excitation/Emission Slits: 1/2nm

Integration time: 0.1sec

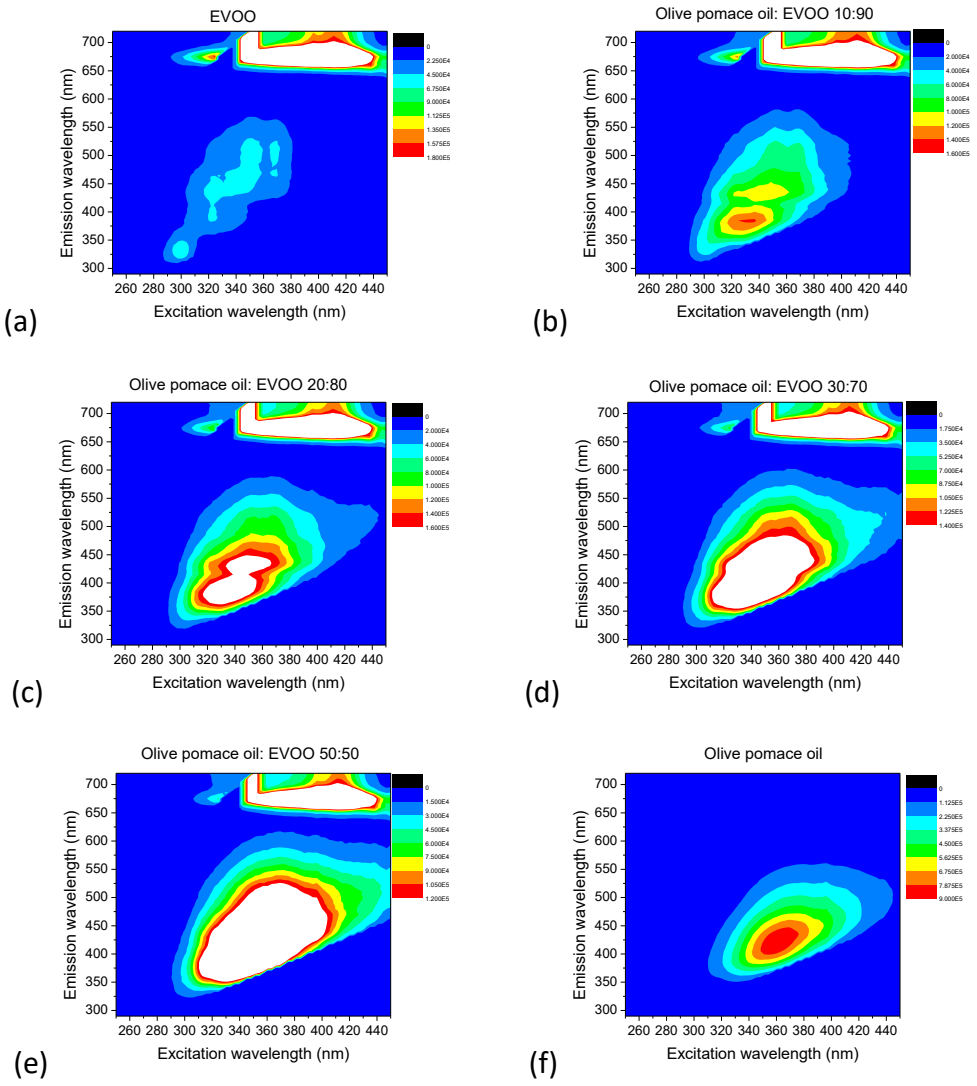

Figures 6.5.8 (a-f): Contour maps of oils. (a) extra virgin olive oil (EVOO), (b) 10:90 olive pomace oil: EVOO, (c) 20:80 olive pomace oil: EVOO, (d) 30:70 olive pomace oil: EVOO, (e) 50:50 olive pomace oil: EVOO, (f) olive pomace oil

Pure extra virgin olive oil (EVOO) and pure olive pomace oil present differences in their fluorescence spectra, as discussed in section 6.5.1.2. Adding olive pomace oil in the EVOO, increase of intensity at excitation wavelengths 310-394nm and emission wavelengths 375-500nm is observed, due to polyphenols. This is a principle for discriminating the adulterated EVOO with olive pomace oil qualitatively.

6.5.2.2 Adulteration with corn oil

The absorbance spectra in the visible region 400-550nm (2nm interval) of pure extra virgin olive oil (EVOO) and pure corn oil are totally different. EVOO presents 3 absorbance peaks at 414, 458 and 486nm, related to carotenoids. These absorbance peaks are absent at the absorption spectrum of corn oil. When corn oil is added to

the EVOO (Extra Virgin Olive Oil), differences at the intensity of absorbance peaks below 500nm are observed, as seen in Fig. 6.5.9 below:

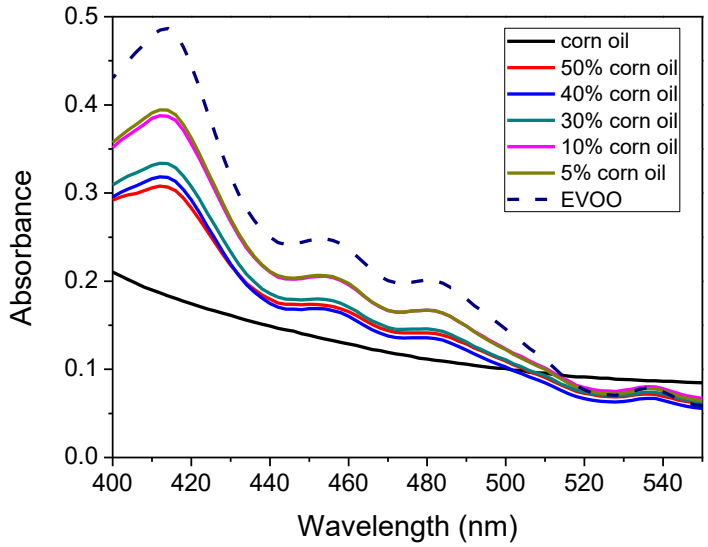

Figure 6.5.9: Absorbance spectra of EVOO, corn oil and mixtures in the visible region (400-550nm)

Mixtures of EVOO and corn oil measured had the following voltage percentages: 5, 10, 30, 40 and 50% v/v corn oil in EVOO. Absorption peaks of EVOO at 414, 458 and 486nm, corresponding to carotenoids, and at 536nm, corresponding to chlorophylls, present lower absorbance, as changing the volume percentage of corn oil in the mixture.

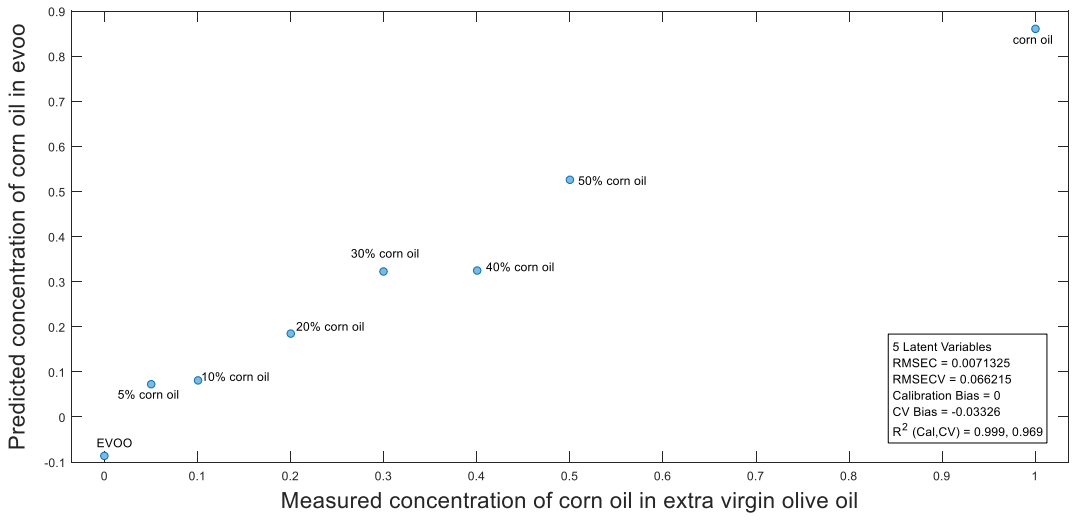

(a)

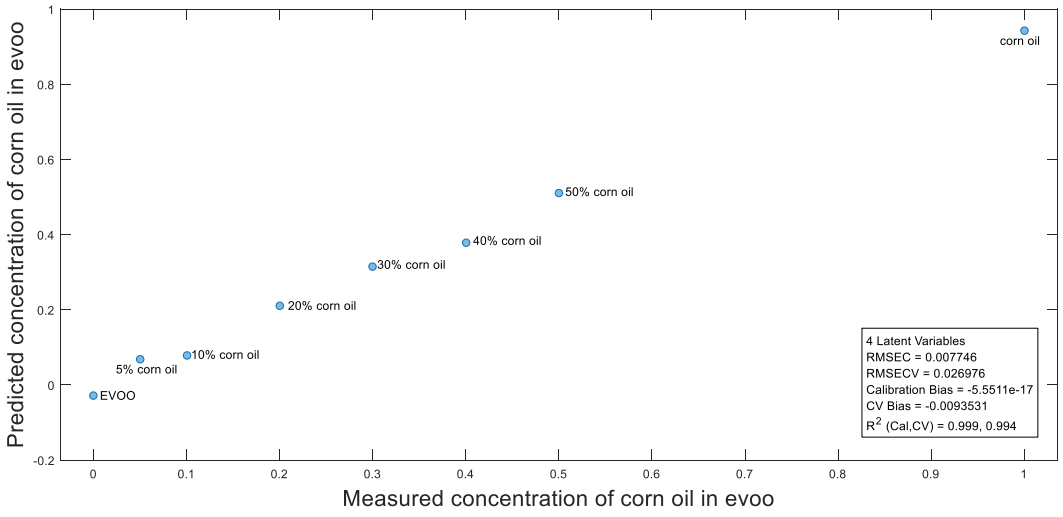

(b)

Figures 6.5.10 (a and b): PLS plots at the visible region. (a) Mean-centering pre-treatment of data, leave-one-out cross validation, RMSECV=6.6% (b) Mean-centering and Savitzky-Golay 1st derivative pre-treatment of data, leave-one-out cross validation, RMSECV=2.7%

As shown in Fig. 6.5.10, PLS model was employed to predict the volume percentage of seed oil in EVOO in this particular region (400-550nm). Mean-centering pre-treatment of the absorbance data was made, the leave-one-out cross validation was applied and the RMSECV is 6.6%. By pre-treating the data with mean-centering and Savitzky-Golay 1st derivative, the RMSECV is equal to 2.7%, which is a satisfying result for the detection of corn oil in EVOO.

6.5.2.3 Adulteration with sunflower oil

The sunflower oil is a common adulterant of extra virgin olive oil (EVOO) and many scientific journals have been reported for detecting the adulteration of EVOO *(Sikorska, Khmelinskii, & Sikorski, Analysis of Olive Oils by Fluorescence Spectroscopy : Methods and Applications, 2011), (Skevin, 2011), (Downey, McIntyre, & Davies, 2002)*. Several series of EVOO and sunflower oil mixtures have been performed, measured, employing Absorption and Fluorescence Spectroscopy, and analyzed on this purpose.

6.5.2.3.1 Absorption Spectroscopy and PLS regression

Mixtures of extra virgin olive oils (EVOO) and sunflower oils were performed, using different oils, and with different volume percentages. They are discussed as different series below:

1. EVOO (olive oil 12) and Sunflower oil (Carrefour)

EVOO was adulterated with sunflower oil in different volume percentages: 5, 10, 15, 20, 30, 40, 50, 60, 75 and 85% v/v sunflower oil in evoo. Measuring the absorbance of these samples (undiluted) in the visible region 400-800nm, by 2nm interval, and employing a 10mm path length cuvette, the absorption spectra are plotted (Fig. 6.5.11):

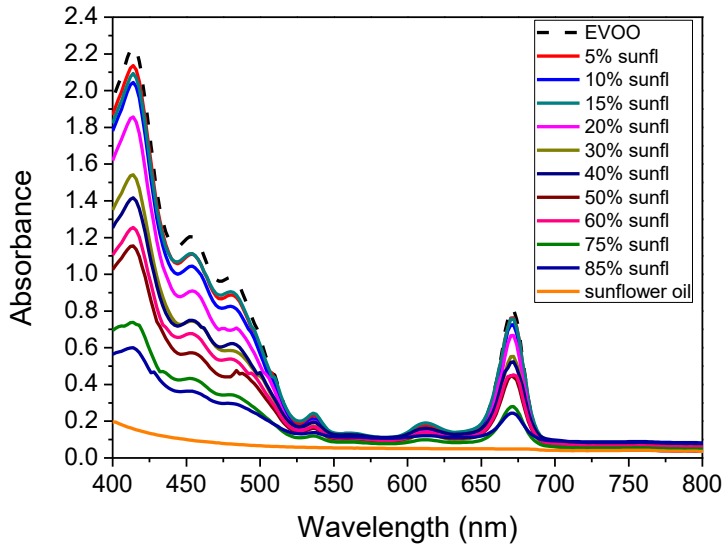

Figure 6.5.11: Absorption spectra of mixtures in the visible region (400-800nm)

It is observed that sunflower oil has no absorbance peaks at this wavelength region (400-800nm), but evoo presents 6 main absorbance peaks, as discussed before (section 6.5.1.1). The mixtures have the same absorption shape as evoo, but the absorbance intensity of carotenoids (especially at 414nm) decreases, as the volume percentage of sunflower oil increases. Consequently, a qualitatively discrimination of adulteration can be achieved only by observing the absorbance peak at 414nm, attributed to carotenoids.

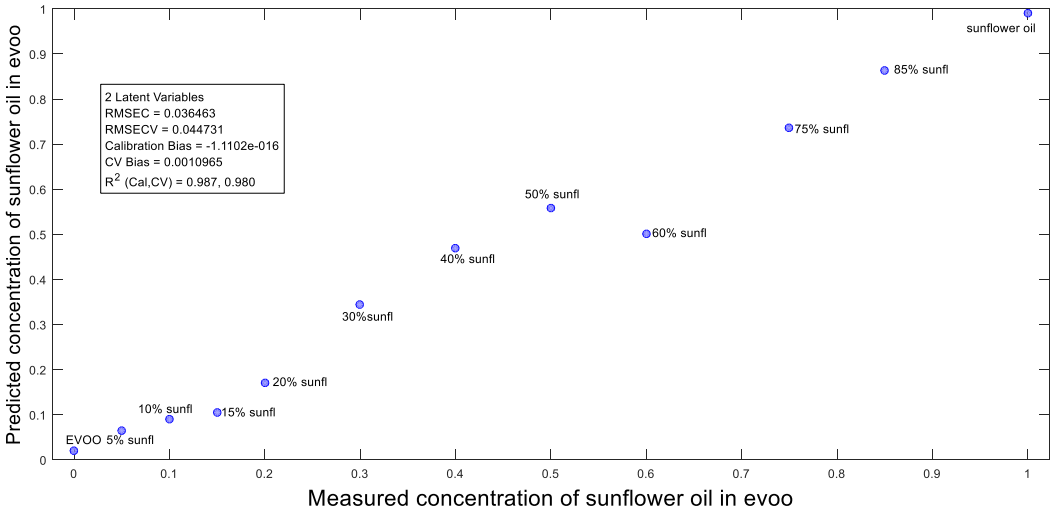

Figure 6.5.12: PLS plot at the visible region.

PLS regression model (via Matlab and PLS-Toolbox) was applied (see Fig. 6.5.12) to these data (mean-centering pre-treatment of spectra, leave-one-out cross validation) and the resulting RMSECV (root mean square error of cross validation) was 4.5%, which is an interesting outcome for detecting the adulteration.

2. EVOO (Μάλες Ιεράπετρα or olive oil 2) and Sunflower oil (Sol)

Sunflower oil in volume percentages 1, 2, 4, 8, 10, 12.5, 15, 20, 25, 30, 60, 80% v/v was added to extra virgin olive oil. Mixtures, pure sunflower and olive oils were placed in a 2mm path length cuvette, undiluted and measured at the visible wavelength region 400-800nm, by a 2nm interval. Absorption spectra were plotted (Fig. 6.5.13):

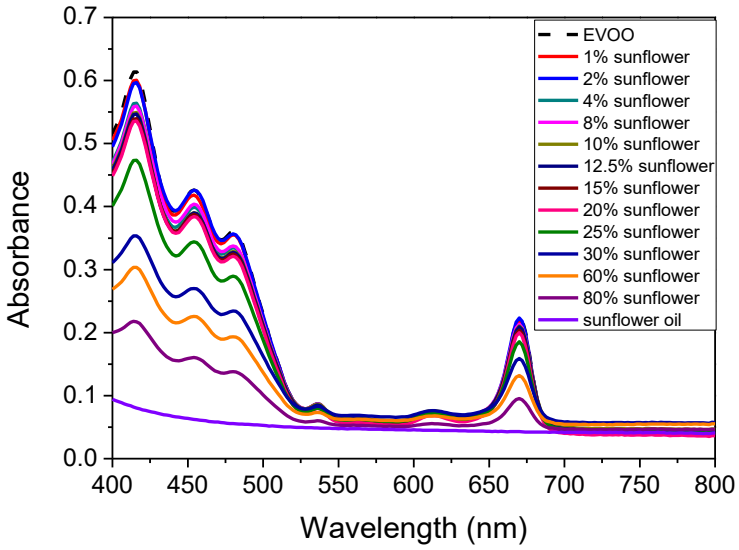

Figure 6.5.13: Absorption spectra of pure oils and mixtures at the visible region (400-800nm)

Pure extra virgin olive oil and mixtures of evoo with sunflower oil show 3 main absorbance peaks at 414, 458 and 486nm, related to carotenoids and three absorbance peaks at 537, 611 and 672nm, attributed to chlorophyll, in contrast to the absorption spectrum of sunflower oil, where these peaks are absent. Concerning the absorbance peak at 414nm (carotenoids absorption), pure evoo shows the most intense absorbance and mixtures tend to have lower absorbance intensities at this specific wavelength (414nm). So, there is a discrimination of oils and qualitatively detection of adulterants in evoo.

As observed from the absorption spectra at the visible region (400-800nm), the absorbance peak at 414nm, which corresponds to carotenoids, is a good indicator to discriminate the adulteration of extra virgin olive oil (evoo) with sunflower oil. On this purpose, the control of linearity of the sunflower concentration in evoo versus the absorbance peak at 414nm was printed in Fig. 6.5.14:

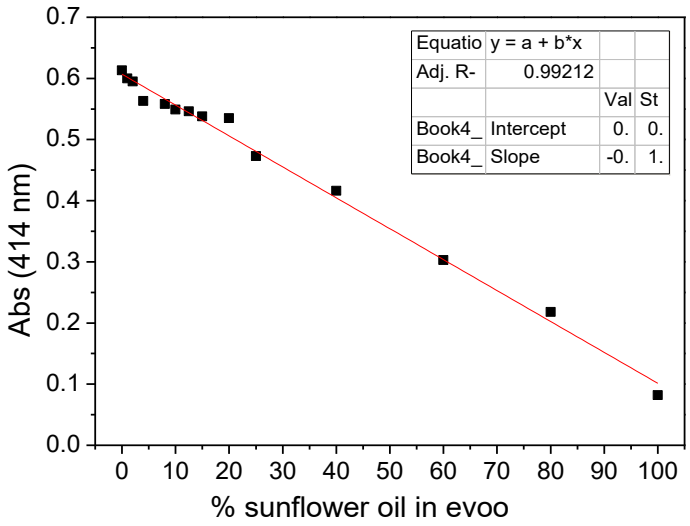
Equatio y = a + b*x
Adj. R- 0.99212
Val St
Book4_ Intercept 0. 0.
Book4_ Slope -0. 1.
Abs (414 nm)
% sunflower oil in evoo

(a)

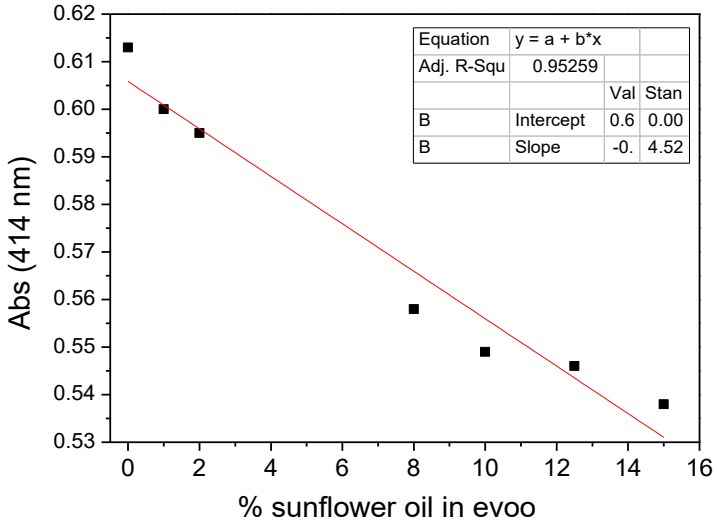
Equation y = a + b*x
Adj. R-Squ 0.95259
Val Stan
B Intercept 0.6 0.00
B Slope -0. 4.52
Abs (414 nm)
% sunflower oil in evoo

(b)

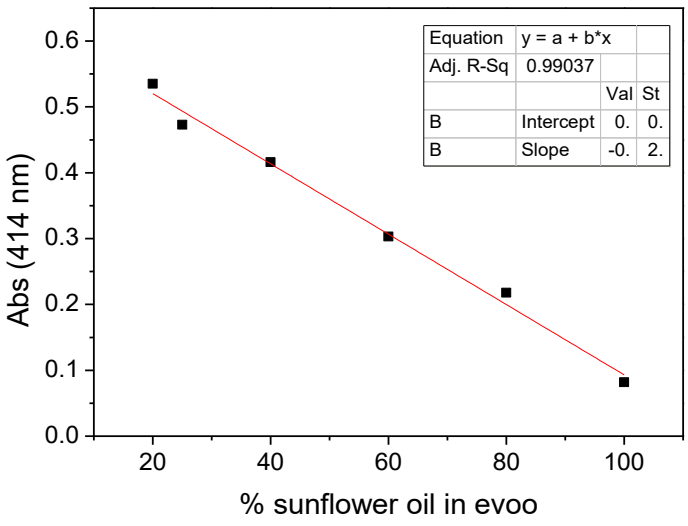
Equation y = a + b*x
Adj. R-Sq 0.99037
Val St
B Intercept 0. 0.
B Slope -0. 2.
Abs (414 nm)
% sunflower oil in evoo

(c)

Figures 6.5.14 (a- c): Mixtures of sunflower oil and evoo vs Absorbance peak at 414nm. (a) All mixtures vs Absorbance peak at 414nm, (b) Low concentrations of sunflower oil in evoo ($\leq 15\%$ sunflower oil in evoo) and (c) High concentrations of sunflower oil in evoo ($\geq 20\%$ sunflower oil in evoo)

As seen, the absorbance peak at 414nm falls linearly as the concentration of sunflower oil in evoo increases (Fig. 6.5.14 a). R^2 coefficient is 0.992, very close to 1, which means that is a linear equation. I separated the mixtures in two categories – low sunflower concentration ($\leq 15\%$) and higher sunflower concentration ($\geq 20\%$). R^2 coefficients are 0.952 and 0.99, respectively, very close to 1. There is a linear dependence of sunflower concentration in evoo with the absorbance peak at 414nm, which corresponds to carotenoids, and the adulteration of evoo can be defined qualitatively only by measuring the absorbance of the sample at this specific wavelength.

Moreover, the absorption spectra were inserted to the PLS regression model, in order to control the adulteration of evoo with the sunflower oil with statistical method:

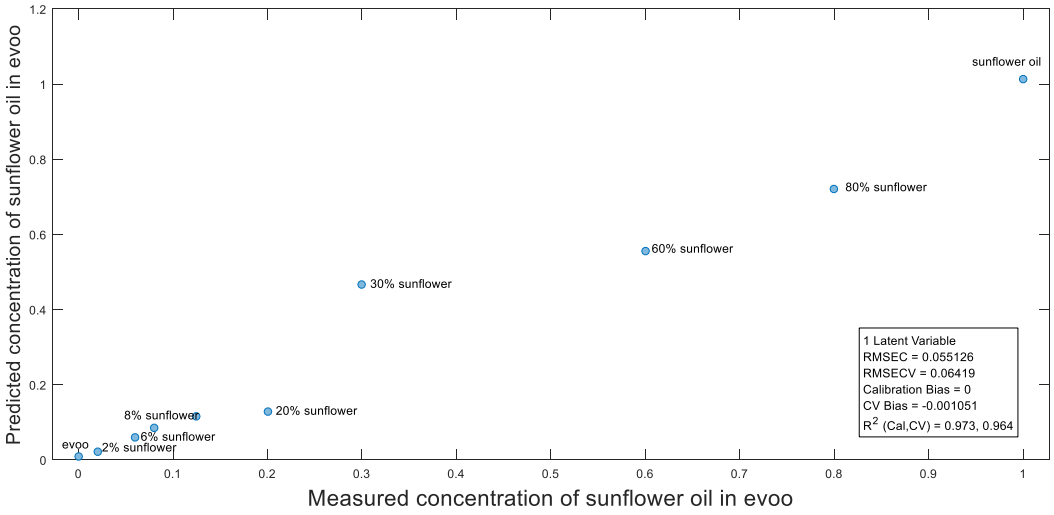

Figure 6.5.15: PLS plot at the visible region

PLS regression model (Fig. 6.5.15) was applied to these absorption spectra (400-800nm) (mean-centering pre-treatment of spectra, leave-one-out cross validation) and the RMSECV was 6.4%.

Evaluating the predictive ability of the PLS regression model, external validation was carried out, by dividing the samples in two groups (calibration and validation sets). The calibration and validation sets are composed of 10 and 5 samples, respectively. Samples included in the validation set have volume percentages of 4, 10, 15, 25 and 40% v/v sunflower oil in evoo and RMSEP (Root Mean Square Error of Prediction) is evaluated (Fig. 6.5.16).

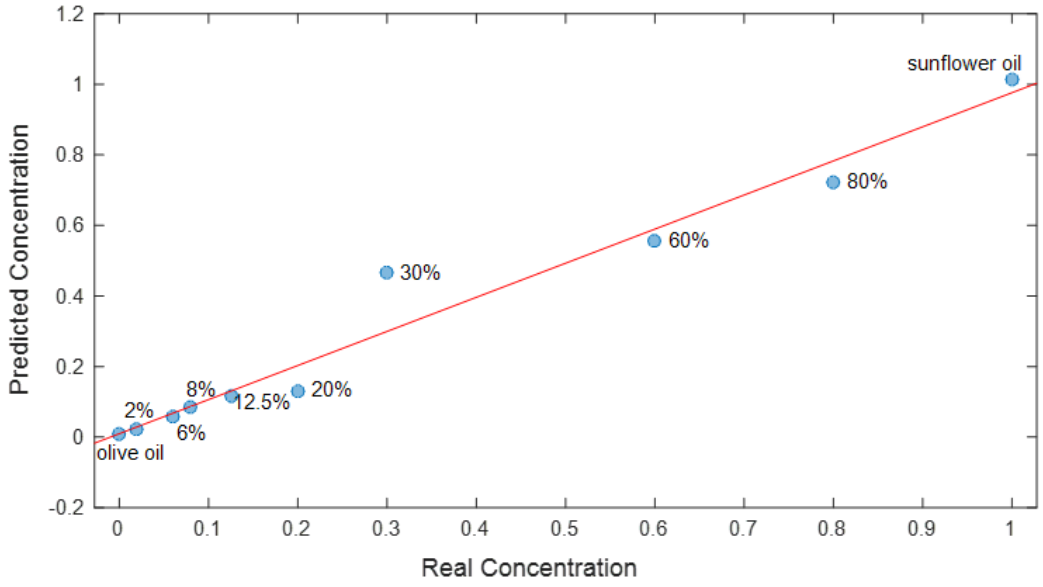

Figure 6.5.16: PLS plot for the calibration set

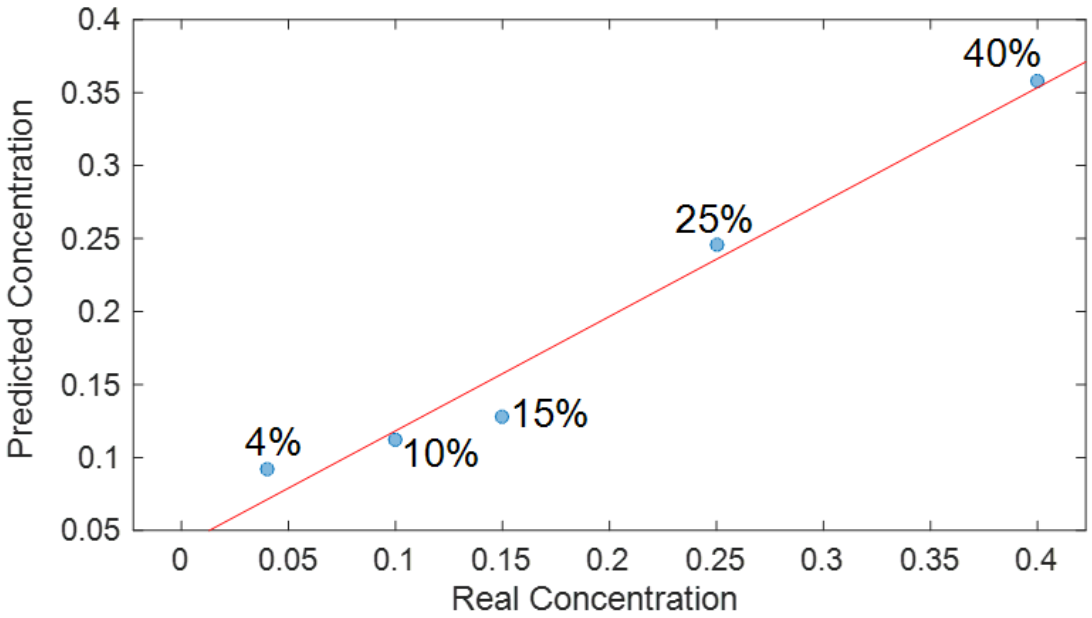

Figure 6.5.17: PLS plot for the validation set

The PLS plot for the calibration set (Fig. 6.5.16) presents the actual concentration of sunflower oil in evoo (x-axis) versus the predicted concentration (y-axis). PLS regression model shows the value of R^2 coefficient as 0.965 and RMSECV as 5.5%. Concerning the PLS plot for the validation set (Fig. 6.5.17) that contains 5 samples out of 15 in total, R^2 coefficient is equal to 0.971 and the RMSEP equals to 3.2%. These results are promising in detection of seed oils in extra virgin olive oil, by applying the visible absorption spectroscopy.

3. <u>EVOO (Dafnes) and Sunflower oil (Mr. Grand)</u>

Mixtures prepared, contained 0.5, 1, 2, 4, 5, 6, 8, 10, 12.5, 15, 20, 30, 40 and 50% v/v sunflower oil in extra virgin olive oil (evoo).

Using the UV absorption spectroscopy at wavelengths region of 220-280nm, by 0.5nm step, the samples were diluted 1% v/v in n-hexane, placed in a 2mm path length quartz cuvette and the background measured was the cuvette full of the solvent (n-hexane).

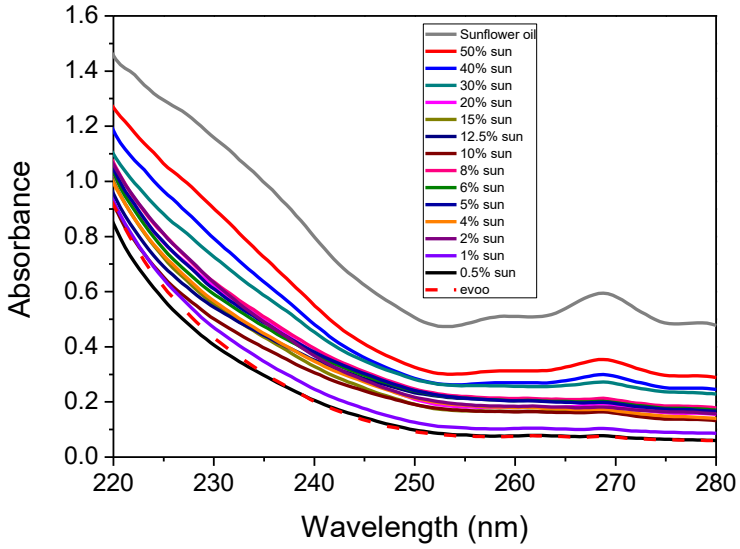

Figure 6.5.17: Absorption spectra of mixtures and pure oils at the UV region 220-280nm.

As seen in Fig. 6.5.17, the absorbance of pure evoo and mixtures have the same shape and do not have any absorbance peaks, except from the mixtures with 30, 40 and 50% v/v sunflower in evoo. Pure sunflower oil and the adulterated olive oils, containing volume percentages 30, 40 and 50% sunflower oil present an absorbance peak at 268nm, which is related to conjugated trienes.

As observed at the following plots (Fig. 6.5.18), when mean-centering pre-treatment of the data was performed and the leave-one-out cross validation was applied, the PLS model was evaluated and RMSECV was equal to 2.9%. The same prediction (RMSECV=2.9%) was achieved, when Savitzky-Golay 1st derivative pre-treatment of spectral data was performed and the venetian blinds cross validation applied. However, by pre-treating the spectra with Savitzky-Golay method, using 2nd derivative and the venetian blinds cross validation, RMSECV was 2.4%. These RMSECV values indicate that the UV absorption spectroscopy at wavelengths of 220-280nm are valuable for detecting extra virgin olive oil adulteration with sunflower oil in low volume percentages.

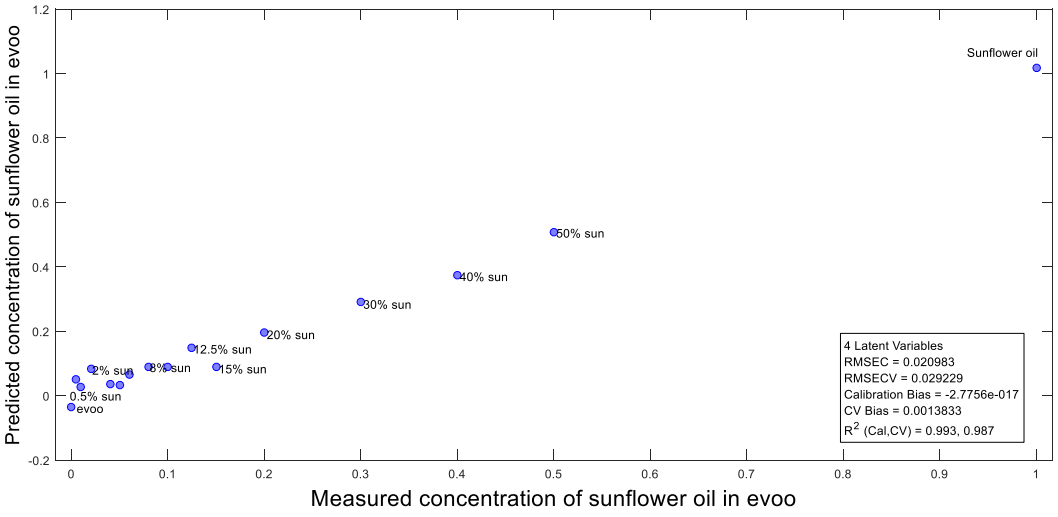
Predicted concentration of sunflower oil in evoo
Measured concentration of sunflower oil in evoo
Sunflower oil
50% sun
40% sun
30% sun
20% sun
12.5% sun
15% sun
2% sun
0.5% sun
evoo
4 Latent Variables
RMSEC = 0.020983
RMSECV = 0.029229
Calibration Bias = -2.7756e-017
CV Bias = 0.0013833
R2 (Cal,CV) = 0.993, 0.987

(a)

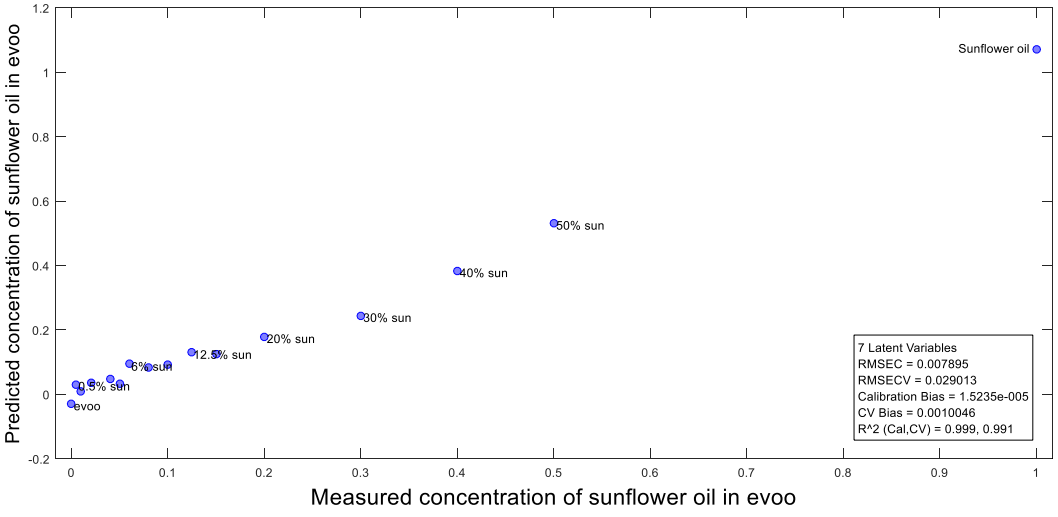
Predicted concentration of sunflower oil in evoo
Measured concentration of sunflower oil in evoo
Sunflower oil
50% sun
40% sun
30% sun
20% sun
12.5% sun
6% sun
0.5% sun
evoo
7 Latent Variables
RMSEC = 0.007895
RMSECV = 0.029013
Calibration Bias = 1.5235e-005
CV Bias = 0.0010046
R^2 (Cal,CV) = 0.999, 0.991

(b)

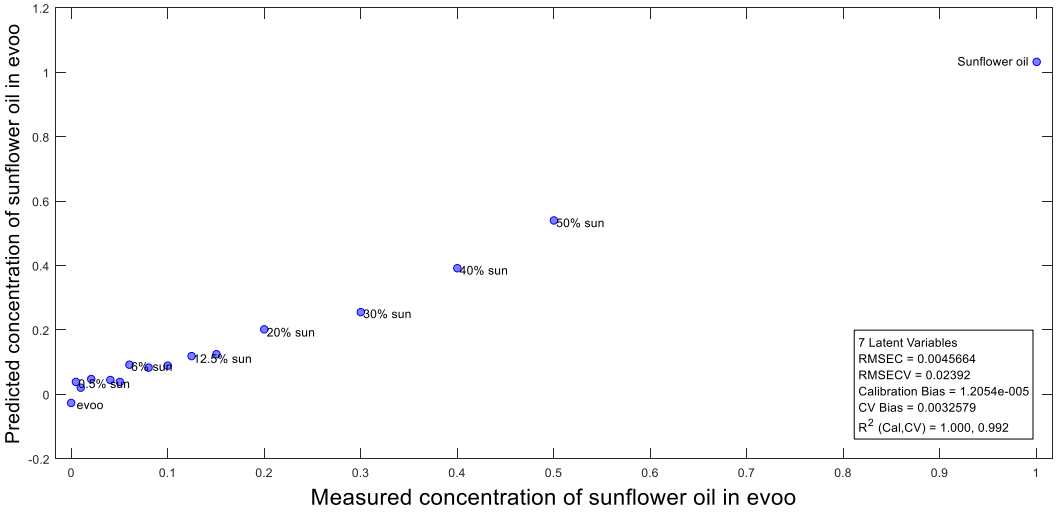
Predicted concentration of sunflower oil in evoo
Measured concentration of sunflower oil in evoo
Sunflower oil
50% sun
40% sun
30% sun
20% sun
12.5% sun
6% sun
0.5% sun
evoo
7 Latent Variables
RMSEC = 0.0045664
RMSECV = 0.02392
Calibration Bias = 1.2054e-005
CV Bias = 0.0032579
R2 (Cal,CV) = 1.000, 0.992

(c)

Figures 6.5.18 (a-c): PLS plots at the UV region (220-280nm). (a) Mean-centering pre-treatment of data, leave-one-out cross validation, RMSECV=2.9% (b) Savitzky-Golay 1st derivative, Venetian blinds cross validation, RMSECV=2.9% (c) Savitzky-Golay 2nd derivative, Venetian blinds cross validation, RMSECV=2.4%

Experimental measurements were performed by employing UV absorption spectroscopy at the wavelengths region of 260-410nm (2nm interval). Samples were diluted 1% v/v in hexane and placed in a 10mm path length cuvette, while the background was the solvent.

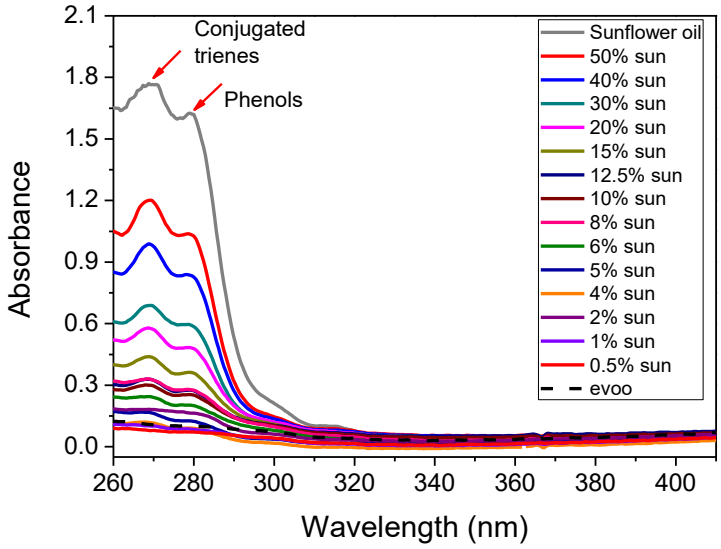

Figure 6.5.19: Absorption spectra of oils at the UV region (260-410nm)

Pure sunflower oil spectrum shows two absorbance peaks at 268 and 278nm, related to conjugated trienes and phenols, respectively, in contrast to pure extra virgin olive oil spectrum. When the volume percentage of sunflower oil in evoo increases, absorbance peaks appear. This effect actually appears when the volume percentage of sunflower in evoo is above 6%.

Employing the PLS model (mean-centering pre-treatment of spectra, venetian blinds cross validation), RMSECV equals to 5.6%. If spectral data are pre-treated with mean-centering and Savitzky-Golay 1st derivative processes and leave-one-out cross validation is applied, the value of RMSECV is equal to 7.1%, as shown in Fig. 6.5.20:

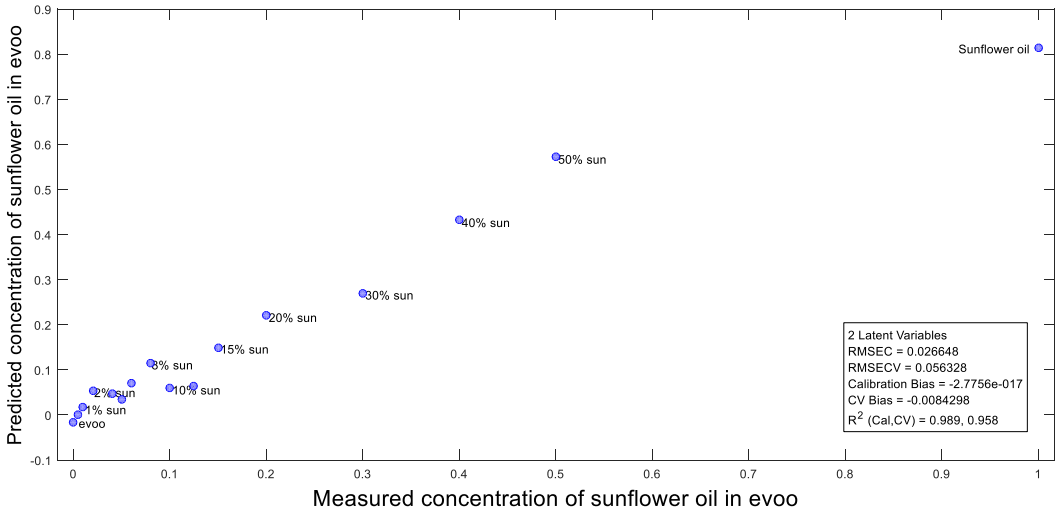

(a)

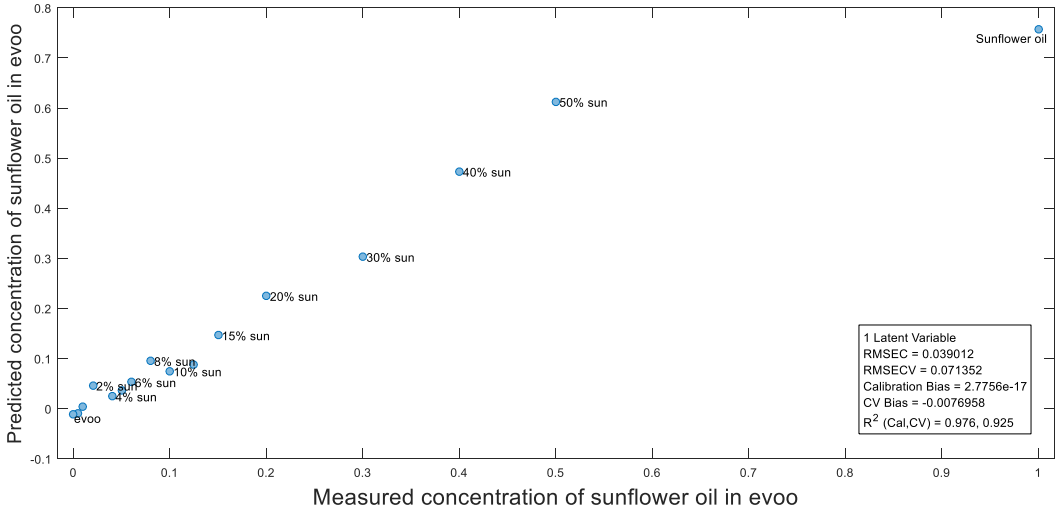

(b)

Figure 6.5.20 (a and b): PLS plots at the UV region (260-410nm). (a) Mean-centering pre-treatment of data, venetian blinds cross validation, RMSECV=5.6% (b) Mean-centering and Savitzky-Golay 1st derivative pre-treatment of data, leave-one-out cross validation, RMSECV=7.1%

Calculating the K_{270} and ΔK indexes (as mentioned at section 4.2.2) from Eq. 4.1 and 4.2, the results are shown below:

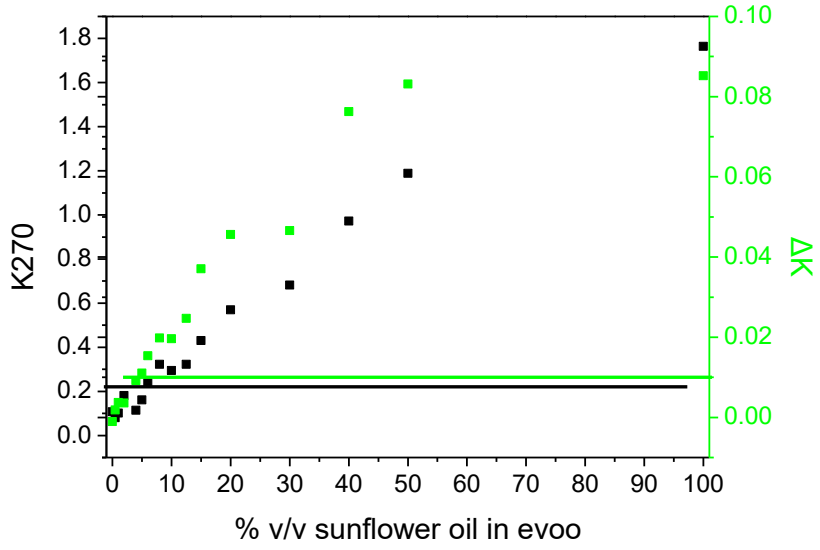

Figure 6.5.21: Indexes K_{270} and ΔK of the mixtures

Looking at the K and ΔK index values, it can be observed that samples containing 6% v/v sunflower oil and up are not characterized as extra virgin olive oils, according to European instructions for the authentication of evoo (IOOC, 1991). This is an indicative detection of adulteration of extra virgin olive, only by calculating the K indexes, coming out from the UV absorption spectra.

Furthermore, experiments were performed in the Visible wavelength region of 400-800nm (2nm interval). Samples were undiluted and placed in 2mm path length cuvette. Absorption spectra are shown in the following figure:

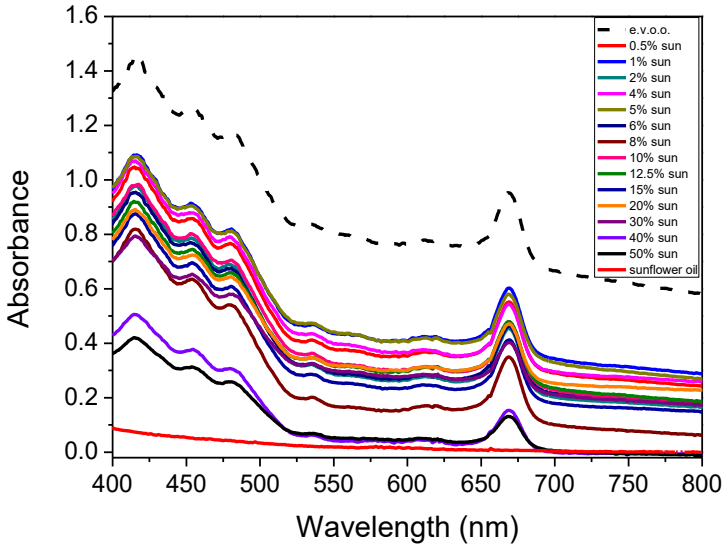

Figure 6.5.22: Absorption spectra of samples at visible region (400-800nm)

From Fig. 6.5.22, pure extra virgin olive oil presents three main absorbance peaks at 414, 453 and 482nm, corresponding to carotenoids and one absorbance peak, corresponding to chlorophylls. These peaks are absent in pure sunflower oil. Mixtures present the same absorbance peaks with evoo, but have lower absorbance values.

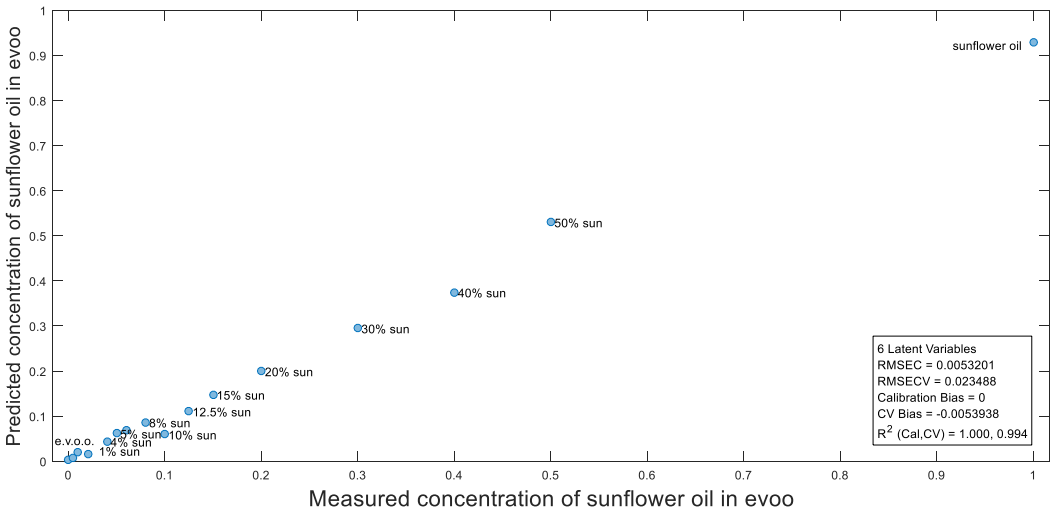

(a)

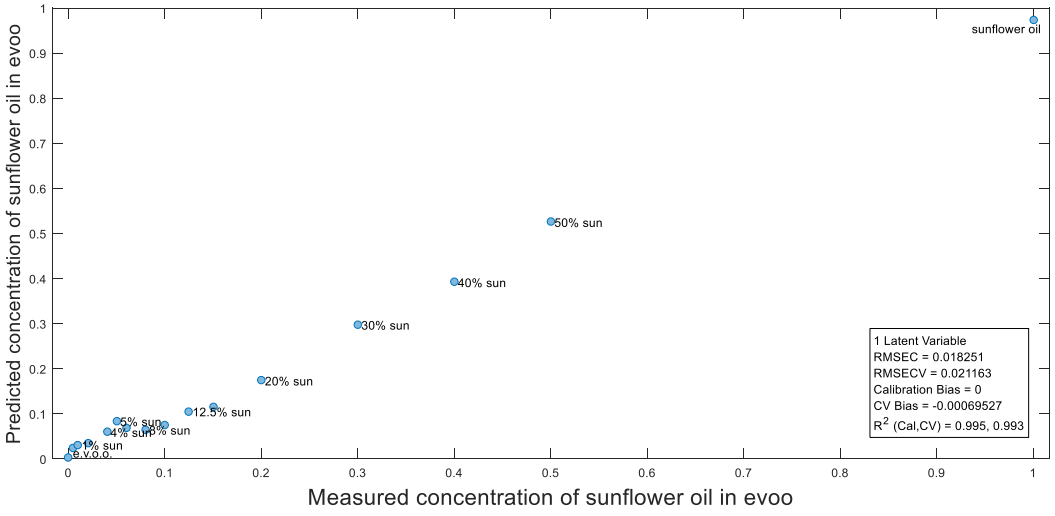

(b)

Figures 6.5.23 (a and b): PLS plots at the visible region (400-800nm). (a) Mean-centering pre-treatment of data, leave-one-out cross validation, RMSECV=2.3% (b) Mean-centering+ Savitzky-Golay 1st deriv. and leave-one-out cross validation, RMSECV=2.1%

Processing the absorbance data with mean-centering pre-treatment and applying the leave-one-out cross validation, PLS model shows the value of RMSECV equal to 2.3%. A lower prediction was achieved, when the pre-treatment of data was mean-centering and Savitzky-Golay 1st derivative processes and the leave-one-out cross

validation was applied. The RMSECV was equal to 2.1%, by applying the previous parameters, as shown in Fig. 6.5.23. The combination of absorption spectroscopy with PLS regression method leads to quantitative measurement of adulterant concentration of sunflower oil in extra virgin olive oil.

4. EVOO (Androulidia) with Sunflower oil (Mr. Grand)

Mixtures were prepared as: 0.5, 1, 2, 4, 5, 6, 8, 10, 12.5, 20, 30, 40, 50% v/v sunflower oil in extra virgin olive oil.

Applying the UV absorption spectroscopy, the absorption spectra of samples at the wavelengths region 220-280nm (0.5nm interval) are shown below (Fig. 6.5.24):

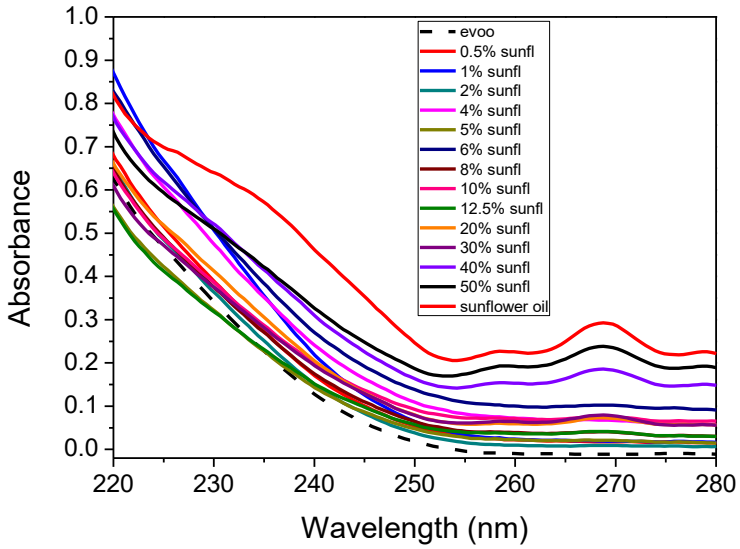

Figure 6.5.24: Absorption spectra of samples at the UV region (220-280nm)

The samples were diluted 1% v/v in n-hexane and placed in a 2mm path length quartz cuvette. As seen in Fig. 6.5.24, extra virgin olive oil presents no absorbance peaks at this region, but, as the volume percentage of sunflower oil in evoo increases, an absorbance peak at 268nm appears, especially for mixtures containing 20% v/v sunflower oil and up. Pure sunflower oil also presents this absorbance peak at 268nm, corresponding to conjugated trienes.

PLS regression model was applied to these absorption data, as seen in Fig. 6.5.25. Data were pre-treated in three different procedures and two different cross validation methods. Mean centering pre-treatment procedure and leave-one-out cross validation show the value of RMSECV equal to 3.1%, but Savitzky-Golay (Savgol in brief) using 1st derivative pre-treatment process and venetian blinds cross validation applied show that RMSECV equals to 2.9%. When the absorption data are pre-treated with mean-centering and Savitzky-Golay 2nd derivative processes and the leave-one-out cross validation is applied, the value of RMSECV was equal to 4.6%.

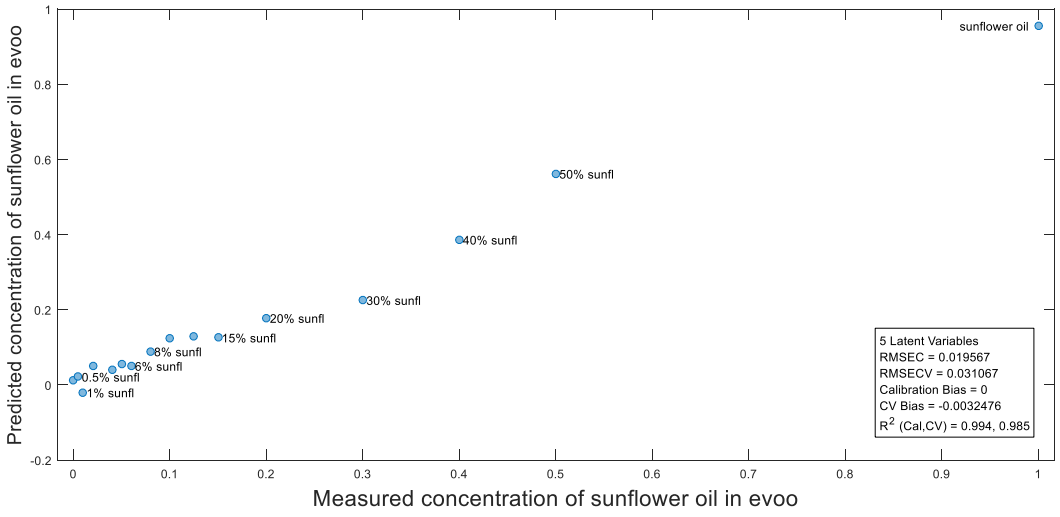
sunflower oil
50% sunfl
40% sunfl
30% sunfl
20% sunfl
15% sunfl
8% sunfl
6% sunfl
0.5% sunfl
1% sunfl
5 Latent Variables
RMSEC = 0.019567
RMSECV = 0.031067
Calibration Bias = 0
CV Bias = -0.0032476
R2 (Cal,CV) = 0.994, 0.985
Predicted concentration of sunflower oil in evoo
Measured concentration of sunflower oil in evoo

(a)

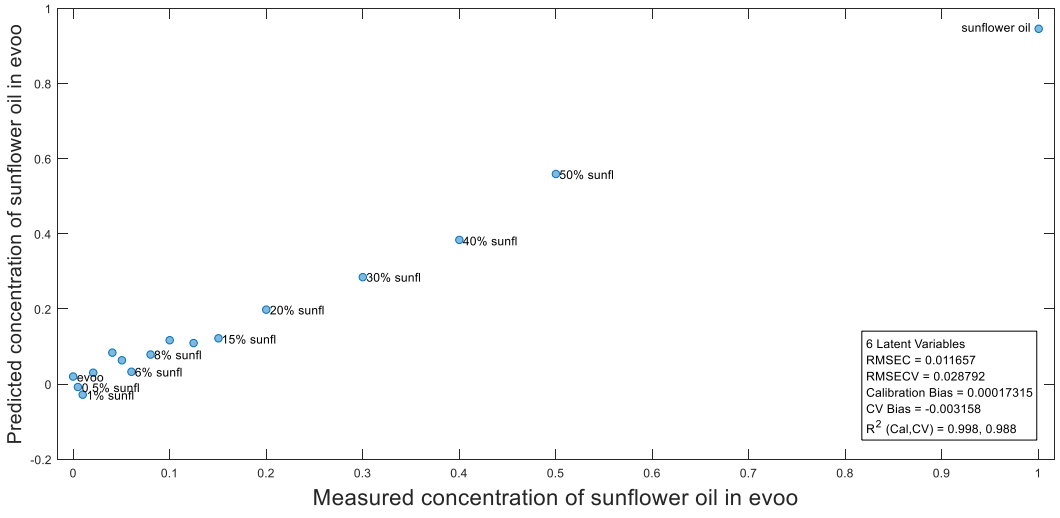
sunflower oil
50% sunfl
40% sunfl
30% sunfl
20% sunfl
15% sunfl
8% sunfl
6% sunfl
evoo
0.5% sunfl
1% sunfl
6 Latent Variables
RMSEC = 0.011657
RMSECV = 0.028792
Calibration Bias = 0.00017315
CV Bias = -0.003158
R2 (Cal,CV) = 0.998, 0.988
Predicted concentration of sunflower oil in evoo
Measured concentration of sunflower oil in evoo

(b)

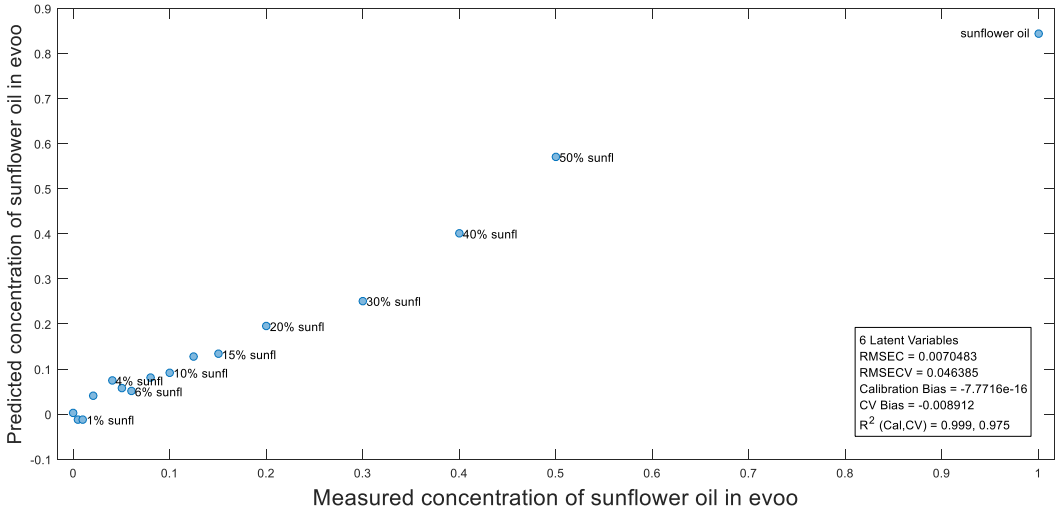
sunflower oil
50% sunfl
40% sunfl
30% sunfl
20% sunfl
15% sunfl
10% sunfl
4% sunfl
6% sunfl
1% sunfl
6 Latent Variables
RMSEC = 0.0070483
RMSECV = 0.046385
Calibration Bias = -7.7716e-16
CV Bias = -0.008912
R2 (Cal,CV) = 0.999, 0.975
Predicted concentration of sunflower oil in evoo
Measured concentration of sunflower oil in evoo

(c)

Figures 6.5.25 (a-c): PLS plots at the UV region (220-280nm). (a) Mean-centering pre-treatment of data and leave-one-out cross validation, RMSECV=3.1% (b) Mean-centering+Savgol 1st derivative pre-treatment of data and leave-one-out cross validation, RMSECV=3.9% (c) Mean-centering+Savgol 2nd derivative pre-treatment of data and leave-one-out cross validation, RMSECV=4.6%

Consequently, even if the absorption spectra do not show significant differences of the mixtures, PLS regression model can indicate a low detection limit for the adulteration of evoo with sunflower oil by the absorption spectra of samples in the UV wavelength region 220-280nm.

Testing the UV absorption wavelength region of 260-410nm, by a 2nm step, and employing a 10mm path length cuvette, samples were diluted 1% v/v in n-hexane and their absorption spectra are printed below (Fig. 6.5.26):

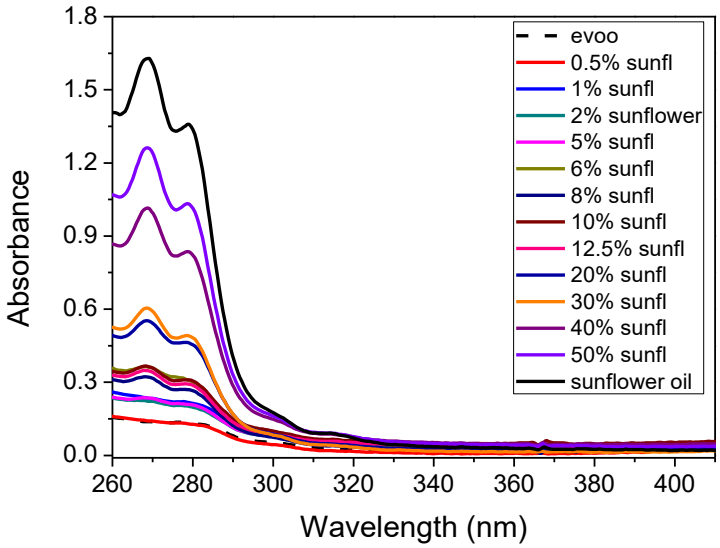

Figure 6.5.26: Absorption spectra of mixtures at region 260-410nm

It is observed that extra virgin olive oil presents a shoulder at 280nm, corresponding to phenols. On the other side, sunflower oil and mixtures present two absorbance peaks at 268 and at 278nm, corresponding to conjugated trienes and phenols, respectively. Concerning the absorbance values at 266, 270 and 274nm, indexes K_{270} and ΔK can be calculated (from Eq. 4.1 and 4.2). Their values are plotted vs the concentration below (Fig. 6.5.27):

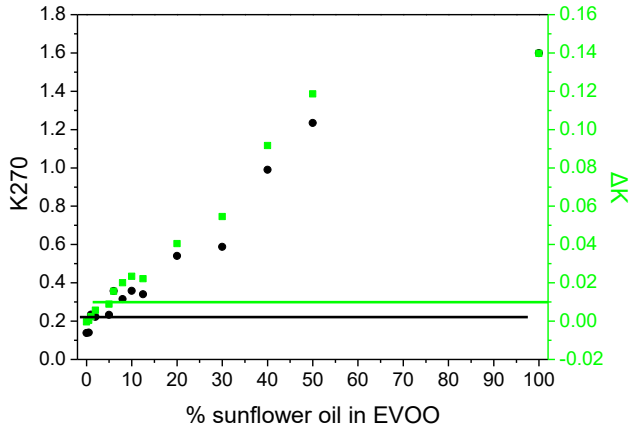

Figure 6.5.27: Indexes K_{270} and ΔK vs concentration

As observed, the values of K_{270} are below the limit of 0.22 (for extra virgin olive oil) for samples with lower than 5% v/v sunflower oil in evoo. Similarly, ΔK values are below 0.01 (this is the limit for characterizing an olive as an extra virgin olive oil) for mixtures containing lower than 6% v/v sunflower oil. These results recommend that UV absorption spectroscopy at the wavelength region of 260-410nm is a promising technique for the detection of the adulteration of evoo with sunflower oil in low limits as 5% v/v.

Moreover, Visible absorption Spectroscopy was applied to the mixtures, which were undiluted at this stage. More specifically, samples were measured at the wavelength region 400-800nm, by a 2nm step, in a 2mm path length cuvette.

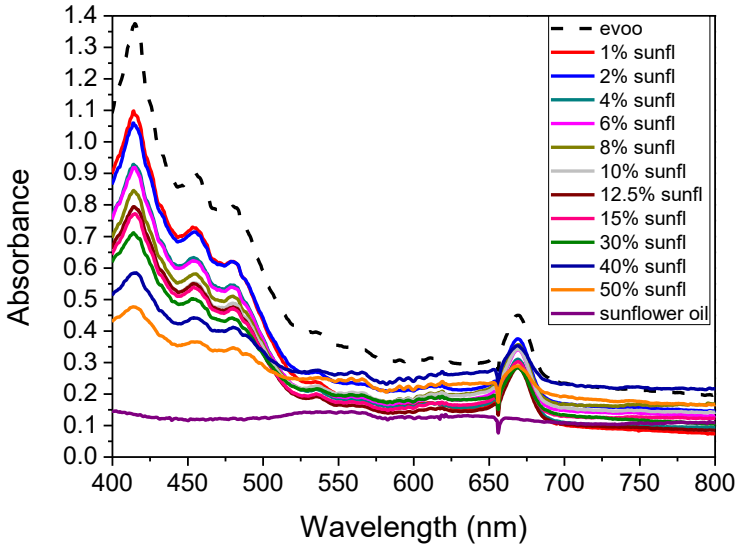

Figure 6.5.28: Absorption spectra of mixtures at the visible region 400-800nm

From Fig. 6.5.28, it is noticed that pure sunflower oil presents no absorbance peaks, in contrast to evoo and the mixtures containing various concentrations of sunflower and extra virgin olive oils. There are 4 main absorbance peaks present in evoo, 3 of

them at 414, 453 and 482nm related to carotenoids and one at 668nm, corresponding to chlorophylls group. In a more careful glance, it is observed that as the concentration of sunflower oil in evoo is increased, the absorbance intensity of the peak at 414nm decreases.

PLS regression model was applied to the absorption data, while the absorption spectra were pre-treated with mean-centering process and leave-one out cross validation was implemented. RMSECV was equal to 4.6%, which is a low detection limit. When mean-centering and Savitzky-Golay 1st derivative processes were applied to the absorption data and leave-one-out cross validation was employed, the RMSECV was equal to 5.4%, as can be seen in the following plots (Fig. 6.5.29):

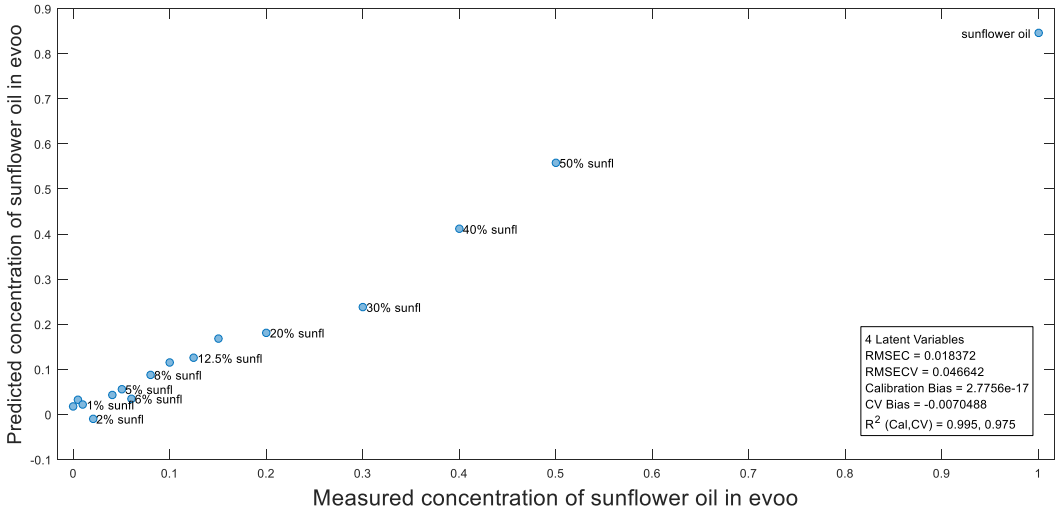

(a)

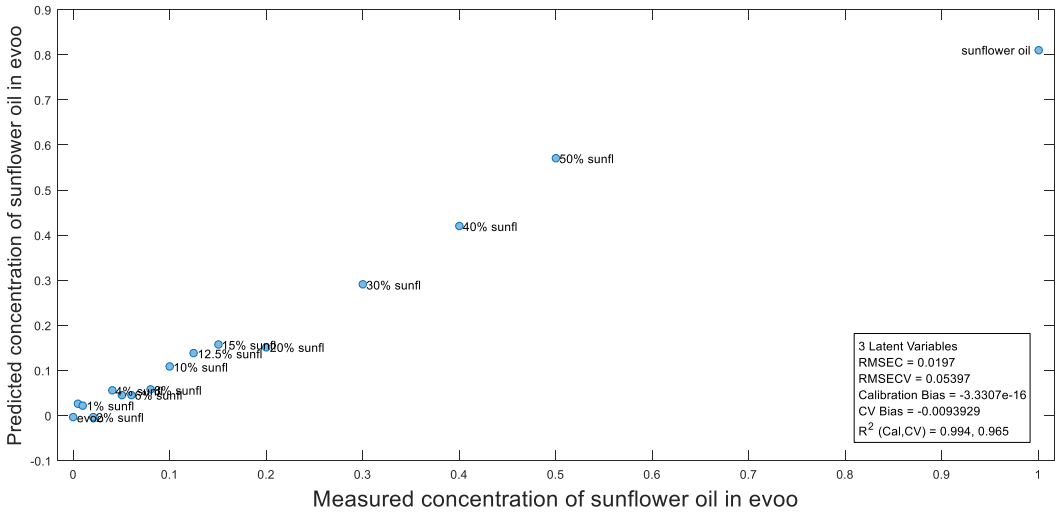

(b)

Figure 6.5.29 (a and b): PLS plot at the visible region 400-800nm. (a) Mean centering pre-treatment and leave-one-out cross validation, RMSECV=4.7% (b) Mean centering+ Savgol 1st derivative and leave-one-out cross validation, RMSECV=5.4%

5. <u>EVOO (Kerasia) with Sunflower oil (Carrefour)</u>

The mixtures were prepared as: 0.5, 1, 2, 4, 6, 8, 10, 12.5, 15, 20, 30, 40, 60 and 80% v/v sunflower oil in extra virgin olive oil. Diluting the samples in n-hexane (1% v/v oil in n-hexane) and placing the solutions in a 10mm path length quartz cuvette, the absorption spectra at the UV region 260-410nm (2nm interval) are shown below (Fig. 6.5.30):

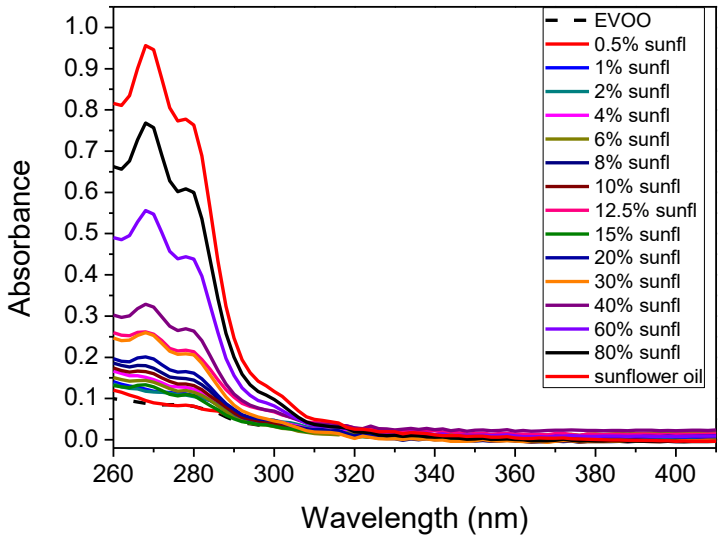

Figure 6.5.30: Absorption spectra of mixtures at the UV region 260-410nm.

Extra virgin olive presents no absorbance peaks at this UV region, in contrast to the sunflower oil, that presents one broad absorbance peak at 268nm, corresponding to conjugated trienes and one absorbance peak at 280nm, related to phenols. As the concentration of sunflower oil in extra virgin olive oil (evoo) decreased, the absorbance peaks at 268 and 280nm decreased too. Taking into account the absorbance values at 266, 270 and 274nm and the Eq. 4.1 and 4.2, K_{270} and ΔK indexes were calculated and plotted vs the concentration of sunflower oil in extra virgin olive oil.

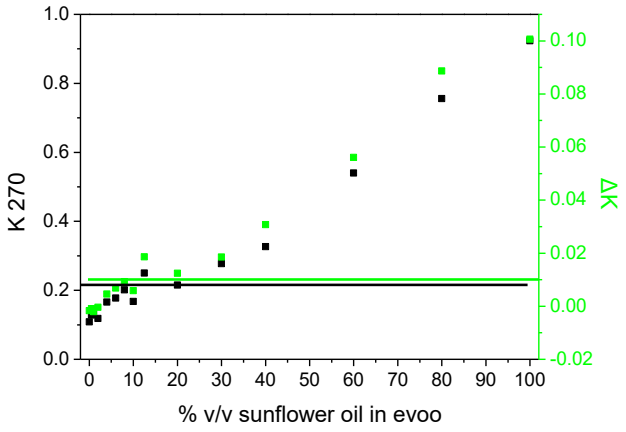

Figure 6.5.31: Indexes K_{270} and ΔK vs concentration of sunflower oil in evoo.

As observed from Fig. 6.5.31, samples containing up to 20% v/v sunflower oil in evoo can be characterized as extra virgin olive oils, according to the European instructions (IOOC, 1991). Evaluation of the absorption spectra at the wavelength region 260-280nm, data were pre-treated with mean-centering process and the leave-one-out cross validation was applied, PLS model showed the value of RMSECV equal to 4.7%. When the absorption data were pre-treated with Savitzky-Golay 1st derivative process and the venetian blinds cross validation was applied, the value of RMSECV was equal to 5%, as shown in the following plots (Fig. 6.5.32):

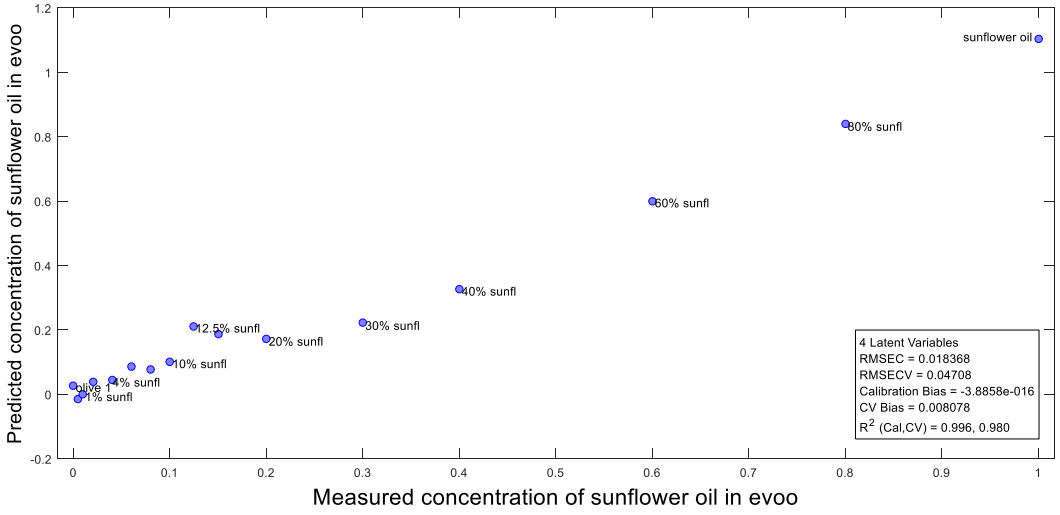

(a)

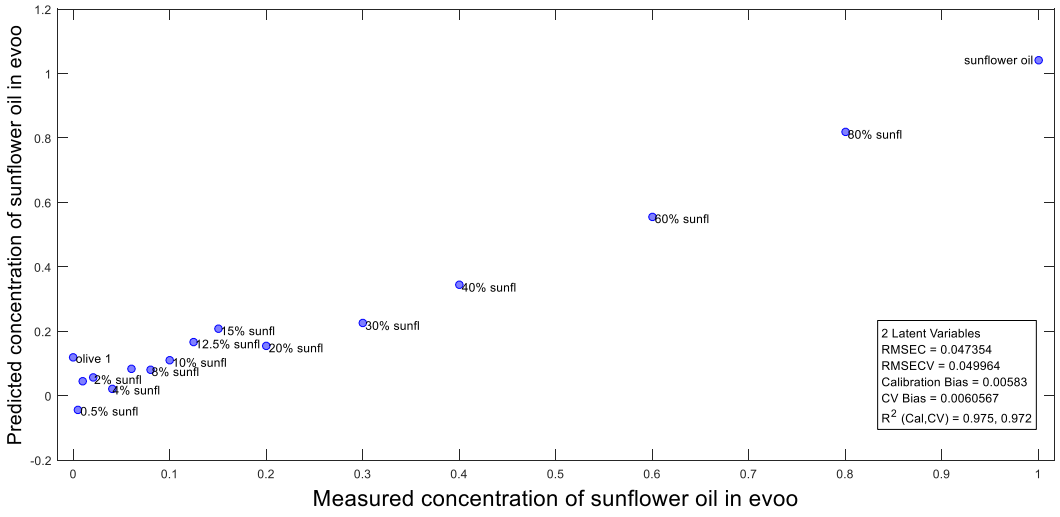

(b)

Figures 6.5.32 (a and b): PLS plots at the UV region (260-410nm). (a) Mean-centering pre-treatment of data and leave-one-out cross validation, RMSECV=4.7% (b) Savitzky-Golay 1st derivative and venetian blinds cross validation, RMSECV=5%

Moving on to the visible absorption 400-800nm (2nm interval), samples were undiluted and placed in a 2mm path length cuvette.

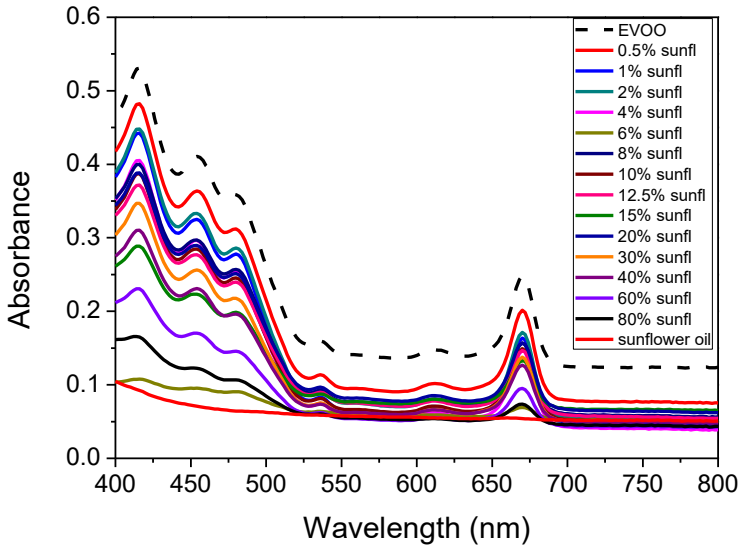

Figure 6.5.33: Absorption spectra at the visible region.

As observed (Fig. 6.5.33), extra virgin olive oil presents 4 main absorbance peaks at 414, 455, 482nm (corresponding to carotenoids) and 670nm (corresponding to chlorophylls). Contrariwise, sunflower oil presents no absorbance peaks at the visible region. While the concentration of sunflower oil is increased in the mixture, the intensity of the absorbance peaks, related to carotenoids, is decreased.

PLS model was employed to evaluate these data, without any pre-treatment and leave-one-out cross validation was implemented, so the RMSECV was equal to 5.5%, as seen at Fig. 6.5.34 (a). When the absorption data were pre-treated with mean centering process and the leave-one-out cross validation was applied, the RMSECV was equal to 8.7%, as seen at Fig. 6.5.34 (b).

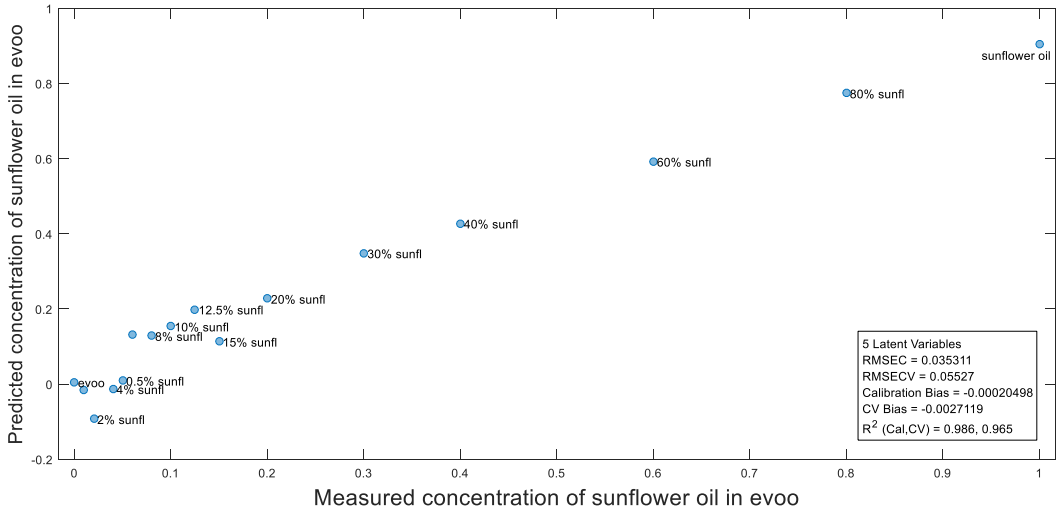

(a)

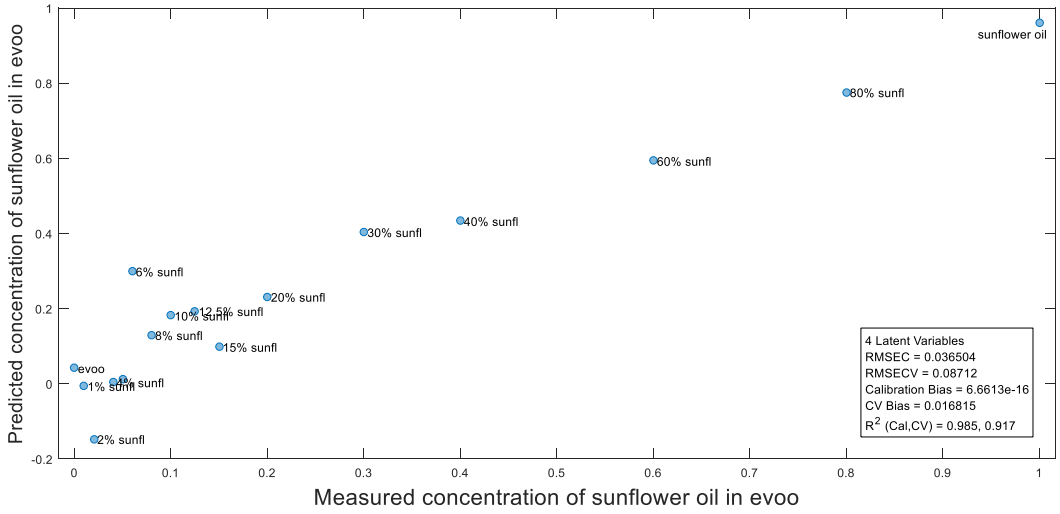

(b)

Figures 6.5.34 (a and b): PLS plots at the visible region (400-800nm). (a) None pre-treatment of data and leave-one-out cross validation, RMSECV=5.5% (b) Mean-centering pre-treatment of data and leave-one-out cross validation, RMSECV=8.7%

The next step for the evaluation of these absorption spectra was to apply the PLS model to a smaller wavelength region, where the carotenoids absorb, namely at 400-500nm. Samples that were evaluated at this step where the ones containing up to 20% v/v sunflower oil in evoo, as seen in Fig. 6.5.35:

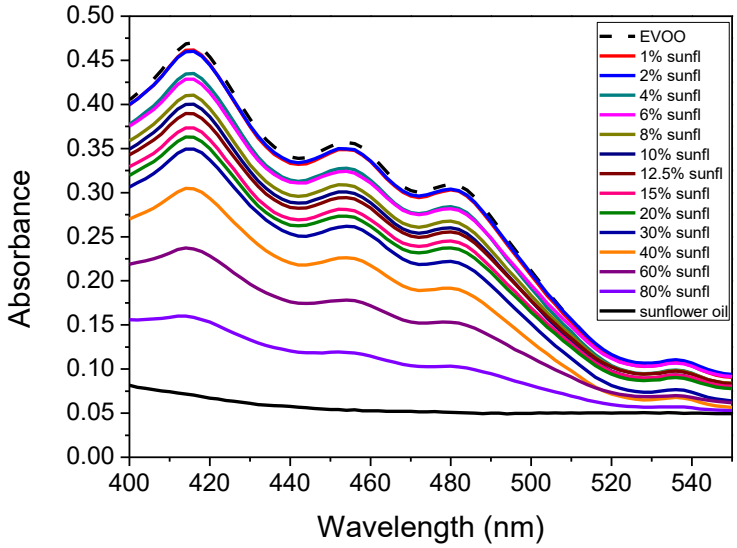

Figure 6.5.35: Absorption spectra of mixtures in the visible region 400-550nm

A discrimination of the mixtures cannot be achieved just by the spectra. This is the reason for the evaluation by PLS model (Fig. 6.3.36). Data were pre-treated by mean-centering process, leave-one-out cross validation was employed and RMSECV was 2.2%, which is a low limit.

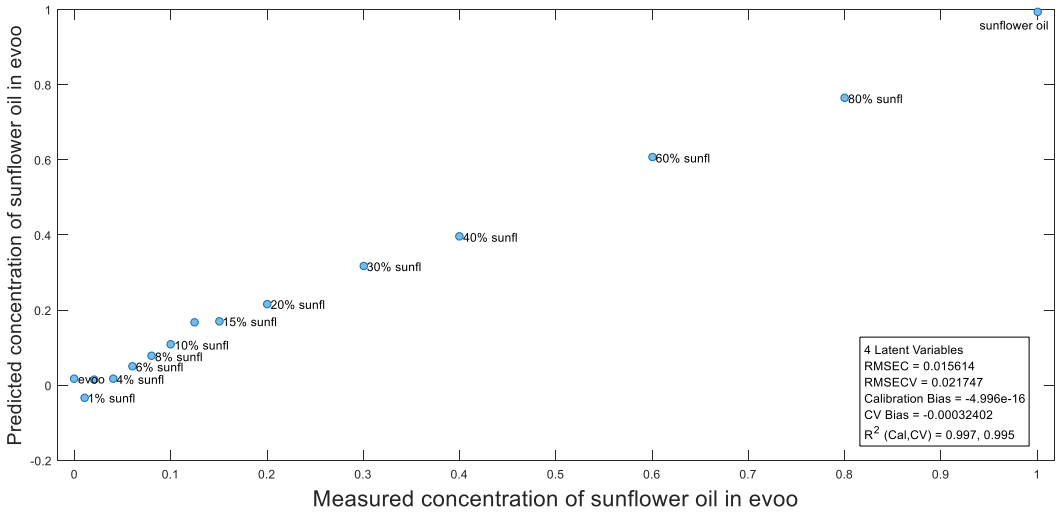

Figures 6.5.36: PLS plot at the visible region (400-550nm). Mean centering if spectral data and leave-one-out cross validation, RMSECV=2.2%

6. EVOO (Kalamayka) with Sunflower oil (Carrefour 2)

The last series of evoo adulteration is presented here. Mixtures prepared were: 1, 2, 3, 5, 6, 7, 8, 10, 12.5, 15% v/v sunflower oil in extra virgin olive oil. Employing the visible absorption spectroscopy, at the wavelength region 400-550nm (2nm interval), samples were placed in a 2mm path length cuvette and measured.

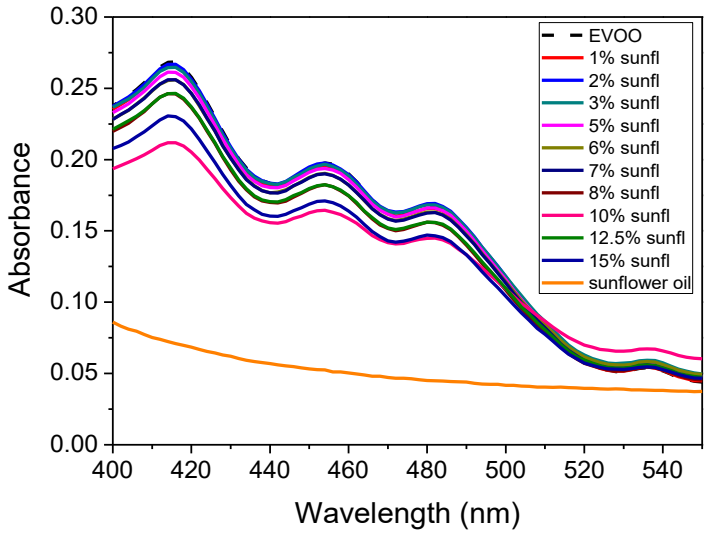

Figure 6.5.37: Absorption spectra of mixtures at region 400-550nm.

Figure 6.5.37 shows the absorption spectra of the samples mentioned before at the visible region 400-550nm. Sunflower oil presents no absorbance peaks. Extra virgin olive oil, on the other hand, presents 3 main absorbance peaks at 414, 454 and 482nm, corresponding to carotenoids and one shoulder at 536nm, corresponding to chlorophylls.

A discrimination of the adulteration of evoo cannot be achieved only by looking at the spectra, so PLS model was applied on this purpose. Data were not pre-treated, at first sight, the leave-one-out cross validation was applied and the value of RMSECV was equal to 2.7% (Fig. 6.5.38 (a)). Then, the mean-centering pre-treatment of spectral data was implemented with the same cross validation and the value of RMSECV increased to 4% (Fig. 6.5.38 (b)), low enough for the detection of adulterant of extra virgin olive oil.

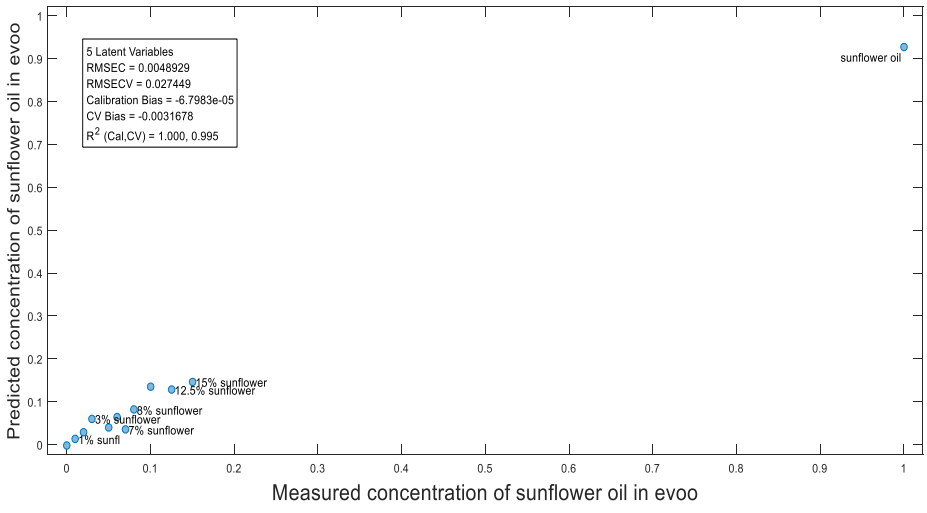

(a)

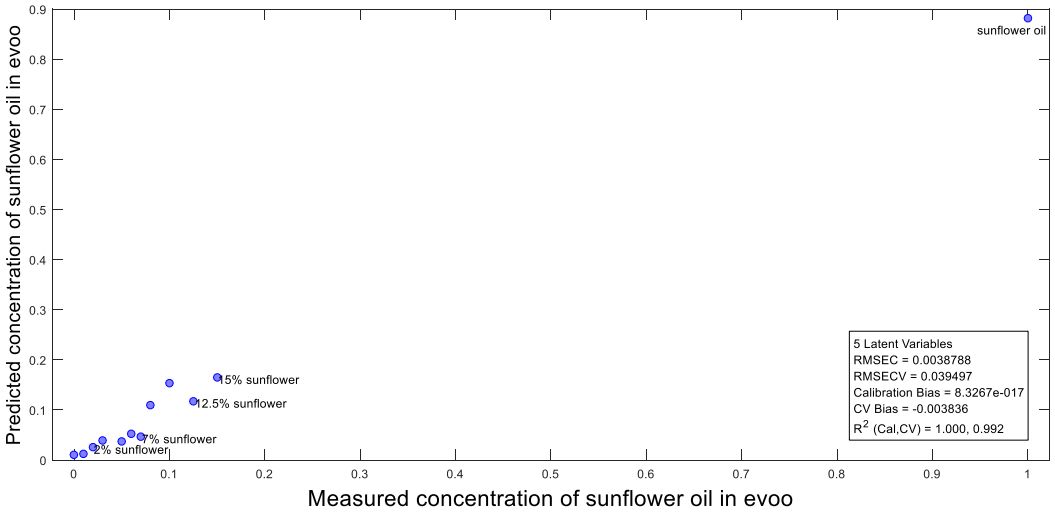

(b)

Figures 6.5.38 (a and b): PLS plots at visible region 400-550nm. (a) None pre-treatment of data and leave-one-out cross validation, RMSECV=2.7% (b) Mean-centering pre-treatment of data and leave-one-out cross validation, RMSECV=4%

Diluting the samples in n-hexane (1% v/v oil in solvent), the oils were placed in a 10mm path length quartz cuvette and measured in spectrophotometer at the UV region 250-300nm, while the background was measured by using the same cuvette with the solvent.

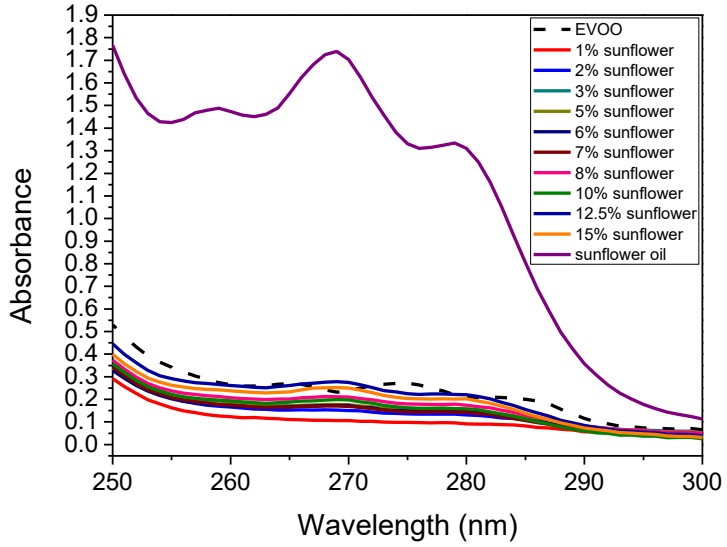

Figure 6.5.39: Absorption spectra of samples I the UV region 250-300nm.

As observed from Fig. 6.5.39, pure sunflower oil present three absorbance peaks at 258, 268 and 280nm, corresponding to conjugated trienes *(Kapoulas & Andrikopoulos, 1987)* and phenols, respectively. Extra virgin olive oil absorbs at 275nm,

corresponding to unsaturated fatty acids. Getting the values of absorbance at 266, 270 and 274nm and eq. 4.1 and 4.2, ΔK values were calculated and plotted vs the concentration of sunflower oil (Fig. 6.5.40).

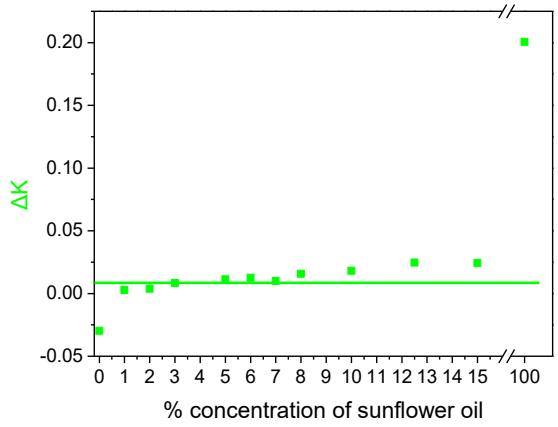

Figure 6.5.40: ΔK values vs samples

It is observed clearly from Fig. 6.5.40 that samples containing up to 4% v/v sunflower oil in evoo can be characterized as extra virgin olive oils, according to eq. 4.3.

Applying the PLS regression model with leave-one-out cross validation, without pre-treating the data, RMSECV was equal to 1.9%, the lowest limit achieved to all adulteration series.

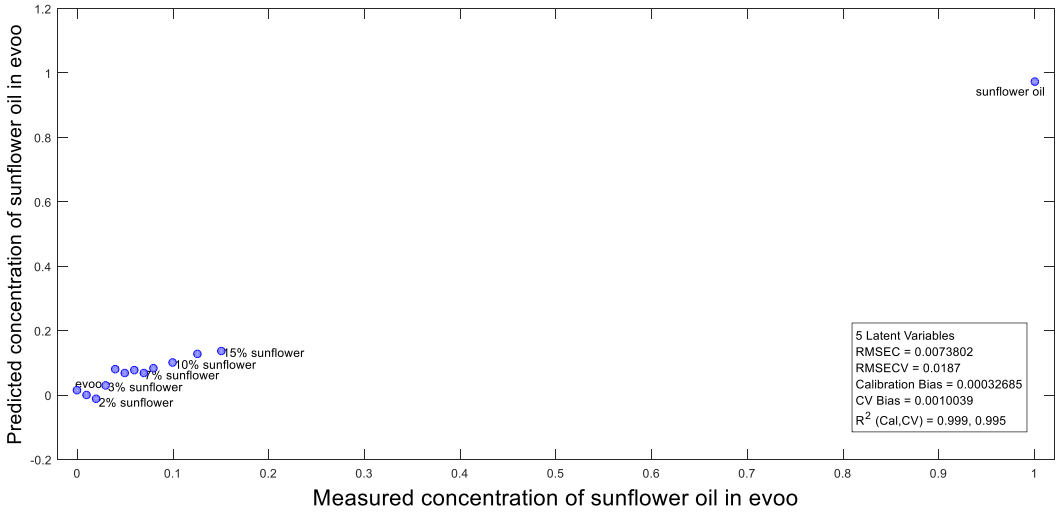

(a)

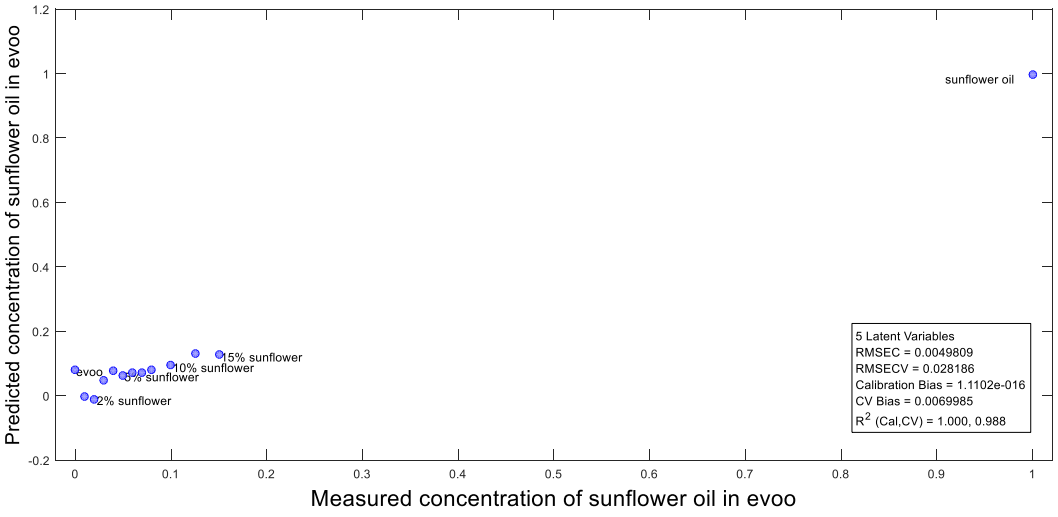

(b)

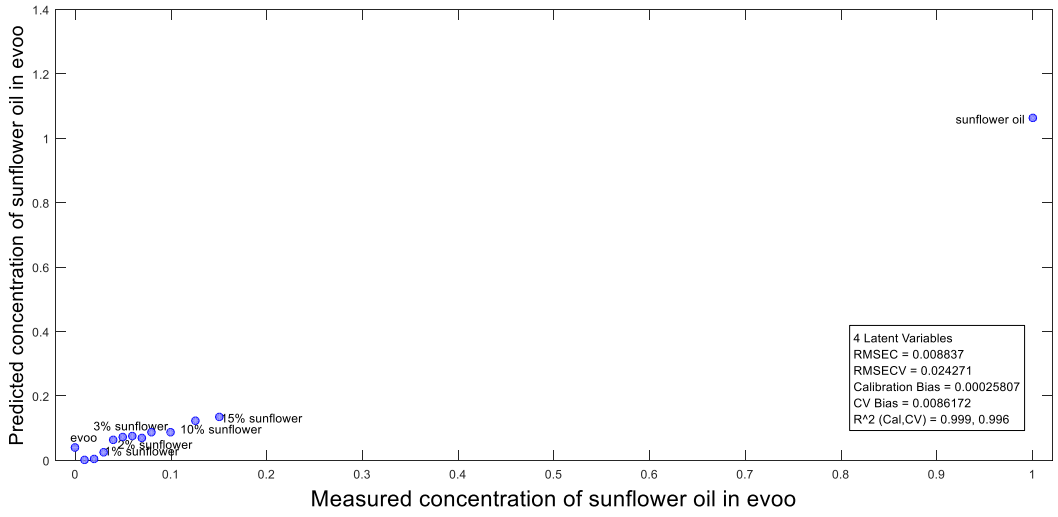

(c)

Figures 6.5.41 (a-c): PLS plots at UV region 250-300nm. (a) None pre-treatment of data and leave-one-out cross validation, RMSECV=1.9% (b) Mean-centering pre-treatment of data and leave-one-out cross validation, RMSECV=2.8% (c) Savitzky-Golay 1st derivative and leave-one-out cross validation, RMSECV=2.4%

6.5.3 Fluorescence Spectroscopy and PLS regression

1. EVOO (olive oil 12) and Sunflower oil (Carrefour)

Mixtures prepared were: 5, 10, 20, 30 and 50% v/v sunflower oil in extra virgin olive oil. Samples were measured in Front Face geometry (FF), without any dilution and placed in a 10mm path length cuvette. The excitation wavelength was 355nm and emission wavelengths were at region 360-700nm (5nm interval), while the slits of excitation and emission were set to 1 and 2nm, respectively.

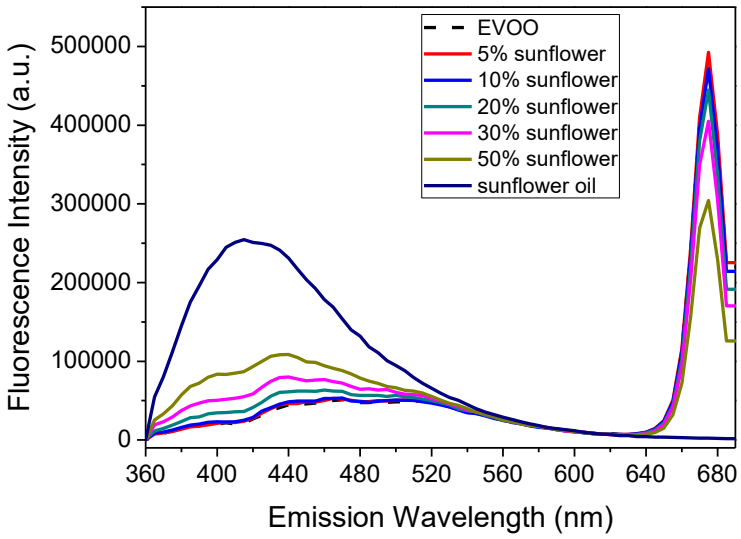

Figure 6.5.42: Emission spectra of samples (λ_{exc}=355nm)

From Fig. 6.5.42, two main fluorescence bands appear, at 415 and 676nm, corresponding to polyphenols and chlorophylls, respectively. Pure sunflower oil presents only one fluorescence peak, at 415nm, while there is no peak at 676nm. Extra virgin olive oil and mixtures present both fluorescence peaks. As the concentration of sunflower oil increases in the mixtures, the fluorescence peak of polyphenols increases, but the chlorophylls fluorescence decreases. So, a preliminary discrimination of adulterated evoo can be achieved only by the emission spectra, when excited at 355nm.

2. <u>EVOO (Dafnes) and Sunflower oil (Mr. Grand)</u>

Mixtures prepared were: 0.5, 1, 2, 4, 5, 6, 8, 10, 12.5, 15, 20, 30, 40 and 50% v/v sunflower oil in extra virgin olive oil. Samples were measured in Front Face geometry (FF), without any dilution and placed in a 10mm path length cuvette. The excitation wavelength was 355nm and emission wavelengths were at region 360-600nm (5nm interval), while the slits of excitation and emission were set to 3 and 5nm, respectively.

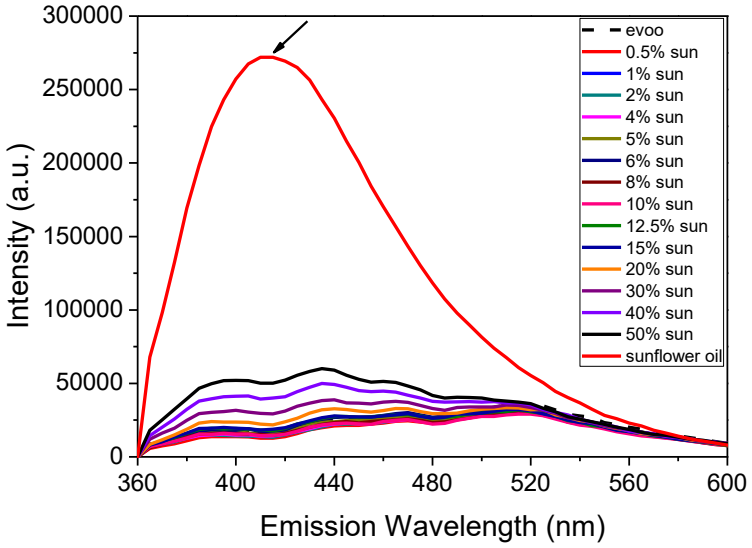

Figure 6.5.43: Emission spectra of mixtures, when excited at 355nm.

As seen in Fig. 6.5.43, pure sunflower oil presents a broad fluorescence band at 412nm, corresponding to phenolic compounds. As the concentration of sunflower oil decreases, the fluorescence intensity at 412nm decreases too, because pure extra virgin olive oil presents a very low intensity at this emission wavelength. Emission wavelengths above 600nm are not included in the spectra, because of the high intensity of chlorophyll at 670nm.

Discrimination of adulterated oils cannot be easily achieved from the fluorescence spectra. Applying the PLS regression model (mean-centering pre-treatment on the spectra and leave-one-out cross validation), RMSECV was equal to 9%, as seen at the following plot (Fig. 6.5.44):

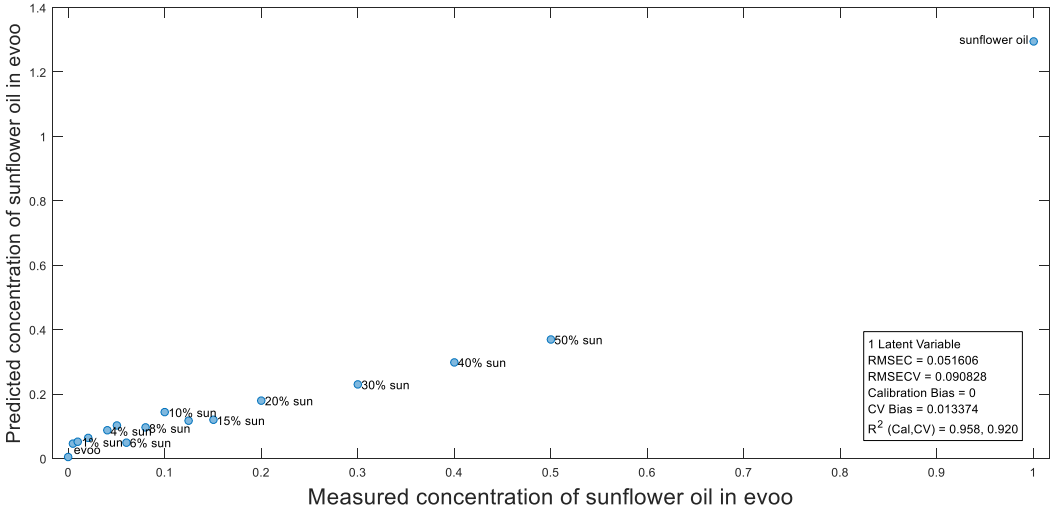

Figure 6.5.44: PLS plot of emission spectra of oils, when excited at 355nm.

3. EVOO (Androulidia) with Sunflower oil (Mr. Grand)

Mixtures prepared were: 0.5, 1, 2, 4, 5, 6, 8, 10, 12.5, 15, 20, 30, 40 and 50% v/v sunflower oil in extra virgin olive oil. Samples were measured in Front Face geometry (FF), without any dilution and placed in a 10mm path length cuvette. The excitation wavelength was 355nm and emission wavelengths were at region 360-600nm (5nm interval), while the slits of excitation and emission were set to 3 and 5nm, respectively.

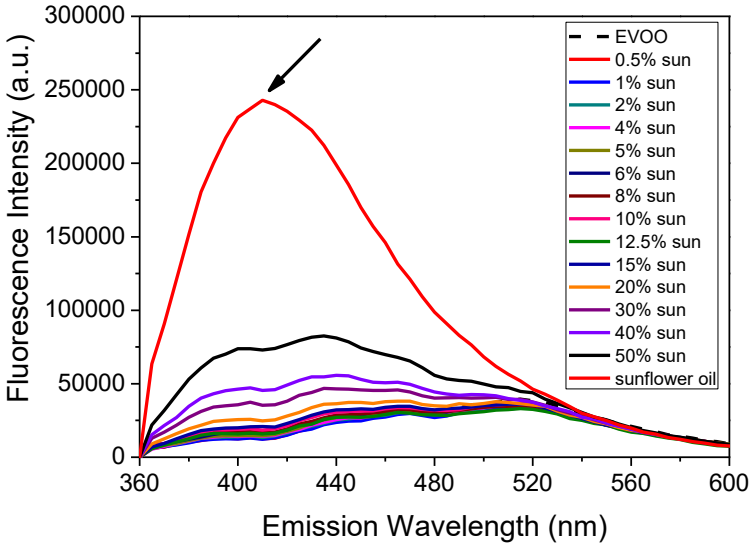

Figure 6.5.45: Emission spectra of mixtures, when excited at 355nm.

As it is observed, pure sunflower oil present an intense fluorescence at 412nm, corresponding to phenolic compounds. Oil mixtures and pure extra virgin olive oil present a lower intensity at 412nm.

PLS regression model was employed to these emission spectra and were pre-treated with mean-centering, Savitzky-Golay 1st derivative and Savitzky-Golay 2nd derivative processes, respectively (Fig. 6.5.46 (a, b, c), and leave-one-out cross validation was applied. The respective values of RMSECV were equal to 8.5, 9 and 7.3%.

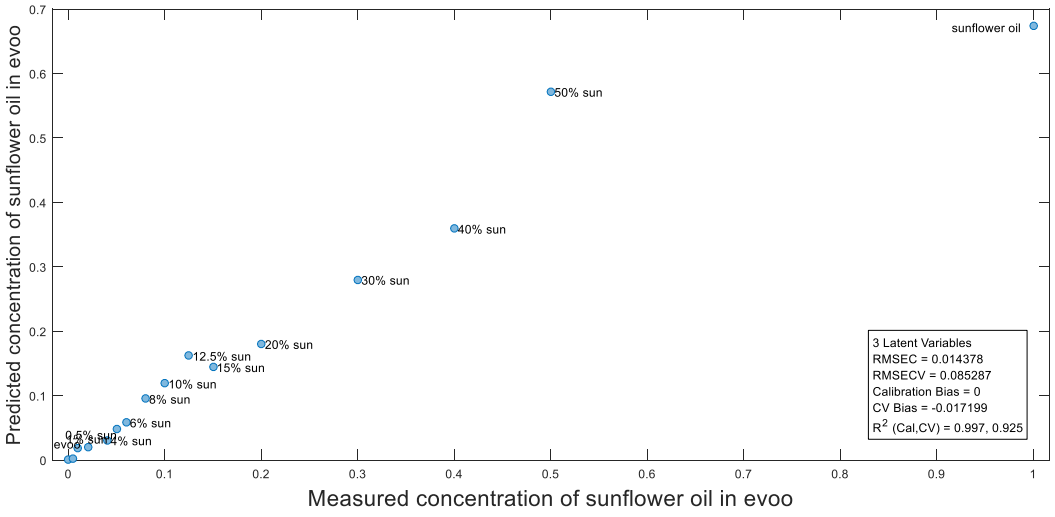
Predicted concentration of sunflower oil in evoo
Measured concentration of sunflower oil in evoo
sunflower oil
50% sun
40% sun
30% sun
20% sun
12.5% sun
15% sun
10% sun
8% sun
6% sun
3 Latent Variables
RMSEC = 0.014378
RMSECV = 0.085287
Calibration Bias = 0
CV Bias = -0.017199
R2 (Cal,CV) = 0.997, 0.925

(a)

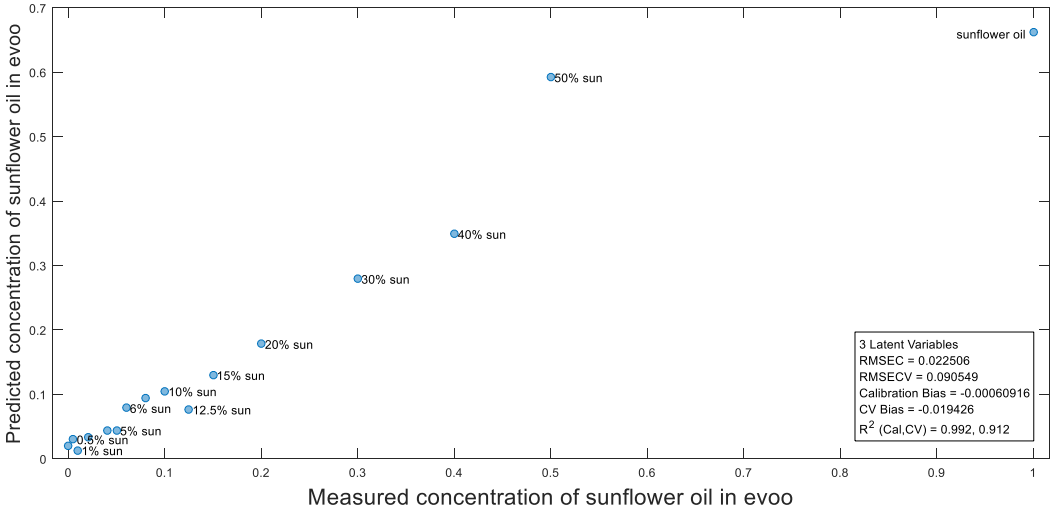
Predicted concentration of sunflower oil in evoo
Measured concentration of sunflower oil in evoo
sunflower oil
50% sun
40% sun
30% sun
20% sun
15% sun
10% sun
6% sun
12.5% sun
5% sun
1% sun
3 Latent Variables
RMSEC = 0.022506
RMSECV = 0.090549
Calibration Bias = -0.00060916
CV Bias = -0.019426
R2 (Cal,CV) = 0.992, 0.912

(b)

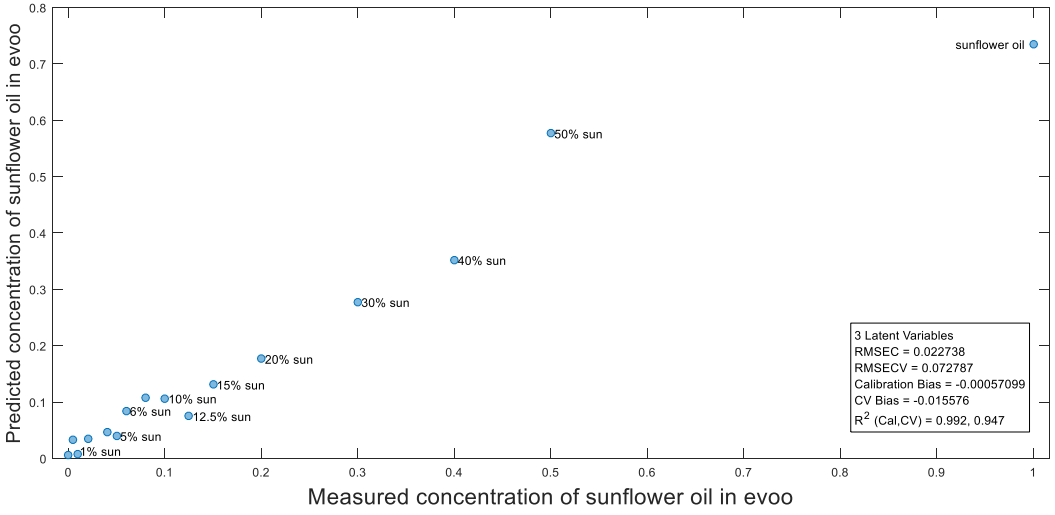
Predicted concentration of sunflower oil in evoo
Measured concentration of sunflower oil in evoo
sunflower oil
50% sun
40% sun
30% sun
20% sun
15% sun
10% sun
6% sun
12.5% sun
5% sun
1% sun
3 Latent Variables
RMSEC = 0.022738
RMSECV = 0.072787
Calibration Bias = -0.00057099
CV Bias = -0.015576
R2 (Cal,CV) = 0.992, 0.947

(c)

Figures 6.5.46 (a-c): PLS plots of emission spectra. (a) Mean-center pre-treatment of data and leave-one-out cross validation, RMSECV=8.5% (b) Savitzky-Golay 1st derivative pre-treatment of data and leave-one-out cross validation, RMSECV=9% (c) Savitzky-Golay 2nd derivative and leave-one-out cross validation, RMSECV=7.3%

6.6 Time-resolved Fluorescence Spectroscopy

Laser Induced Fluorescence was employed to measure the extra virgin olive and sunflower oils fluorescence. Experimental setup, as mentioned in section 4.5, contained a pulsed Nd:YAG laser operated at 1064nm, repetition rate at 10Hz, pulse duration 8ns and average power 48mW. In order to measure the fluorescence of oils, third harmonic frequency (at 355nm) was applied to the samples. Sunflower oil and extra virgin olive oil's fluorescence spectra are seen below (Fig. 6.6.1 and 6.6.2):

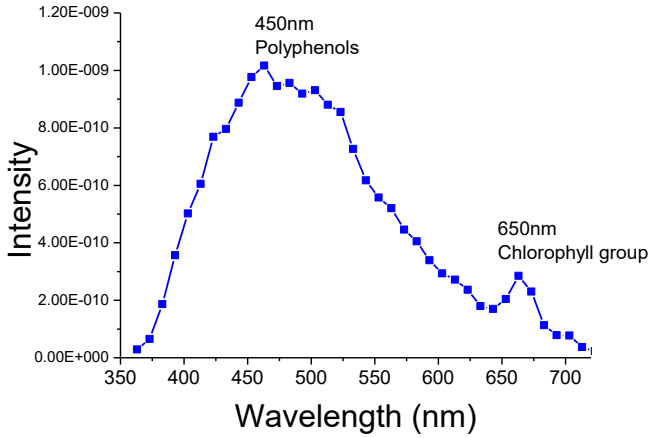

Figure 6.6.1: Emission of Sunflower oil, excited at 355nm

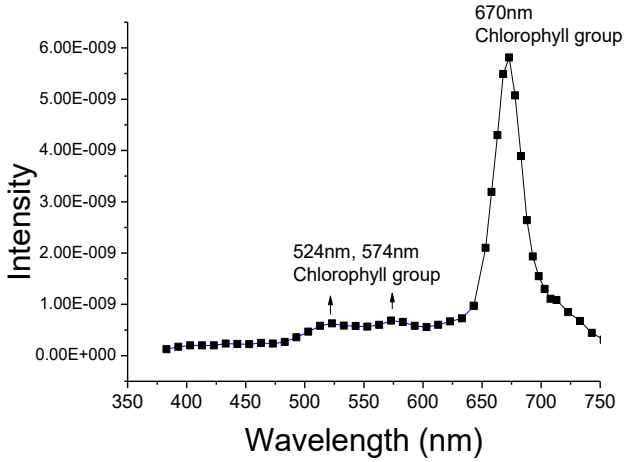

Figure 6.6.2: Emission of Extra virgin olive oil, excited at 355nm.

It is observed that these fluorescence spectra seem about the same, as measured with a commercial Fluorometer. Concerning the fluorescence of extra virgin olive oil

in the emission range 640-800nm, where chlorophyll emit, time decay of fluorescence is plotted:

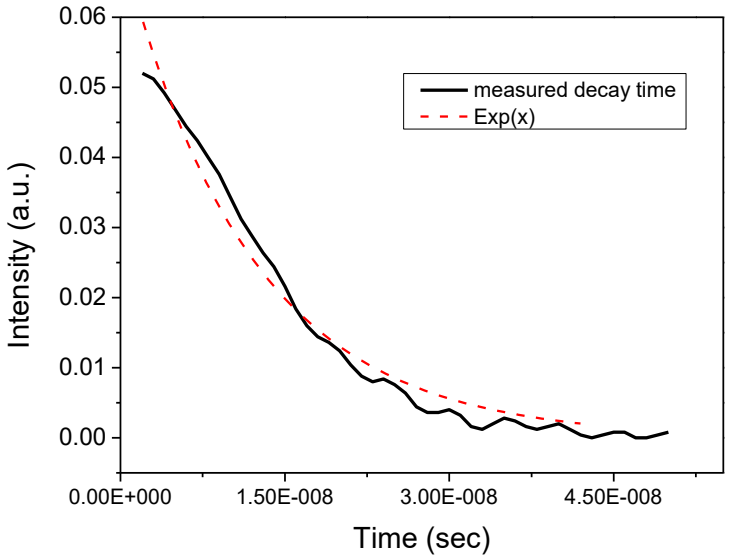

Figure 6.6.3: Time decay of chlorophyll and exponential fitting

The fitting used $(\exp(Ax))$ in Fig. 6.6.3 was not the most suitable, so the time decay of chlorophyll could not be extracted. This process remains in a preliminary study, hoping that this technique can be implemented to the discrimination between olive oils and the detection of adulteration of extra virgin olive oils, by the time decay of fluorophores, contained in the oils.

Chapter 7:

Experimental Results of Tsikoudia and Discussion

A preliminary study of absorbance and fluorescence measurements of the grape distillate *Tsikoudia* will be discussed in this section, since it has not been discussed by other scientific groups in this field, as seen in the literature.

Samples of Tsikoudia have been stored in the fridge before measured. Before any experimental process, they were taken out of fridge for about one hour at room temperature. As mentioned at section 2.2.2, every sample was made from one variety of grapes and their pH was measured using a pH meter, as shown in Table 7.1 below:

Variaty	Ph	Abbreviation
Dafni	4.40	Da
Vidiano	4.15	vi
Thrapsathiri	4.07	th
Mantilari	4.25	ma
Plyto 1	4.15	p1
Plyto 2	4.07	p2
Soultanina Arxanes	4.31	s1
Mosxato Alagni	4.15	mo
Soultanina Arkaloxwri	3.95	s2
Voidomatos Siteia	4.37	vo
Kotsifali Arkaloxwri	3.44	ko

Table 7.1: Values of pH of tsikoudia samples and their abbreviations

7.1 Absorption measurements

Tsikoudia samples were measured in the UV region (230-450nm) by a 2nm interval, using a 10mm path length cuvette and the absorption spectra were recorded (Fig. 7.1). The samples are undiluted and the background measurement was a dilution of water: ethanol 70: 30.

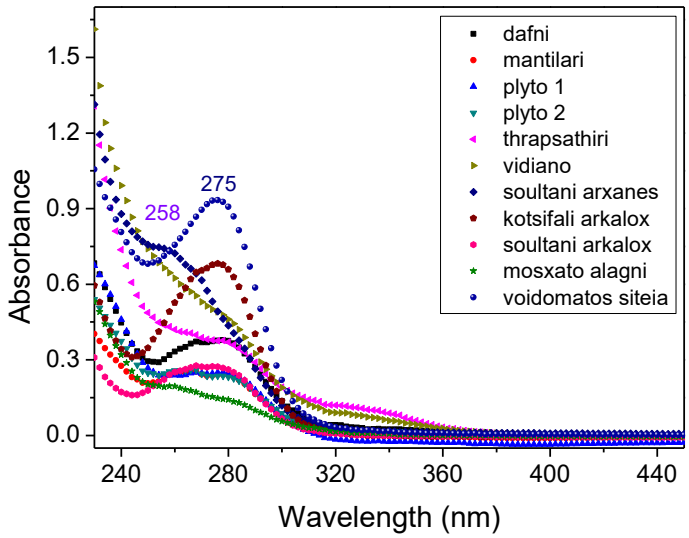

Figure 7.1: Tsikoudia samples: Absorption spectra of different varieties of grapes

As seen on the figure, different varieties of grapes present a different behavior in the absorption spectrum. All samples do not absorb in the visible region, they are transparent to visible light, as tsikoudia is a crystal clear liquid. Absorbance at 258nm is attributed to benzoic acids, at 275nm to flavanols and a shoulder at about 325nm can be related to flavanones *(Robards, Prenzler, Tucker, Swatsitang, & Glover, 1999)*, *(Roussis, et al., 2008)*.

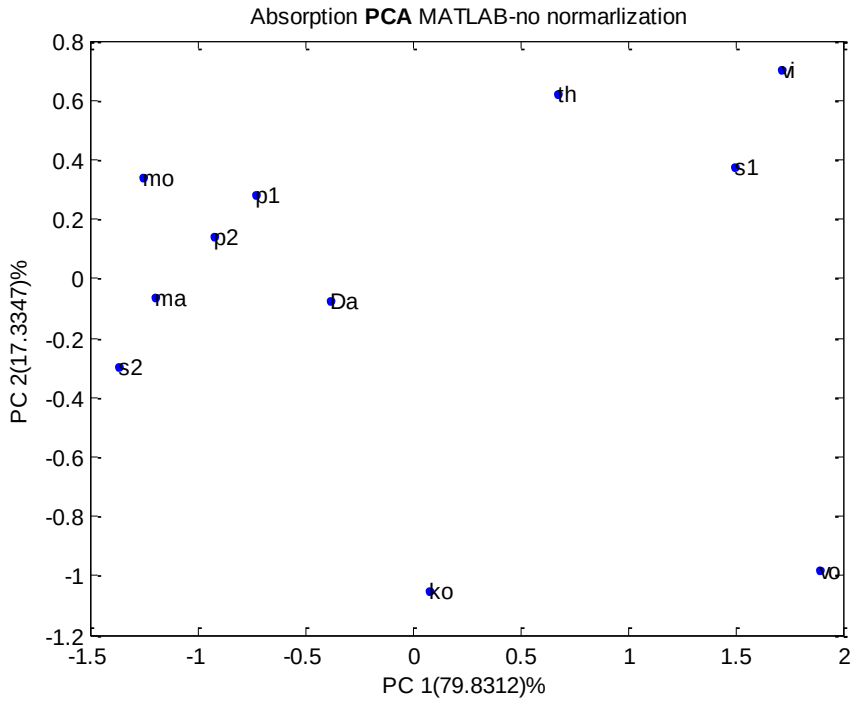

Figure 7.2: PCA score plot of different grape varieties without any pretreatment of data

PC 1 and PC 2 factors at the previous figures explain the 79.8% and 17.3% of the non-pretreated data. As it can be observed from the PCA plots, varieties of Plyto are contained in the same group with Mosxato variety (coming from Alagni, Heraklion) and Thrapsathiri variety, while the variety of Soultanina, coming from Alkaloxwri, are close to Voidomatos and Kotsifali varieties.

Based on the loading plots below, it can be observed that the grape varieties were differentiated by the absorbance peaks at 275nm, corresponding to phenolic compounds, such as flavonoids (Fig. 7.3). It is observed that PC2 has a negative correlation, in contrast to PC1, that has a positive correlation to the data.

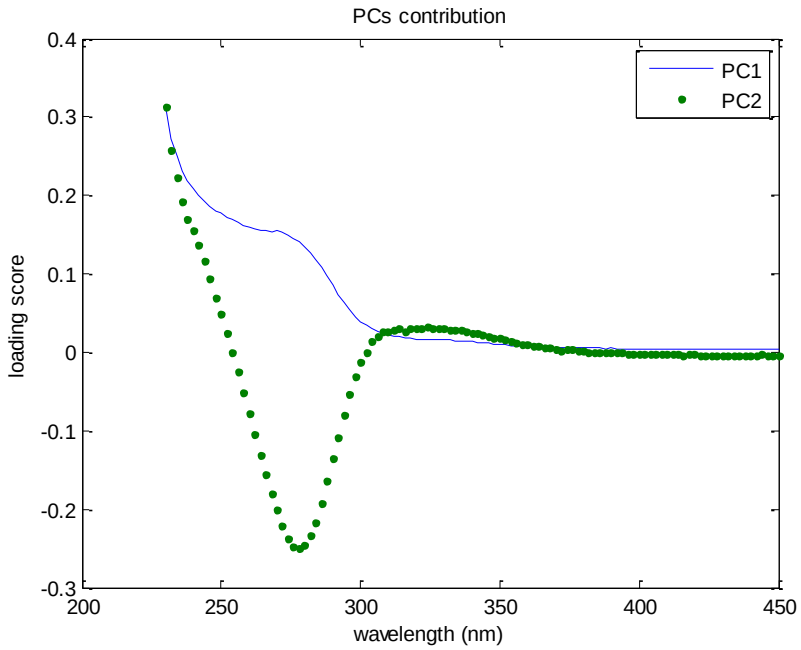

Figure 7.3: PCA loading plots of different grape varieties without any pretreatment of data

As a conclusion, Tsikoudia samples, coming from different grape varieties, can be differentiated by their absorption spectra at the UV region, where there are different absorption peaks, combined with PCA technique.

7.2 Fluorescence measurements

Employing the EEFS, we created contour maps of the samples from different grape varieties, with the following experimental parameters:

Excitation wavelength region: 230-340nm, 2nm interval

Emission wavelength region: 290-500nm, 2nm interval

Excitation slit: 1nm

Emission slit: 3nm

Integration time: 0.2sec

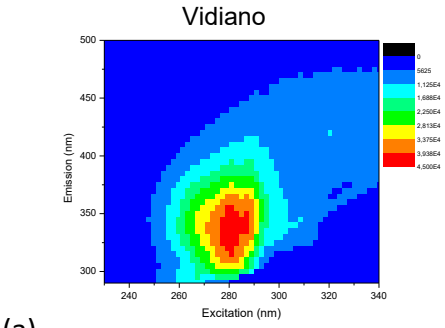
Vidiano
Emission (nm)
Excitation (nm)

(a)

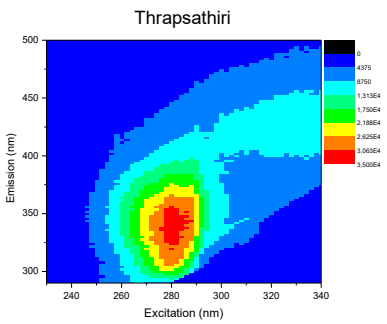
Thrapsathiri
Emission (nm)
Excitation (nm)

(b)

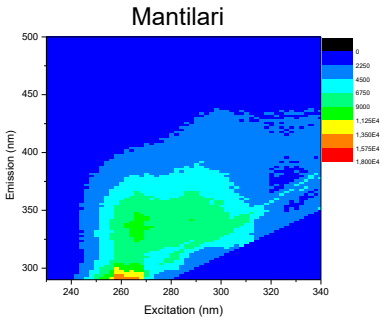
Mantilari
Emission (nm)
Excitation (nm)

(c)

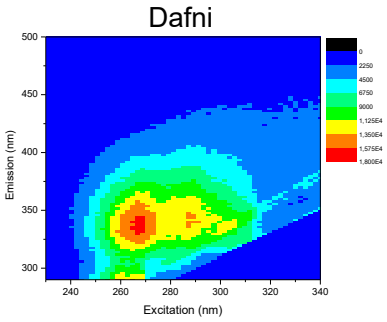
Dafni
Emission (nm)
Excitation (nm)

(d)

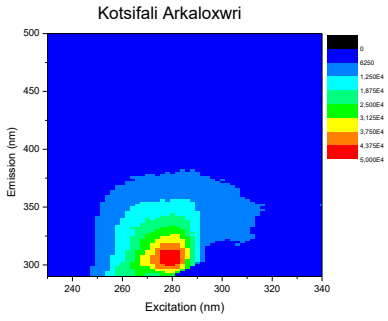
Kotsifali Arkaloxwri
Emission (nm)
Excitation (nm)

(e)

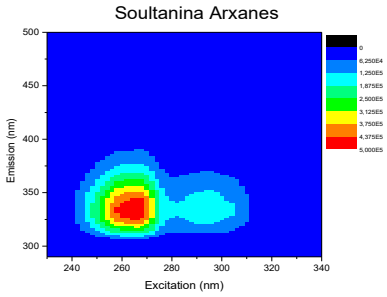
Soultanina Arxanes
Emission (nm)
Excitation (nm)

(f)

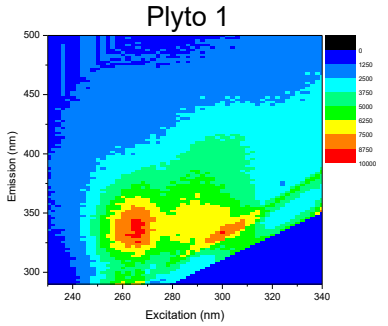
Plyto 1
Emission (nm)
Excitation (nm)

(g)

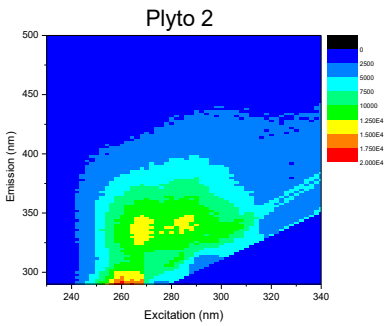
Plyto 2
Emission (nm)
Excitation (nm)

(h)

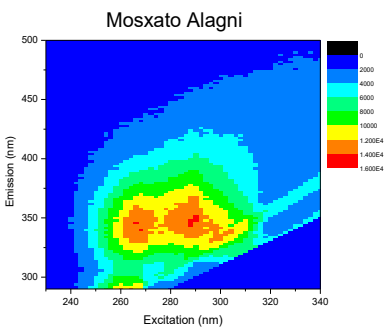
Mosxato Alagni
Emission (nm)
Excitation (nm)

(i)

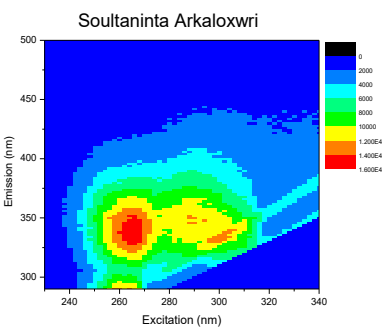
Soultaninta Arkaloxwri
Emission (nm)
Excitation (nm)

(k)

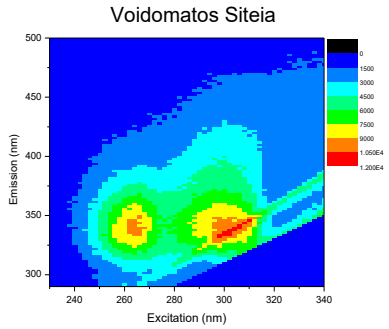

(l)

Figures 7.4 (a-l): Contour maps of tsikoudia from different grape varieties

The contour maps observed in Fig. 7.4 are characteristic examples of the tsikoudia samples and there are a lot of differences in their emission spectra. The fluorescence maps exhibit one common feature, they do not emit in the visible region. When samples were excited at the range of 260-295nm, the emission occured at the range of 310-340nm. As Tothova *et.al.* claimed, two characteristic fluorophores in distillates could be related to these spectra. Benzoic acids emit at 350nm, when excited at the range 250-280nm and tyrosine and tyrosol emit at 302nm, when excited at 276nm *(Tothova, Sadecka, & Majek, 2009)*. Because of the large variety of substances contained in the distillates, it cannot be determined which of the fluorophores are absent in the distillates, in order to guarantee the exact compounds that are related to the tsikoudia samples.

Combining the information from the absorption spectra, the samples of tsikoudia do not absorb or emit in the visible region, because of their transparency.

To sum up, even though the Tsikoudia samples were under preliminary study, UV-Vis Absorption and Fluorescence spectroscopic techniques, due to their simplicity, non-invasive interaction and rapidness, are good candidates for discriminating the different varieties of distillates. This study can be further proceeded, if more samples of tsikoudia coming from different grape varieties are tested, in combination with Statistical Analysis, in order to control the samples' quality.

Conclusions:

The Master thesis presented was focused on the identification, authentication and quality control of agro-products, especially in olive oils and tsikoudia. By applying Absorption Spectroscopy at the Ultraviolet and Visible region and Fluorescence Spectroscopy, identification and discrimination between olive and seed oils and grape distillate (Tsikoudia) were achieved. More specifically, the identification of Cretan virgin olive oils was achieved by means of Absorption Spectroscopy at the UV-Vis region of electromagnetic radiation and Fluorescence Spectroscopy, using the Front Face Geometry, in combination with Statistical Analysis.

Discrimination of different varieties of olives and grapes was also achieved by the Optical Spectroscopic techniques. Evaluating the differences between the olive oils and seed oils, the adulteration of extra virgin olive oils with seed oils was detected by mixing these oils in different concentrations and the detection limit was as low as 2% v/v seed oil in evoo, as PLS regression model showed. Laser Induced Fluorescence (LIF) spectroscopy was applied to the olive oils as a preliminary study and this is a promising technique for the authentication of olive oils, combined with Time Resolved Fluorescence, in order to estimate the time decay of the fluorophores contained in the olive oils.

Future Plans:

As the olive oil industries are interested in the authentication and identification of the extra virgin olive oil worldwide, the Optical Spectroscopic techniques, combined with Statistical Analysis, are promising to control efficiently the quality of oils, and generally liquid foods, in a low-cost, fast, non-invasive way. It could become a compact, commercial system, that oil companies could provide to their customers the essential information needed for the product. A database of oils from all over Greece could be set, in order to discriminate the oils by their geographical origin, olive variety, quality control and the adulteration with low-grade oils and seed oils.

References:

(n.d.). Retrieved from http://eur-lex.europa.eu/legal-content/en/ALL/?uri=CELEX:31991R2568.

(n.d.). Retrieved from http://www.coherent.com/downloads/AboutMeasuringLaserPowerndEnergyOutputFinal.

Abdi. H., &. W. (2010). Principal component analysis. *Wiley Interdisciplinary Reviews: Computational Statistics, 2*(4), 433-459.

Angerosa, F., Campestre, C., & Giansante, L. (2006). Analysis and Authentication. In D. Boskou, *Olive Oil: Chemistry and Technology* (pp. 113-172). AOCS.

Atkin, P. W. (n.d.). Κανόνες επιλογής και ροπές μετάβασης. In P. W. Atkin, *Φυσικοχημεία.* CUP.

Beltrán, G., Ruano, M. T., Jiménez, A., Uceda, M., & Aguilera, M. P. (2007). Evaluation of virgin olive oil bitterness by total phenol content analysis. *Eur. J. Lipid Sci. Technol, 108*, pp. 193-197.

Bendini, A., Cerretani, L., Carrasco-Pancorbo, A., Gómez-Caravaca, A., Segura-Carretero, A., Fernández-Gutiérrez, A., & Lercker , G. (2007). Phenolic Molecules in Virgin Olive Oils: a Survey of Their Sensory Properties, Health Effects, antioxidant activity and analytical methods. An overview of the last decade. *Molecules, 12*, 1679-1719.

Bertolucci, H. a. (1989). *Symmetry and Spectroscopy.* Dover Publications.

Boskou, D., Blekas, G., & Tsimidou, M. (1996). Olive oil adulteration. In Olive Oil Chemistry and Technology. In D. Boskou. AOCS Press: Champaign, IL, Chapter 8 (pp 121-133).

Casale, M. C. (2010). The potential of coupling information using three analytical techniques for identifying the geographical origin of liguria extra virgin olive oil. *Food Chemistry, 118*, 163-170.

Castleden, R. (2005). Huge quantities of olive oil were produced and it must have been a major source of wealth. The simple fact that southern Greece is far more suitable climatically for olive production may explain why the Mycenaean civilization made far greater advances in . In *London and New York: Routledge* (p. 107).

Cozzolino, D., Kwaiatkowski, J. M., Dambergs, R. G., Cynkar, W. U., Janik, L. J., Skouroumounis, G., & Gishen, M. (2008). *Talanta, 74*, 711.

Dankowska, A. (n.d.). *Discrimintion of edible oilve oils by mens of UV spectropfotometry with the use of SPA-LDA.*

Díaz, T. G., Merás, I. D., Correa, C. A., Roldan, B., & Cáceres, M. I. (2003). Simultaneous Fluorometric Determination of Chlorophylls A and B and Pheophytins A and B in Olive Oil by Partial Least-Squares Calibration. *Journal of Agricultural and Food Chemistry, 51*(24), 6934-6940.

Domenici, V., Ancora, D., Cifelli, M., Serani, A., Veracini, C. A., & Zandomeneghi, M. (2014). Extraction of Pigment Information from Near-UV Vis Absorption Spectra of Extra Virgin Olive Oils. *Journal of Agriculural and Food Chemistry*.

Downey, G., Mcintyre , P., & Davies, A. N. (2003). Geographic Classi? cation of Extra Virgin Olive Oils From the Eastern Mediterranean by Chemometric Analysis of Visible and Near-Infrared Spectroscopic Data. *Applied Spectroscopy, 57*(2), 158-163.

Downey, G., McIntyre, P., & Davies, A. N. (2002). Detecting and Quantifying Sunflower Oil Adulteration in Extra Virgin Olive Oils from the Eastern Mediterranean by Visible and Near-Infrared Spectroscopy. *J. Agric. Food Chemistry, 50*(20), 5520-5525.

Eitenmiller, R. R., Ye, L., & Landen, W. O. (2008). Vitamin E: Tocopherols and Tocotrienols. In *In Vitamin Analysis for the Health and Food Sciences.* 2 edn CRC Press, New York.

Elmer, P. (n.d.). *http://www.perkinelmer.com/product/lambda-950-uv-vis-nir-spectrophotometer-l950*.

Enderlein, J., Ambrose, P. W., Goodwin, P. M., & Keller, R. A. (n.d.). Fluorescence Detection of Single Molecules applicable to small volume assays.

(2001). Fluoromax-3. Jobin Yvon Inc.

Foot, C. J. (n.d.). Einstein A and B coefficints. In C. J. Foot, *Atomic Physics.* Oxford University Press.

Fotakis, C., Christodouleas, D., Kokkotou, K., Zervou, M., Zoumpoulakis, P., Moulos, P., . . . Calokerinos, A. (2013). NMR metabolite profiling of Greek grape marc spirits. *Food Chemistry, 138*, 1837-1846.

Frehse. (1925). Physical methods, apparatus, etc. *Analyst, 50*, 361-362.

Fuentes, E., Báez , M. E., Bravo, M., Cid, C., & Labra, F. (2012). Determination of Total Phenolic Content in Olive Oil Samples by UV–visible Spectrometry and Multivariate Calibration. *Food Anal. Methods, 5*, 1311-1319.

Galani-Nikolakaki, S., Kallithrakas-Kontos, N., & Katsanos, A. A. (2002). Trace elements analysis of Cretan wines and wine products. *The science of the total environment, 285*, 155-163.

Galili, E. (1997). "Evidence for Earliest Olive-Oil Production in Submerged Settlements off the Carmel Coast, Israel". *Journal of Archaeological Science, 24*, 1141-1150.

Garcia-Gonzalez, D., & et.al. (n.d.). Infrared, Raman and Fluorescence Spectroscopies:Methodologies and Applications. In R. Aparicio, & J. Harwood, *Handbook of olive oil, Analysis and Properties* (Vol. II). Springer.

Gardiner, A. H. (1916). Notes on the Story of Sinuhe. *Paris: Librairie Honoré Champion*.

Guilbault, G. G. (1990). *Practical Fluorescence.*

Guimet, F., Boqué, R., & Ferré, J. (2004). Cluster Analysis Applied to the Exploratory Analysis of Commercial Spanish Olive Oils by Means of Excitation-Emission Fluorescence Spectroscopy. *J. Agric. Food Chem., 52*, 6673-6679.

Guimet, F., Ferré, J., & Boqué, R. (2005). Rapid detection of olive–pomace oil adulteration in extra virgin olive oils from the protected denomination of origin “Siurana” using excitation–emission fluorescence spectroscopy and three-way methods of analysis. *Analytica Chimica Acta, 544*, 143-152.

GUTIÉRREZ, F., Albi, M. A., Palma, R., Rios, J. J., & Olias, J. M. (1989). Bitter Taste of Virgin Olive Oil: Correlation of Sensory Evaluation and Instrumental HPLC Analysis. *Journal of Food Science, 54*(1), 68-70.

Holman, R. T., & Edmondson, P. R. (1956). Near-Infrared Spectra of Fatty Acids and Some Related Substances. *Anal. Chem., 28*(10), 1533-1538.

http://www.sfakia-crete.com. (n.d.). Retrieved from http://www.sfakia-crete.com/sfakia-crete/raki.html.

http://www.we-love-crete.com. (n.d.). Retrieved from http://www.we-love-crete.com/tsikoudia.html.

IOOC. (1991). Commission Regulation (EEC) No 2568/91 of 11 July 1991 on the characteristics of olive oil and olive-residue oil and on the relevant methods of analysis.

Kapoulas, V. M., & Andrikopoulos, N. K. (1987). Detection of virgin olive oil adulteration with refined oils by second-derivative spectrophotometry. *Food Chemistry, 23*, 183-192.

Kennell, N. M. (2001). "Most Necessary for the Bodies of Men: Olive Oil and its By-products in the Later Greek Gymnasium" in Mark Joyal (ed.), In Altum: Seventy-Five Years of Classical Studies in Newfoundland,. In *in Mark Joyal (ed.), In Altum: Seventy-Five Years of Classical Studies in Newfoundland* (pp. 119-33).

Kiritsakis, A. K. (n.d.). *Olive oil, From the tree to the table* (II ed.).

K-MAC spectrometer. (n.d.). Korea.

Kokkinofta, R. I., & Theocharis, C. R. (2005). Chemometric Characterization of the Cypriot Spirit “Zivania”. *Journal of Agricultural and Food Chemistry, 53*, 5067-5073.

Kyriakidis, N., & Skarkalis, P. (2000). Fluorescence Spectra Measure- ment of Olive Oil and Other Vegetable Oils. *83*, 1435-1439.

L-Diez. (2003). Rapid Quantitative Assessment of the Adulteration of Virgin Olive Oils with Hazelnut Oils Using Raman Spectroscopy and Chemometrics. *J. Agric. Food Chem., 51*, 6145-6150.

Mignani, A. G. (2011). Visible and near-infrared absorption spectroscopy by an integrating sphere and optical fibers for quantifying and discriminating the adulteration of extra virgin olive oil from Tuscany. *Anal. Bioanal. Chem., 399*, 1315-1324.

Obeidat, S.M., Khanfar, M.S., & Obeidat, W.M. (2009). Classification of Edible Oils and Uncovering Adulteration of Virgin Olive Oil Using FTIR with the Aid of Chemometrics. *Aust. J. Basic & Appl. Sci., 3*(3), 2048-2053.

(2013). Olive oil virgin, crops processed, production data for 2013. Food and Agricultural Organization of the United Nations, Statistics Division.

ÖZDEMIR, D., & ÖZTÜRK, B. (2007). J. Food and Drug Analysis. *15*(1), 40-47.

P.J.A., S. (2003). Multivariate statistics for the Environmental Sciences. Hodder-Arnold.

Passaloglou-Emmanouilidou, S. (1990). A comparative study of UV spectrophotometric methods for detection of olive oil adulteration by refined oils. *Z Lebensm Unters Forsch, 191*, 132-134.

Perkin Elmer Fluorescence Spectroscopy. (n.d.).

Petrakis, P., Touris, I., Liouni, M., Zervou, M., Kyrikou, I., Kokkinofta, R., . . . Mavromoustakos, T. M. (2005). Authenticity of the Traditional Cypriot Spirit “Zivania” on the Basis of 1H NMR Spectroscopy Diagnostic Parameters and Statistical Analysis. *Journal of Agricultural and Food Chemistry, 53*, 5293-5303.

Phillipidis, A., Poulakis, E., Papadaki, A., & Velegrakis, M. (2016). Comparative Study Using Raman and Visible Spectroscopy of Cretan Extra Virgin Olive Oil Adulteration with Sunflower Oil. *Analytical Letters*.

Poulli, K. I. (2005). Classification of edible and lampante virgin olive oil based on synchronous fluorescence and total luminescence spectroscopy. *Analytica Chimica Acta, 542*, 151-156.

Poulli, K. I. (2007). Rapid synchronous fluorescence method for virgin olive oil adulteration assessment. *Food Chemistry, 105*, 369-375.

Poulli, K. M. (2006). (2006). Synchronous fluorescence spectroscopy for quantitative determination of virgin olive oil adulteration with sunflower oil. Anal. Bioanal. Chem., 386, 1571-1575. *Analytical Bioanalytical Chemistry, 386*, 1571-1575.

RAQUEL MATEOS, CONCEPCIOÄ N GARCIÄA-ORTIÄZ CIVANTOS, & JUAN CASTRO. (2005). Direct Spectrophotometric Determination of Bitterness in Virgin Olive Oil without Prior Isolation by pH Gradient. *J. Agric. Food Chem., 53*, 9615-9619.

Reusch, W. (n.d.). Retrieved from Spectroscopy: http://www2.chemistry.msu.edu/faculty/reusch/VirtTxtJml/Spectrpy/UV-Vis/spectrum.htm

Riley, F. R. (2002). "Olive Oil Production on Bronze Age Crete: Nutritional properties, Processing methods, and Storage life of Minoan olive oil". *Oxford Journal of Archaeology, 21*(1), 63-75.

Robards, K., Prenzler, D. P., Tucker, G., Swatsitang, P., & Glover, W. (1999). Phenolic compounds and their role in oxidative processes in foods. *Food Chemistry, 66*(4), 401-436.

Rodriguez, R. I., Delgado, M. F., Garcia, J. B., Crecente, R. M., Martin, S. G., & Latorre, C. H. (2010). Comparison of several chemometric techniques for the classification of orujo distillate alcoholic samples from Galicia (northwest Spain) according to their certified brand of origin. *Analytical Bioanalytical Chemistry, 397*, 2603-2614.

Rogovaya, M., Sinitsyn, G. V., & Khodasevich, M. A. (2014). A Principal Component Analysis of Transmission Spectra of Wine Distillates. *Optics and Spectroscopy, 117*(5), 839-843.

Rosales, F. G., Perdiguero, S., Gutiérrez, R., & Olias, J. M. (1992). Evaluation of the bitter taste in virgin olive oil. *JAOCS, 69*(4), pp. 394-395.

Roussis, I. G., Lambropoulos, I., Tzimas, P., Gkoulioti, A., Marinos, V., Tsoupeis, D., & Boutaris, I. (2008). Antioxidant activities of some Greek wines and wine phenolic extracts. *Journal of Food Composition and Analysis, 21*, 614-621.

Sadecka, J., & Tothova, J. (2007). (2007): Fluorescence spectroscopy and chemometrics in the food classification − a review. 25: . *Czech J. Food Sci., 25*, 159–173.

Schuster, R. (December 2014). *"8,000-year old olive oil found in Galilee, earliest known in world".* Haaretz.

Sikorska, E., Góreckib, T., Khmelin, I. V., Sikorskid, M., & Kozioła, J. (2005). Classification of edible oils using synchronous scanning fluorescence spectroscopy. *Food Chemistry, 89*, 217-225.

Sikorska, E., Khmelinskii, I., & Sikorski, M. (2011). Analysis of Olive Oils by Fluorescence Spectroscopy : Methods and Applications. In D. Boskou, *Olive Oil - Constituents, Quality, Health Properties and Bioconversions* (pp. 63-89).

Sikorska, E., Romaniuk, A., Khmelinskii, I. V., Herance , R., Bourdelande, J. L., Sikorski, M., & Kozioł, J. (2004, January). Characterization of Edible Oils Using Total Luminescence Spectroscopy. *Journal of Fluorescence, 14*(1), 25-35.

Skevin, D. (2011). *Croatian Journal of Food Technology, Biotechnology and Nutrition, 6*(3-4), 117-122.

Skevin, D., Kraljić, K., Miletić, L., Obranović, M., Neđeral, S., & Petričević, S. (2011). Adulteration of Oblica Virgin Olive Oil with Edible Sunfl ower and Refi ned Olive Pomace Oil. *Croatian Journal of Food Technology, Biotechnology and Nutrition, 6*(3-4), 117-122.

Stark, A. (2002). Olive oil as a functional food: Epidemiology and nutritional approaches. *Nutr. Rev., 60*, 170-176.

Tenenhaus, M., Esposito Vinzi, V., Chatelinc, Y.-M., & Lauro, C. (2005, January). "PLS path modeling". *Computational Statistics & Data Analysis, 48*(1), 159-205.

Torrecilla, J. S. (2010). A Novel Method To Quantify the Adulteration of Extra Virgin Olive Oil with Low-Grade Olive Oils by UV−Vis. *J. Agric. Food Chem., 58*(3), 1679-1684.

Tothova, J., Sadecka, J., & Majek, P. (2009). Total luminescence spectroscopy for differentiating between brandies and wine distillates. *Czech Journal of Food Science, 27*(6), 425-432.

Undenfriend, S. (1962). *Fluorescence Assay in Biology and Medicine.* Academic Press, New York.

Vinzi, V., Chin, W., Henseler, J., & et al. (2010). Handbook of Partial Least Squares.

Ward, K., Scarth, R., Daun, J. K., & Thorsteinson, C. T. (1994). Comparison of High-Performance Liquid Chromatography and Spectrophotometry. *Journal of the American Oil Chemists' Society, 71*(9), 931-934.

West, W. (2014). Absorption of electromagnetic radiation. Eastman Kodak Company, Rochester, New York.: Access Science. doi:http://dx.doi.org/10.1036/1097-8542.001600

White, P. J. (1995). Conjugated diene, anisidine value, and carbonyl value analysis. In N. A. Eds. K. Warner, *Methods to Assess Quality and Stability of Oils and Fat-Containing Foods* (pp. 159-178). Champaign, IL (USA): AOCS Press.

Wójcicki, K. K. (2015). Spectroscopic techniques and chemometrics in analysis of blends of extra virgin with refined and mild deodorized olive oils. *Eur. J. Lipid Sci. Technol., 117*, 92-102.

Wold, S. S. (2001). PLS-regression: a basic tool of chemometrics. *Chemometrics and Intelligent Laboratory Systems, 58*, 109-130.

Xie, L., Ye, X., Liu, D., & Ying, Y. (2009). *Food Chemistry, 114*, 1135.

Yang. (2001). Comparison of Near-Infrared, Fourier Transform-Infrared, and Fourier Transform-Raman Methods for Determining Olive Pomace Oil Adulteration in Extra Virgin Olive Oil. *JAOCS, 78*(9), 889-895.

Zhang. (2011). Quantitative detection of adulterated olive oil by Raman spectroscopy and chemometrics. *J. Raman Spectrosc., 42*, 1784-1788.

Zhang. (2011). Rapid Authentication of Olive Oil by Raman Spectroscopy Using Principal Component Analysis. *Analytical Letters, 44*, 2209-2220.

Zou. (2009). Rapid Authentication of Olive Oil Adulteration by Raman Spectrometry. *J. Agric. Food Chem., 57*, 6001-6006.

Βαλαβανίδης, Α. (2008). Υπεριώδης και Ορατή Φασματοσκοπία. In Α. Βαλαβανίδης, *ΒΑΣΙΚΕΣ ΑΡΧΕΣ ΜΟΡΙΑΚΗΣ ΦΑΣΜΑΤΟΣΚΟΠΙΑΣ ΚΑΙ ΕΦΑΡΜΟΓΕΣ ΣΤΗΝ ΟΡΓΑΝΙΚΗ ΧΗΜΕΙΑ.* ΣΥΓΧΡΟΝΑ ΘΕΜΑΤΑ.

(1991). ΠΑΡΑΡΤΗΜΑ IX. In *ΚΑΝΟΝΙΣΜΟΣ (ΕΟΚ) αριθ. 2568/91 ΤΗΣ ΕΠΙΤΡΟΠΗΣ.*

Τραχανάς, Σ. (2005). *Κβαντομηχανική Ι.* ΠΕΚ.